Purdue University
Purdue e-Pubs

Open Access Dissertations | Theses and Dissertations

8-2016

The role of mechanical loading in chondrocyte signaling pathways

Qiaoqiao Wan
Purdue University

Follow this and additional works at: https://docs.lib.purdue.edu/open_access_dissertations

 Part of the Biomechanics and Biotransport Commons

Recommended Citation
Wan, Qiaoqiao, "The role of mechanical loading in chondrocyte signaling pathways" (2016). *Open Access Dissertations*. 877.
https://docs.lib.purdue.edu/open_access_dissertations/877

This document has been made available through Purdue e-Pubs, a service of the Purdue University Libraries. Please contact epubs@purdue.edu for additional information.

Graduate School Form
30 Updated 12/26/2015

PURDUE UNIVERSITY
GRADUATE SCHOOL
Thesis/Dissertation Acceptance

This is to certify that the thesis/dissertation prepared

By Qiaoqiao Wan

Entitled

THE ROLE OF MECHANICAL LOADING IN CHONDROCYTE SIGNALING PATHWAYS

For the degree of Doctor of Philosophy

Is approved by the final examining committee:

Sungsoo Na
Chair

Bumsoo Han

Hiroki Yokota

Jiliang Li

To the best of my knowledge and as understood by the student in the Thesis/Dissertation Agreement, Publication Delay, and Certification Disclaimer (Graduate School Form 32), this thesis/dissertation adheres to the provisions of Purdue University's "Policy of Integrity in Research" and the use of copyright material.

Approved by Major Professor(s): Sungsoo Na

Approved by: George R. Wodicka 7/12/2016

Head of the Departmental Graduate Program Date

THE ROLE OF MECHANICAL LOADING IN CHONDROCYTE SIGNALING PATHWAYS

A Dissertation

Submitted to the Faculty

of

Purdue University

by

Qiaoqiao Wan

In Partial Fulfillment of the

Requirements for the Degree

of

Doctor of Philosophy

August 2016

Purdue University

West Lafayette, Indiana

I dedicate this dissertation to my husband, Wenhan Huang, who has been helping and supporting me throughout my PhD study. I dedicate this dissertation to my parents, Runfeng Ni and Xianchun Wan, who have always loved me and provided me extensive supports.

ACKNOWLEDGMENTS

I wish to thank my mentor, Dr. Sungsoo Na, for his sustained support and effort to help me becoming a better researcher and a better person. I will proudly carry his name with me for the rest of my scientific career. I would also like to thank the members of my thesis advisory committee, Dr. Hiroki Yokota, Dr. Jiliang Li and Dr. Bumsoo Han.

I would like to thank the past and current members of the Dr. Yokota laboratory who collaborated with us in the various scientific projects that I participated, especially Dr. Ping Zhang, Dr. Shinya Takigawa, Dr. Wenxiao Xu, Dr. Kazunori Hamamura, Dr. Joon W. Shim and Andy Chen.

I would like to thank the past and current members of the Dr. Han laboratory who collaborated with us in the 3D agarose gel project, Dr. Altug Ozcelikkale, Dr. Seungman Park and Dr. Soham Ghosh.

I would like to thank the past and current members of the Na laboratory, Seungjoo Kim, Euhye Cho, Yu-Hui Lai, ThucNhi TruongVo, Bo Sun, Jeffery Joll and Hannah Steele, for their help with research projects as well as their friendship.

I would also thank my friends who supported me and provided numerous entertaining activities in my free time.

TABLE OF CONTENTS

Page

Page

Page

Page

LIST OF TABLES

LIST OF FIGURES

Figure Page

Figure Page

Figure Page

Figure Page

ABBREVIATIONS

2D	Two-demensional
3D	Three-dimensional
AG	Agarose gel
AMPK	AMP-activated kinase
Bleb	Blebbistatin
CaMKKs	calmodulin-dependent kinase kinases
cAMP	Cyclic adenosine monophosphate
Col	Collagen
COX-2	Cyclooxygenase-2
CytoD	Cytochalasin D
ECM	Extracellular matrix
ER	Endoplasmic reticulum
ERK	Extracellular signal-regulated kinase
ESs	Effect sizes
F-actin	Filamentous actin
FAC	Focal adhesion complex
FAK	Focal adhesion kinase
FAs	Focal adhesions
FoxO	Forehead transcription factors
FPs	Fluorescent proteins
FRET	Fluorescence resonance energy transfer
GEF	Guanine nucleotide exchange factor
IL1β	Interleukin 1β
iNOS	Inducible-nitric oxide synthases

JNK	C-Jun N-terminal kinase
LIF	Leukaemia inducing factor
LINC	Linkers of the nucleoskeleton to the cytoskeleton
LKB1	liver protein kinase B1
MAPK	Mitogen-activated protein kinases
MEKK	MAP kinase kinase kinase
MKKs	MAP kinase kinases
MMPs	Matrix metalloproteinases
MSK	MAPK- and stress kinase-activated protein kinase
mTOR	Mechanistic target of rapamycin
NF-κB	Nuclear factor-κB
NO	Nitric oxide
OA	Osteoarthritis
PGE2	Prostaglandin E2
Pyk2	Proline-rich tyrosine kinase 2
ROCK	Rho-associated protein kinase
SEM	Standard error of the mean
VEGF	Vascular endothelial growth factor
VCAM-1	Vascular cell adhesion molecule-1
TAK	TGFβ-activated kinase
TIMPs	Tissue inhibitors of metalloproteinases
TNFα	Tumor necrosis factor alpha
TNFR	TNF receptor
TRAF	TNF-receptor activated factor
TRPV4	Transient receptor potential vanilloid 4

ABSTRACT

Wan, Qiaoqiao. Ph.D., Purdue University, August 2016. The Role of Mechanical Loading in Chondrocyte Signaling Pathways. Major Professor: Sungsoo Na.

Chondrocytes are a predominant cell type present in articular cartilage, whose integrity is jeopardized in joint degenerative diseases such as osteoarthritis (OA). In the chondrocytes of patients with OA, the elevated levels of inflammatory cytokines such as interleukin 1β (IL1β) and tumor necrosis factor α (TNFα) have been reported. These cytokines contribute to degradation of cartilage matrix by increasing activities of proteolytic enzymes. In addition to their contribution to proteolytic enzymes, these cytokines adversely affect anabolic activity of chondrocytes by inhibiting the production of proteoglycans and type II collagen. Therefore, blocking the action of these cytokines is a potential strategy to prevent cartilage degradation. Accumulating evidence suggests that mechanical loading contributes to the regulation of cartilage homeostasis. However, the underlying mechanisms are not clear as to how varying magnitudes of mechanical loading trigger differential intracellular signaling pathways at sub-cellular levels, which consequently lead to selective matrix synthesis or degradation. Furthermore, it is not known whether the loading-magnitude dependent responses are linked to degenerative diseases such as OA.

Tyrosine kinases such as Src and focal adhesion kinase (FAK) are known to play a crucial role in OA progression. We hypothesized that mechanical loading regulates the sub-cellular activation pattern of Src/FAK, and acts as a suppressor of the OA- or inflammatory cytokine-driven signaling activities. We used live cell imaging approach in conjunction with fluorescence resonance energy transfer (FRET)-based biosensors to investigate real-time molecular events at the sub-cellular level in live chondrocytes. Using two-dimensional (2D) cell culture and shear stress application, we found that

Src is activated by inflammatory cytokines (i.e., IL1β and TNFα), and is regulated by shear stress in a magnitude-dependent manner. Importantly, the cytokine-induced Src activation can be suppressed by moderate shear stress (5 dynes /cm^2) and the ER stress inhibitor.

Next, to investigate the sub-cellular activation pattern of Src and FAK in response to inflammatory cytokines and mechanical loading, we used lipid raft-targeting (Lyn-FAK and Lyn-Src) and non-lipid raft-targeting (KRas-FAK and KRas-Src) biosensors. We also developed a three-dimensional (3D) cell culture system using collagen-coupled agarose gels to mimic the physiologically relevant cell microenvironment. The activities of Lyn-Src, KRas-Src and Lyn-FAK were up and down regulated by high (> 10 μl/min) and moderate (5 μl/min) interstitial fluid flow, respectively, but KRas-FAK did not respond to the flow. We also found that Src activation by loading was blocked by inhibition of FAK, while inhibition of Src did not affect FAK activities, suggesting that FAK is necessary for interstitial fluid flow-induced Src activity. In contrast, Src was necessary for inflammatory cytokine-induced FAK activation. Furthermore, we developed a 3D *ex vivo* system that uses murine cartilage explants. This system in conjunction with 3D FRET imaging allowed us to visualize sub-cellular signaling activities of Src and FAK that closely mimic *in vivo* setting. We found that intermediate loading can inhibit inflammatory cytokine-induced activities of Lyn-Src, KRas-Src and Lyn-FAK, but not KRas-FAK.

AMP-activate kinase (AMPK) is a master regulator of cellular energy balance that activates when the ratio of (AMP+ADP)/ATP increases. Imbalance of AMPK regulation contributes to the development of diabetes, cardiovascular diseases, cancer, and found most recently, OA. In healthy cartilage, the treatment of IL1β and TNFα decreases AMPK activity, while how mechanical loading influences AMPK activities needs to be clarified. The recent design of FRET-based AMPK biosensors that can target various subcellular compartments (PM-AMPK targets plasma membrane, Cyto-AMPK target cytosol, Nuc-AMPK targets nucleus, ER-AMPK targets endoplasmic reticulum (ER), Golgi-AMPK targets Glogi apparatus, and Mito-AMPK

targets mitochondria) enable the study about the regulation of AMPK compartmentalization by physical stimulus. The AMPK activities were upregulated by shear stress in 2D environment, while only Nuc- and PM-AMPK are responsive to loading in 3D environment, suggesting culture dimensionality alters the mechanosensitivity of chondrocytes. To examine potential factors responsible for discrepancies between different culture models, we evaluated roles of cytoskeleton in mechanotransduction in 2D and 3D cultures and found that the differential cytoskeletal networks contribute to the distinct signaling in 2D versus 3D model.

1. INTRODUCTION

1.1 Introduction

OA is currently the most common form of arthritis, and is associated with various risk factors, including overuse of joint and overt inflammation [1,2]. The chondrocytes that sparsely distributed in cartilage are constantly exposed to a combination of compression [3], shear stress [4], and hydrostatic pressure [5]. Physiological loading is associated with reduced expression of MMPs [6, 7], while pathological loading, on the other hand, induces elevated production of matrix metalloproteinases (MMPs) and reduced expression of extracellular matrix (ECM) components, such as Type II collagen and aggrecan [8, 9].

FAK and Src play both direct and indirect roles in regulation of signaling cascades responsible for cell survival [10], differentiation, proliferation [11], mobility, mechanotransduction [4], and inflammatory signaling activities [12]. Upon the stimulation by chemical or mechanical factors, FAK is autophosphorylated at Tyr397 to unmask SH2 binding domain for the binding of Src. The formation of Src and FAK complexes enables FAK to phosphorylate other downstream molecules, such as paxillin, p130Cas, and α-actinin, to activate subsequent signaling pathways [13]. FAK and Src are known to respond to cytokines and mechanical stimulations, resulting in anabolic [14, 15] or catabolic [16] reponses in chondrocytes. Interestingly, recent reports indicate that distinct signaling mechanisms are responsible for their activation at different subcellular compartments [17–19]. However, to this date, it is still unknown how various stimulations differentially regulate FAK and Src activities at different subcellular locations, and subsequently leads to the progression or alleviation of OA.

In chapter 2, we utilized the live cell imaging approach in conjugation with FRET-based biosensors to investigate real-time molecular events in C28I2 human chondro-

cytes in 2D setup. We found that fluid flow and the inhibition of ER stress selectively regulate subcellular Src kinases, and appear to interact with Src-mediated signaling pathways that are important for cartilage health. In the chapter 3, we further employed a 3D *in vitro* cell culture system as well as a 3D *ex vivo* system using murine cartilage explants to maintain C28I2 human chondrocytes in a physiologically relevant microenvironment. The effect of different magnitudes of fluid flow and cytokines on Src/FAK signaling at subcellular levels was examined. Our findings demonstrated that the integrin activity is required for and highly localized with FAK activity in lipid rafts, which is essential to further activate Src signaling by fluid flow; while under cytokine treatment, FAK is a downstream molecule of Src. The proline-rich tyrosine kinase 2 (Pyk2) depletion and moderate loading suppress cytokine-activated Src/FAK activities, suggesting their potential therapeutic roles in OA.

We observed discrepancies between signaling activities in 2D versus 3D culture. To elucidate potential factors contributing to the difference, in the Chapter 4, we tested roles of cytoskeleton in signaling transduction. The imbalance of AMP-activate kinase (AMPK) activity has been recently found to contribute to OA development. AMPK is a master regulator of cellular energy balance that get activated when the ratio of (AMP+ADP)/ATP increases [20]. In healthy cartilage, the treatment of IL1β and TNFα decreases AMPK activity [21], while how mechanical loading influences AMPK activity is not well understood. In chapter 4, we utilized new-developed FRET-based AMPK biosensors that can specifically target subcellular compartments of cells to visualize the response of AMPK activities under various stimuli at different locations. We found culture dimensionality results in differential signaling activities of chondrocytes in response to loading, and the cytoskeleton is one of factors responsible for the distinct cellular activities in different culture environments.

1.2 Articular cartilage and chondrocytes

Articular cartilage is a type of highly specialized connective tissue that lines between the opposing bone surfaces to provide lubricated layers for articulation movement with a very low frictional coefficient. It is 2 to 4 mm thick layer that covers the gliding surface of joint. Unfortunately, cartilage is lack of blood vessels, lymphatic and nerves, and has very limited ability to repair and heal by itself. The cartilage has high compressive strength and is resistant to wear under normal circumstances. However, aging, injuries and obesity cause the excessive degeneration of cartilage, which subsequently leads to OA. OA is featured for symptoms including joint locking, pain, tenderness and dysfunction. In this regards, it is pivot to understand mechanisms underlying cartilage degeneration to prevent the initiation of OA [22].

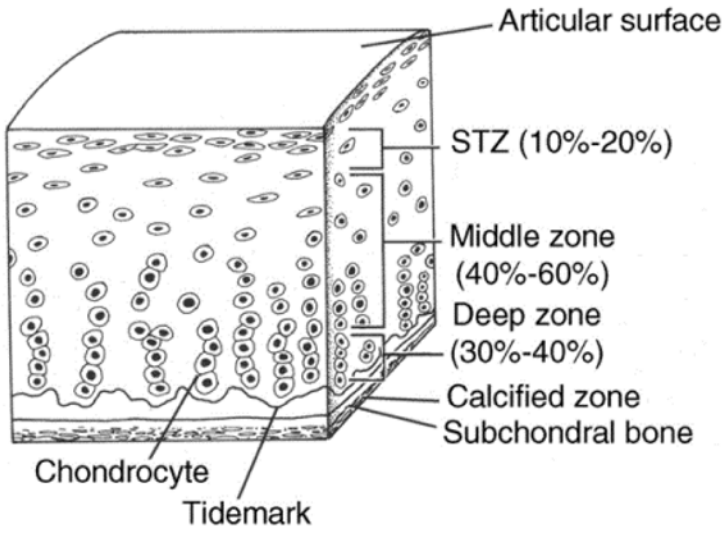

Fig. 1.1.: Schematic diagram of articular cartilage zones. The healthy cartilage can be divided into four zones from top to bottom: superficial zone, transitional/middle zone, deep zone, and calcified cartilage zone [23].

1.2.1 The structure of articular cartilage

Although the composition of articular cartilage can vary among species, it consists of the same components and the same structure. Articular cartilage can be vertically divided into four unique, and highly ordered zones: the superficial zone, the middle (transitional) zone, the deep zone, and the calcified zone (Figure 1.1). The composition, mechanical properties of the matrix, and cell functions differ with the depth from the cartilage surface. Recent studies found the existence of this highly organized structure significantly improves the function of cartilage [22]. The thinnest articular cartilage zone, superficial zone, makes up ∼10 to 20 % of articular cartilage thickness and has the highest collagen content [23] and consists of two layers. The first layer is a clear sheet containing little polysaccharide but no chondrocytes. It covers the joint surface. The second layer has a higher collagen concentration but a lower proteoglycan concentration as compared to other zones. In this layer, the collagen fibrils are organized parallelly to the cartilage surface to resist the strong shear stress that generated during articulation of joints and to regulate the travel of molecules in and out of cartilage. The damage of collagen fibrils at this layer will alter the mechanical behavior of the tissue and is the first sign of OA development [24]. The middle zone is located inside of superficial zone and makes up ∼40 to 60 % of cartilage thickness. Chondrocytes in this zone are characterized for highly active synthetic organelles, like ER and Golgi apparatus. As compared with superficial zone, it contains higher concentration of proteoglycans; lower concentration of water and collagen; but interestingly, lager diameter collagen fibrils. This zone is the first layer in cartilage that absorb compressive forces [25]. The deep zone occupys ∼30 % of cartilage thickness. In the deep zone, chondrocytes align perpendicular to the joint surface. This zone is featured for the largest diameter of collagen fibrils, the highest concentration of proteoglycans, and the lowest concentration of water. These properties collectively enable cartilage to resist great compression and maintain the integrity of cartilage under normal loading environments [23]. The calcified zone is a very thin layer of

calcified cartilage that lies between the deep zone and the subchondral bone. In the calcified zone, chondrocytes are smaller than those in other zones, and have smaller numbers of ER and Golgi apparatus, suggesting the lower level of synthetic activity of chondrocytes. The collagen fibrils in this zone tightly bound to subchondral bone to secure the cartilage to the bone [22]. Taken together, chondrocytes in different zones experience distinct microenvironments and are exposed to various types and magnitudes of mechanical loading in daily activities.

1.2.2 Extracellular matrix

Adult articular cartilage does not contain blood vessels, nerves, or lymphatics, which consequently leads to limited ability to self-repair and regrow. Chondrocyte is the only cell type in healthy cartilage and occupys less than 5 % of the cartilage volume. The remainder 95 % is ECM, consisting of tissue fluid (65-80 %), collagen ($\sim$10 %), proteoglycans (10-15 %) and a small amount of non-collagenous proteins and glycoproteins. The structural macromolecules form networks that shape the tissue and gain articular cartilage the ability to withstand significant mechanical loads, in some cases, can be more than multiple times of body weight. The tissue fluid contains water, gases, small proteins, metabolites, and a large amount of cations to neutralize the negative charge brought by proteoglycans. Most of the water is maintained within the matrix by the large aggregating proteoglycans and can not move freely. The confined water contributes to the resistance to compression, while upon the application of compression, the free-moving water generates shear stress along the joint surface that stimulates chondrocyte cellular activities [26].

There are three classes of structural macromolecules in articular cartilage, collagen, proteoglycans, noncollagenous proteins and glycoproteins. Collagen is distributed evenly throughout the depth of cartilage, and is the structural backbone of ECM by mechanically trapping water and proteoglycans in collagenous meshwork. Some noncollagenous proteins are involved to organize and stabilize the collagenous

meshwork, and also serve as connectors assisting the interaction between chondrocytes and ECM. The most abundant collagen in articular cartilage is the type II collagen, which is specifically exist in cartilage and is a biomarker of chondrocyte differentiation [27]. Collagen II contains a high content of hydroxylysine as well as glucosyl and galactosyl residues. These two components are required for the connection between collagen and proteoglycan to form ECM networks [28]. There are two types of proteoglycans in articular cartilage: aggrecans (consists of 90 % of proteoglycan mass) and smaller proteoglycans (consists of 10 % of proteoglycan mass). Aggrecans contain a protein core filament, and large amounts of chondroitin sulfate and keratin sulfate chains, which noncovalently associated with hyaluronic acid and other noncollagenous proteins on the core filament to form large proteoglycan aggregates. These aggregates can have sizes ranged from hundreds to more than ten thousands nm [29]. The smaller proteoglycans do not directly contribute to the mechanical behavior of cartilage; instead, their binding to other macromolecules might affect chondrocyte functions. Articular cartilage contains a wide variety of noncollagenous proteins, while only a small part of them have been identified and studied. Some of these molecules have been found can help to organize the structure of matrix, secure chondrocytes to ECM [30], and get involved in inflammatory signaling [31].

1.2.3 The mechanical behaviors and properties of cartilage

The mechanical properties of cartilage are determined using a confined compression test with a creep mode or a relaxation mode. In the creep mode, the load applied on cartilage tissue is constant and the displacement is measured; and in the relaxation mode, the displacement applied on tissue is constant and the force is measured. In the creep test, the displacement is rapid at the initial time points, then the rate of deformation will slow down and the displacement reaches its maximum (Figure 1.2). The proteoglycan is negatively charged due to its sulfate and carboxyl groups, and the repulsive force generated by these negative charges spread out proteoglycan

aggregates, which consequently occupy a large volume and hold a large amount of tissue fluid in cartilage. The collagen framework confines the swelling proteoglycan aggregates. In the creep test, upon the application of compression on cartilage, the negatively charged aggrecans are squeezed together, while in this process, the repulsive force increases, leading to the increase of cartilage stiffness. The proteoglycan is considered responsible for the constant displacement at later time points. Therefore, the loose collagen framework and nonaggregated proteoglycan in damaged cartilage will lead to compromised tissue stiffness. The measurements in creep test can be used to obtain two material properties, the stiffness and the permeability. The typical Youngs modules of cartilage is in the range of 0.45 to 0.80 MPa, which is really soft as compared to the values of steel is 200 GPa and wood is 10 GPa. Using Darcys law, the permeability of typical cartilage is in the range of 10^{-15} to 10^{-16} m^2 [32]. Values can change through the depth of the tissue: the permeability is highest near the surface of the joint, and is lowest in the deep zone [33].

1.2.4 Chondrocytes

The chondrocyte is the only cell type that sparsely distributed in articular cartilage. In different zones of cartilage, chondrocytes differ in cell size, morphology and metabolic activities, but all of them encapsulated with ECM and do not have cell-cell contacts. The number of chondrocytes in matrix is much lower than cell numbers in other tissues, while they are responsible for the maintenance and repair of ECM in its vicinity via balancing the degradation of the macromolecules by degradative enzymes with their replacement by synthesizing matrix components, including proteins and glycosaminoglycan side chains. To perform these functions, chondrocytes sense the biochemical signals and mechanical changes of the cartilage. In health cartilage, chondrocytes are responsible for the synthesis of appropriate macromolecules, which will be further assembled to be highly organized framework [25]. With aging or obesity, the production level of ECM by chondrocytes decreases dramatically, and thereby

contributes to the onset of OA. The mutations in genes for cartilage-specific proteins, including aggrecans, link proteins, and type II collagens have been correlated with heritable disorders of cartilage.

Due to the lack of blood vessels in cartilage, chondrocytes obtain nutrients and oxygen primarily by diffusion from the synovial fluid or subchondral bones, which limits the number of cells that can survive in cartilage. To survive and perform functions under low oxygen (the oxygen tension in deep layers is 1 % as compared with 24 % in atmosphere) and malnutrition tensions, chondrocytes prefer anaerobic pathways that metabolizing glucose to lactate [34]. The metabolic state of chondrocytes in healthy human cartilage is maintained at minimum level, resulting in very limited self-healing ability of cartilage. Moreover, chondrocytes have very limited potential for division and replication in healthy adult articular cartilage [22,35]. In this regards, the maintenance of cartilage is paramount to maintain the joint integrity and health.

1.3 Osteoarthritis

OA is the most common form of progressive joint diseases. It impairs the physical movement of 27 million Americans. Joint pain, stiffness and swelling are most common clinical symptoms associated with OA. Normal chondrocytes maintain the balance between ECM synthesis and degradation; but in OA chondrocytes, the excessive expression of MMPs, aggrecanases and other enzymes [36] compromises ECM integrity. At the level of clinical signs, OA patients are not suffered from the overt inflammation as compared to those with rheumatoid arthritis, while an elevated expression level of cytokines has been found in the synovial tissue of OA [1]. At the cellular level, it has been found that OA chondrocytes express genes typical of inflammatory responses [37]. Therefore, even though the cause of OA is still under debate, multiple factors that lead to inflammation are regarded to contribute to the early development of OA. Additionally, factors that result in the overuse of joint, including joint instability, obesity, aging, intra-articular mineral deposition, and joint muscle

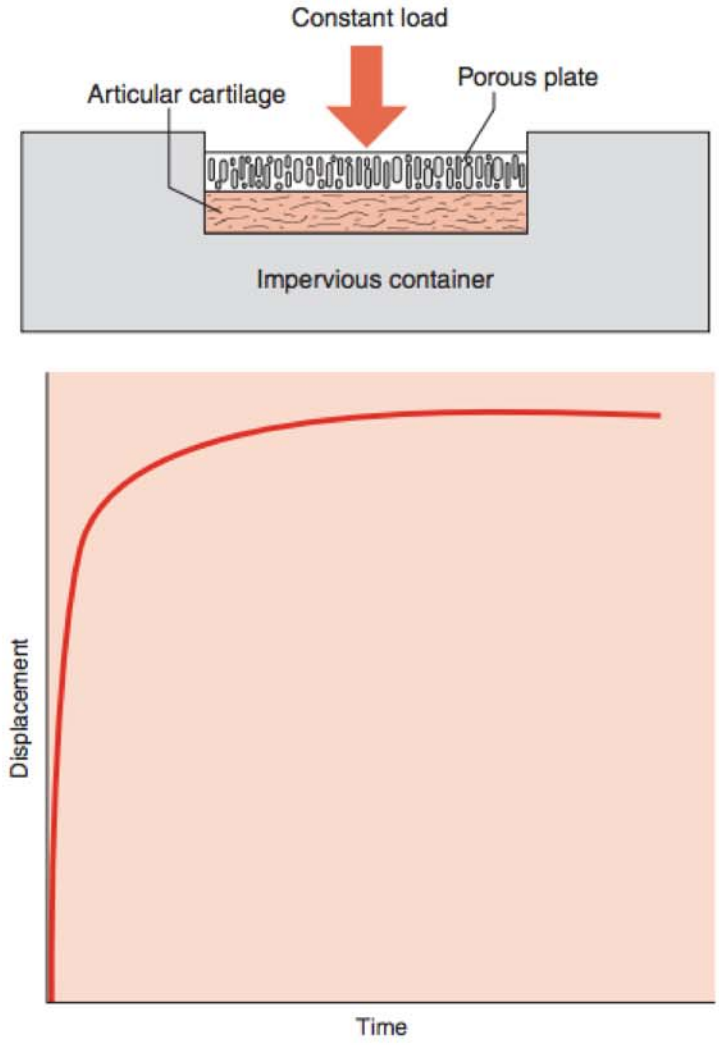

Fig. 1.2.: A schematic showing the device used to test the confined compression of cartilage. The cartilage explant is placed under a porous slice, and is loaded during the test. A plot showing confined compression test of cartilage. A constant force is applied on the cartilage and the resulting displacement is measured over time. The cartilage deforms rapidly at the earlier time points and large amounts of tissue fluid are squeezed out of the cartilage. Then the displacement reaches its maximum, and the deformation becomes zero [32].

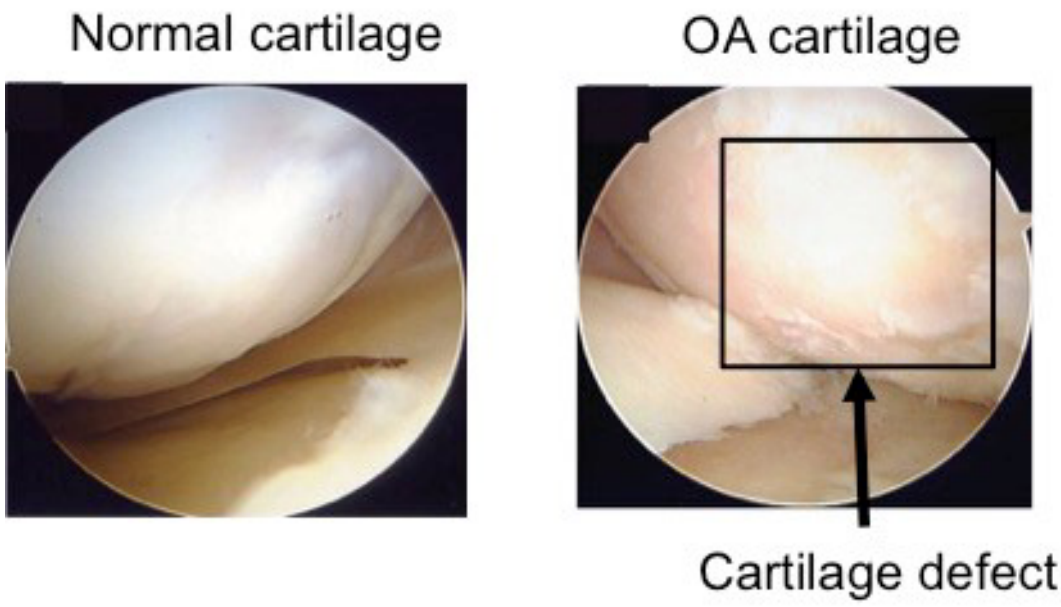

Fig. 1.3.: The comparison between normal and OA cartilage. The black box denotes cartilage defect. The arthroscopic view shows the difference between healthy cartilage and OA cartilage. The healthy cartilage present smooth and rigid surface, while the OA cartilage shows obvious cartilage loss and wear at the medial femoral condyle and tibia [38].

weakness, increase the expression levels of cytokines and MMPs [2] and are considered as risk factors of OA. However, the underlying mechanisms are still undetermined as to how inflammatory cytokines and varying types of mechanical forces differentially regulate chondrocyte intracellular signaling and ultimately alter cartilage matrix.

1.3.1 The initiation and progression of OA

The ECM of cartilage is highly dynamic and undergoes constant remodeling. At the initial state of ECM degradation, the chondrocyte will activate anabolic mechanism to counteract the degeneration process. This stage is featured for increased chondrocyte proliferation rate, intracellular metabolic activities, and synthesis of ECM components. The loss of cartilage integrity greatly increases the diffusibil-

ity of growth factors that have been found to be responsible these repair activities. Moreover, advanced lesions in cartilage are capable to increase the expression level of growth factor by chondrocytes to further activate repair process. Eventually, the repair and degradation will reach a new balance, in which the increased anabolic activities equal catabolic activities. Nevertheless, the cartilage has very limited repair ability, and might not be able to reach another new balance if the newly established balance is broken again, which consequently leads to the progression of OA, ultimately causing symptoms that experienced by patients.

During the progression of OA, the degeneration of ECM by proteinases exceed the synthesis, resulting in a net loss of cartilage matrix. In this process, the content of ECM is considerably decreased, including type II collagen and proteoglycan, and the distribution of proteoglycan becomes uneven in OA cartilage (Figure 1.3). In addition to the reduced content, the shorter collagen fibers that degenerated by proteinases in OA cartilage lead to reduced elastic modules, fibrillation and fissure formation [39]. Moreover, the organization of collagen meshwork is disoriented, and collagen fibrils are found widely separated. As the result of the changed collagen II and the impaired ECM networks during OA development, the mechanical microenvironment of chondrocytes is significantly changed, influencing cellular functions of chondrocyte [40]. The loose ECM structure transfers greater loads to the underlying subchondral bones and stimulates the growth of subchondral bones towards the articular surface [41], preceding the cartilage damage. This feedback loop consequently drives the progression of OA. Therefore, it is paramount to develop chemical and mechanical therapies that prevent collagen II degradation and loss; and the understanding of signaling pathways in chondrocytes that is responsible for these processes are indeed essential.

1.3.2 Proteinases

MMPs produced by chondrocytes or synovial cells are mainly responsible for the degeneration of the ECM. MMP1 degrades type I, II and III collagen; MMP2 digests gelatins, type IV, V, VII, X, and XI collagen, fibronectin and proteoglycans; MMP3 cleaves proteoglycans, type IV, VII, IX and XI collagen, and fibronectin. MMP9, MMP8 and MMP13 also play crucial roles in the degradation of cartilage matrix. ADAMs is another group of proteinases that can degrade the aggrecans core proteins [42]. The excessive expression of MMP genes has been found in the initiation of OA in animal models as well as in human patients. In healthy cartilage, the synthesis and activation of MMPs are under strict control by chondrocytes, while in OA cartilage, MMPs excessively degrade endogenous ECM as well as newly synthesized ECM components. The uncontrolled degradation of these newly produced ECM molecules might induce a total loss of cartilage integrity and initiate inflammatory responses [43]. Tissue inhibitors of MMPs (TIMPs), including TIMP1, 2, 3 and 4, are capable to control the cartilage degradation by inhibiting the activities of MMPs. Most interestingly, both TIMP1 and TIMP2 also promote the growth of chondrocytes, which might assist matrix turnover in the early stage of OA [44]. However, with the development of OA, the expression level of MMPs in cartilage will be substantially higher than that of TIMP, and the activities MMPs can not be rescued by the insufficient amount of TIMP [42].

1.3.3 Inflammatory cytokines

OA development is characterized by cartilage erosion as well as synovial inflammation. An increased expression of inflammatory cytokines, such as IL1β and TNFα, has been reported using immunolocalization technology in OA cartilage by Tetlow [45]; abnormal mechanical and oxidative stresses are possible factors that promote the cytokine production. IL1β and TNFα excessively produced by synoviocytes, or chondrocytes substantially elevate MMPs expression, while on the other hand, inhibit

ECM production by chondrocytes. Moreover, the expression level of natural antagonists of the IL-1 receptor (IL-1Ra), competing with IL1 for the IL receptor, is downregulated in OA cartilage, which further enhances the catabolic effect of IL-1 on ECM.

IL1β and TNFα contribute to the catabolic processes in OA progression by significantly increasing the expression of matrix degrading enzymes such as MMP1, MMP3, MMP13 and an disintegrin and metalloproteinase with thrombospondin-1 domains (ADAMTS)4 [37, 46–49]. These digestive enzymes degrade collage type II fibrils in superficial layers of cartilage, and this denaturation of collagen is regarded as the first sign of OA development. In addition to promoting the production of MMPs and other proteinases by chondrocytes, IL1β and TNFα elevate the expression of prostaglandin E2 (PGE2) and nitric oxide (NO) via mitogen-activated protein kinases (MAPK) and nuclear factor κB (NFκB) signaling pathway [50]. On the other hand, these cytokines adversely reduce anabolic activity of chondrocytes by reducing the gene expression of proteoglycans and type II collagens [47, 51, 52]. Moreover, IL1 has been reported to contribute to other cytokines production such as TNFα, IL1 and LIF (leukaemia inducing factor) [53, 54], inducing additive effects that further promote proteinase production and suppress matrix synthesis. TNFα also has been found to promote the production of IL1, IL6 and IL8, and activates sensory neurons that induce pains [55]. The inhibition of these inflammatory actions using anti-inflammatory drugs is a strategy to prevent OA progression. IL1 receptor antagonist has been shown prevent OA progression in animal models as well as clinical trials [56]; and the anti-TNFα treatment has been found can reduce the pain and the inflammatory process in OA. Although the significant roles of IL1 and TNFα in cartilage health are well known, the signaling involved in inflammation of cartilage needs further studies.

IL1β is a member of IL-1 family. Its active form exists in extracellular space and consists of 153 amino acid residues [58]. During the inflammation of cartilage, chondrocytes, osteoblasts, synoviocytes, and mononuclear cells elevate the synthesis

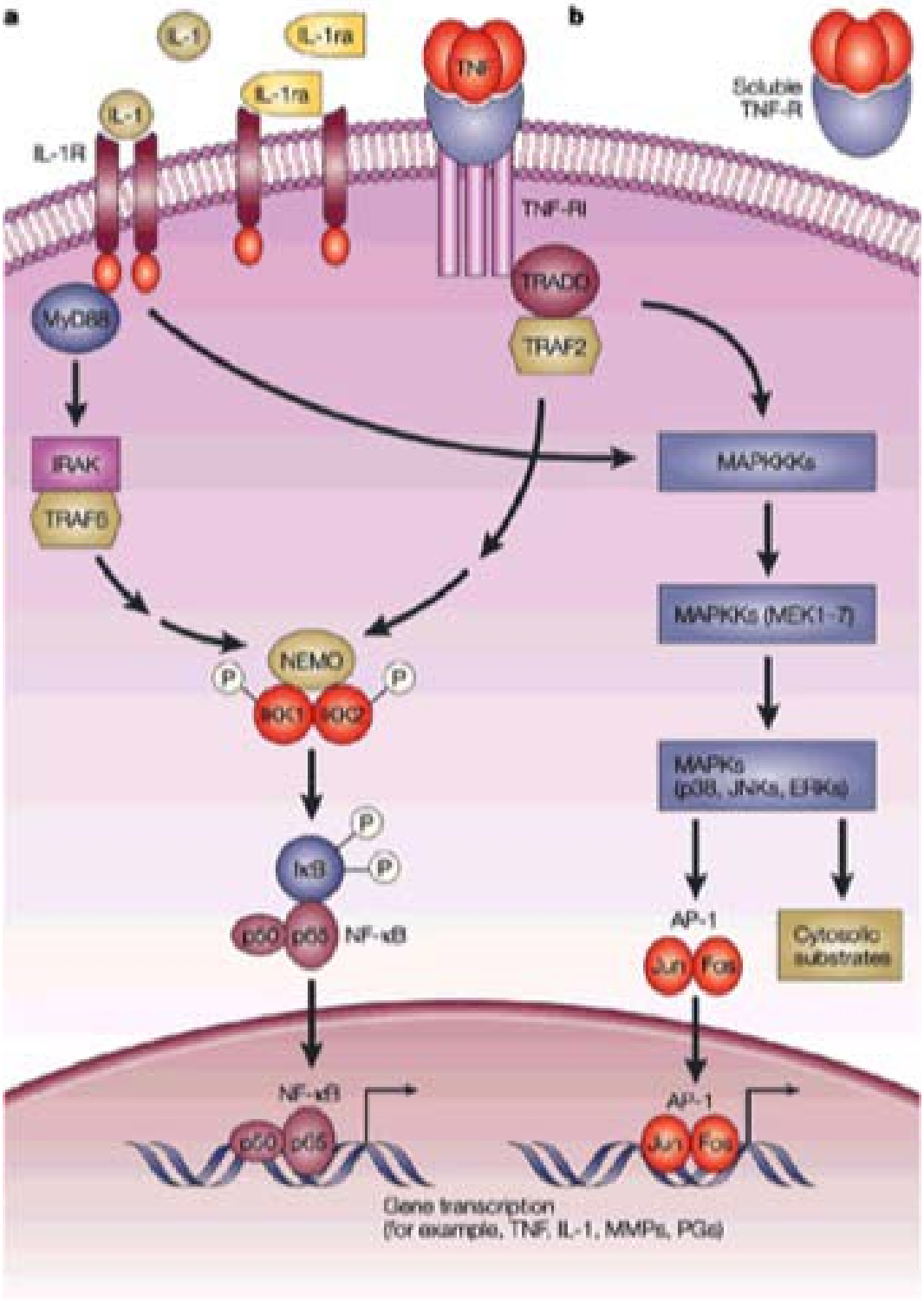

Fig. 1.4.: TNFα and IL1β induced signaling pathways [57].

of IL1β, and release it to the synovial fluid, synovial membrane, cartilage, and the subchondral bone layer [59]. The IL1β binds to IL1 receptor families that are called the Toll and IL1 receptor (TIR) family, including IL-1R1 and IL-1R2, and initiates inflammatory signaling cascades. The expression of IL-1R1 is elevated on the surface of chondrocytes in OA patients. The interaction between IL1β and IL-1R1 triggers mechanisms as shown in Figure 1.4A, while the binding of IL1β on IL-1R2 have no ability to activate further intracellular signal [60].

Two pathways form the essential core of IL1β-induced intracellular signaling cascades: MAPKs and NFκB [50]. The MAPK pathways coordinate activation of gene transcription, protein synthesis, cell cycle machinery, cell apoptosis, and cell differentiation. All MAPK pathways involve a three-tiered signaling module. The first titer is MAP kinase kinase kinases (MEKKs). MEKKs are serine/threonine-specific kinases and can activate MAP kinase kinases (MKKs). The second titer is MKKs. MKKS phosphorylate both hydroxyamino acids of the Thr-X-Tyrosin motif (TEY in extracellular signal regulated kinase (ERK)1/2,TPY in c-Jun N-terminal kinases (JNKs), TGY in p38 kinases) on MAPKs, which is the third titer [61]. Three types of MAPKs, including ERK1/2, JNKs and p38, are ubiquitously expressed and are capable to phosphorylate a wide selection of transcription factors. The p38 pathway also stabilizes the mRNAs and enables mRNA translation by activating MAPK-activated protein kinase (MAPKAPK)-2. NF-κB, a key element in proinflammatory signaling pathway, regulates genes that encoding cytokines (IL1,IL2, IL6, IL12, and TNFα), chemokines (IL-8 and MIP-1α), and inducible effector enzymes (inducible-nitric oxide synthases (iNOS) and cyclooxygenase-2 (COX-2)) [62].

Upon the binding of IL1β to TIR, the adapter protein MyD99 is recruited, which further activate TRAF6 protein, leading to the activation of Tp12, MEKK3 and TGFβ-activated kinase (TAK)1. Tp12 activates ERK pathway; MEKK3/TAK1 activates JNK and p38MAPK; and TAK1 regulates the phosphorylation of the IκB kinase complex (IKK), thereby activates NF-κB [63]. In recent years, the MEKK2, as well as MAPK- and stress kinase-activated protein kinase (MSK) have been found can

increase the transcriptional activity of NF-κB p65 [64], suggesting the NFκB pathway is cross-linked with MAPK pathways in IL1β-induced inflammatory signaling, as shown in Figure 1.4. The activation of these signaling pathways blocks the synthesis of ECM components, such as type II collagen and aggrecans; activates the synthesis of enzymes, including MMP-1, MMP-3, MMP-13, ADAMTS-4, which have deleterious effects on cartilage integrity; induces its secretion of other cytokines, for example, TNFα, IL-6, IL-8 and CCL5 chemokine, and activates a number of other compounds, including NO, phospholipase A2 (PLA2), cyclooxygenase-2 (CPX-2), prostaglandin E2 (PGE2), and reactive oxygen species (ROS).

TNFα is a member of tumour necrosis factors family (TNF superfamily). TNFα is produced by the same group of cells that synthesize IL1β, and is secreted to the same elements as IL1β [65]. Basically, TNFα activates the same MAPK signaling as IL1β, though via a different mechanism (Figure 1.4B). There are two isotypes of TNF receptors located on the plasma membrane of chondrocytes. TNF-R1 (p55, CD120a, and TNFRSF1a) can bind to TNF in both soluble and membrane forms, and TNF-R2 (p75, CD120b, and TNFRSF1b) can only be activated in membrane form [66]. The binding of TNFα to TNF-R1 forms the TNF-TNFR complex, which will further couple with TRADD adapter protein and other adapter proteins, such as TRAF2, c-IAP1, c-IAP2, and RIP1, to form a complex. This complex binds TAK1, TAB1, and TAB2, resulting in the activation of the most two important transcription pathways, NF-κB and ERK/MAPK [67]. Additionally, the interaction of TNFα and TNF-R1 changes the conformation of the complex, recruit FADD and pro-Caspase 8, and eventually leads to cell death [68]. The binding of TNFα to the TNF-R2 receptor activates the interaction of TRAF2, TRAF3, c-IAP1, and c-IAP2, which further activate JNK and NF-κB signaling pathways [67]. Progranulin (PGRN), an anti-inflammatory growth factor, has been shown to incorporate both TNF-R1 and TNF-R2. The elevated expression level of PGRN in OA patients indicates its potential roles as a natural antagonist of TNF interfering with the TNFα-induced inflammatory signaling [69]. The major difference between IL1β- and TNFα-induced

signaling is that the TNFα also activates apoptotic pathways [70, 71]. The improved understanding of signaling nodes may benefit in developing a therapeutic strategy that specifically inhibits inflammatory signaling with less side effects and alleviates OA symptoms.

1.3.4 Anti-inflammatory cytokines

Several cytokines have anti-inflammatory functions, such as IL-4, IL-10 and IL-13, which are capable to inhibit the inflammatory effects of both IL1β and TNFα.

IL4 has been found have a strong chondroprotective effect by inhibiting the production of MMPs and preventing the variation in proteoglycan synthesis in OA progression. The increased expression levels of IL4 in synovial fluid and its receptors in blood have been identified in OA patients as compared to the healthy control group [72]. With the treatment of IL4, the synthesis of inflammatory cytokines, including IL1β, TNFα, IL6, and other inflammatory mediators, such as PGE2, COX-2, PLA2, and iNOS, are inhibited in chondrocyte cultures [73]. However, the sensitivity of OA chondrocytes to IL4 is decreased, which impairs the ability of IL4 to prevent the rapid erosion of the cartilage [74]. IL4 shares a same group of receptors with IL13, including IL-4Rα, IL-13Rα1, and IL-2Rγc. The formation of IL-4Rα and IL-2Rγc complexes (complex I) is required for the binding of IL4, and the attachment of IL-4Rα and IL-13Rα1 (complex II) promotes the binding of both IL4 and IL13. The interaction of complex I and IL4 is associated with the activated phosphorylation of JAK1/STAT3/STAT6 cascades [75].

Similar to IL4, IL10 shows chondroprotective effect in OA cartilage. It stimulates the production of ECM components, such as type II collagen and aggrecans, downregulates the expression of TNFα and IL1β, inhibits the synthesis of MMPs, and inhibits the apoptosis of chondrocytes [76]. The attachment of IL10 to the subunit of IL-10R1 changes its conformation to enable the binding of this complex to IL-10R2 subunit [77], and the intracellular signaling cascade is started, leading to the acti-

vation of SMAD1/SMAD5/SMAD8, ERK1/2 MAP, and consequently elevates the synthesis of bone morphogenetic protein 2 and 6 (BMP-2 and 6). BMP proteins are capable to induce mesenchymal cells transform to chondrocytes, and stimulate their proliferation [78].

IL13 has been found have strong anti-inflammatory and chondroprotective effects on chondrocytes in OA articular cartilage and synovial membrane. IL13 has inhibitory effects on the production of IL1β, TNFα, and MMPs; elevates the expression of IL-1Ra, which competes with IL1β to binding receptors, leading to inhibited effects of IL1β; and blocks the synthesis of COX-2 and PGE2 [79]. As stated in paragraph about IL4, the interaction of IL-4Rα and IL-13Rα1 is required for the binding of IL13. Upon its attachment to receptors, IL13 activates the cascades IL-4Rα/JAK2/STAT3 and IL-13Rα1/TYK2/STAT1/STAT6 [80].

1.3.5 Mechanical loading affects cartilage health

Table 1.1: Forces experienced by chondrocytes *in vivo*

Force Type	Intensity
Compression (Standing)	3.5MPa [3]
Compression (Stair Climbing)	10-20MPa [81]
Shear Stress	
Hydrostatic Pressure	3-10MPa [5]
Osmotic Stress	
Tensile	

Chondrocytes live in a complex and harsh mechanical environment, and they are exposed to a combination of compression, shear stress, hydrostatic pressure, osmotic

stress, and tensile stretch (Table 1.1). The compression experienced by chondrocytes during standing is ∼3.5 MPa and during stair climbing is 10-20 MPa [3, 81]. The compression applied on cartilage induces synovial fluid flow along the surface and eventually results in shear stress [4]. The hydrostatic pressure due to the retained fluid by charged proteoglycans is ranged from 3 to 10 MPa [5]. Osmotic stress is usually resulting from the sudden changes in solute concentration around chondrocytes during joint movement [82]. Tensile only occurs in some stretch activities. Upon mechanical stimulation, chondrocytes sense mechanical stresses and convert them into the intracellular signaling cascades; and consequently change metabolic activities of chondrocytes. Accumulating evidences demonstrate that mechanical loading has either anabolic or catabolic effect on chondrocyte activities.

Moderate exercises prevent OA progression

Besides pain relief treatment and joint replacement, there is no non-invasive therapy can completely prevent the progression of OA [25]. Recently, moderate exercises have been recommended to OA patients as an alternative physical therapy, considering the fact that it significantly benefits in the health of articular cartilage. At clinic level, exercises have been shown can decrease the risk of knee OA [83], and improves function in OA [84]. A recent research investigated the effects of anti-inflammatory drugs, simple analgesics and exercises on OA. Results demonstrated that the effect sizes (ESs) of pain and function for exercises are comparable to estimates for drugs (Table 1.2) [85]. Therefore, the exercise is regarded as a potential therapeutic strategy of managing OA conditions and the improved understanding of how moderate loading influence chondrocyte functions is demanding [86].

At tissue level, physiological loads promote the integrity of ECM, increase the content of glycosaminoglycan in cartilage [87], and enhance the cartilage repair by chondrocytes [2,88]. The goal of physical therapies is to impede joint damage by inhibiting catabolic activity and activating anabolic activity. Experiments using cartilage ex-

Table 1.2: The efficacy of various therapies for knee OA [85]

Therapy	ES_{pain}	$ES_{function}$
Strengthening	0.32	0.32
Aerobic	0.52	0.46
Water-based	0.19	0.26
Acetaminophen	0.14	0.09
Oral NSAIDs	0.29	1
Topical NSAIDs	0.44	0.36

plants, 3D cultures and monolayer cultures have shown that dynamic compression, shear stress and hydrostatic pressure at moderate intensities are able to promote chondrocyte anabolic activities by increasing expression levels of aggrecan and type II collagen [63, 89–95] and adversely decreasing the production of degenerative enzymes (Table 1.3). The study using animal models with antigen-induced arthritis found that moderate loads not only inhibited IL1β or TNFα-induced transcriptional activation of COX-2, PGE2, NO, MMPs and ADAMTS-5, but also upregulated the production of anti-inflammatory cytokine IL-10, suggesting the anti-inflammatory effect of physiological loading on cartilage [96, 97]. In addition to increased anabolic activities, the proliferation of chondrocytes was also elevated in response to moderate mechanical stimulation [98–100]. But the duration and intensity of stimulation required for the beneficial responses appears to be dependent on a number of factors, including loading type, frequency, intensity and duration.

Injurious loading promotes OA progression

On the contrary to the physiological loading, the injurious loading is one major factor of OA onset and progression. Overuse of joints results in catabolic effects by directly damaging the cartilage ECM and breaking the balance of chondrocytes

Table 1.3: The effect of physiological loading on chondrocytes

Loading type	Model	Effect
Passive motion	OA rabbit cartilage explant	↓ GAG degradation, COX-2, MMP1, and IL1β ↑ IL10 [96, 97]
Passive motion	Rat cartilage explant	↓ MMP3 and ADAMTS5 [89]
4-8% strain	Rabbit cartilage	↓ IL1β-induced NO and NF-κB [63]
15% compression	Chondrocytes in agarose gel	↓ NO, IL1β-induced NO, COX-2, and PGE2 ↑ Aggrecan expression [90, 91]
20% strain	Rat chondrocytes	↓ IL1β-induced MMPs [92]

activities [101]. The aberrant expressions of proinflammatory cytokines, proteolytic enzymes and ECM components induced by overloading have been reported in numerous studies (Table 1.4), and are regarded as evident signs of arthritis [8]. The application of osmotic stress upregulated the production of MMP-3 and -13 [102]; the strain at high rates (0.1 and 1/sec, 50 % strain, peak stress at 12 MPa) reduced protein biosynthesis [103]; the repetitive impact loading of 5 MPa at 0.3 Hz resulted in collagen structure damage and chondrocyte apoptosis [104, 105]; a single impact load at 4.5 MPa leaded to chondrocyte apoptosis in bovine cartilage explants; and a load at 7-20 MPa induced degradation of cartilage ECM [106, 107]. The MAPK and Rac/MKK7/c-Jun signaling pathways have been found are responsible for loading-induced upregulation of MMP3/ADAMTS5 and COX-2, respectively [108]. In addition to its direct effect on chondrocyte catabolic activities, the deleterious loading also stimulates the production of vascular endothelial growth factor (VEGF), which is capable to upregulate the expression of ADAMTS5 and MMPs and downregulate the expression of TIMPs [109, 110]. Taken together, these chronic or acute high loads might consequently initiate and promote OA development. To adopt exercises as therapeutic strategies that can relieve the inflammation symptoms of OA, a better

understanding of the intracellular activities in chondrocytes under different magnitudes and types of loading is required.

Table 1.4: The effect of deleterious loading on chondrocytes

Loading type	Model	Effect
50 % Compression	Bovine cartilage	↑ MAPKs, COX-2, MMP3, and ADAMTS5 ↓ Type II collagen, Fibronectin [96]
20 dyne/cm^2 stress	Human chondrocytes	↑ COX-2, Rac, c-Jun, and JNK2 [111]
15 % strain	Rabbit chondrocytes	↑ IL1β, NO, and NF-κB [63]
50 % compression	Bovine cartlage	↑ VEGF, MMP1, 3, 13, and ↓ TIMP [109]

1.3.6 ER stress promotes OA progression

In addition to cytokines and mechanical loading, inappropriate induction of cellular stress to the ER is deleterious to cartilage. The ER stress-induced accumulation of abnormal proteins leads to adaptive cellular responses, including suppression of mutant protein synthesis, elevated expression of molecular chaperones , which increase the probability of correcting unfolded or misfolded proteins, and activation of degradative enzymes to remove abnormal proteins [112]. The phosphorylation of eukaryotic translation initiation factor 2 subunit alpha (eIF2α) is upregulated by ER stress to reduce overall translation in the cell and the synthesis of mutant misfolded proteins [113]. Notably, some genes escape the block imposed by eIF2α phosphorylation and get upregulated; one of these is MMP. A recent study found that salubrinal, a small molecule that can alleviate ER stress by selectively dephosphorylating eIF2α [114], inhibits IL1β- and TNFα-induced MMP activities [115]. Although the dephosphorylation of eIF2α inhibits MMP activities, little has been known about the role of eIF2α in cytokines- and mechanical loading-induced signaling.

1.4 Signaling mechanisms for mechanotransduction in chondrocytes

Mechanical loading plays a crucial role in cartilage homeostasis and remodeling. The mechanical force-induced cell responses can be acute responses that occur within seconds to minutes, including changes in calcium and cAMP levels, and regulation of membrane ion channels, or long-term changes that occur over hours to months, such as changes in cell morphology, and regulation of ECM production [116]. With the increasing interest in mechanotransduction in chondrocytes, different model systems have been developed. These include studies on monolayer cultures subjected to stretch or shear stress, and both static and dynamic compression of cartilage explants or cells in 3D scaffolds. Molecular mechanisms considered for mechanotransduction in chondrocytes include MAPK/ERK pathway, Ca^{2+} ion channel and integrin-mediated signaling.

1.4.1 MAPK/ERK signaling

As discussed in earlier paragraph, MAPK/ERK pathway play pivot roles in cytokine-induced signaling pathways in chondrocytes. Moreover, it is further identified as highly responsive to mechanical stimulation. In response to continuous pressure of 90 kPa for 60 min, the expression of ERK increased by 73 %, and the application of pressure for 360 min leaded to 32 % increase of ERK expression [117]. A study found that the application of fluid flow on chondrocytes reduced the gene expression of aggrecans by activating ERK pathway [118]. Another study using microarray analysis showed that p38 MAPK and ERK1/2 pathways were involved in a wide variety gene expression in chondrocytes under hyperosmotic stress [119].

1.4.2 Calcium channel

Ca^{2+} is a key second messenger that controls many cellular functions, like cell metabolism, cell proliferation, gene transcription, cell contraction as well as mechan-

otransduction. Many studies have identified that Ca^{2+} signaling can be regulated by compression [120, 121], fluid flow [122], hydrostatic pressure [123], and osmotic stress [124]. The transient receptor potential vanilloid 4 (TRPV4) channel is the most well studied Ca^{2+} channel. It was first found can be activated by hypotonicity-induced cell swelling. A recent study showed that the blocking of TRPV4 diminished the chondrocyte responses to hypoosmotic stress, and TRPV4 activation promoted chondrocyte responses. Moreover, the activation of TRPV4 was capable to restore the defective cell volume caused by IL-1 [125].

1.4.3 Integrin-mediated mechanotransduction

Integrin is a group of transmembrane glycoprotein consisting of an α and a β subunit. The combination of 16 types of α and 8 types of β subunits form more than 20 different kinds of integrin receptors. Some receptors have specific binding to ligands: for example, $\alpha5\beta1$ and $\alpha V\beta1$ bind fibronectin, $\alpha6\beta1$ and $\alpha6\beta4$ bind laminin; $\alpha V\beta3$ binds vitronectin andosteopontin; $\alpha1\beta1$, $\alpha2\beta1$, and $\alpha11\beta1$ bind type II and type VI collagen. In chondrocytes, $\alpha1\beta1$, $\alpha5\beta1$, $\alpha10\beta1$ and $\alpha V\beta5$ are highly expressed [126]. Each subunit contains an extracellular domain, providing the binding site for ECM; a transmembrane domain, and a cytoplasmic tail, transducing the mechanical signals to intracellular signaling molecules or the actin cytoskeleton. Adapter proteins, like paxillin, Src and tensin connect the cytoplasmic tail of integrin with cytoskeleton and other signaling molecules (Figure 1.5). The interaction between integrin and ECM is required for the integrin-mediated mechanotransduction. The absence of ECM components or the inhibition of integrin activity totally abolishes integrin response to shear stress [127]. The composition of ECM also determines the transduction of mechanical signal and the regulation of cellular response. It has been found that chondrocytes binding to fibronectin show a maximal response to mechanical stimulation, while the binding to type II collagen shows a less degree of response, and the binding to poly-l-lysine gives the minimal response [128]. Chondrocytes attached to

fibronectin showed a higher degree of membrane hyperpolarization induced by 0.33 Hz mechanical stimulation than cells adherent to type II collagen. This hyperpolarization response was abolished by blocking $\alpha 5\beta 1$ integrin [128]. The rigidity of ECM is another significant factor of integrin-mediated FAK activity. The phosphorylation level of Tyr 397 increased with the elevated rigidity of a 3D collagen matrix [129].

Upon the binding of integrin to ECM ligands, the actin cytoskeleton interacts with β integrin and other adapter proteins, to form actin stress fibers. The actin filaments transmit mechanical signaling through the cell. The importance of actin in mechanotransduction has been shown that the Cytochalasin D (selective actin inhibitor) abolishes the mechanical stimulation-induced hyperpolarization [131]. The remodeling of F-actin has been observed in response to hydrostatic pressure in chondrocytes in monolayer culture, or dynamic compression in chondrocytes in 3D agarose scaffolds [132]. The cyclic pressure of 15 MPa impairs the intact actin network, and 30 MPa almost totally abolishes actin structure, leading to cell retraction [133]. 10-15 % compression on chondrocytes results in punctate actin network as compared to the uniform cortical actin structure in non-loaded cells [134]. The increased punctate actin structure was also observed in chondrocytes in 3D agarose gels under cyclically compression [135].

Upon the formation of stress fibers, the Rho-associated protein kinase (ROCK) and downstream Rho GTPases are activated. Rho GTPases are important regulators of chondrocyte development and maturation. RhoA, Rac1 and Cdc42 are three most common types of Rho GTPases. In chick chondrocytes, elevated Rac1 expression induced chondrocyte enlargement and MMP13 overexpression [136], while inhibition of Rac1 blocked MMP-13 production [137]. Ren and colleagues [138] showed that periodical mechanical stress field in the range of 0 to 200 kPa at 0.1 Hz elevated Rac1 activities in chondrocytes. RhoA also plays roles in cartilage degradation. A recent OA rodent study showed that cartilage damage was alleviated with the treatment of Rho kinase inhibitor AS1892802 [139]. Using 0.5 Hz unconfined dynamic compression, results showed that loading upregulated iNOS gene expression in a RhoA-dependent

manner, suggesting RhoA may be involved in OA initiation in response to abnormal mechanical stimuli [135].

To transduct mechanical forces to nucleus, the linkers of the nucleoskeleton to the cytoskeleton (LINC) complex is required. The crucial roles of LINC complex has been identified recently. It regulates cell division, cytoskeletal organization, organelle positioning and cell proliferation [140]. The LINC complex physically link the nuclear envelop with the cytoskeleton to transmit physical forces. The LINC complex contains SUN proteins, nesprins, and Klarsicht/ANC-1/Syne homologue (KASH) domain proteins. On the nucleoplasmic side, the SUN domains interact with the lamina; on the cytoplasmatic side, the KASH domains bind to cytoskeleton via nesprins [141]. Although the importance of LINC complexes has been recognized, how mechanical stimuli activate transcriptional genes are not well understood.

1.5 FAK and Src

The further integrin clustering brought with the reorganization of actin cytoskeleton forms focal adhesion complex (FAC). The formation of FAC, containing enzymes and their substrates, accelerates the reaction rate and increases the reaction opportunity (Figure 1.5). FAK is the first molecule that is recruited to the location of forming FAC. Upon activation, it autophosphorylates and create a Src-homology-2 (SH2) binding domain, which allows the binding of Src and Fyn. The newly formed complex of Src-FAK phosphorylates other molecules near FAC [142]. FAK and Src have been found play crucial roles in mechanotransduction in many organs and tissues, including bone, cartilage, heart, lungs, and blood vessels. Additionally, the loading-induced integrin activation leads to the activation of protein kinase C (PKC), which play roles in regulation of MAPK signaling pathways [143],suggesting the possible cross-link between integrin/Src/FAK and MAPK signaling.

1.5.1 FAK and Src as targets for OA treatment

The physiological functions of FAK/Src signaling have been explored. It regulates chondrocytes proliferation, differentiation, apoptosis, mobility, and ECM production [144]. A study found that the silence of FAK by siRNA decreased cell proliferation rate and prevented chondrocyte differentiation [11]; and FAK inhibitor significantly reduced chondrocyte viability [10]. Additionally, FAK and Src can upregulate the gene transcription of MMPs, iNOS and NO. It has been shown that reduced MMP expression has been observed with the treatment of FAK antisense [145,146]; and the treatment of Src inhibitor completely abolished iNOS expression and NO production in chondrocytes [144, 147].

Recent studies showed that integrin/Src signaling plays a major role in MAPK/ERK and Rho GTPases signaling [144, 148]. Blockage of integrin activity downregulates Rho/ROCK gene expression and prevents cytoskeleton formation in chondrocytes [149]; and in FAK knock-out mice, the loss of FAK abolished GTPase Rho regulation by fibronectin [150]. Therefore, a deeper understanding of FAK/Src signaling is important, and can be a potential strategy for OA prevention and treatment.

1.5.2 structure of FAK and Src

FAK consists of three major domains, an N-terminal FERM (band 4.1, ezrin, radixin, moesin homology) domain, a central kinase domain, and a C-terminal domain. The FERM domain localizes FAK to the plasma membrane, facilitates the binding of epidermal growth factor receptor (EGFR) and the platelet-derived growth factor receptor (PDGFR) to FAK, and promotes further activation of FAK by binding to actin- or membrane-associated adaptor proteins. The C-terminal domain contains two proline-rich subunits that are binding sites for SH3 domains. The association of SH3 binding domain and p130Cas is required for the cell migration by activating Rac at membrane. The C-terminal domain also consists a FAT region, which connects FAK to focal adhesions (FAs) by binding to paxillin and talin. And it also bind to

the activator of Rho-family GTPases, including p190 RhoGEF [130]. There are nine members in the Src family, including Src, Lck, Hck, Fyn, Blk, Lyn, Fgr, Yes, and Yrk. All family members share the same SH1, SH2, SH3, and SH4 domains, while at their N-terminus, there are 50-70 residues that are divergent among family members. Src contains a very short C-terminal tail, which contains an autophosphorylation site. At inactive state, the interaction motifs of these domains stay inward and lock the kinase via intramolecular interactions [151].

1.5.3 The interaction between FAK and integrin

The interaction between FAK and integrin was first found from the studies shown that the phosphorylation of FAK was induced by cell attachment to fibronectin or integrin activation by antibodies [152]. A latter study showed that the existence of β cytoplasmic domain of integrin is required for FAK activation mediated by integrins [153], suggesting a very simple model that the FAK directly associate with the cytoplasmic domain of integrins upon activation. Nevertheless, the membrane distal amino acid in the cytoplasmic domain has been found is necessary for integrin-induced FAK activation *in vivo* [152], indicating the first model is too simple to explain FAK-integrin interation. Another model is proposed and suggests that cytoskeleton and cytoskeletal proteins, including talin, paxillin and tesin, transduce the activation of integrin that in turn activate FAK. A study supports the second model showing that the treatment of Cytochalasin D, an actin cytoskeleton inhibitor, abolishes FAK phosphorylation and activation induced by integrin clustering, while calcium is not directly involved in FAK phosphorylation induced by integrin, as to the depletion of calcium using thapsigargin fails to alter FAK activity [154].

1.5.4 The association of FAK and Src

Growth factors as well as the binding of integrins to ECM can activate the FAK phosphorylation. Upon the activation of FAK, the autophosphorylation of Tyr-397

site on FAK generates a binding site for the SH2 domain of Src to form complexes [155]. The binding of Src to FAK activates Src activity by altering the interaction of SH2 domain and C-terminal regulatory tyrosine residue [156]; and additionally prevents dephosphorylation of FAK by cellular tyrosine phosphatases [157]. The activated Src would further phosphorylate FAK on other tyrosine residues (like Tyr-576 and Tyr-577) and create more binding sites for SH2 domains [158]. The C-terminal Src kinase could negatively regulate the activity of FAK/Src complex by releasing Sh2 domain of Src from FAK [159].

1.5.5 TNFα or IL1β-induced FAK/Src signaling

The FAK/Src signaling is essential for TNFα- and IL1β-induced cell motility, survival [160] and inflammatory gene expression [12]. The TNFα-induced MMP production is regulated by FAK and Src activities. FAK-deficient cells exhibited much lower MMP9 secretion as to normal cells, and JNK might be involved in this FAK-mediated MMP regulation [161]. In a mice model, the expression level of TNFα shared a similar pattern to those of MMP2 and MMP9; and the inhibition of FAK and ERK blocked the TNFα-stimulated MMP2 and MMP9 production [162, 163]. It also has been found that the phosphorylation of Src mediated TNFα-induced MMP production through ERK signaling pathway [164]. However, the mechanisms are under debate as to how FAK and Src transduce signals to downstream molecules in inflammatory signaling. A recent finding showed that FAK inhibition significantly prevented TNFα-induced MAPK activation, and subsequently reduced the production of vascular cell adhesion molecule-1 (VCAM-1), which plays important roles in inflammation [165]. Moreover, it has been found that although FAK is essential for MAPK activation, but it is not required for NFκB or JNK activation by TNFα [166]. Interestingly, contradictory results have been shown that FAK regulates TNFα-induced inflammation response via NFκB pathway; and FAK deficiency in fibroblasts abolished TNFα-induced IL6 production by inhibiting NFκB signaling,

but did not affect the activities of MAPKs [167]. Src activation also has been found to be involved in in TNFα-stimulated NFκB signaling by upregulating IKK activity [168]. A recent study demonstrated that TNFα elevated phosphorylation of Src and NFκB, as well as the production of MMP9; and the treatment of Src, MAPK, or JNK1/2 inhibitor abolished TNFα-induced NFκB phosphorylation and translocation. A study using Src-null and FAK-null mouse embryo fibroblasts showed that FAK expression activates IL6 production, while Src expression was inhibitory to IL6 production [166]. This result provides the evidence for a Src-independent FAK signaling pathway. Taken together, cytokine treatment elevates Src/FAK via NFκB, MAPK and ERK signaling pathways [169], leading to elevated MMP expression.

Table 1.5: Chondrocyte intracellular activity in response to mechanical stimulation

Loading type	Model	Effect
Ultrasound	Rabbit	↑ Integrin, MERK1/2, FAK/Src, ERK1/2, PI3K and Akt, ↑ Matrix synthesis, ↓ MMP [14, 170]
Stress	Rat	↑ FAK/Src, MEK1/2, ERK1/2, PI3K and Akt, ↑ Matrix synthesis, ↓ MMP [15, 170]
Ultrasound	Human	↑ FAK/Src, p130 Cas, CrkII and ERK phosphorylation [148]
Cyclic strain	Human	↑ FAK, β-catenin and paxillin [171]
Compression	Bovine	↑ Src and ERK, ↑ Cell spreading and contraction, ↑ MMP [16]

1.5.6 Mechanical loading-induced FAK/Src signaling

Mechanical environment changes and matrix binding initiate integrin-mediated FAK/Src signaling. In chondrocytes, $\alpha5\beta1$ integrin is the prominent integrin, and highly expressed in OA chondrocytes [172]. The attachment of integrins to ECM is essential for integrin signaling. A study found that the phosphorylation levels of

FAK, Pyk2 and ERK were higher in adherent chondrocytes as compared to those in suspended chondrocytes [173].

When chondrocytes are exposed to mechanical stimulus, FAK and Src are first molecules to be concentrated to the newly formed FAC. Table 1.5 lists studies about FAK/Src regulations by mechanical loading. A study demonstrated that the activation of integrin/FAK signaling is essential for ECM production by chondrocytes in response to ultrasound [14]. Another study found the treatment of either integrin or Src inhibitor reduced ultrasound-induced ERK phosphorylation level, which indicates integrins and Src are upstream molecules of ERK [148]. The periodic mechanical stress has been shown could elevate chondrocyte proliferation and matrix synthesis through Src-ERK1/2 signaling cascade [170]. The same group further evaluated the role of FAK in this Src-mediated signaling cascade. They found that the reduction of FAK phosphorylation level attenuated the phosphorylation of ERK1/2 and consequently abolished periodic mechanical stress-induced chondrocyte proliferation and matrix production, but can't affect Src activation [15]. Additionally, it has been found that Src and FAK activities upregulate loading-induced MMP expression [16]. Under mechanical loading, there are two signaling pathways involved in FAK and Src-mediated MMP regulation. Upon FAK autophosphorylation, Src binds to FAK and phosphorylates FAK at Tyr 861 and Tyr 925. The phosphorylation of Tyr 925 leads to the binding of GRB2 to FAK, which activates Ras and the ERK2/MAPK cascade, leading to elevated MMP expression [174]. The second pathways involves in JNK signaling. The Src/FAK complexes phosphorylate p130Cas and paxillin [175], and the phosphorylated p130Cas together with CrkII upregulate the activity of Dock180, a Rac GEF. The elevated Rac activity by Dock180 activates the JNK signaling and ultimately increases MMP2 and MMP9 activities [176]. Although the known importance of FAK/Src in loading- and cytokine-induced cartilage maintenance, whether different loading can differentially regulate Src/FAK and even reverse cytokine-stimulated FAK/Src activation is unknown.

1.5.7 The differential activities of FAK and Src at different microdomains of plasma membranes

The lipid bilayer of the cell plasma membrane contains different subdomains: the regions of plasma membrane that are rich in cholesterol and sphingolipids are termed lipid rafts; and the surrounding regions are termed non-lipid rafts. It has been found that most FAK may translocate to rafts upon cell adhesion [177]; the inhibition of caveolin, a raft protein, blocked the FAK phosphorylation and integrin activation [178]; and the disruption of rafts by MβCD downregulated FAK activities [179]. On the other hand, Src is localized at lipid rafts as well as non-lipid rafts. It has been found that Src concentrates at the non-lipid rafts at resting state, which can be rapidly activated [180, 181]; and the other population of Src is stored in endosomes and can be transported to lipid rafts via actin filaments upon stimulation [17]. Studies suggest that different microdomains of plasma membranes may function distinctly as segregated signaling platforms [182], for example, Akt activities at different microdomains are regulated differentially [183]. The kinetic characteristics of Src [184] and FAK [185] under growth factors are also different in and outside of lipid rafts; and upon thermoactivation, Src at lipid rafts regulates PI3K/Akt signaling, while Src at non-lipid rafts regulate MAPK/ERK pathways [186]. However, it remains unclear how FAK and Src activities in different microdomains respond to cytokine and mechanical stimulations in chondrocytes.

1.5.8 Proline-rich tyrosine kinase 2 (Pyk2)

Pyk2 is highly similar to FAK in sequence (46 % identical and 65 % similar) and structure, but its expression is not as ubiquitous as FAK. Pyk2 is not phosphorylated in epithelial [173], neural [187] and smooth muscle cells [188]; but predominantly expressed in macrophages and osteoclasts [189]. Upon activation, Pyk2 creates a binding site for SH2 domain of Src, resulting in Src activation. Pyk2 shares some functions with FAK [190], for example, in FAK-null fibroblasts, Pyk2 can compensate

FAK activity to promote cell retraction [191]. Pyk2 also performs different functions from FAK: it can impair GAP activity towards Cdc42 [192], but not FAK; FAK is essential for Rho guanine nucleotide exchange factors (GEFs) localization to FA, but not Pyk2 [191]. However, the roles of Pyk2 in chondrocyte activities are not well studied, and how it interacts with FAK and Src under cytokine and mechanical loading is also unknown.

1.6 AMPK signaling in osteoarthritis

In 1987, AMPK was first found as a protein kinase that was activated by the increased amounts of AMP [193]. It is a sensor of cellular energy that maintains the energy balance, both at the cellular level and at the whole body. Once activated by rising ratio of (AMP+ADP)/ATP, AMPK phosphorylates multiple downstream targets to initiate catabolic regulatory pathways that generate ATP, whilst downregulate anabolic signaling and other cellular activities that consume extra ATP [20]. Recent studies indicate that, in addition to balancing energy metabolism, AMPK also coordinates several other mechanisms, such as anti-inflammation and increasing tissue stress resistance. Regarding its potent roles in human health, its dysfunction leads to diverse disorders such as cardiovascular diseases, diabetes, cancer and OA. Widely used drugs like metformin for diabetes II, and salicylates for anti-inflammation are acting to activate AMPK, while its roles in OA is not very well clarified.

1.6.1 The structure of AMPK

AMPK exists throughout eukaryotes as a heterotrimer, consisting of α, β, and γ subunits (Figure 1.6). The layout of all domains of AMPK is well understood. In mammals, two genes code for α (α1, α2), two for β (β1, β2), and three for γ subunits (γ1, γ2, γ3). The phosphorylation of Thr172 on α2 isoform by upstream kinases triggers AMPK activation and are regarded as the sign for AMPK activation [194]. Start from the N-terminal end, the α subunit consists of the catalytic kinase domain

(α-KD), a small auto-inhibitory domain (α-AID), a linker and the α-C-terminal domain (α-CTD) [195]. The catalytic activity of α-KD is compromised by α-AID, and the reorientation of the α-AID contributes to the activation of AMPK. The pivot phosphorylation site, Thr172 is located next to α-CTD. The active conformation of α-CTD is required for the access of phosphatases to Thr172 to activate AMPK activity [196]. The β subunits contain two domains, the carbohydrate-binding module (β-CBM), and the β-CTD. The β-CBM is responsible for the binding of AMPK to glycogen, but its physiological roles are not clear. The γ subunite contains four repeats of cystathionine-β-synthase (CBS) sequence. The second CBS site remains empty, the fourth site binds AMP, and the first and the third sites can bind AMP, ADP or ATP to perform regulatory functions. The binding of AMP to the first site promotes the kinase activity of AMPK, and the binding of AMP or ADP to the third site suppresses Thr172 dephosphorylation [197].

1.6.2 The AMPK-related disease

The importance of AMPK is implicated in many diseases, and its activation is suspected to extend healthspan by reducing risks for atherosclerosis, heart attack, stroke, type II diabetes, overweight, cancers, autoimmunity and cartilage diseases. In addition to several widely used drugs, regular consumption of vinegar, and moderate alcohol ingestion has been found achieve health-protective AMPK activation.

Cardiovascular diseases (CVDs)

CVD includes a class of disease related to heart or blood vessels, and it is the leading cause of death globally. A randomized clinical trial enrolling 156 patients showed that the AMPK activator reduces chronic congestive heart failure [199], and animal studies showed that the activation of AMPK has been shown can reduce risk for heart attack, stroke and congestive failure [200]. Although the downregulation of protein synthesis by AMPK play some roles in CVD prevention, the impact of AMPK

activation on CVDs is prominently due to its ability to activate endothelial nitric-oxide synthase (eNOS). The activation of eNOS preserves the structure and function of the vascular system by increasing the concentration of NO [201]. The AMPK also downregulates the activation of NF-κB and oxidative stress, two factors that contribute to the atherogenesis and thrombosis [202]. However, excessive activation of AMPK in the heart leads to deleterious impact. The heart disease Wolff-Parkinson-White syndrome results from genetic mutation on AMPK genes in 2 isoform. This mutation restricts the binding of ATP, and thus increases basal phosphorylation level of Thr172, which results in constitutive activation of AMPK and over-accumulation of glycogen in cardiomyocytes [203]. Interestingly, a study found that the exercise-induced shear stress stimulates the expression of eNOS via AMPK signaling [204]. This is one of the very rare studies about the impact of physical stimulus on AMPK activities.

Type II diabetes

Type II diabetes, a type of metabolic disorder featured high blood sugar and insulin resistance, affects 29.1 million American in 2012, and costs 550 billion annually. Obesity and lack of exercise are two primary factors contributing to this disease. The number of patients suffered from type II diabetes has boomed markedly since 1960. The insulin resistance is believed strongly associated with obesity, which leads to excessive triacylglycerol in liver and skeletal muscle. In addition to triacylglycerol, the increased level of diacylglycerol appears to downregualte the insulin-signaling pathway by activating protein kinase C in muscle as well as in liver [205]. Treatments to activate AMPK pathways are expected to prevent lipid accumulation in liver and muscle by enhancing the degradation and inhibiting the synthesis of fat [206]. AICAR mimics the activating effects of AMP on AMPK and reverses obesity and insulin resistance in animal models [207, 208]; A-769662, a direct AMPK activator, increases the oxidation of fat and decreases body weight in rats [209]; metformin, a drug to

treat type II diabetes, also highly activates AMPK [210]. Although AIRCAR regulate AMPK activity indirectly, studies have confirmed their therapeutic effects on insulin resistance and weight control are indeed mediated by AMPK [211].

Cancer

Types of cancer have been found related to AMPK signaling, including breast, prostate, and colorectal cancer [212]. The downregulation of AMPK-α2 has been found in hepatocellular carcinoma [213]. The most important link between AMPK and cancer can be liver protein kinase B1 (LKB1), a classical tumor suppressor, which is located at the upstream of AMPK. Peutz-Jeghers patients with the mutations that lack of LKB1 activity are tend to develop malignant cancers [214]; and the mutations in LKB1 gene are common in patients with cancer: up to 30 % of lung cancers, 20 % of cervical cancers, and 10 % of melanomas [215]. Although other AMPK-related kinases are also regulated by LKB1, AMPK is the most pivot kinase because of its ability to inhibit mTORC1. mTORC1 regulates various biosynthetic pathways to enhance proliferation and inhibit apoptosis, leading to accumulation of mutations and survival of pre-cancerous stem cells [216]. Drugs to activate AMPK activities, such as metformin, phenformin, and A-769662 have been shown delayed the onset of tumor in tumor-prone mice [217]. Moreover, diabetic patients on metformin had lower incidence of cancer than those taking other medications [218].

Inflammatory disorders

Inflammatory disorders arise when inflammation mistakenly destroys healthy tissue of the body, resulting in fever, rash, joint swelling, and potential fatal build up of blood proteins in vital organs. AMPK has anti-inflammatory effects by attenuating the production of inflammatory cytokines, and preventing the activation of immune cells, including dendritic cells, neutrophils and T cell [219]. At inactive state, immune cells utilized mainly oxidative metabolism; while upon activation, they tend to use

aerobic glycolysis instead, and this process is inhibited by AMPK activation [220]. The AMPK-β1-deficient mice have suppressed fatty acid oxidation that consequently increases the content of pro-inflammatory diacylglycerols. A-769662 has been found an increase fatty acid oxidation [221]. AMPK activator, metformin, berberine, and AICAR, can effectively prevent sclerosis and colitis in murine models [222–224], and some of these inhibitory effects are stem from the inhibited activity of NF-κB. Salicylate, the natural product, promotes fatty acid oxidation by activating AMPK activity [225].

Neurodegenerative disorders

Neurodegeneration occurs when the structure or function of neurons is impaired. In US, Alzheimers disease affects 5.4 million people, Parkinsons disease affects half million, and Huntingtons disease affects 30 thousand people. These diseases are irreversible and incurable, therefore, the prevention of neurodegeneration is crucial. AMPK activation promotes autophagy, a crucial process to maintain healthy neurons [226], suggesting preventive roles of AMPK in neurodegeneration. Additionally, inflammation is suspected to contribute to this neurodegeneration. A study found that AMPK activator suppressed inflammation on cultured microglia [227]. AMPK activation has been shown to aid Alzheimers prevention by suppressing the expression of BACE1 protease, which is required for the accumulation of extracellular amyloid-β [228]. The possibility of developing dementia is reduced by 25 % in diabetic patients on metformin as compared to those not taking medications [229].

Osteoarthritis

It has been discovered that the AMPK activity is highly activated in normal chondrocytes and cartilage, while its activity is suppressed in OA chondrocytes, injured chondrocytes, and cytokine-treated chondrocytes [21]. The AMPK activator attenuates catabolic pathways, and this response declines during ageing [230]. The LKB1

is involved in the regulation of AMPK activity in chondrocytes. The silence of LKB1 activity enhances catabolic responses of chondrocytes to cytokine treatment [231]. The NAD+-dependent protein deacetylase silent information regulator 1 (SIRT1) is a downstream mediator of AMPK regulating chondrocyte metabolism. Activation of SIRT1 upregulates ECM production and inhibits chondrocyte apoptosis [232], and the inhibition of SIRT1 enhances chondrocyte responses to cytokines [233]. Using mice models, the knockout or the mutation of SIRT1 promotes OA progression [234]. Moreover, a positive feedback loop about SIRT1, LKB1 and AMPK has been discovered. Activation of AMPK enhances the activity of SIRT1 by upregulating intracellular NAD+, and the activated SIRT1 deacetylates and activates LKB1 that eventually further promotes AMPK activation [230]. Recent studies found that AMPK activator notably suppress the IL-1 and TNFα-induced catabolic response of chondrocytes, including the elevated production level of MMP-3, MMP-13, and NO [21, 235].

1.6.3 The signaling properties of AMPK

What is the mechanism of AMPK activation? The AMPK signaling is switched on by ATP depletion, and plays critical roles in maintaining the homeostasis of cellular energy. The adenylate kinase reaction of 2ADP$\leftrightarrow$ATP + AMP is tightly controlled to maintain equilibrium in most eukaryotic cells. In normal cells, the ratio of ATP : ADP at 10 : 1 drives the adenylate kinase reaction to produce ADP and to maintain the AMP at a low level. However, in stressed cells, the ATP : ADP ratio reduces by driving the reaction towards AMP. Because the AMP basal concentration starts at a very low level, the AMP concentration becomes a sensitive indicator of metabolic stress. The activation of AMPK signaling promotes catabolic pathways to produce more ATP, and simultaneously inhibits anabolic activities that consume ATP.

The initiation of AMPK activity

The complex containing the LKB1, a tumor-suppressor gene, is the principal upstream kinase that phosphorylates Thr172 of AMPK [194, 236], and this is the first evidence linked AMPK with cancer. The binding of AMP to AMPK promotes the phosphorylation of Thr172 by LKB1 and inhibits the dephosphorylation by protein phosphatase even in the presence of physiological concentration of ATP [237]. In addition to LKB1, with the rise of intracellular Ca^{2+}, which often indicate cellular stress, Ca^{2+}/calmodulin-dependent kinase kinases (CaMKKs) further activates Thr172, which is an alternate pathway to activate AMPK in the absence of changes in AMP levels. This CaMKKs-mediated AMPK activation occurs in many cells. The TAK1 and ataxia telangiectasia mutated (ATM) are also identified as upstream kinases of AMPK, however, the physiological roles of these two kinases in regulating AMPK phosphorylation are not well understood, and require further studies. For instance, the TAK1 is involved in AMPK activation by tumor necrosis factor, but not that induced by TNF or IL1β, suggesting TAK1 might partially regulate the activation of AMPK [238].

The downstream of AMPK signaling

Researches have revealed several signaling pathways involved in AMPK signaling, and many of them aid the regulation of autophagy and oxidative stress. CRTC-1, a cytoplasmic co-activator of CREB, is a phosphorylation target located at the downstream of AMPK. The phosphorylation of CRTC-1 by AMPK prevents its nuclear translocation and inhibits CRTC-CREB pathway, and consequently extends the lifespan of C. elegans [239]. AMPK mediates caloric restriction- and heat stress-induced CRTC inhibition, while its roles in some hormones-or phytochemicals-induced CRTC inhibition needs to be clarified.

SIRT1, an enzyme that deacetylates proteins, regulates cellular energy metabolism and cell survival. The AMPK activation elevates the intracellular concentration of

NAD+, which further stimulate the SIRT1 activity. SIRT1 has the ability to induce mitochondrial biogenesis by activating PGC-1α, and it is capable to potentiate its owns activity by promoting the expression of Nampt that increases NAD+ [240]. Interestingly, SIRT1 has been found to deacetylate LKB1 kinase, which consequently stimulates the activation of AMPK. This positive feedback loop can potentiate AMPK [241].

Forehead transcription factors (FoxOs) are involved in crucial cellular functions. AMPK phosphorylates FoxO3, and further promotes the resistance of cells to oxidative stress. The constitutively active AMPK extends the lifespan of C. elegans [242]. The AMPK-FoxO3 pathway are integrated with other signaling pathways. FoxO3 is capable to inhibit NF-κB signaling by elevating the expression of inhibitory kappaB genes. IKKα and IKKβ, upstream kinases of NF-κB, can phosphorylate FoxO3 and initiate the degradation of FoxO3 [243]. Increased NF-κB activities are closely associated with chronic inflammation. Both *in vivo* and *in vitro* data showed that the activation of AMPK inhibits the activity of NF-κB. Metformin, an AMPK activator, inhibits NF-κB signaling and alleviates inflammation in endothelial cells [244].

The mechanistic target of rapamycin (mTOR) is widely involved in regulatory signaling induced by cytokines, excessive nutrients and energy, and is known to inhibit autophagy. Two mechanisms underlying how AMPK inhibits mTOR complex have been revealed, either by directly phosphorylating the Raptor, or by phosphorylating the tuberous sclerosis protein 2 (TSC2) that can inhibit mTOR. In the first mechanism, the phosphorylation of the Raptor component by AMPK triggers the dissociation of mTORC1 from the ULK1 complex, which is required for the formation of autophagosome. AMPK also has been found can directly binding to the ULK1 complex and activate autophagy [245]. However, the phosphorylation sites in the ULK1 by AMPK havent been identified yet.

AMPK can phosphorylate the Rab-GTPase activator protein (Rab-GAP) TBC1D1 to accelerate glucose uptake. TBC1D1 is essential to insulin-mediated glucose uptake in muscle cells. It binds to the glucose transporter GLUT4, and maintains the Rab

family of small G proteins in their inactive state. The phosphorylation of TBC1D1 by AMPK alters its Rab-GAP activity, which promotes trafficking of the GLUT-4 vesicles to the plasma membrane and leads to the increase of glucose uptake [246].

Malonyl-CoA is critical for fatty acid synthesis, and also inhibits fatty acid uptake by mitochondria. The reduced amount of malonyl-CoA inhibits fatty acid synthesis and promotes fatty acid oxidation [247]. AMPK phosphorylates acetyl-CoA carboxylase that lowers the concentration of malonyl-CoA. A single injection of AICAR significantly activates AMPK activity, which subsequently suppresses malonyl-CoA activity and upregulates insulin-stimulated glucose uptake in muscle 24 h after injection [208].

1.6.4 The dark side of AMPK

While AMPK activation has been demonstrated act as a protective response to various stresses, accumulating evidences indicate that excessive AMPK activity in cancer cells can have deleterious effects. The silence of AMPK using siRNA diminishes the growth of LNCaP, an androgen-sensitive prostate adenocarcinoma cell line [248]. The knockdown of AMPK in pancreatic cancer cells diminishes their ability of resistance to glucose starvation [249]. In tumor cells with low pH, upregulated-AMPK activity increases glucose consumption, resulting in the induction of oxygen-sparing phenotypes [250]. More evidences support that AMPK activation is a strategy used by tumor cells to adapt to nutrient-deprived and hypoxic tumor microenvironments [251–253]. The pro-tumorigenic ability of AMPK is also linked with Src signaling, which will be described in details in the next section.

1.6.5 AMPK and integrin/Src/FAK

The proton beam irradiation inhibits the gene expression of β1integrin, FAK, Src, and MAPK, and simultaneously, increases the phosphorylation of AMPK to inhibit cell adhesion and spreading [254], and the mutation of integrin and the silence of β3

integrin prevents tumor formation in liver [255], while the direct link between integrin and AMPK is not clearly clarified in these studies. Emerging data indicates that activation of integrin is required for the phosphorylation of AMPK. The neutralization of β1 integrin using anti-integrin antibody completely reversed CCNI-stimulated AMPK activation in endothelial cells. CCNI is known to highly express in cancer cells and to promote angiogenesis in endothelial cells [256]. Interestingly, it has been found that the activation of AMPK reduces the expression of β1 integrin and inhibits the phosphorylation of β1 integrin signaling targets in colon cancer cells [257]; the treatment of A-769662, an AMPK activator, reduces the abundance of β1-integrin on cell surface [258]. These data suggest a negative loop between AMPK and integrin that tightly controls and prevents its excessive activation. However, the adiponectin-stimulated integrin activation is inhibited by the inhibitor and mutant of AMPK [259]; and the AMPKα2 is required for the phosphorylation of β3 integrin [260]. This discrepancy in integrin activity in responses to AMPK might attributable to differences in certain genetic traits among different cell line that used in researches. Additionally, evidence supports a role of AMPK activity in integrin-related signaling. The expression of integrin-linked kinase (ILK), an adaptor connecting integrin to cytoskeleton, is regulated via AMPK-mediated signaling [261].

Regarding the pivot roles of Src in cancer progression, emerging evidences revealed the interaction between AMPK and Src in cancer development. AMPK activation has been demonstrated as the result of c-Src activation independent of AMP level human papillomavirus (HPV)-transformed cells [262], and the same group found that the activation of c-Src signals through LKB1 to AMPK is the hallmark of cancer cell transformation [263]. And the inhibition of Src activity abolished AMPK phosphorylation in breast cancer cells [264]. Fyn, another member of Src family kinase, has been found increases AMPK activity by upregulating the expression of LKB1 [265]. Additionally, the Src has been found mediate AMPK signaling in aortic endothelial cells [266] and tubular epithelia cells [267]. Several studies showed contradictory results indicating AMPK regulates the phosphorylation of Src: it is required for the

phosphorylation of Src family kinase, Fyn [260]; Src is activated by metformin in a AMPK-dependent manner [268]; and the inhibition of AMPK by selective AMPK inhibitor, compound C, impairs Src activity [269]. The interplay between AMPK and Src is still unclear, and requires further studies.

Very few studies about FAK and AMPK have been performed. Mulberry have been identified to inhibit the migration of vascular smooth muscle cells by two distinct pathways: AMPK-mediated and FAK-mediated, while crosslink between these two signaling is not clear [270].

1.6.6 The AMPK activities at various subcellular compartments

AMPK regulate various cellular functions, one solution to perform multi-task within the different cellular spaces is compartmentalization. It has been known that several environmental factors stimulate AMPK travels between the nucleus and cytosol. After heat shock or oxidant exposure, AMPK translocate from cytosol to nuclei with the assistance of nuclear exporter Crm1, and this shuttling behavior is abolished in high-density cell culture, for which AMPK is only exist in cytoplasm [271]. AMPK containing different units has been found in different compartments. AMPK with $\alpha 2\beta 1$ is confined in cytoplasm, while upon the stimulation of fatty acid oxidation, $\alpha 2\beta 2$ is capable to rapidly translocate to the nucleus [272]. In addition to nucleus and cytoplasm, several studies revealed that in response to stress, AMPK could accumulate near plasma membrane [273, 274], mitotic apparatus [275], and the basal bodies of primary cilia [276]. To visualize the dynamic activities of AMPK at various subcellular microdomains without cell lysis, the FRET-based AMPK biosensors with modifications to target specific compartments have been developed. In 2011, Tsou and colleagues successfully designed Cyto-AMPK and Nuc-AMPK to monitor the AMPK activities in cytoplasm and nuclei, correspondingly [277]. Recently, a series of AMPK biosensors that can target ER, mitochondria, Golgi apparatus, plasma membrane and lysosome have been developed with improved specificity, gaining insights

into the dynamic signaling activities at subcellular levels with high spatiotemporal precision [278]. Thus, we employed these biosensors to evaluate the activities of AMPK in response to mechanical or chemical stimulations and their interaction with integrin/FAK/Src signaling at different compartments.

1.7 3D culture alters cellular cues

The direct effects of mechanical loads on intracellular signaling that lead to progression of OA cannot be investigated over time in patients, so numerous studies were performed based on *in vivo*, *ex vivo* and *in vitro* models.

In living animal experiments, application of mechanical loading generates strain within the whole matrix, and impacts cells via natural cell-matrix connections. With the development of various genetic modified mice, it becomes possible to correlate changes in cartilage structure with specific molecule activities in chondrocytes. While *in vivo* studies provide valuable data, it shows drawbacks, including the uncontrolled parameters within the whole animal, the variability among animals, and the raised ethical and economical issues. Experiments using *ex vivo* cartilage explants have been shown to be able to maintain cell 3D morphology, provide native ECM, and simplify the complexities of *in vivo* experiments. Results suggest that cells in the explant exhibit similar loading-induced cellular responses to those measured *in vivo* [279]. *in vitro* monolayer cell culture is a highly simplified experiment model widely used in cell-based studies. However, the flat and hard plastic or glass surfaces fail to allow cells to keep their physiological morphology and native interactions with ECM and other cells [280]. Many cell types, including chondrocytes that isolated from tissues become excessively flatter, function aberrantly, and lose their phenotype when placed on 2D substrates [281, 282]. To narrow the gap between 2D cell culture and *in vivo* studies, 3D cell culture has been developed to mimic *in vivo* 3D environments and is regarded as an appealing approach to improve the traditional *in vitro* cell culture

model [280]. It has been shown that cultured cells in 3D culture could maintain some tissue-specific phenotypes [22].

The 3D culture can be categorized into two culture systems, scaffold-free or scaffold-based. In the scaffold-free system, cell spheroids generate their own ECM, and has been shown to promote cell survival and maintenance of stem cell phenotype [283]. This spheroid system is highly popular in cancer and stem cell studies, however, due to the lack of standardized procedures to produce uniform and consistent spheroids, the scaffold-free system cant be widely used in drug development. In the scaffold-base system, scaffolds can made of a wide range of natural or synthetic materials to extend the options available to researchers. Several cell types have been found can regain their physiological morphology and cellular function when seeded in 3D scaffolds: encapsulation of dedifferentiated chondrocytes in agarose gels regains their spherical morphology and phenotype [284]; dedifferentiated mammary epithelial cells redifferentiate when maintained on floating collagen membranes [285]. Several microenvironmental cues that presented in 3D versus cultures are known to affect cell function.

1.7.1 Cell adhesion, Cell morphology and cytoskeleton

All animal cells are in constant close contact with the surrounding ECM and neighboring cells. Studying biological processes on flat, 2D plastic or glass substrates does not consider the importance of natural 3D environment on cellular functions. Cells in 2D and 3D are very different in morphology (Figure 1.7). Cells grown on 2D substrates are flat and spreading one the plate due to no support for spreading in the vertical dimension. One consequence of this is that monolayer cells have an artificial lower and upper surface polarity. This polarity is required to functions of some cell types, such as epithelial cells, but for most of other cell types, like chondrocytes, the 2D substrate failed to provide the microenvironment that cells experience *in vivo* [287]. This apical-basal polarity directly impact cell function by increasing the

resistance to apoptosis [288]. Beyond this forced polarity, the flattening cells growing on 2D substrates can better respond to stimulations as a result of increased exposure of membrane receptors to the activators (increase the surface-to-volume ratio) [289]. Contradictory to 2D monolayer culture, cells growing in 3D culture systems form aggregates or spheroids within the matrix, and maintain their spherical morphology that resembles its natural shape *in vivo*. The formation of aggregates also allows cell-cell interactions and cell-ECM interactions, such that cells embedded in 3D culture can closely emulate the cellular processes in the body [290].

The organization, composition and the number of adhesions are important for tissue phenotype, tissue mechanical stability, tissue repair, cell motility, proliferation, differentiation, morphogenesis, and intra/intercellular signaling [291]. For the *in vitro* studies, cells are isolated from native cell-cell and cell-ECM interactions, and are placed into a artificial enviroment that provided by substrates. The 2D culture system provides adhesions to the ECM on one face of the cell, while the 3D model allows adhesions all around the cell surface [292]. This variation could result in the different cellular responses in 2D versus 3D culture. However, how adhesions in varying culture models impact cell signaling and function remains unclear.

The importance of cytoskeleton in 2D cell culture has been well established. However, different from that in 2D model, cells *in vivo* as well as in 3D gel culture, having much less dense actin stress fibers. And the organization of microtubular cytoskeleton is also distinct in different culture models [293]. As to the cytoskeletal networks in 3D matrix are very different to cells on 2D culture, how the differential cytoskeletal organization, in turn, influence cell signaling and function can be topics to be examined.

1.7.2 Materials for 3D scaffold-based cell culture

The 2D culture usually grows cells on glass or tissue culture plastic dishes, while 3D cultures utilize different methods to support cells in 3D, including forced-floating,

hanging drop, agitation-based approaches, matrices and scaffolds, and microfluidic cell culture platforms (Figure 1.8) [294]. Scaffold-based 3D cultures are most widely used and can be produced by mixing a cell suspension with a liquid matrix followed by cross-linking of the network [295]. The cross-linking process can be regulated by temperature, pH, chelating agents, and the exposure to ultraviolet light [296]. Hydrogels are popular scaffolds for 3D cell culture due to their high water content (>90 %), macroporous structure, controlled shapes and sizes, and the wide range of chemical/mechanical properties for various applications [297]. Synthetic materials have well-controlled chemical composition and tunable degradability, while naturally derived materials are biocompatible and are capable to provide cell adhesion sites. Natural biomaterials includes collagen, fibrin, HA, agarose, are of particular interest to researchers thanks to their generally good biocompatibility, and low toxicity [298].

Collagen

Collagen is a type of elongated fibril that plays crucial roles in most connective tissues. The highly organized 3D collagen network is required for the integrity of ECM and is undergoing constant dynamic remodeling. It is a widely used natural component in tissue engineering. The three most common types of collagen are: Type I (skin, tendon and bone), Type II (cartilage), Type III (blood vessel walls). Type II collagen is the most abundant collagen in articular cartilage. Findings showed that small type II collagen fibers with diameter of <10 nm widely exist in all three zones; larger fibers with diameter of ∼34 nm are organized parallel to the surface and only exist in superficial zone; fibers with diameter of 70-100 nm distribute in the middle zone; and fibers with diameter of ∼140 nm are only exist in the deep zone [299]. Glutaradehyde (GA) is commonly used to crosslink collagens to prevent contraction of matrices during cell growth, but its existence leads to cytotoxicity [300]. The advantages and disadvantages of collagen crosslinking techniques have been extensively examined [301]. The cross-linked collagen is more resistant to deformation

and flow than that was not crosslinked. Many studies of cell activities show that the existence of collagen alters cell migration, attachment, adhesion and differentiation [302].

Alginate

Alginates are linear anionic polysaccharides consisting of β-D-mannuronic acid and C5-epimer α-L-guluronic acid. It is extracted from the cell walls of brown algae, and will form a viscous gum when bind with water. Although the production process will significantly affect properties of alginate, well-processed alginates with high purity are capable to maintained consistent mechanical properties for cell growing. Alginate has been used to maintain various types of cells for its ability to provide physiological conditions, easy dissolution to harvest cells, transparency for imaging, and porous structure that allows diffusion [303].

Chitosan

Chitosan is a linear polysaccharide made of β-linked D-glucosamine and N-acetyl-D-glucosamine, and has molecular weight ranged from 300 kD to 1000 kD. It is produced by treating shells of shrimp with the alkali. It is soluble in organic acids and can be easily accessed in chemical reactions. The physical and chemical properties of chitosan are highly dependent on the number of protonated amino groups in the polymer chain, and are controlled different process conditions. These features make it an attractive option for wide applications in researches [304].

Agarose gel for chondrocyte studies

Synthetic and natural polymers, such as polyethylene glycol, alginate, and agarose, are allowing the creation of 3D models [305]. The agarose gel has been extensively used in cartilage study for maintaining long-term chondrocyte suspension cultures.

It is able to mimic the nature of cartilage tissue as to high water content and the presence of pores where offer a gentle and cyto-compatible condition for chondrocytes. Numerous studies demonstrated that agarose is capable to maintain the chondrocyte phenotypes [99, 306–309] and improve ECM synthesis [310, 311]. Moreover, agarose provides a similar load-support mechanism as articular cartilage [312, 313]. These properties of agarose enable the investigation of the response of chondrocytes to chemical and mechanical stimulus.

1.8 FRET based biosensors

Live cell imaging using FRET-based biosensors becomes increasingly appealing due to its high spatial and temporal resolution in visualizing dynamic intracellular molecular activities in live cells [314]. Two different types of FRET-based biosensors are available in terms of their design strategies, intramolecular and intermolecular FRET biosensors. Intramolecular FRET-based biosensors are advantageous in live cell imaging because they allow the use of simple ratiometric imaging approach to monitor and analyze FRET changes [315]. They are constructed by fusing donor and acceptor fluorescent proteins (FPs) to interacting molecules, for example, a FRET-based Cyto-Src biosensor consists of a cyan fluorescent protein (CFP), a SH2 binding domain, a Src substrate peptide, and a yellow fluorescent protein (YFP) (Fig. 1.9a). When the Src substrate does not bind to SH2 (inactive state), the cyan excitation (at 433nm) gives yellow emission (at 530nm). Upon phosphorylation of Src substrate, the intramolecular binding of the Src to the SH2 domain leads to a conformational change of the biosensor, which abolishes the strong FRET from CFP to YFP (Figure 1.9b). Thus, by monitoring the changes in FRET between CFP and YFP, we can measure the Src activities [184]. Biosensors targeting different subcellular microdomains also have been developed. To observe the FAK and Src activities at lipid raft regions, the Lyn-FAK and Lyn-Src were constructed by fusing myristoylation and palmitoylation sites derived from Lyn at the N-terminus of the Cyto-Src and Cyto-FAK biosensors; and

the KRas-Src and KRas-FAK were constructed by attaching polybasic-geranylgeranyl to the C-terminus of the Cyto-Src and Cyto-FAK biosensors [17, 185].

Similar to the structure of Cyto-Src, cytosolic AMPK (Cyto-AMPK) biosensor consists of the ECFP, an FHA1 domain, an AMPK substrate motif, and Venus cpV E172. To specifically bind to different subcellular locations, different sequences are fused to Cyto-AMPK: plasma membrane (PM-AMPK), Golgi apparatus (Golgi-AMPK), endoplasmic reticulum (ER-AMPK), nucleus (Nuc-AMPK) and mitochondria (Mito-AMPK). The phosphorylation of the AMPK substrate will lead to the binding of FHA1 substrate to the binding domain, resulting in the fluorescence resonance transfer from the donor (ECFP) to the acceptor (YFP variant Venus). Hence, AMPK activities can be visualized as changes of the emission ratio of the YFP/CFP. The specificity of the biosensors has been characterized thoroughly in earlier studies [278, 316].

With the similar strategy, other biosensors such as RhoA [317], Ras [318], Rac1, Cdc42 [319] GTPases, Ca^{2+} [320], proteases [321], cyclic adenosine monophosphate (cAMP) [322], phosphor-lipids [323], integrin [324] have been developed. FRET-based biosensors can be used as a powerful tool in visualizing the spatiotemporal activation map in live cells under cytokines and mechanical loading.

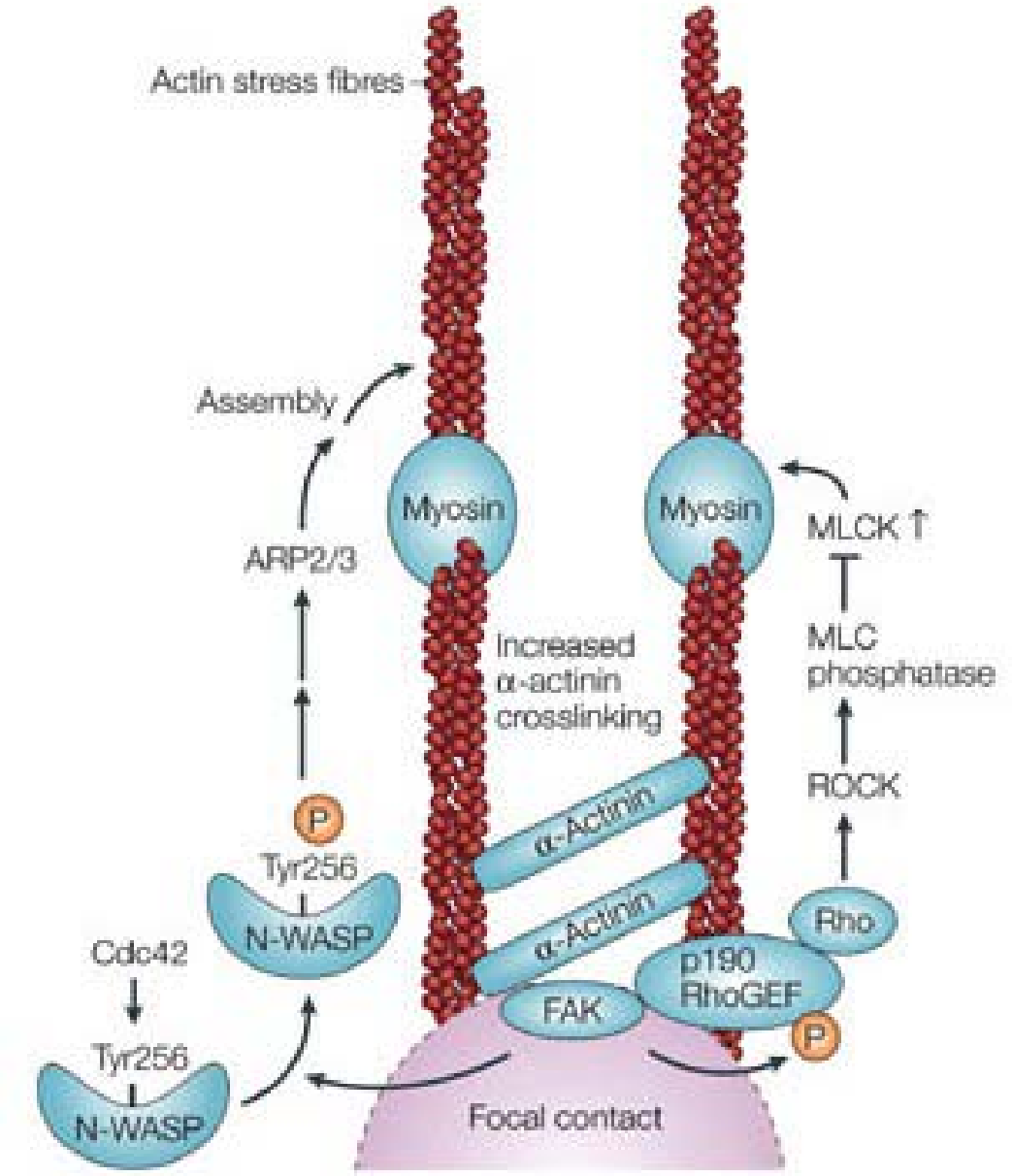

Fig. 1.5.: A schematic showing FAK interact with integrin at focal adhesion sites. The binding of integrins to ECM stimulates integrin-binding proteins, like paxillin and talin, to recruit FAK and vinculin to the focal adhesion sites. The complex binds to actin cytoskeletal filaments and is mediated in the transduction of physical stimulus. The focal adhesion is a dynamic structure and is undergoing constantly remodeling in response to external stimulation [130].

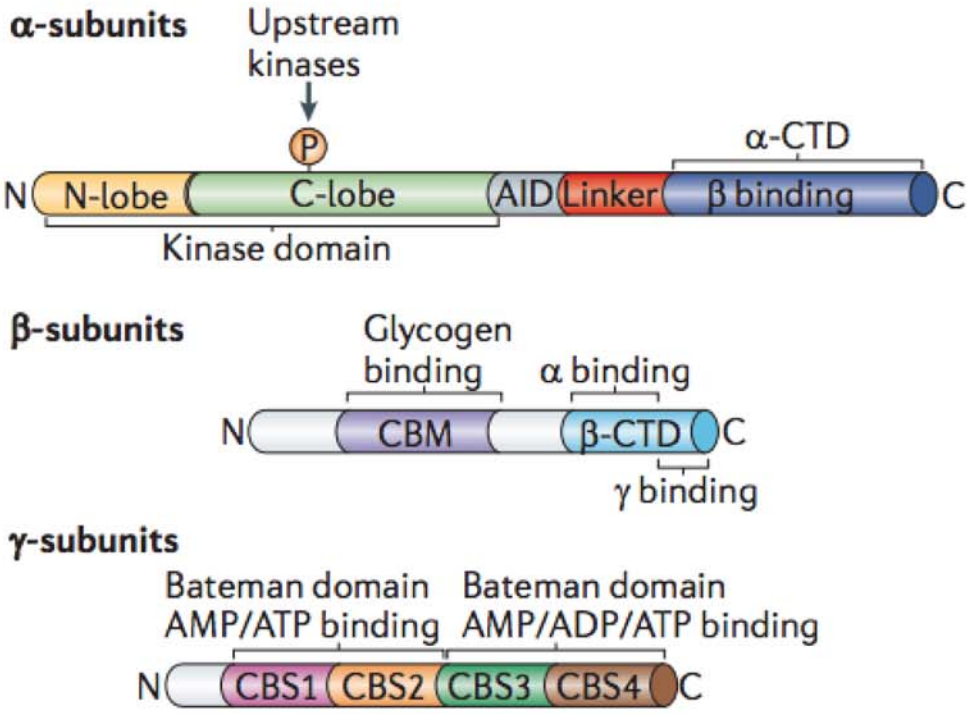

Fig. 1.6.: A schematic showing AMPK structure. AMPK consists of α, β, and γ subunits. The α-CTD binds to the β domain, and the β-CTD binds to the γ domain [198].

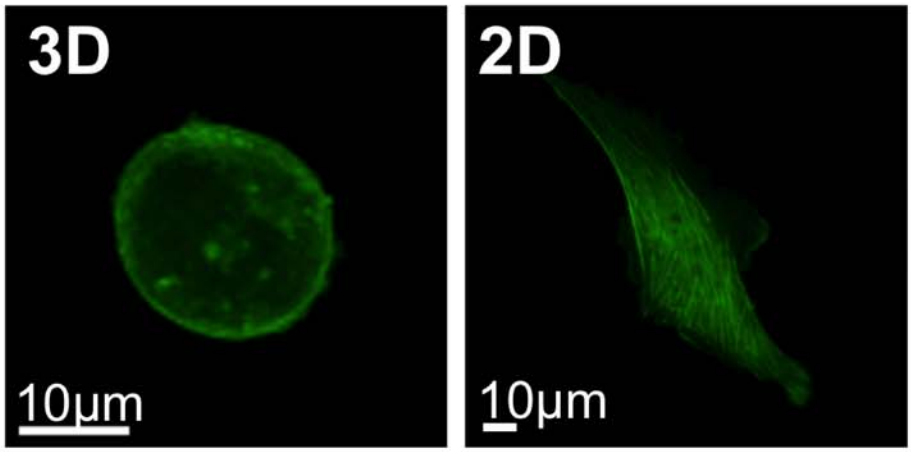

Fig. 1.7.: The differential cell morphology and actin cytoskeleton structure in 3D versus in 2D. The chondrocytes were cultured in a 3D agarose construct or on a 2D culture dish. The cell in 3D is spherical and shows bright actin dots; while the cell in 2D culture is well spreading and develops strong actin fibrils across through the cell. As compared to the cell in 2D, the cell growing in 3D matrix is much smaller, and shows more physiological-relevant cell morphology.

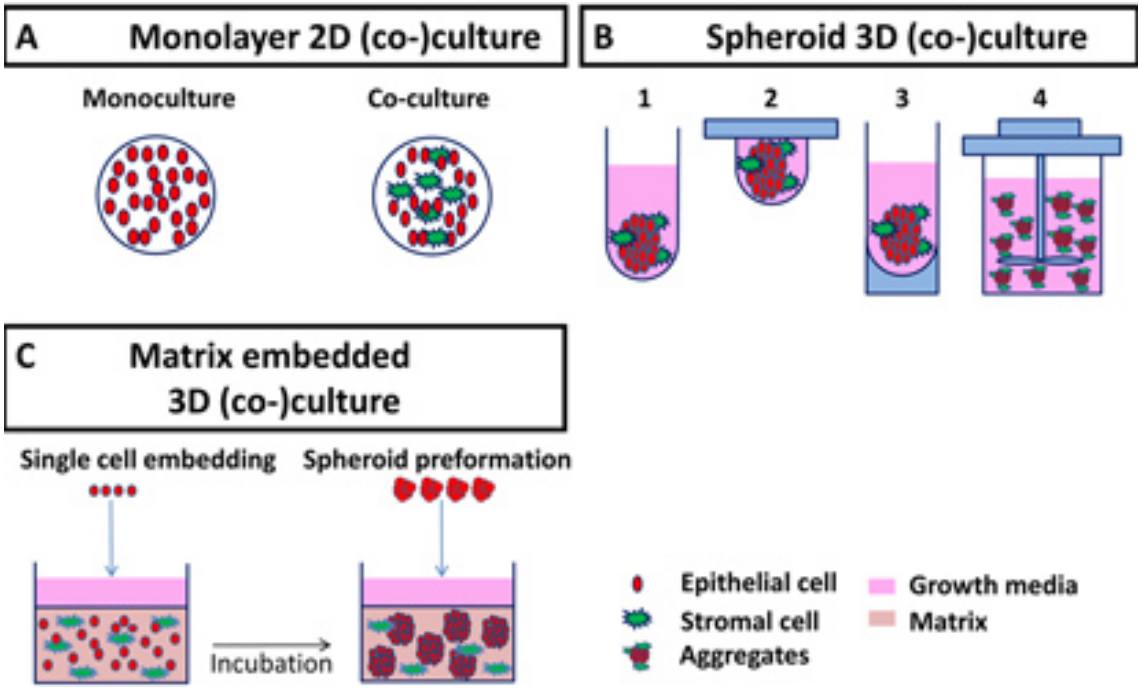

Fig. 1.8.: 2D versus 3D culture models [286]. (A) The 2D monolayer culture or co-culture on flat and rigid substrates. (B) The forced floating spheroid culture on nonadhesive surfaces. (C) The 3D scaffolds culture in 3D matrix.

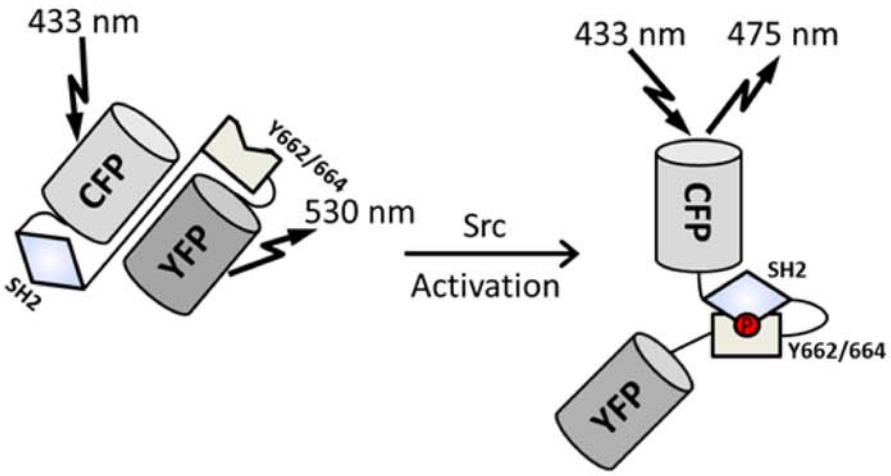

(a) The structure of a Src biosensor

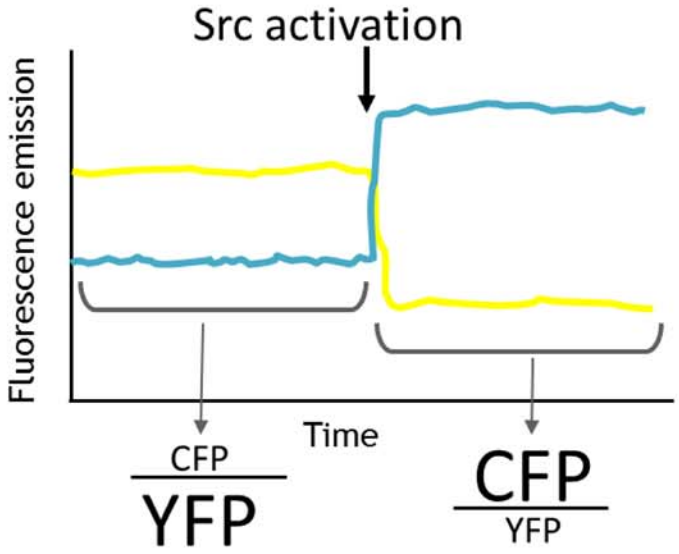

(b) The fluorescence emission curves showing Src activation

Fig. 1.9.: A FRET-based Cyto-Src biosensor. (A) The structure of Cyto-Src biosensor, which consists of CFP, SH2 binding domain, Src phosphorylation site, and YFP. At inactive state, CFP is close to YFP, while upon activation, the binding of SH2 domain to substrate apart CFP from YFP. (B) A Curve showing the emission ratio value of CFP and YFP intensity before and after Src activation.

2. DISTINCTIVE SUBCELLULAR INHIBITION OF CYTOKINE-INDUCED SRC BY SALUBRINAL AND FLUID FLOW

2.1 Introduction

In healthy cartilage, chondrocytes play an essential role in maintaining the balance between anabolism and catabolism. However, injurious loading and excessive secretion of cytokines lead to ECM degradation [16, 162, 163]. TNFα and IL1β contribute to cartilage matrix degradation by increasing activities of proteolytic enzymes, including MMPs and ADAMTS [37]. Moreover, these cytokines inhibit the production of proteoglycans and type II collagen [47]. Therefore, blocking the action of these cytokines is a potential strategy to prevent cartilage degradation. Besides proinflammatory cytokines, excessive mechanical loading is another factor that contributes to OA progression [101]. However, physiological mechanical loading is capable to promote cartilage homeostasis [87]. Application of gentle loading has been shown to inhibit IL1-induced matrix degradation as well as expression of MMPs and ADAMTS [96]. In addition of moderate loading, the reduction of ER stress using salubrinal, a chemical agent, has been shown inhibits TNFα- and IL1β-induced MMP activities by inhibiting eIF2α phosphorylation [115]. Src activities are known to be involved in ECM regulation by chondrocytes, and play critical roles in mechanotransduction and inflammatory signaling [144, 145]. Recent reports indicate that they can be activated at different subcellular locations [17, 185]. Although studies about how Src activities regulate downstream signaling cascades in response to inflammatory cytokines and loading have improved our understanding of the role of Src in OA progression, little is known about whether the site-specific activities of Src are differentially regulated by mechanical loading or cytokines; whether their activities are loading magnitude

dependent; whether mechanical loading suppresses cytokine-induced signaling activities. To visualize Src activities at different subcellular locations, two FRET-based Src biosensors were used: Lyn-Src FRET biosensor targeting lipid rafts and Cyto-Src FRET biosensor existing around cell membrane.

2.2 Materials and methods

2.2.1 Src and FAK biosensors

FRET-based, cyan fluorescent protein (CFP)-yellow fluorescent protein (YFP) biosensors were used for monitoring Src and FAK activities in the cytosol (Cyto-Src), lipid rafts of the plasma membrane (Lyn-Src and Lyn-FAK), and non-lipid rafts of the membrane (KRas-Src and KRas-FAK). The Cyto-Src biosensor consists of CFP, a binding domain of an effector protein (SH2 domain), a truncated Src substrate peptide and YFP. The lipid rafts-targeted Src and FAK biosensors were produced by fusing acylation substrate sequences derived from Lyn kinase to the N-terminal of Cyto-Src and Cyto-FAK biosensors, respectively. The non-lipid rafts-targeted Src and FAK were produced by attaching polybasic-geranylgeranyl to the C-terminus of the Cyto-Src and Cyto-FAK biosensors, respectively. The activation promotes the intramolecular binding of the SH2 domain to the truncated Src or FAK domain within the biosensor, which leads to a conformational change of the biosensor and the decrease of FRET efficiency from CFP to YFP. Hence, Src and FAK activities can be visualized as changes of the emission ratio of the CFP/YFP. The specificity of the biosensors has been well characterized previously [17, 18, 184].

2.2.2 Chemical reagents and siRNAs

Two types of proinflammatory cytokines, TNFα (Sigma; 10 ng/ml) and IL1β (Sigma; 1 ng/ml), were used. Salubrinal and guanabenz (both from Tocris Bioscience), inhibitors of eIF2α phosphatase, were used to test the effect of phosphoryla-

tion of eIF2α on Src activity. We also used Pyk2 siRNA (Santa Cruz), eIF2α siRNA and non-specific control (NC) siRNA (Origene). Cytochalasin D (Sigma; 1 μg/ml) was used to disrupt actin filaments. Methyl-beta-cyclodextrin (MβCD; Sigma; 10 mM) was used to extract cholesterol from the lipid rafts of the plasma membrane. PP2 (Sigma; 10 μM) was used to block Src activities, and PF228 (Sigma; 1 μM) was used to inhibit FAK activities. The 3D agarose gels were produced by using SAPHAPHA (Sigma) to conjugate agarose gel (Sigma) with Type I collagen (Sigma).

2.2.3 Cell culture, transfection, and western blotting

The human chondrocyte cell line C28/I2 was used. Cells were cultured in Dulbecco's modified Eagle's medium (DMEM; Lonza) containing 10 % FBS (Hyclone) and 1 % penicillin/streptomycin (Lonza), and maintained at 37 °C and 5 % CO_2 in a humidified incubator. Neon transfection system (Invitrogen) was used to transfect Src biosensors into the cells. After transfection, the cells were transferred to a type II collagen-coated glass bottom dish or μ-slide cell culture chamber (Ibidi) and incubated in serum-free, antibiotic-free DMEM for 2436 h before imaging experiments. For Western blotting, cells were grown in the presence and absence of salubrinal or guanabenz and lysed in a radioimmunoprecipitation assay (RIPA) buffer. Isolated proteins were fractionated using 10 % SDS gels and electro-transferred to Immobilon-P membranes. The membrane was incubated for 1 h with primary antibodies followed by 45 min incubation with secondary antibodies conjugated with horseradish peroxidase (Cell Signaling). We used antibodies against eIF2α (Cell Signaling), phosphorylated eIF2α (p-eIF2α; Thermo), and β-actin (Sigma). Signal intensities were quantified with a luminescent image analyzer (LAS-3000, Fujifilm).

2.2.4 Shear stress application

Fluid flow-induced shear stress has been shown to play a crucial role in the development and progression of osteoarthritis. During imaging, a unidirectional flow

was applied to the cells grown in the -slide cell culture chamber (Ibidi) at 37 °C. The chamber was perfused with HEPES-buffered (20 mM), phenol red-free DMEM without serum to maintain the pH at 7.4. Because the shear stress of 2 to 10 dynes/cm^2 has been shown to affect chondrocyte signaling and metabolism either positively or negatively, we used this flow range in this study. The shear stress was applied to the cells by controlling the flow rate of a peristaltic pump (Cole-Parmer). A pulse dampener (Cole-Parmer) was used to minimize pulsation of the flow due to the pump.

2.2.5 3D agarose-chondrocytes constructs

The collagen-coupled agarose gels were prepared as stated before [325]. The collagen solution was reacted with 10-fold molar excess of the sulfo-SANPAH in PBS at room temperature for 4 h in the dark room to produce 1.2 mg/ml collagen solution. The 4 % agarose solution was prepared using sterile PBS, autoclaved, and cooled to 40 °C. Three parts of 4 % agarose solution were combined with one part of collagen-sulfo-SANPAH solution to yield the mixture 3 % agarose and 0.3 mg/ml collagen. The mixture was exposed under UV light for 20 min to allow the activation of the photoreactive groups of the sulfo-SANPAH, and conjugate the collagen to CH groups in the agarose. After conjugation, the agarose mixture cooled down and washed with 10-folds excess sterile PBS for five times over 3 days to remove the unbound collagen and sulfo-SANPAH. Collagen + agarose gels were prepared as described previously but without addition of the sulfo-SANPAH. Agarose gels were prepared without addition of collagen and sulfo-SANPAH. Before transfection, 3 % modified agarose gels were melted at 45 °C and cooled to 37 °C. Two parts of 3 % agarose gel were mixed with one part of 3 × DMEM to produce the mixture of 2 % agarose and 0.2 mg/ml collagen. Transfected chondrocytes were suspended in the 2 % agarose-collagen gel; and the mixture was injected into a flow chamber. The cell-gel construct was cooled at room temperature for 30 min to allow gelling, and then the gel was supplemented with fresh DMEM and transferred to incubator for 24 hours before imaging.

2.2.6 Bovine cartilage explant culture and transfection

The stifle joints from bovine were received from local slaughterhouse. The skin and synovial membrane were removed to expose cartilage surface. During this process, the exposed cartilage surface should be constantly rinsed with sterile PBS. Thin cartilage slice were harvested by scalpelling the outer layer of cartilage and washed five times with PBS. The clean explants were cultured in 24 well plates with DMEM medium (supplemented with 10 % serum and 1 % antibiotics) and incubated overnight. The *in vivo*-jet PEI (Polyplus) was used to transfect chondrocytes in cartilage explant with Src and FAK biosensors following manufactures manual. 12 hours after transfection, explants were mixed with 2 % agarose-collagen gels supplemented with DMEM. The explant-agarose constructs were incubated overnight before imaging.

2.2.7 Microscopy and image analysis

Images were obtained by using a Nikon Ti-E inverted microscope equipped with an electron-multiplying charge-coupled device (EMCCD) camera (Evolve 512; Photometrics), a filter wheel controller (Sutter Instruments), and a Perfect Focus System (Nikon) that maintains the focus during time-lapse imaging. The following filter sets (Semrock) were used: CFP excitation: 438/24 (center wavelength/bandwidth in nm); CFP emission (483/32); YFP (FRET) emission: 542/27. To minimize photobleaching, cells were illuminated with a 100 W Hg lamp through an ND64 ($\sim$1.5 % transmittance) neutral density filter. Time-lapse images were acquired at intervals of 2 min with a 40 $\times$ (0.75 numerical aperture) objective. FRET images for Src activity were generated with NIS-Elements software (Nikon) by computing an emission ratio of CFP/YFP for individual cells over time. The FRET ratio images were scaled according to the color bar. To quantify the kinetics of the FRET responses of Src biosensors, the discrete time derivatives of the emission ratios, Y, were calculated and the associated curves were fitted using the Gaussian functions: $Y = A \cdot exp[-0.5 \cdot ((t-\mu)/\sigma)2]$. The parameter A represents the maximal rate of FRET ratio change upon stimu-

lation, μ the time point where the rate of FRET ratio change reaches the maximal value, and σ the duration of the rate of FRET ratio change. The rate of FRET ratio change in response to cytokines was assumed to follow a Gaussian distribution. This assumption was tested by the D'Agostino-Pearson (omnibus K2) normality test.

2.2.8 Statistical analysis

Statistical data are presented as the mean ± standard error of the mean (SEM). One-way ANOVA followed by Dunnett's post hoc test was used to determine the statistical differences. Student's t-test was used to compare two groups. Statistical analyses were conducted using Prism 5 software (GraphPad Software). $p<0.05$ was considered significant. In the time course data, * indicates the time point after which the Src activity becomes significantly different from that at 0 min.

2.3 Results

2.3.1 2.3.1 Activation of Src at different subcellular locations by TNFα and IL1β

To determine whether the cytokines would differently affect Cyto-Src in the cytosol and Lyn-Src in the lipid rafts of the plasma membrane, we transfected either Cyto-Src or Lyn-Src biosensor into C28/I2 cells and plated the cells on a type I collagen-coated glass bottom dish. The spatiotemporal activities of Src in the cells were assessed by monitoring changes in the emission ratio of CFP/YFP of the biosensors [184, 326]. Cells were imaged for 10 min without treatment, and then were imaged for 2 hours with TNFα (10 ng/ml) or IL1β (1 ng/ml). Cyto-Src activities were increased by the treatment of TNFα or IL1β and reached a maximal at 90 min by TNFα (10.0 %) and at 80 min by IL1β (7.1 %). Its activities after 10 min of the cytokine treatment were significantly different from those at time 0, and the activation level was maintained for 2 hours (Figure 5.1A). Lyn-Src activities were also activated by TNFα or IL1β

application, while they showed a slower increase than that of Cyto-Src (Figure 5.1B). The FRET ratio increased and reached the peak value at 120 min by TNFα (10.2 %) and at 110 min by IL1β (11.6 %). The Lyn-Src activities after 50 min of the cytokine treatment were significantly different from those at time 0. We also observed that cytokine induced Lyn-Src activities were initially decreased (Figure 5.1B). However, the decreased Src activity following cytokine application was not significantly different from that at 0 min.

Since the temporal profiles of Cyto-Src and Lyn-Src activities were different, we further determined the kinetics and magnitudes of the FRET response of Src biosensors. $t_{\frac{1}{2}}$ is the amount of time required for Src to reach the half-maximal activity level. Notably, the mean and standard deviation of $t_{\frac{1}{2}}$ values of Cyto-Src (TNFα: $t_{\frac{1}{2}}$ = 16.25$\pm$2.63 min; IL1β: $t_{\frac{1}{2}}$ = 22.22$\pm$6.24 min) were significantly lower than those of Lyn-Src (TNFα: $t_{\frac{1}{2}}$ = 53.33$\pm$5.87 min; IL1β: $t_{\frac{1}{2}}$ = 53.33$\pm$3.23 min) (Figure 5.2A). To evaluate a rate of activation changes in response to TNFα and IL1β, we computed time derivatives of activation levels and the estimated rate was fitted to a Gaussian function. Based on the DAostino-Perason (omnibus K2) normality test, the p values for all experimental conditions were higher than the cut-off value, 0.05, indicating that the data follow a Gaussian distribution. In the fitting curve, the rate of the changes in Cyto-Src activity reached the maximal value earlier than that in Lyn-Src (Figure 5.2B). Compared to Lyn-Src, Cyto-Src activities showed significantly lower mean time parameters in the Gaussian curves (Cyto-Src + TNFα: 17.59 $\pm$ 2.51; Cyto-Src + IL1β: 20.02 $\pm$ 7.78; Lyn-Src + TNFα: 60.11 $\pm$ 3.87; Lyn-Src + IL1β: 63.19 $\pm$ 4.37). However, differences in the level and duration of Src activation were not statistically significant (Figure 5.2C-D).

Study has shown that activation of Src is associated with its translocation to the plasma membrane via the actin cytoskeleton [327]. To determine the roles of the actin cytoskeleton and lipid rafts in these differential Src activation at different microdomains by cytokines, cells were pretreated with Cytochalasin D (CytoD) for 1 h to disrupt the actin cytoskeleton or with MβCD for 1 h to extract cholesterol

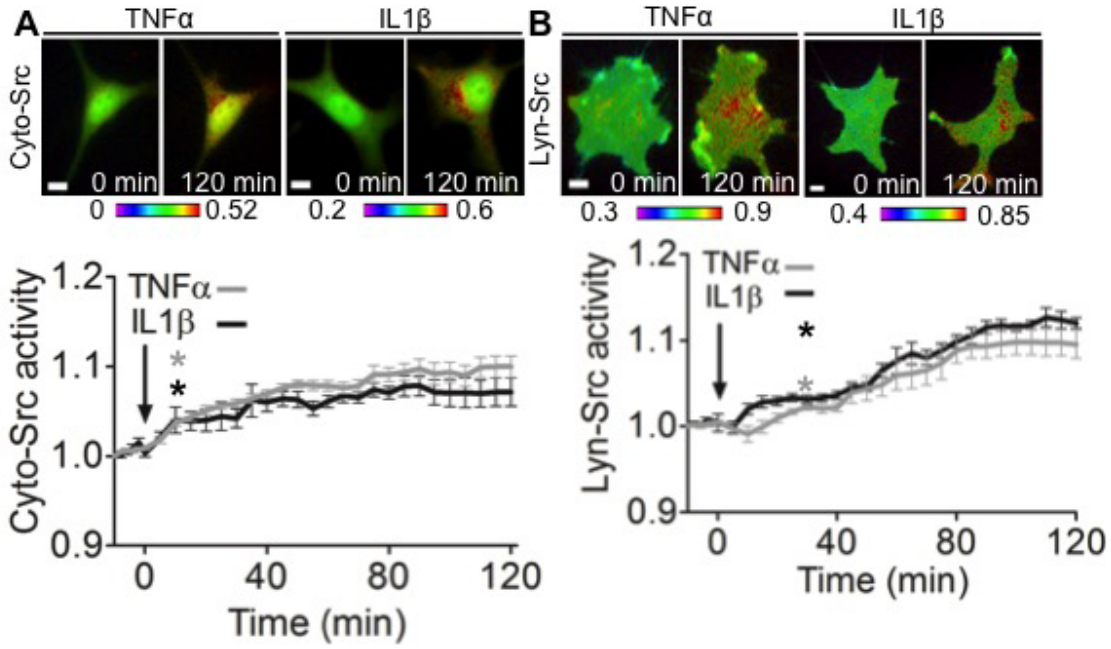

Fig. 2.1.: TNFα and IL1β activate both Cyto-Src and Lyn-Src. The FRET ratio images and time courses of Src activities under fluid flow. Color bars represent emission ratio of CFP/YFP of the biosensor, an index of Cyto-Src activation. The FRET ratio images were scaled according to the corresponding color bar. For each time-lapse imaging experiment, the images from the same cell were taken. The CFP/YFP emission ratios were averaged over the whole cell and were normalized to time 0. (A,B) The FRET ratio images and time courses of Cyto-Src activities (A) and Lyn-Src activities (B) under treatment with TNFα (grey) and IL1β (black). N=8 (TNFα), 9 (IL1β) cells in (A); 6 (TNFα), 9 (IL1β) cells in (B). Scale bars, 10 μm. * p<0.05.

from the plasma membrane. CytoD partially blocked Cyto-Src activation, and it completely inhibited Lyn-Src activation (Figure 2.2E). MβCD reduced both Cyto-Src and Lyn-Src activations, although to a lesser degree to Cyto-Src. Collectively, these data suggest that the actin cytoskeleton and lipid rafts are essential components for cytokine-induced Lyn-Src activation (Figure 2.2A-E).

2.3.2 Magnitude-dependent regulation of Lyn-Src by fluid flow

To determine the effect of fluid flow on Src activities in chondrocytes, cells transfected with either Lyn-Src or Cyto-Src biosensor were plated on flow chamber. During imaging, the cells were subjected to no flow for 10 min, and then flow-induced shear stress at 2, 5, or 10 dyne/cm^2 for 1 h. Lyn-Src was responsive to fluid flow in a magnitude-dependent manner (Figure 2.3B). In response to shear stress at 5 dyne/cm^2, a rapid Lyn-Src inhibition occurred (9.7 % decrease). In contrast, shear stress at 10 dyne/cm^2 led to marked Lyn-Src activation (14.9 % increase). However, Cyto-Src activity was not altered under flow induced shear stress in all magnitudes (Figure 2.3A). These differential activity patterns and time-courses of Src by shear stress suggest that mechanotransduction mechanisms for Src activities might be different depending on the magnitude of the applied loading and compartmental localization of Src.

To further explore the potential contribution of eIF2α in Src activity in response to shear stress, cells cotransfected with Src biosensor and either eIF2α or NC siRNA were subjected to 10 dyne/cm^2 shear stress for 1 h. Cyto-Src in C28/I2 cells transfected with eIF2α or NC siRNA failed to respond to shear stress (Fig. 2.4C). The cells transfected with eIF2α siRNA showed Lyn-Src activation (3.9 % FRET increase) in a less degree than that of NC siRNA treated cells (9.6 % FRET increase) (Fig. 2.4D). These results demonstrate that eIF2α siRNA partially prevents the activation of Lyn-Src in response to 10 dyne/cm^2 shear stress.

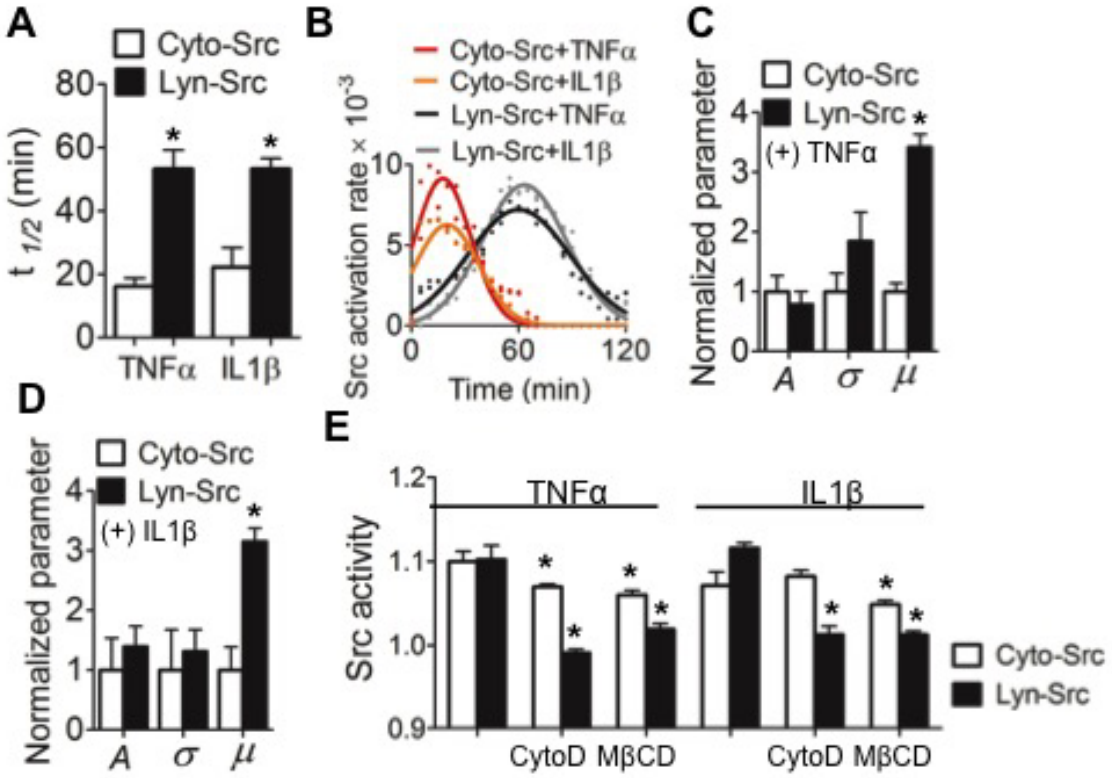

Fig. 2.2.: Differential dynamics of Cyto-Src and Lyn-Src activation by TNFα and IL1β. (A) The $t_{\frac{1}{2}}$ values of Src response to TNFα and IL1β. * p<0.05 between Cyto-Src and Lyn-Src. (B) Gaussian function curves determined by curve fitting of the rate of mean FRET changes over time under cytokine treatment. (C, D) The parameter A represents maximal velocity, μ represents the time point that reach the maximal velocity, and σ represents reaction duration for Lyn- or Cyto-Src. The normalized values of A, μ, and σ for Cyto-Src and Lyn-Src activities that were calculated by parameter fitting in cells under treatment with TNFα (C) or IL1β (D). n>6 cells. * p<0.05 between Cyto-Src and Lyn-Src. (E) The response of Src activities to cytokines in cells pretreated with CytoD (1 μg/ml, 1 h) to disrupt actin filaments or MβCD (10 mM, 1 h) to extract cholesterol from the plasma membrane. The Src activities at 2 hours after cytokine treatment were normalized to time 0. n>9 cells. * p<0.05 compared to the group treated with a corresponding cytokine alone.

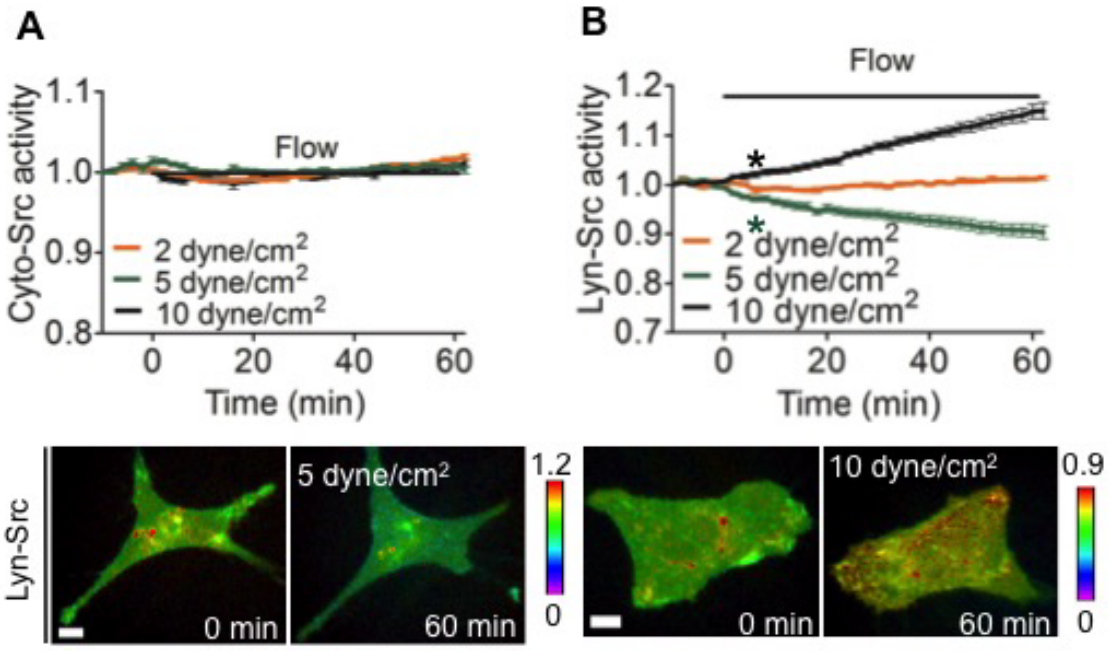

Fig. 2.3.: Fluid flow induces magnitude-dependent Lyn-Src activities. (A) Cyto-Src activity is not altered by fluid flow. n>7 cells. (B) Selective Lyn-Src activities in response to different magnitudes of fluid flow. n>7 cells. Scale bars, 10 μm. * $p<0.05$.

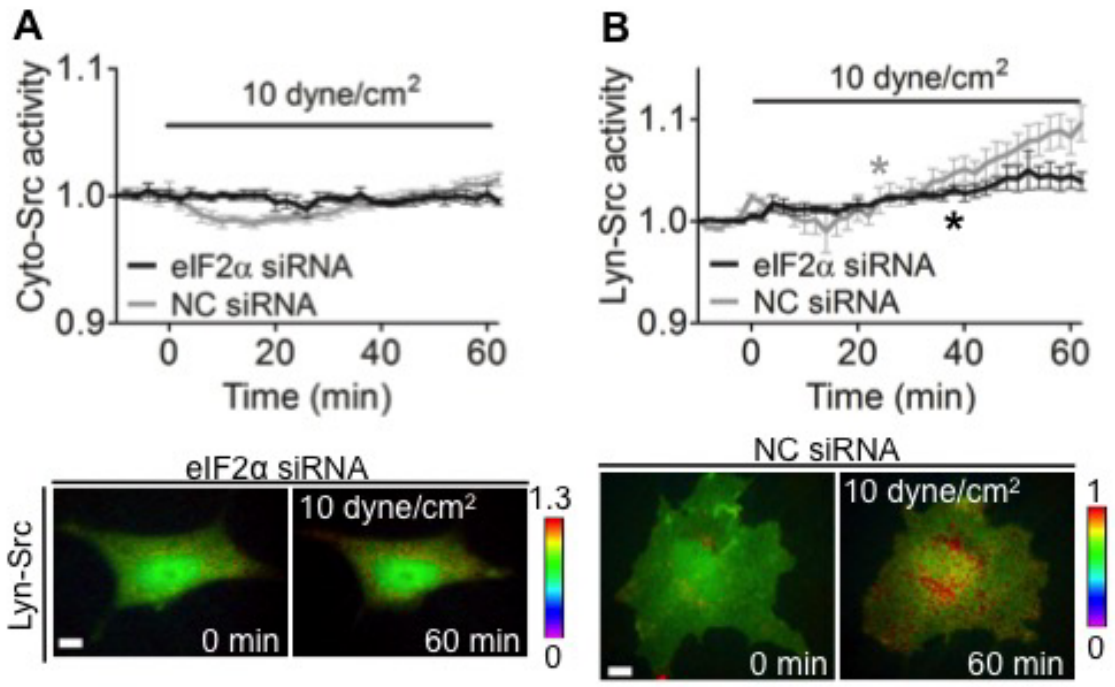

Fig. 2.4.: eIF2α is partially involved in fluid flow-induced Lyn-Src activation. C28/I2 cells were cotransfected with either Lyn-Src or Cyto-Src biosensor and eIF2α or NC siRNA, and then subjected to fluid flow (10 dynes/cm^2) during FRET imaging. (A) Cyto-Src with siRNA under fluid flow. n>7 cells. (B) Lyn-Src with siRNA under fluid flow. n>7 cells. * p<0.05.

To observe the inhibitory effect of fluid flow at 5 dyne/cm^2 on Lyn-Src activities, we pretreated cells with IL1β or TNFα for 2 h before the application of fluid flow. Shear stress at 5 dyne/cm^2 substantially reduced the activation level of cytokine-induced Lyn-Src activities (TNFα: 10.1 % decrease at 60 min; IL1β: 6.5 % decrease at 60 min) (Fig. 2.5A).

2.3.3 The inhibitory effect of salubrinal and guanabenz on Cyto-Src

Western blotting revealed that incubation with 10 μM salubrinal and 10 μM guanabenz elevated the phosphorylation level of eIF2α by 40 $\pm$ 9 % and 29 $\pm$ 19

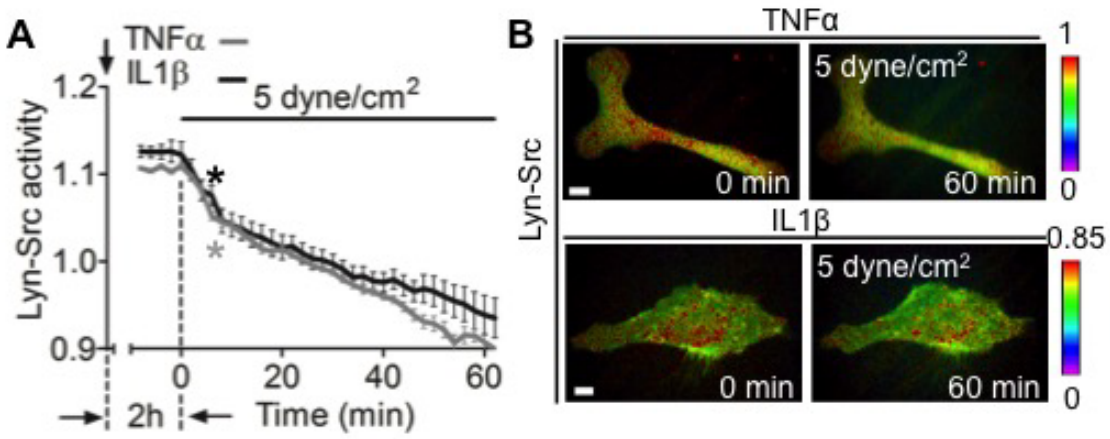

Fig. 2.5.: Lyn-Src activity in cytokine-treated cells under fluid flow (5 dynes/cm^2). Cells transfected with a Lyn-Src biosensor were pretreated with cytokines for 2 hour before FRET imaging. n>7 cells. Scale bars, 10 μm.* p<0.05.

%, respectively (Figure 5.6A,B). Salubrinal decreased Cyto-Src activity in a dose-dependent manner (Figure 2.6C). Although a lower concentration (1 and 2 μM) did not detectably alter Cyto-Src activity, salubrinal at 5, 10, and 20 μM significantly decreased it (5 μM: 10.9 %; 10 μM: 10.0 %; and 20 μM: 11.7 % after 60 min). Guanabenz at 10 and 20 μM also decreased Cyto-Src activity, while lower concentrations did not affect it (10 μM: 9.7 %; 20 μM: 10.1 % at 60 min). In contrast to Cyto-Src that was inhibited by the application of salubrinal or guanabenz, Lyn-Src activity was not altered by either salubrinal or guanabenz (Figure 2.6D), suggesting that salubrinal and guanabenz may differentially affect Src activity depending on the compartmental location of Src within the cell.

The treatment of salubrinal and guanabenz is known to increase phosphorylation of eIF2α (as shown in Figure 2.6A, B) [114, 328]. To further examine whether the inhibition of Src by salubrinal is associated with eIF2α, we cotransfected C28/I2 cells with either eIF2α or negative control (NC) siRNA and Src biosensor. The FRET changes of the transfected cells were visualized under 10 M salubrinal. Silencing eIF2α by siRNA abolished the inhibitory effect of salubrinal on Cyto-Src as compared to the NC siRNA (Figure 2.7A). Salubrinal did not alter Lyn-Src activity in C28/I2 cells cotransfected with the eIF2α or NC siRNA (Figure 2.7). Moreover, we measured the basal level of Src activity before salubrinal treatment. Bar graph demonstrated that the silencing of eIF2α significantly decreased the basal level of Cyto-Src activity ($* \ p < 0.01$), but not the basal level of Lyn-Src activity as compared to the negative control siRNA treated cells (Fig. 2.7C).

We further investigated the effect of salubrinal and guanabenz on Src activities in C28I2 cells that were pretreated with IL1β or TNFα. C28/I2 cells incubated with one of the cytokines for 2 hours before the application of salubrinal or guanabenz. Both salubrinal and guanabenz substantially reduced cytokine-induced Cyto-Src activities (Figure 2.8A). After 6 min of drug application, Cyto-Src activities are statistically significant different from those at 0 min. However, salubrinal and guanabenz failed to inhibit Lyn-Src activation (Figure 2.8B).

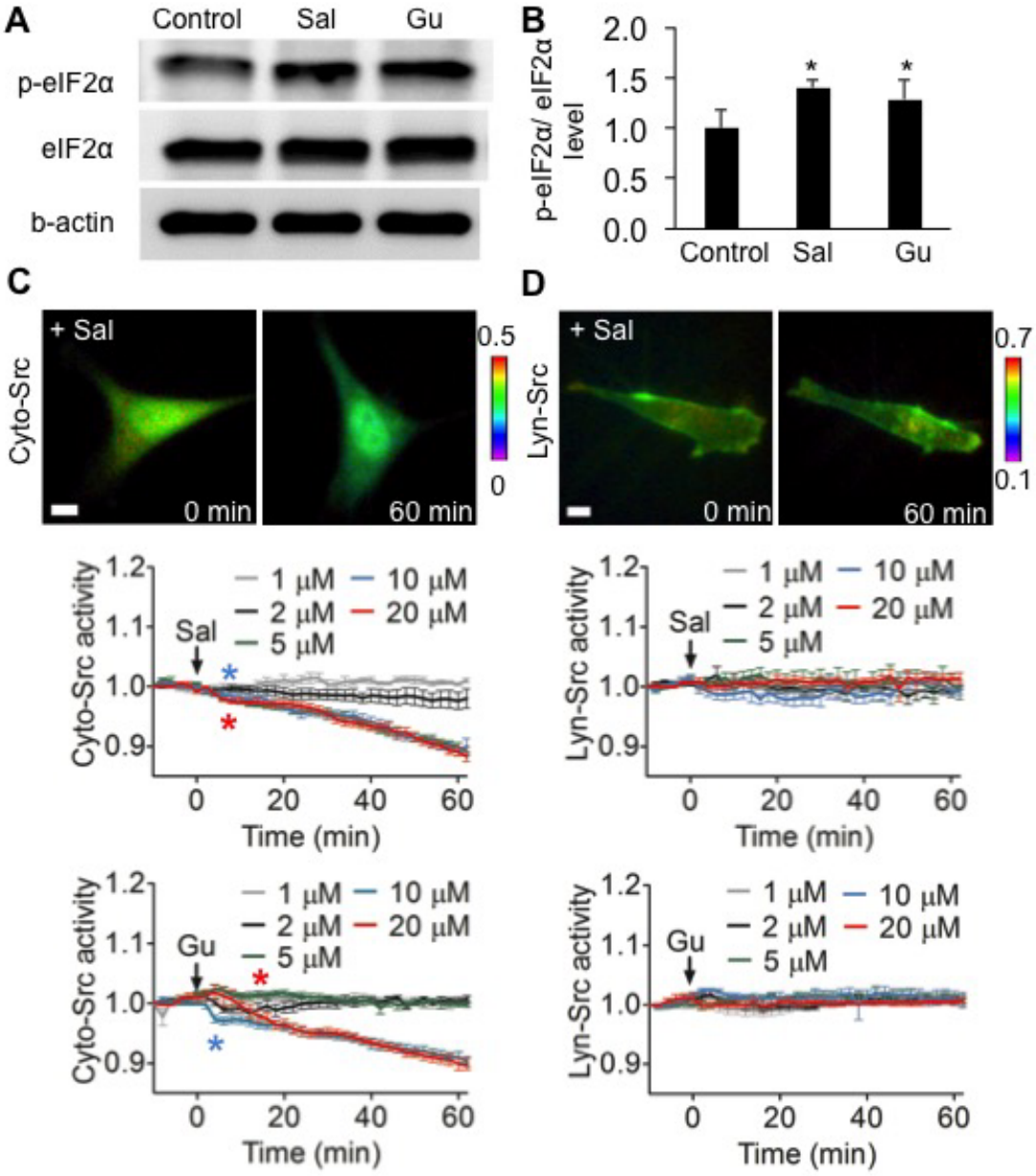

Fig. 2.6.: Salubrinal (Sal) and guanabenz (Gu) increase phosphorylation of eIF2α and decrease Cyto-Src activities. (A) Western blots showing the elevated level of p-eIF2α by salubrinal and guanabenz. (B) Staining intensity of p-eIF2α, normalized by intensity of eIF2α. (C) Cyto-Src activity by salubrinal and guanabenz. (D) Lyn-Src activity by salubrinal and guanabenz. Scale bars, 10 μm. n>7 cells. * p<0.05.

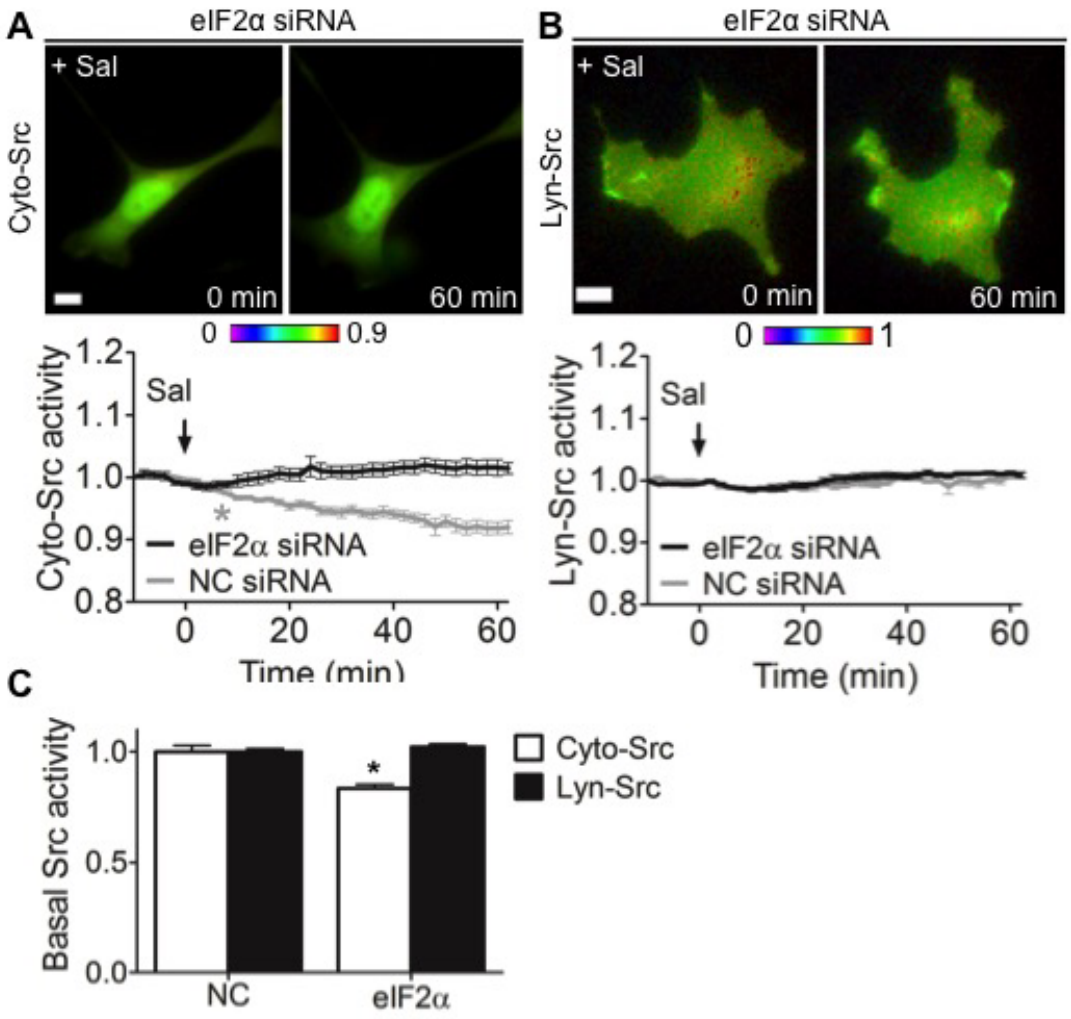

Fig. 2.7.: Involvement of eIF2α in salubrinal-driven Cyto-Src activity. C28/I2 cells were cotransfected with Cyto-Src or Lyn-Src biosensor, and eIF2α or NC siRNA, and then treated with 10 μM salubrinal for 1 hour during imaging. (A) eIF2α siRNA blocks inhibitory effect of salubrinal on Cyto-Src activity. (B) Lyn-Src activity is not altered by eIF2α siRNA. Scale bars, 10 μm. n>7 cells. (C) The basal level of Src activity in C28/I2 cells expressing NC or eIF2α siRNA. n>7 cells. * p<0.05 compared to the corresponding NC group.

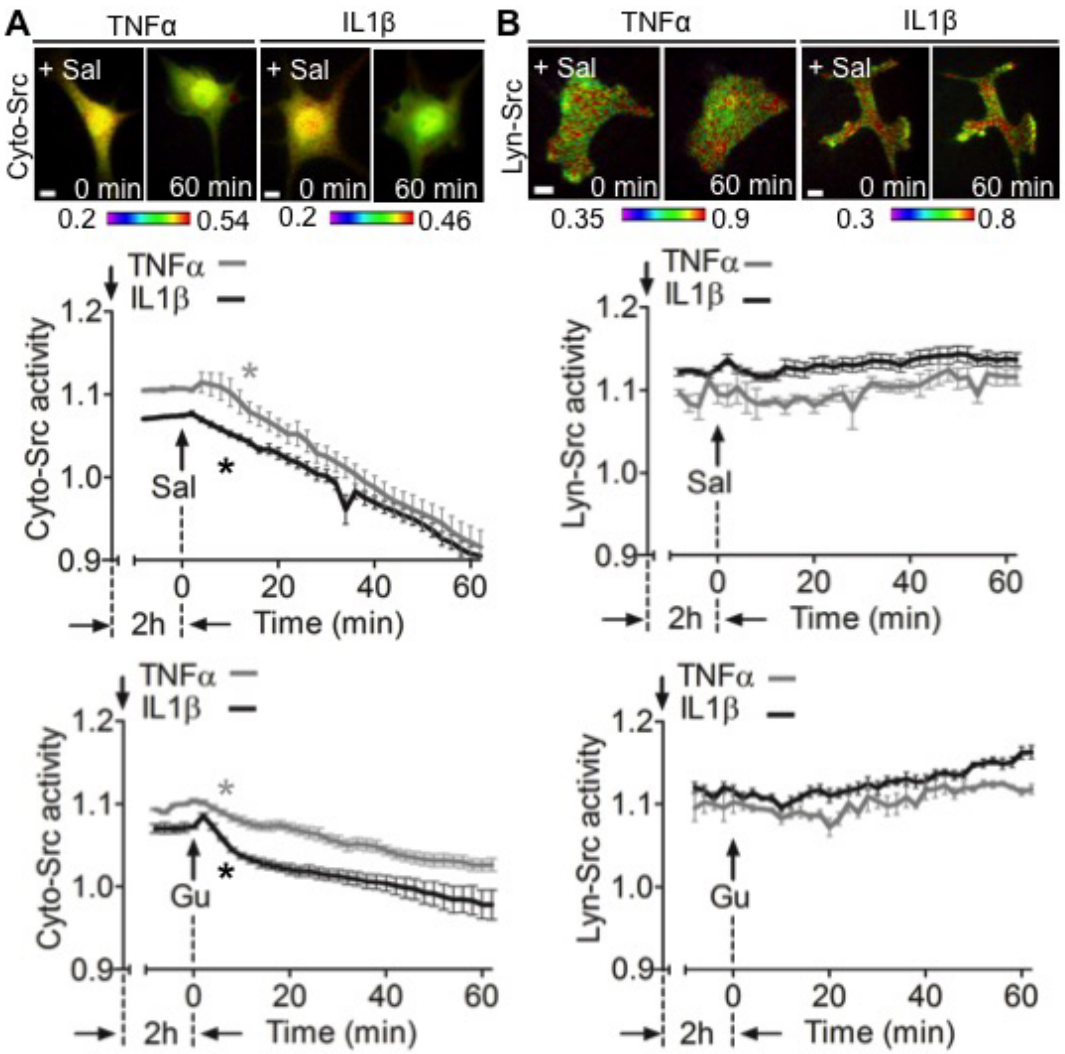

Fig. 2.8.: Salubrinal and guanabenz inhibit cytokine-induced Cyto-Src activity. C28/I2 cells transfected with either Cyto-Src or Lyn-Src biosensor were pretreated with TNFα or IL1β for 2 hours before incubating with salubrinal or guanabenz. (A) Effect of salubrinal and guanabenz on cytokine-induced Cyto-Src activity. (B) Cytokine-induced Lyn-Src activity is not altered by salubrinal or guanabenz. Scale bars, 10 μm. n>7 cells. * p<0.05.

2.4 Discussion

We employed live cell imaging in conjunction with FRET-based Src biosensors to determine the spatiotemporal activities of Src in C28/I2 human chondrocytes. Lyn-Src biosensor targeting lipid raft of the plasma membrane and Cyto-Src biosensor existing in cytosol were used to monitor Src activities in different microdomains. We first demonstrated that Src proteins in the cytosol and lipid rafts were activated by TNFα and IL1β with distinct dynamic patterns. Although the role of the inflammatory cytokines in regulating Src activation has been documented, its spatiotemporal activation pattern has not been known. We observed that the cytokine-induced Src activation occurred earlier in the cytosol than that in the lipid raft region of the plasma membrane. Since it is considered that Src activation requires its translocation to the plasma membrane via the actin cytoskeleton, our observations suggest that upon stimulation, Src moves quicker to the non-lipid rafts than to the lipid rafts of the plasma membrane. Taken together, the result is consistent with previous studies showing that translocation of Src from the cytosol to the non-raft region is faster than that to the raft region of the plasma membrane.

It has been reported that TNFα and IL1β differently affect degenerative joint diseases such as osteoarthritis. However, their differential effects on Src activity are not known. We observed that Cyto-Src activities by TNFα were significantly higher than those by IL1β, while Lyn-Src activities under the two cytokines were not significantly different. Although the exact mechanism is not clear, it is possible that Cyto-Src and Lyn-Src would differently interact with inflammatory signaling components, such as TNF receptor DEATH domain (TRADD), TRAF2, and GRB2. Another possibility is that TNFα would stimulate the release of IL1β, which may further increase TNFα-induced Cyto-Src activity. In this study, however, the primary aim was to evaluate the role of mechanical force and salubrinal in the cytokine-induced Src. Investigating Src responses to different cytokines or interaction between TNFα and IL1β is an important subject. Further consideration is necessary to elucidate the

molecular mechanism underlying the differential Src activities at different subcellular locations in response to various cytokines.

There are several lines of evidence that Src can be activated at the different locations within the cell, such as in the cytoplasm, along the actin cytoskeleton, or on the plasma membrane. Thus, we evaluated the possibility that Src may be activated in the cytoplasm before it is mobilized to the cell periphery or plasma membrane upon cytokine stimulation. To test this possibility, we disrupted the actin cytoskeleton and monitored Src activity in the cytosol and lipid rafts of the plasma membrane. While disruption of the actin cytoskeleton using CytoD blocked Src activation in the lipid rafts, it did not completely inhibit cytosolic Src activation, suggesting that some population of cytosolic Src may be activated in the cytoplasm, without translocation through the actin cytoskeleton (Figure 2.9). These results support the previous findings that activation of Src at the lipid rafts of the plasma membrane requires its translocation through the actin cytoskeleton and that Src can be activated in the cytoplasm. However, our data cannot distinguish whether cytosolic Src near the plasma membrane outside the lipid rafts, which may not require translocation, is activated or other focal adhesion proteins at the plasma membrane, such as vinculin or talin, are involved in this cytosolic Src activation. Further studies are needed to elucidate the underlying mechanism for this dynamically distinct Src activation at different cellular compartments.

Fluid flow-induced shear stress (5 dynes/cm^2) was able to significantly inhibit the cytokine-induced Src activity at the lipid rafts. This result is consistent with previous findings that lipid rafts of the plasma membrane are involved in Src mechanotransduction. On the contrary, cytosolic Src was not responsive to the shear stress. We previously reported that local mechanical force applied from the cell surface using a small (4.5 mm in diameter) magnetic bead induces highly localized cytosolic Src activity and does not yield global FRET changes of the Src biosensors within the cytoplasm. We do not know whether cytosolic Src does not respond to shear stress that is evenly distributed over the cell surface, or activation of the cytosolic Src by shear

stress is not sufficient to yield detectable FRET changes from a substantial pool of Src biosensors in the cytosol. We also observed that Src activities at the lipid rafts of the plasma membrane are selectively up- or down-regulated by different magnitudes of shear stress; moderate (5 dynes/cm^2) and high (10 dynes/cm^2) shear stress decrease and increase Src activity in the lipid rafts, respectively. This result is consistent with previous reports on fluid flow magnitude-dependent small GTPase RhoA activities and MMP13 activities in chondrocytes. We have previously reported that the inhibition of ER stress through eIF2α phosphorylation can decrease expression and activity of degrading enzymes such as MMP13 in C28/I2 human chondrocytes. Here, we used two inhibitors for eIF2α dephosphorylation, salubrinal and guanabenz, and tested whether alleviating ER stress by eIF2α phosphorylation could attenuate the inflammatory cytokine-induced Src activation. In contrast to the nonresponsive Src activity in cytosol under shear stress, we observed that the cytokine-induced Src in the cytosol, but not in the lipid rafts of the plasma membrane, was inhibited by salubrinal or guanabenz. This result suggests that Src at different compartments within the cell may be regulated by different mechanisms; cytosolic Src is downregulated by eIF2α phosphorylation, but Src in the lipid rafts may not be a critical signaling node within an ER stress signaling pathway (Figure 2.9). Our results further suggest that these distinct responses of Src activities are differently regulated by fluid flow.

In summary, our findings of the distinct activation patterns of Src kinases suggest the critical role of mechanical loading and inhibition of ER stress through phosphorylation of eIF2α in arthritic cartilage (Figure 2.9). By selectively regulating subcellular Src kinases, fluid flow and a chemical agent that inhibits ER stress appear to interact with Src-dependent regulatory pathways important for chondrogenesis and cartilage maintenance. The work herein suggests that a proper combination of chemical and mechanical stimuli may present a potential therapeutic strategy for prevention of cartilage loss in joint diseases such as OA. Further studies on the interaction between Src and FAK, and signaling pathways connecting subcellular Src/FAK kinases to FAK in chondrocytes may benefit in developing a therapeutic strategy for joint diseases.

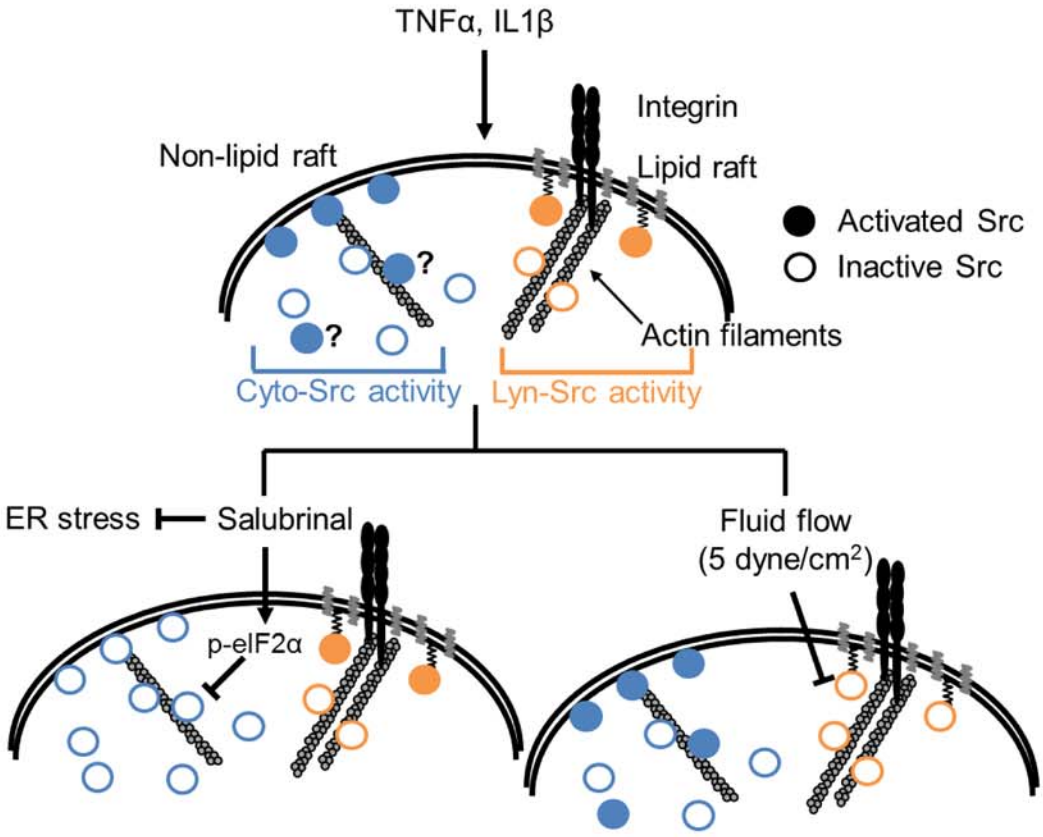

Fig. 2.9.: A proposed model of distinctive Src activities at different subcellular locations. TNFα and IL1β activate Src kinase at the cytoplasm and lipid rafts of the plasma membrane, and actin cytoskeleton and lipid rafts are essential components of the Lyn-Src activation. Salubrinal can inhibit Src kinases in the cytoplasm through phosphorylation of eIF2α, but not in the lipid rafts of the plasma membrane. In contrast, fluid flow at 5 dynes/cm^2 decreases integrin-mediated Src kinase in the lipid rafts of the plasma membrane, but it did not significantly affect the level of Src activation in the cytoplasm.

3. DISTINCT SUBCELLULAR ACTIVATION PATTERNS OF SRC AND FAK BY INTERSTITIAL FLUID FLOW AND CYTOKINES

3.1 Introduction

FAK and Src are tyrosine kinases that play crucial roles in fundamental cellular functions that include cell motility, cycle progression and survival [329–331]. They also serve as crucial signaling nodes in integrin-mediated signaling cascades [332]. Because integrins are cell surface receptors and FAK and Src are closely associated with them, it is expected that FAK and Src are activated at the plasma membrane. For example, in response to flow-induced shear stress, FAK is activated at focal adhesions [333]. Direct activation of integrin 1 alone is shown to be sufficient to activate FAK [334]. Localized mechanical force using a bead coated with fibronectin, which is known to bind to integrins, induces Src activation at the plasma membrane [184]. Therefore, the plasma membrane is believed to be the primary activation site for FAK and Src [332]. However, recent evidence suggests that FAK and Src can be differently regulated depending on their location within the membrane domains such as lipid rafts and non-lipid rafts [17, 185]. The molecular relationship between FAK and Src and their roles in the signaling pathways are also shown to be distinct depending on the membrane microdomains [17, 185]. For example, Src in the lipid rafts regulates the phosphoinositide 3-kinase (PI3K)/Akt sigaling, whereas Src in the non-lipid rafts regulates mitogen-activated protein kinase/extracellular signal-regulated kinase (MAPK/ERK) signaling [186]. The response of FAK in the lipid rafts to platelet-derived growth factor (PDGF) is much stronger and faster than that of FAK in the non-raft regions [18]. Therefore, the mechanism of their domain-specific regulation by external stimuli, including mechanical force and growth factors, as well

as their relationship, seems very complex and there is a need to understand this mechanism in various physiological conditions.

In addition to the responsiveness of FAK and Src to mechanical force and growth factors, they are known to respond to inflammatory cytokines. We have recently reported that Src is upregulated by inflammatory cytokines such as tumor necrosis factor α (TNFα) and interleukin 1β (IL1β) and that its temporal activation profiles are different in the cytosol and plasma membrane [19]. Because of the involvement of FAK and Src in inflammatory signaling, they are important in cartilage pathology. For example, phosphorylation of Src and FAK elevates the gene transcription of matrix metalloproteinases (MMPs) [145,146]. FAK is upregulated in both osteoarthritis and rheumatoid arthritis tissues [335]. Inhibition of FAK [11] and Src [336] decreases chondrocyte proliferation and promote gene expression, thus maintaining chondrocyte phenotype. They also contribute to osteoarthritis progression by significantly elevating the expression of matrix degrading enzymes while inhibiting the gene expression of proteoglycan and type II collagen [37, 47, 48]. Despite the importance of FAK and Src in the inflammatory signaling, the detailed mechanism of the interaction among FAK and Src activities, mechanical stimuli, and inflammatory cytokines in the different membrane domains (i.e., lipid rafts and non-rafts) is not known.

Current understanding of the cell behavior and signaling has been derived primarily from studying cells cultured on two-dimensional (2D) surfaces. However, it has been recently recognized that there are considerable differences in various cell functions between 2D and 3D extracellular environments, such as cell shape, differentiation, adhesion, migration, and force sensing [337, 338]. For example, when chondrocytes are isolated from articular cartilage and kept in planar 2D culture, they become flat and lose their cartilage phenotype [281]. Surprisingly, when these dedifferentiated cells are cultured in 3D matrices, they become spherical, similar to their cell shape *in vivo*, and restore the differentiated cartilage phenotype [284]. Similarly, focal adhesion proteins, which play critical roles in mechanotransduction signaling and cytoskeletal organization, are highly expressed in 2D cultures, but are much less

apparent *in vivo* and in 3D cultures [337, 339]. Therefore, the 3D culture model may more closely capture the physiological behavior of cells.

Herein we addressed several questions: 1) Whether/how mechanical force and inflammatory cytokines similarly or dissimilarly regulate Src and FAK activities at different subcellular locations? 2) How FAK interacts with Src under various stimulations? 3) As proline-rich tyrosine kinase 2 (Pyk2) is known to be similar to FAK in sequences and structure [190], what is the role of Pyk2 in the Src and FAK signaling in response to loading and inflammatory cytokines? 4) Whether mechanical loading can alter inflammatory cytokine-activated Src and FAK activities? To monitor FAK and Src activities with high spatiotemporal resolution, we employed FRET-based biosensors: the lipid rafts-targeting (Lyn-FAK and Lyn-Src), and the non-lipid rafts-targeting (KRas-FAK and KRas-Src). C28/I2 chondrocytes transfected with one of the biosensors were mixed with type II collagen-coupled agarose gel to produce 3D chondrocytes-gel constructs that allow integrin activation. During imaging, fluid flow or cytokines was applied to cells in 3D gel constructs. To examine the interactions between Src and FAK, we used pharmacological drugs to specifically inhibit Src or FAK activities. The role of Pyk2 in Src/FAK signaling in response to mechanical or inflammatory cytokine stimulations was examined by silencing the Pyk2 activity using siRNA. A 3D cartilage explant system in conjunction with 3D FRET imaging was developed to further examine the effect of moderate loading on inflammatory cytokine-activated FAK/Src signaling.

3.2 Materials and methods

3.2.1 Integrin, Src and FAK biosensors

The β1 integrin was monitored using mCherry-Integrin-Beta1-N-18 biosensor (Addgene). FRET-based biosensors were used for monitoring Src and FAK activities. The Src biosensor consists of a cyan fluorescent protein (CFP), a binding domain of an effector protein (SH2 domain), a truncated Src substrate peptide and a yellow fluo-

rescent protein (YFP). The FAK biosensor consists of a CFP, a SH2 domain, a FAK substrate peptide and a YFP. The lipid raft-targeting biosensors (Lyn-Src and Lyn-FAK) were produced by fusing acylation substrate sequences derived from Lyn kinase to the N-terminal of Src and FAK biosensors. The non-lipid raft-targeting biosensors (KRas-Src and KRas-FAK) were produced by attaching polybasic-geranylgeranyl sequences to the C-terminus of the Src and FAK biosensors. The activation of the Src or FAK substract promotes the intramolecular binding of the SH2 domain to the truncated Src or FAK domain, which leads to a conformational change of the biosensor and a decrease of FRET efficiency from CFP to YFP. Hence, Src and FAK activities can be visualized as changes of the emission ratio of the CFP/YFP. The specificity of the biosensors has been well characterized previously [17, 18, 184].

3.2.2 Cell culture and transfection

The human chondrocyte cell line C28/I2 was used. Cells were cultured in Dulbecco's modified Eagle's medium (DMEM; Lonza) containing 10 % FBS (Hyclone) and 1 % penicillin/streptomycin (Lonza); and maintained at 37 °C and 5% CO_2 in a humidified incubator. Neon transfection system (Invitrogen) was used to transfect Src and FAK biosensors into the cells. After transfection, cells were cultured in serum-free and antibiotic-free DMEM for 24 hours before imaging.

3.2.3 Chemical reagents and siRNAs

Sulfo-SANPAH (Sigma) were employed to crosslink agarose gel (Sigma) with Type II collagen (Sigma). Agarose (low melting temperature agarose; Lonza) was used to prepare 3D agarose gels. Two types of proinflammatory cytokines, tumor necrosis factor (TNFα; Sigma; 10 ng/ml) and interleukin 1 beta (IL1β; Sigma; 1 ng/ml) were used. Anti-integrin β1 antibody (Santa Cruz Biotechnology; 10 μg/ml) was used to block integrin activities. Methyl-beta-cyclodextrin (MβCD; Sigma; 10 mM) was used to extract cholesterol from the lipid rafts of the plasma membrane. PP2 (Sigma; 10

μM) was used to block Src activities, and PF228 (Sigma; 1 μM) was used to inhibit FAK activities. We also used Pyk2 siRNA and non-specific control (NC) siRNA (Santa Cruz) to study the role of Pyk2 in Src and FAK activities.

3.2.4 3D agarose-chondrocytes constructs

The collagen-coupled agarose gels (AG-Col) were prepared as stated before [325]. Briefly, the collagen solution was reacted with 10-fold molar excess of the sulfo-SANPAH in PBS at room temperature in the dark room for 4 h to produce 1.2 mg/ml Type II collagen solution. The 4 % (wt/vol) agarose solution was prepared using sterile PBS, autoclaved, and cooled to 40 °C. Three parts of 4 % agarose were combined with one part of collagen-sulfo-SANPAH solution to yield the mixture containing 3 % agarose and 0.3 mg/ml collagen. The mixture was exposed under UV light for 20 min to allow the activation of the photoreactive groups of the sulfo-SANPAH that conjugate the collagen to CH groups in the agarose. After conjugation, the agarose mixture was cooled down and washed with 10-folds excess sterile PBS for five times over 3 days to remove the unbound collagen and sulfo-SANPAH. Agarose gels + collagen (AG+Col) were prepared as described previously but without addition of the sulfo-SANPAH. Agarose gels (AG) were prepared without addition of collagen and sulfo-SANPAH. Before transfection, 3 % modified agarose gels were melted down at 45 °C and cooled to 37 °C. Two parts of 3 % agarose gel were mixed with one part of 3 × DMEM containing transfected cells to produce the mixture of 2 % agarose and 1 × DMEM containing cells. The mixture was injected into an Ibidi flow chamber (Ibidi) and cooled at room temperature for 30 min to allow gelling. The gel was supplemented with fresh 1 × phenol red-free DMEM and transferred to incubator for 24 hours before imaging.

3.2.5 Flow velocity measurement

The operating principle underlying our permeability assay is to measure the rate at which the fluorescently labeled molecule travel through the agarose gel. The fluorescent solute used is Alexa Fluor 594-conjugated bovine serum albumin (BSA; Thermo Fisher). Place a drop of BSA-594 in DMEM on a glass coverslip, and measure the average fluorescence light intensity. Repeat this step with different concentrations of BSA-594 to create a standard curve of fluorescence intensity vs. solute concentration. The solute concentration (50 μg/ml; Invitrogen) that was used in subsequent sections is within the linear range of this curve. As shown in SFigure 1a, the background fluorescence images were captured before the addition of fluorescent media. The initial fluorescence images were captured right after the addition of fluorescent media. Time-lapse images were obtained every minute to monitor the perfusion of fluorescent solute. The maximum fluorescence images were captured after the imaging regions are uniformly perfused with fluorescent medium, which can be obtained after 10-30 min depending on the fluid rate. Draw the region of interest (ROI), and calculate the mean fluorescence intensity I_b, I_1, I_2 and I_{max}. Compute the velocity as follows:

$$v = \frac{L(I_1 - I_2)}{(I_{max} - I_b)(t_1 - t_2)} \tag{3.1}$$

where L is the length of the ROI along the loading application direction, t_2 and t_1 are the time points taken the first and the second images, correspondingly.

3.2.6 Permeability measurements and shear stress estimation

Permeability of agarose gel prepared within an open cell scaffold was measured using a custom-designed, gravity-driven permeameter. Agarose solutions were polymerized (30 minutes at 37 °C) within disks (0.125 thick, 0.5 diameter) of hydrophilic polyethylene foam (1545 μm pore size; Small Parts Incorporated, Miami, FL). Silicone rings fitted around the polyethylene disks formed a tight seal between the disk and

walls of the permeameter. A specified volume (approximately 15 mL) of PBS, pH 7.4 was added on top of each collagen/polyethylene composite and fluid flow monitored over time.

The shear stress over the cell surface imposed by interstitial fluid flow can be estimated assuming spherical cells by Brinkman [340].

$$\tau = \frac{3}{\pi}(\frac{\mu Q}{A\sqrt{k}}) \tag{3.2}$$

Where τ is the average shear stress, μ is the viscosity of the fluid, Q is the time-averaged volumetric flow rate, A is the cross sectional area of the gel sample, k is the Darcy permeability.

3.2.7 Immunostaining and confocal microscopy

C28/I2 cells were mixed with AG, AG+Col, or AG-Col gels and cultured for 24 h before staining. The cell-gel constructs were fixed with 4 % paraformldehyde. After rinsing, the cells were permeabilized with 0.5 % Triton X-100 (Sigma) in PBS for 45 min at room temperature, and then incubated with blocking buffer (5 % BSA, serum, 20 % Polyvinylpyrrolidone (Amresco, Solon, OH, USA) in PBS combined into 1:1:1 ratio) overnight at 4 °C. The samples were incubated with primary antibodies against activated β1 integrin (1:500; Millipore, Billerica, MA, USA), or total β1 integrin (1:100; Santa Cruz Biotechnology, Dalla, TX, USA) overnight at 4 °C, and then with Alex Fluor 488 anti-mouse IgG (1:1000; Invitrogen) overnight at 4 °C. Finally, cell nuclei were labeled by DAPI (Sigma). An Olympus Fluoview FV1000 confocal microscope was used to visualize activated/total β1 integrins and cell nuclei. Images were acquired using a 60 × objective lens (1.2 numerical aperture; Olympus).The fluorescence images were selected randomly. The fluorescence signal was quantified by measuring average intensity in individual cells using Fluoview Viewer software (Olympus).

3.2.8 Confocal microscopy and colocalization analysis

An Olympus Fluoview FV1000 confocal microscope was used to visualize β1 integrins and Lyn-FAK activity in chondrocytes co-transfected with β1 integrin and Lyn-FAK biosensors. Images were acquired using a 60 $\times$ objective lens (1.2 numerical aperture; Olympus). Colocalization of β1 integrins and Lyn-FAK activity was calculated from 10 randomly picked cells. Same cells were imaged before and after loading application. The Pearsons correlation coefficient was done with ImageJ plugin called JACoP. Representative images were produced by smooth filter and background subtraction to reduce noise, setting a threshold to highlight high activities, and merged to produce merged view using ImageJ (NIH).

3.2.9 Fluid flow-induced shear stress application

Fluid flow-induced shear stress has been shown to play crucial roles in the development and progression of osteoarthritis. During imaging, the agarose gel construct was perfused with phenol red and serum-free DMEM. The DMEM was supplemented with 20 mM HEPES to maintain the pH at 7.4. A syringe pump (Harvard Apparatus) was employed to apply shear stress to cells by controlling the flow rate through the chamber. Chondrocytes encapsulated in the agarose gel were exposed to pulsatile flow (0.2 Hz) at 2, 5, 10, and 20 μl/min in an Ibidi flow chamber (Ibidi) for 1 hour during imaging (Figure 3.1D).

3.2.10 Mouse cartilage explant culture and transfection

The skin and synovial membrane of mouse joints were removed to expose the cartilage surface. The operation process was accompanied by constantly rinsing the exposed cartilage surface with sterile PBS at 4 °C. Thin cartilage slices were harvested by scalpelling the outer layer of cartilage and were washed five times with steril PBS. The clean explants were transferred to 24 well plates and incubated overnight with

DMEM supplemented with 10 % serum and 1 % penicillin/streptomycin. The *in vivo*-jet PEI (Polyplus) was used to transfect chondrocytes in cartilage explants with Src and FAK biosensors following manufactures manual. 12 hours after transfection, explants were mixed with 2 % Col-AG gels that supplemented with DMEM to produce 3D explant-agarose constructs. These constructs were incubated for another 12 hours before imaging.

3.2.11 FRET Microscopy and image analysis

Images were obtained by using a Nikon Ti-E inverted microscope equipped with an electron-multiplying charge-coupled device (EMCCD) camera (Evolve 512; Photometrics), a filter wheel controller (Sutter Instruments), and a Perfect Focus System (Nikon) that maintains the focus during time-lapse imaging. The following filter sets (Semrock) were used: CFP excitation: 438/24 (center wavelength/bandwidth in nm); CFP emission (483/32); YFP (FRET) emission: 542/27. To minimize photobleaching, cells were illuminated with a 100 W Hg lamp through an ND64 ($\sim$1.5 % transmittance) neutral density filter. Time-lapse images were acquired with a 40$\times$ (0.75 numerical aperture) objective. FRET images for Src and FAK activities were generated with NIS-Elements software (Nikon) by computing an emission ratio of CFP/YFP for individual cells over time. The FRET ratio images were scaled according to the color bar.

3.2.12 Statistical analysis

Statistical data are presented as the mean $\pm$ standard error of the mean (SEM). One-way ANOVA followed by Dunnett's post hoc test was used to determine the statistical differences. Student's t-test was used to compare two groups. Statistical analyses were conducted using Prism 5 software (GraphPad Software). $p<0.05$ was considered statistically significant. In the time course data, * indicates the time point

after which the Src or FAK activity become significantly different from that before stimulation.

3.3 Result

3.3.1 3D cells-agarose gel constructs allow Lyn-Src and -FAK activation under loading

The activation of $\alpha5\beta1$ integrin is required for the initiation of loading-induced Src/FAK signaling. To determine our gel systems can enable integrin activation, immunostaining was employed to measure the $\beta1$ integrin activation levels of C28/I2 cells in agarose gels with different modifications: agarose (AG) gel, collagen-added agarose (AG+Col) gel and collagen-coupled agarose (AG-Col) gel (SFig. 1). The average GFP intensity (integrin) over the whole cell was quantified and normalized to that in the AG gel (SFig. 1B, C). The collagen conjugation significantly elevated the integrin activation level (180.3 % increase) (SFig. 1B), while the total integrin levels in different gels were not significantly different among each other (SFig. 1C). As to Lyn-Src that targeting lipid rafts in chondrocytes is highly responsive to shear stress in 2D cell culture37, to examine whether our gels allow Src/FAK regulation by loading, we mixed chondrocytes transfected with either Lyn-Src or Lyn-FAK with one of three types of gels. To apply loading on C28/I2 chondrocytes in 3D matrix, the cell-gel mixture was injected into a flow chamber. During imaging, chondrocytes were subjected to no flow for 10 min, and then 5 μl/min or 10 μl/min fluid flow for 1 hour. The velocities of flow through agarose gel (2 to 28 μm/min corresponds to 2-20 μl/min flow rate) (SFig. 2A, B), the Darcy permeability ($\sim10^{-14}$ m^2) and estimated shear stress experienced by chondrocytes (2-20 dyne/cm^2 corresponds to 2-20 μl/min flow rate) were characterized (SFig. 3.2C). The Src and FAK activities were assessed by monitoring changes of the emission ratios of CFP/YFP of the biosensors. Z-stack images of Lyn-Src activities were captured to generate orthogonal views (SFig. 3.3A), suggesting similar activity level and uniform activation patterns over the cell. In lat-

ter experiments, the Src or FAK activities were determined by capturing a single z slice through the central region midline of each cell. After the application of 10 μl/min fluid flow, fluid flow failed to regulate the Lyn-Src or Lyn-FAK activities in chondrocytes in either AG or AG+Col gels, while the activities of Lyn-Src as well as Lyn-FAK were elevated significantly (Lyn-Src: 21.5 %, Lyn-FAK: 17.1 %) in AG-Col gels (SFig. 3.3b). Moreover, 5 μl/min fluid flow inhibited activities of Lyn-Src (10.7 % decrease at 14 min) and Lyn-FAK (22.7 % decrease at 59 min) (SFig. 3.3C) in AG-Col gels. AG-Col gels were used for latter experiments in this study.

3.3.2 Fluid flow regulates Src and FAK activities in a magnitude-dependent manner

To determine the Src and FAK activities at different subcellular locations, we transfected chondrocytes with one of these four biosensors: Lyn-Src and Lyn-FAK targeting lipid rafts, and KRas-Src and KRas-FAK targeting non-lipid rafts. 2 μl/min fluid flow did not detectably alter Lyn-Src activity, notably, the intermediate fluid flow reduced the Lyn-Src activity (10.7 % decrease at 14 min) and this inhibitory effect was reversed to basal level at 30 min; while higher intensities significantly elevated Lyn-Src activities (10 μl/min: 21.6 % increase at 59 min; 20 μl/min: 15.0 % increase at 59 min)(Figure 3.1A). KRas-Src activities were upregulated by 10 μl/min (18.5 % increase at 60 min) and 20 μl/min (20.7 % increase at 60 min), while activities were downregulated by 5 μl/min (20.7 % decrease at 60 min) (Figure 3.1B). Lyn-FAK activities were also regulated by fluid flow. 10 μl/min fluid flow significant activated Lyn-FAK (17.1 % increase at 4 min); 20 μl/min fluid flow activated Lyn-FAK and maintained this activation for 1 h (24.0% increase at 59 min); and 5 μl/min fluid flow substantially downregulated Lyn-FAK activities (21.4 % decrease at 60 min) (Figure 3.1C). KRas-FAK activities were not altered by 2, 5 and 10 μl/min fluid flow, but

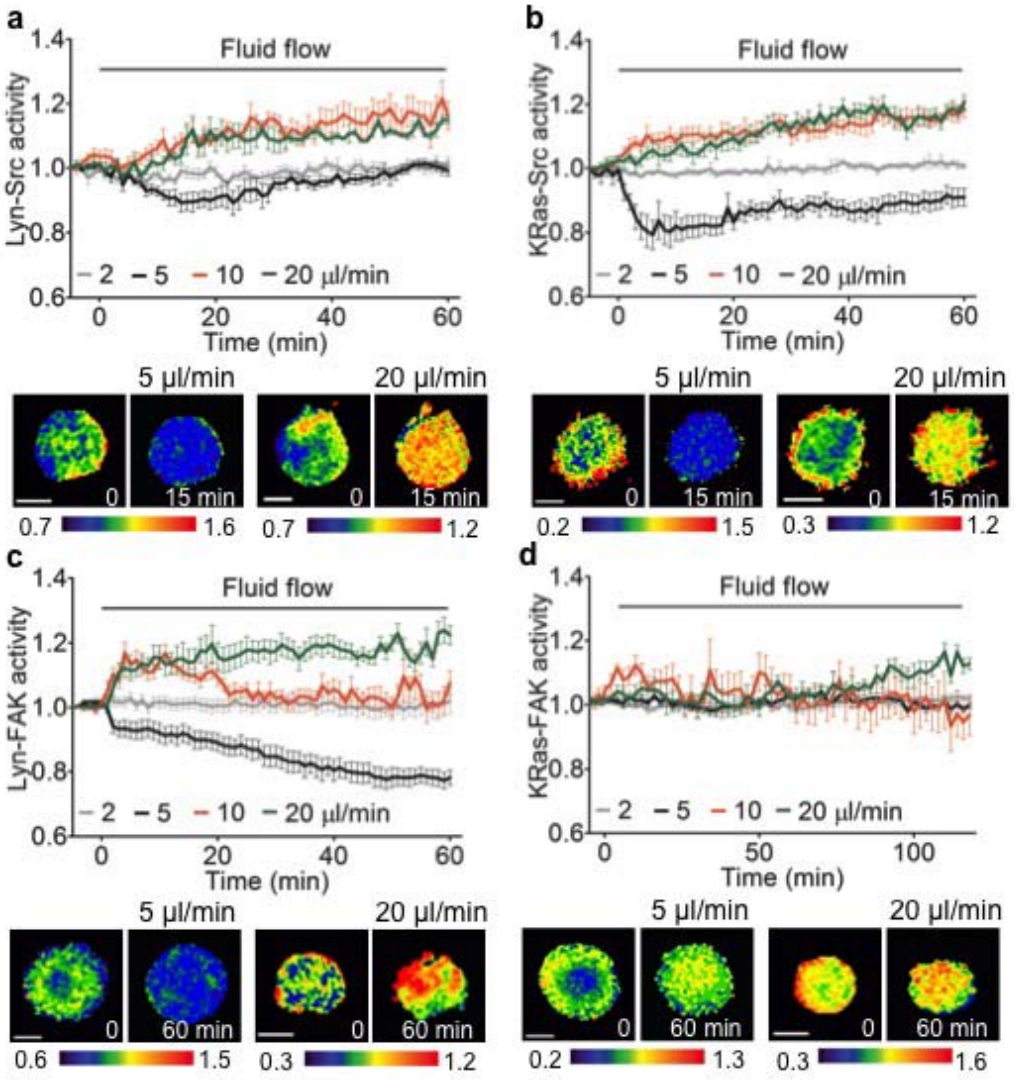

Fig. 3.1.: FAK and Src activities at different subcellular locations are regulated by fluid flow distinctively in a magnitude-dependent manner. The FRET ratio images were scaled according to the corresponding color bar, which represent emission ratio of CFP/YFP of the biosensor. (A) Lyn-Src activities under fluid flow. n=9 (2 μl/min); n=5 (5 μl/min); n=9 (10 μl/min); n=4 (20 μl/min) cells. (B) KRas-Src activities under fluid flow. n=5 (2 μl/min); n=10 (5 μl/min); n=8 (10 μl/min); n=10 (20 μl/min) cells. (C) Lyn-FAK activities under fluid flow. Scale bar, 10 μm. * p<0.05.

slowly upregulated at latter time points by 20 μl/min fluid flow (15.3 % increase at 60 min) (Figure 3.1D).

We further investigated the role of integrin in Src/FAK signaling. We transfected cells with Lyn-Src or Lyn-FAK biosensor. Before imaging, cells were incubated with 10 μg/ml anti-integrin antibody for 1 hour to block integrin activities. By comparing the Src or FAK activities before and after 1 h application of 10 μl/min fluid flow, it showed that the flow-induced Lyn-Src and Lyn-FAK activities were totally abolished by anti-integrin antibody (Figure 3.2A). As to activated integrin clustering in the lipid rafts38 and FAK is closely linked with integrin39, we co-transfected cells with Lyn-FAK and mCherry-β1 integrin biosensors. Using confocal microscopy, the images of FRET CFP, FRET YFP, and RFP were captured before and after 1 h application of 10μl/min fluid flow from the same cell. We observed colocalization of β1 integrin and Lyn-FAK (Figure 3.2C), with Pearson coefficient averaging R = 0.737 (5 μl/min at 0 min), 0.735 (5 μl/min at 60 min), 0.773 (20 μl/min at 0 min), and 0.771(20 μl/min at 60 min) (Figure 3.2B). No significant differences in localization were observed among groups (Figure 3.2B). The representative images in Fig. 2c showed that 5 μl/min fluid flow didnt alter the activation patterns of Lyn-FAK and integrin, but decreased their activation levels; while 20μl/min fluid flow increased the activation level of Lyn-FAK and integrin, and also induced spot activation as shown in enlarged images (Figure 3.2D).

The interactions between Src and FAK in response to fluid flow were explored. Cells transfected with one of Src biosensors were pretreated with 1 μM PF228 (selective FAK inhibitor) for 1 hour. The activities of Src and FAK at 0 and 60 min were recorded, and were normalized to those at 0 min. The fluid flow-induced Lyn-Src and KRas-Src activities were abolished by the treatment of PF228 (Figure 3.3A). On the other hand, with the treatment of PP2, the Lyn-FAK activities were still regulated by fluid flow (5 μl/min: 10.0 % decrease at 60 min; 10 μl/min: 8.6 % increase at 20 min; 20 l/min: 5.5 % increase at 20 min); KRas-FAK activities were not higly responsive to fluid flow (Figure 3.3A). We further examined whether Lyn-FAK activities in lipid

rafts are required for Src activities in non-lipid rafts under fluid flow. Cells transfected with Kras-Src biosensor were pretreated with 10mM MβCD for 1 hour to destroy the lipid rafts of the plasma membrane. The fluid flow-driven KRas-Src activties were blocked by the destruction of lipid rafts (Figure 3.3B). These results demonstrated that Lyn-FAK activity is essential for Src activities in response to fluid flow.

3.3.3 Activation of Src and FAK at different subcellular microdomains by TNFα and IL1β

C28/I2 cells transfected with one of FRET biosensors were imaged for 2 hours under the treatment of IL1β (1 ng/ml) or TNFα (10 ng/ml). Lyn-Src activities were not significantly altered under cytokines (Figure 3.4A). KRas-Src activities increased very fast under IL1β and reached the peak value at 25 min (8.4 % increase); with the treatment of TNFα, its activities increased slower and reached the maxima at 120 min (10.2 % increase) (Figure 3.4B). Activities of Lyn-FAK and KRas-FAK were also substantially activated by cytokines (Lyn-FAK + TNFα: 15.8 % at 120 min; Lyn-FAK + IL1β: 19.0 % at 120 min; KRas-FAK + TNFα: 10.9 % at 120 min; KRas-FAK + IL1β: 16.8 % increase at 115 min) (Figure 3.4C and D).

We determined the interaction between Src and FAK under the stimulation of cytokines using the selective inhibitor of FAK or Src. Before the addition of cytokines, cells transfected with Src biosensor were incubated with PF228 for 1 hour to inhibit FAK activities. The activities of Src and FAK at 0 and 120 min were recorded, and were normalized to those at 0 min. As shown in Fig. 3.5A, with the pretreatment of PF228, the activities of KRas-Src were still upregulated by TNFα and IL1β (TNFα: 10.3 %; IL1β: 9.2 % increase at 120 min), and Lyn-Src is not highly activated by cytokines. However, the activations of Lyn-FAK and KRas-FAK by cytokines were blocked by the PP2 treatment. Results suggested that Kras-Src activity is essential for FAK activities under cytokines.

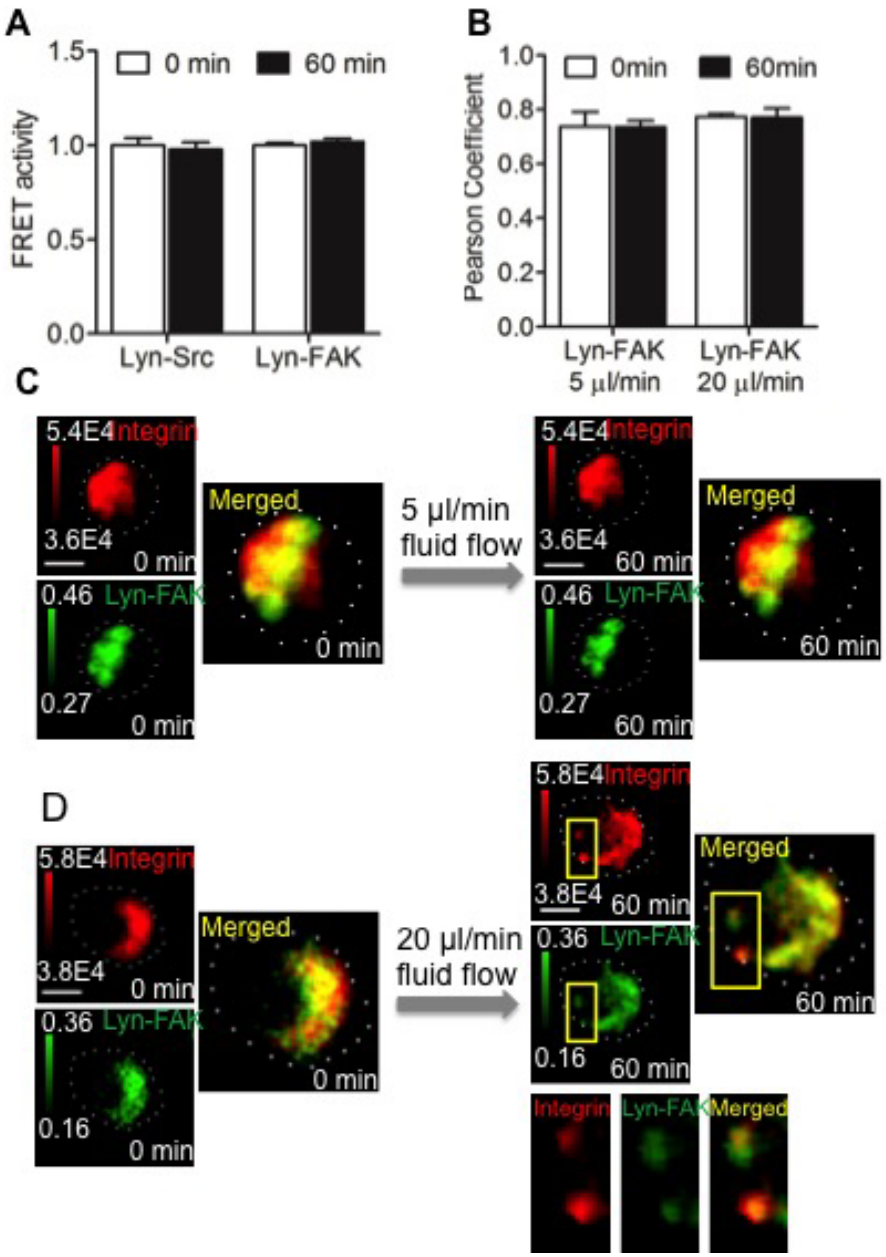

Fig. 3.2.: Integrin activation is required for Lyn-FAK activity under loading. (A) C28/I2 cells transfected with Lyn-Src or Lyn-FAK biosensor were pretreated with 10 μg/ml anti-integrin antibody for 1 hour before subjected to 10 μl/min fluid flow. n>7 cells. (B) C28/I2 cells were co-transfected with Lyn-FAK and mCherry-integrin biosensors. Images taken before and after loading application were analyzed using ImageJ Software to obtain Pearson Coefficient. n>10 cells. (C) Representative images shown integrin (red) merged with Lyn-FAK (green). The enlarged images show the corresponding boxed areas at $\times$ 3 magnification. Scale bar, 10 μm.

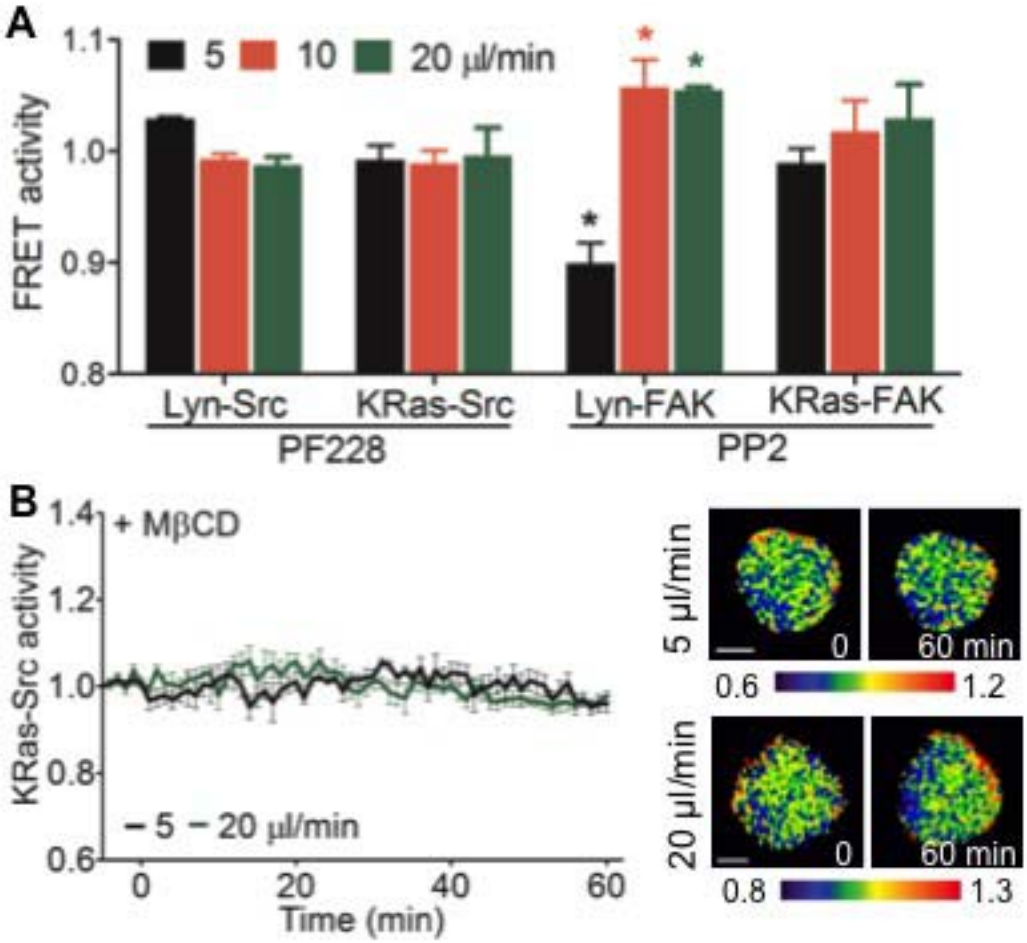

Fig. 3.3.: FAK in lipid rafts is essential for Src activation in response to fluid flow. (A) C28/I2 cells transfected with either Lyn-Src or KRas-Src were pretreated with 1 μM PF228 (selective FAK inhibitor) for 1 h before subjected to different magnitudes of fluid flow. C28/I2 transfected with either Lyn-FAK or KRas-FAK were pretreated with 10 μM PP2 for 1 h before subjected to fluid flow. Bar graph showed Src and FAK activities at 60 min after the application of fluid flow. Activities were normalized to those at 0 min. (B) C28/I2 cells transfected with KRas-Src were pretreated with 10mM MβCD for 1 h to disrupt lipid rafts in plasma membrane. The regulation of KRas-Src by fluid flow was abolished by the treatment of MβCD. Scale bar, 10 μm. n>7 cells. * p<0.05.

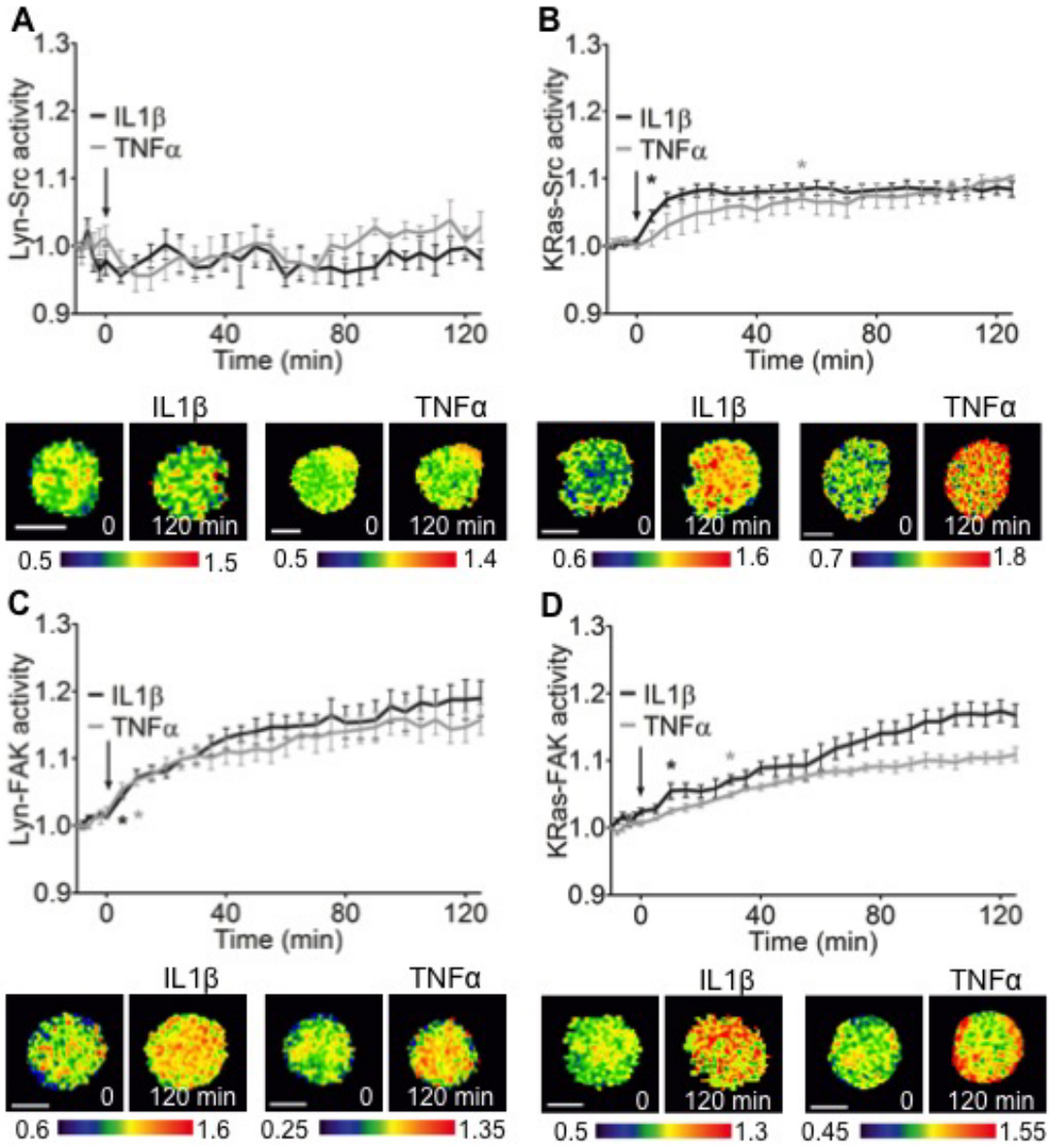

Fig. 3.4.: TNFα and IL1β activate FAK and Src activities. During imaging, C28/I2 chondrocytes were treated with either 10 ng/ml TNFα or 1 ng/ml IL1β for 2 h. (A) Lyn-Src activities under cytokines. (B) KRas-Src activities under cytokines. (C) Lyn-FAK under cytokines. (D) KRas-FAK under cytokines. n>7 cells. Scale bar, 10 μm.* p<0.05.

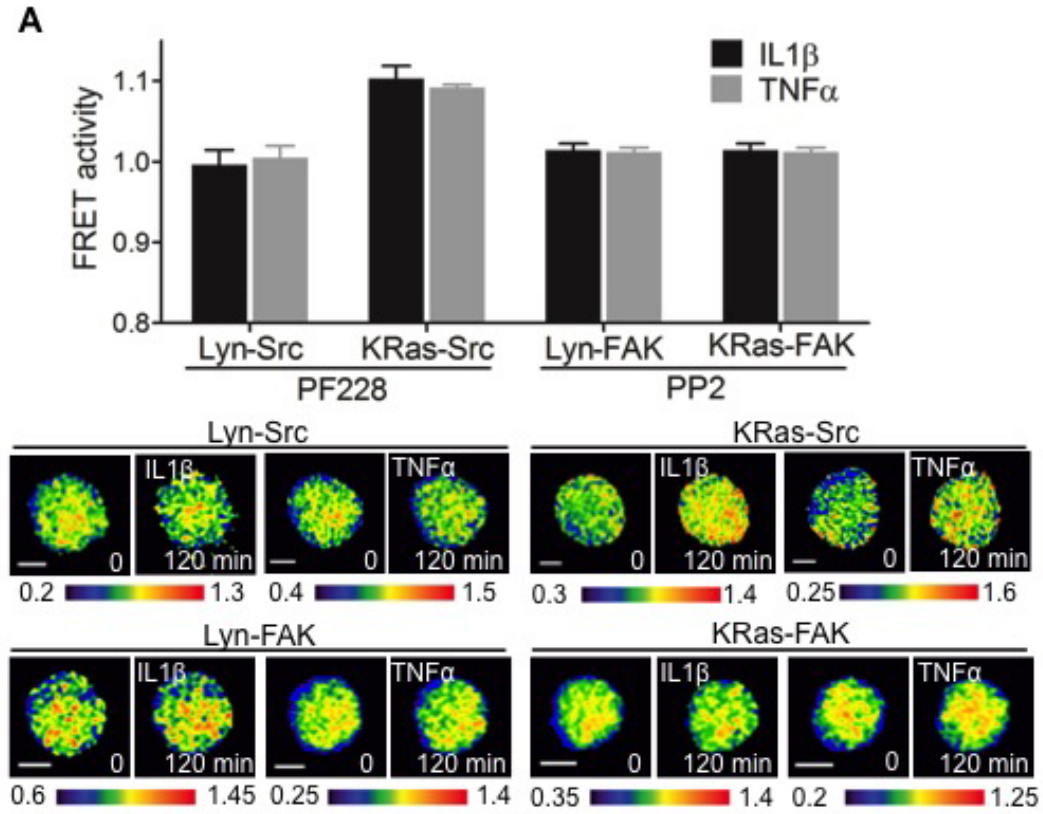

Fig. 3.5.: Src is essential for FAK activation under cytokines. (A) C28/I2 cells transfected with either Lyn-Src or KRas-Src were pretreated with PF228 for 1 h before the treatment of cytokines. C28/I2 transfected with either Lyn-FAK or KRas-FAK were pretreated with PP2 for 1 h before the treatment of cytokines. Bar graph showed Src and FAK activities at 60 min after the application of fluid flow. Activities were normalized to those at 0 min. n>7 cells. Scale bar, 10 μm.* $p<0.05$.

3.3.4 Pyk2 is necessary for cytokine-induced FAK and Src activation

Pyk2 is highly similar to FAK in sequences (46 % identical and 65 % similar) and structures, and has the binding site SH2 domain for Src40. Recent reports have presented conflicting data regarding the interactions between FAK and Pyk259,60. In FAK-null fibroblasts, Pyk2 compensate FAK activity to promote cell retraction35, while it performs different functions from FAK in cell progression40-42. In addition to FAK-Pyk2 interaction, the Pyk2-Src binding plays major roles in monosodium urate monohydrate-induced NO production and MMP-3 expression of chondrocytes 61. To investigate the role of Pyk2 in the loading-driven Src and FAK activities, cells were co-transfected with one of FRET biosensors and Pyk2 siRNA to abolish Pyk2 activities. Src or FAK activities were recorded at 0 or 60 min after flow application, and normalized to those at 0 min. No significant difference was observed between control and Pyk2 siRNA groups, suggesting the silence of Pyk2 failed to block the regulation of FAK and Src by fluid flow (Figure 3.6A). We further examined the role of Pyk2 in Src and FAK activation by cytokines. Fig. 6B shows the Src and FAK activities 2 hour after cytokine treatment. The silence of Pyk2 activity totally blocked the activation of KRas-Src, Lyn-FAK, and KRas-FAK by cytokines; and Lyn-Src activities were still not highly responsive to cytokine stimulation. Results demonstrated that Pyk2 is involved in cytokine-induced Src/FAK signaling.

3.3.5 Intermediate fluid flow suppresses cytokine-induced FAK and Src activation in bovine cartilage explants

To monitor the inhibitory effect of 5 μl/min fluid flow on cytokine-induced FAK and Src activities, we transfected chondrocytes in mouse cartilage explants with one of the FRET biosensors. The transfected explants were mixed with Col-AG gel, and were injected into flow chambers. During imaging, explants were treated with IL1β for 2 hours and then were subjected to 5 μl/min fluid flow for another 1 hour. After 30 min of cytokine treatment, the Lyn-Src activity was significantly upregulated, while

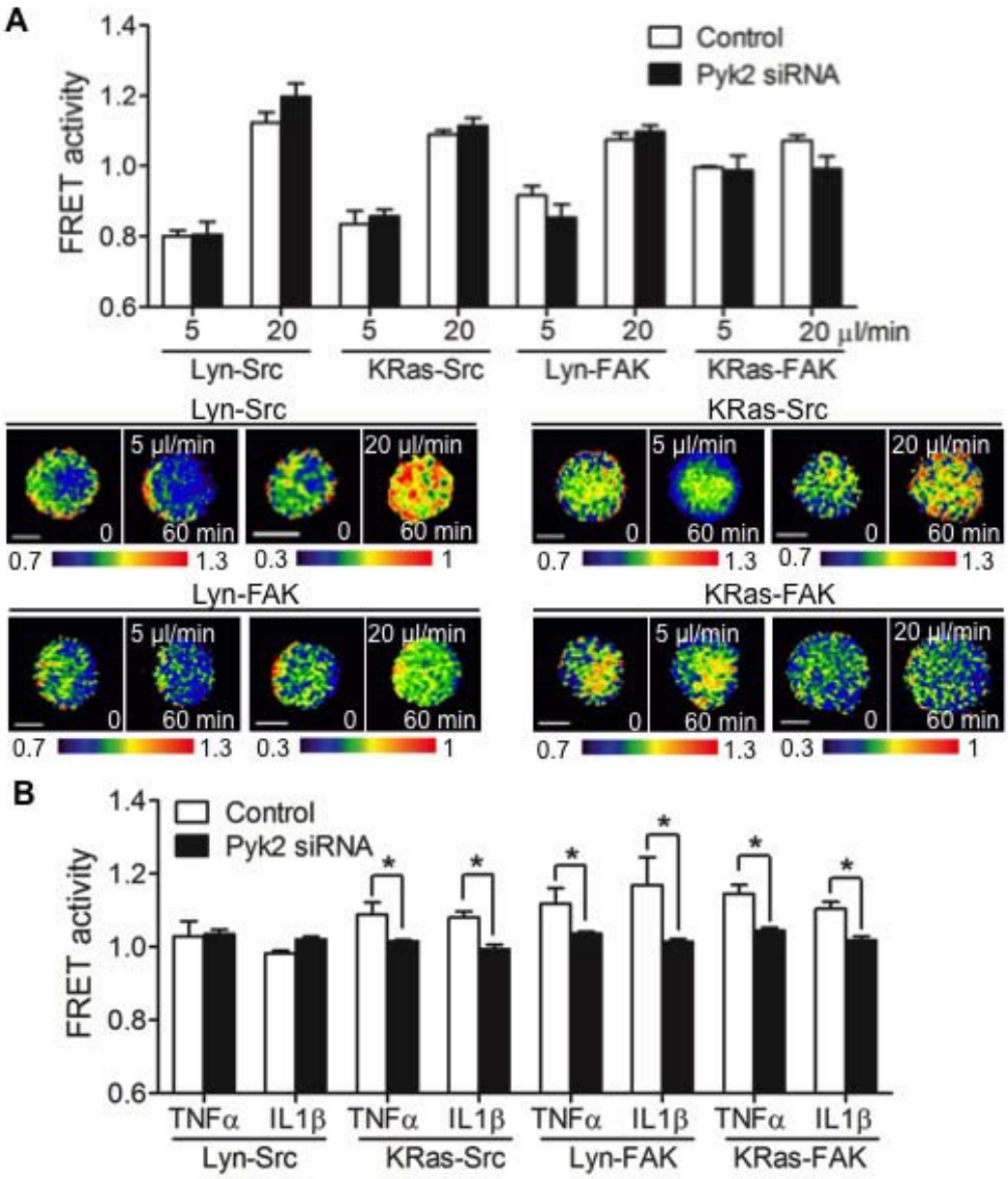

Fig. 3.6.: Pyk2 is involved in cytokine-induced FAK and Src regulation. C28/I2 cells were co-transfected with Pyk2 siRNA to block Pyk2 activity and one of FRET biosensors. (A) Transfected cells were subjected to 5 or 20 μl/min fluid flow for 1 hour. Bar graph showed Src and FAK activities at 60 min after the addition of cytokines. Activities were normalized to those at 0 min. (B) Transfected cells were treated with TNFα or IL1β for 2 hours. Bar graph showed Src and FAK activities at 120 min after the addition of cytokines. Activities were normalized to those at 0 min. Scale bar, 10 μm. n>7 cells. * p<0.05.

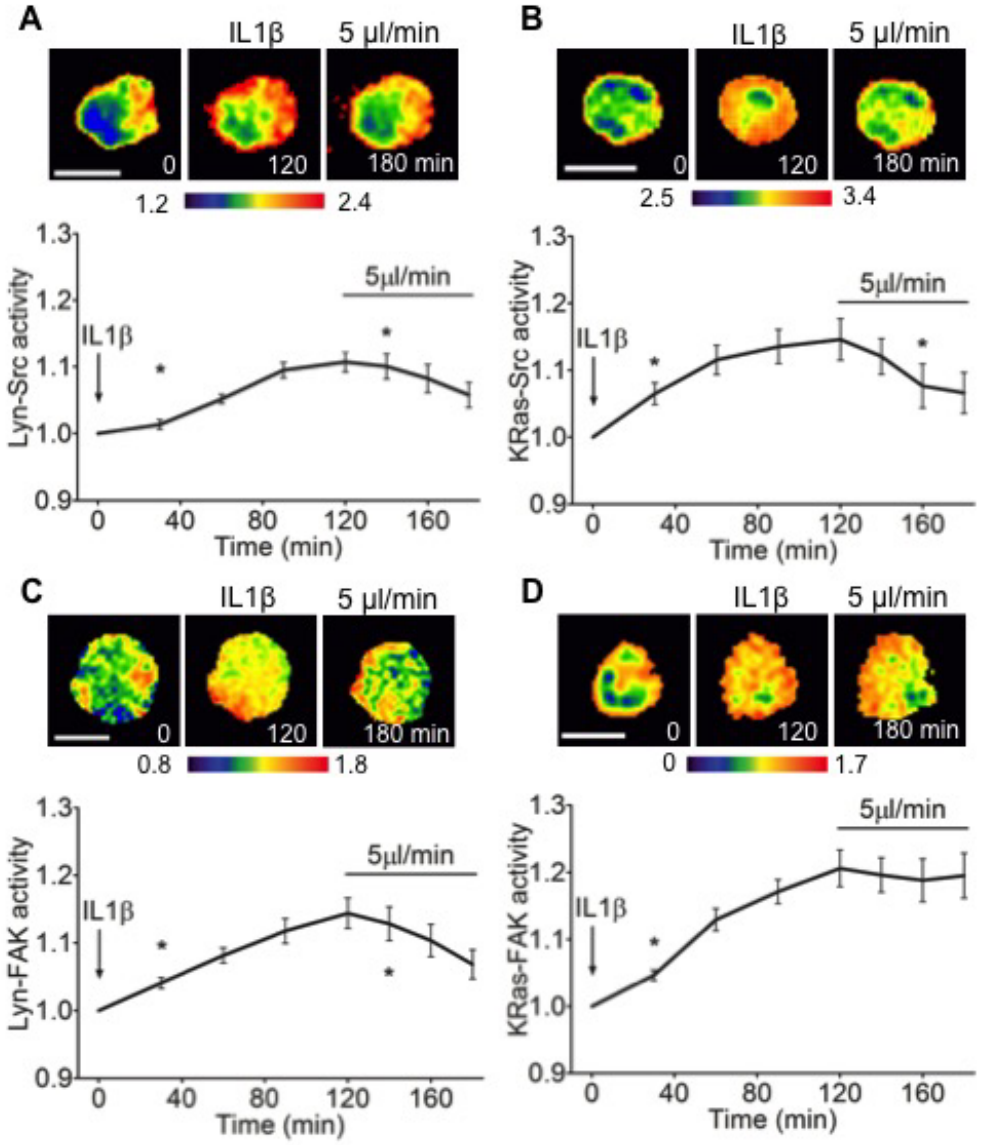

Fig. 3.7.: IL1β-stimulated activation of Lyn-Src, KRas-Src and Lyn-FAK can be reversed by intermediate fluid flow. Chondrocytes in mouse cartilage explants were transfected with one of FRET biosensors. During imaging, cells were treated with IL1β for 2 hours and then subjected to 5 μl/min fluid flow for 1 hour. (A,B) Effect of 5 μl/min fluid flow on IL1-induced Src activity. (C,D) Effect of 5 μl/min fluid flow on IL1β-induced FAK activity. Scale bar, 10 μm. n>7 cells. * p<0.05.

this activation was substantially reduced as compared to that at time 120 min by 5 μl/min fluid flow (Figure 3.7A). The increased activities of KRas-Src and Lyn-FAK by cytokine treatment were also downregulated by 5 μl/min fluid flow (Figure 3.7B and C). KRas-FAK activity was not highly responsive to fluid flow (Figure 3.7D). These results demonstrated that moderate loading might suppress cytokine-induced inflammatory signaling via distinct mechanism.

3.4 Discussion

In this study we employed a 3D type II collagen-conjugated agarose gel-chondrocytes construct in conjunction with live cell imaging to determine the real-time activities of FAK and Src at different microdomains of plasma membrane in C28/I2 human chondrocytes. The agarose gel has been extensively used as 3D cell culture scaffolds due to its nature of high biocompatibility, high water content and the presence of porous structure. Agarose has been found can maintain chondrocyte phonotypes and improve ECM synthesis31 [307, 309, 311]. Although the protein-conjugated agarose gel was also used as a 3D model in chondrocyte studies [341, 342], the effect of collagen conjugation on integrin activation has not been shown. Here we demonstrated that the integrin activation level in chondrocytes that seeded in AG-Col gels was significantly higher than those in AG and AG + Col gels. As to the clustering and activation of integrin are closely associated with lipid rafts [343–345], we used FRET-based Lyn-Src and Lyn-FAK biosensors targeting lipid rafts to determine which gels can enable integrin-mediated Src and FAK activities under loading. Results showed that Lyn-Src and Lyn-FAK activities were regulated by fluid flow in AG-Col gels, but not in AG and AG + Col gels, indicating the conjugation of collagen is required for integrin activation and integrin-mediated Src/FAK signaling. The AG-Col gel was used as the 3D scaffold.

The interstitial fluid flow in knee cartilage is ranged from 6-30 μm/min *in vivo* [346]; and 1.5 body weight generated 12 μm/min interstitial fluid flow in human car-

tilage *ex vivo* [3]. To characterize the flow velocity that experienced by chondrocytes under various rates of fluid flow that applied on gels, BSA-594 was added to culture medium to perfuse agarose gels. The intensity change of the region of interest over time determined the flow velocity in agarose gels (Supplementary Figure 3.2A). Corresponding to 2 to 20 μl/min fluid flow, the flow velocities through agarose gels were ranged from 4.75 to 29.4 μm/min (Supplementary Figure 3.2B), which cover the velocity range in knee cartilage *in vivo*. The estimated shear stress experienced by chondrocytes in agarose gels under 2-20 μl/min flow is ranged from 2 to 20 dyne/cm^2, which is the range widely used in chondrocyte studies *in vitro* [19, 347].

FRET microscopy is a powerful and widely-accepted tool for studying the dynamics of molecular pathways [348]. FRET biosensors employed in this study are designed based on spectral ratiometric methods which distinguish molecular activities in concentration changes and rarely impaired by the out-of-focus signals due to cell thickness [349]. The microscope shifts its focus through the depth of the cell and captures images of various focus planes. After deconvolution, ImageJ compiles the images into a coherent 3D redenring. The Src activity in three different orthogonal planes as shown in Figure 3.2 indicates homogenous distribution and activation level of Src in 3D. Therefore, the Src/FAK activity in the middle plane of the cell was captured and represented the average Src/FAK activity over the whole cell.

Src and FAK are crucial signaling nodes in loading-driven chondrocyte activities3 [15]. Recent studies have shown that Src and FAK at different sub-cellular locations might function distinctly [184]. However, their differential spatiotemporal activities at different microdomains of plasma membrane under different magnitudes of fluid flow are not known. In this study, we observed that the activities of Lyn-Src, KRas-Src and Lyn-FAK were up- or downregulated by fluid flow in a magnitude-dependent manner: moderate (5 μl/min) fluid flow decreased activities, and high (20 μl/min) fluid flow increased activities. This result is consistent with previous reports on loading magnitude-dependent small GTPase RhoA activities [347], Src activities [19], and MMP13 activities 57 in chondrocytes. In contrast to Lyn-FAK,

loading did not alter KRas-FAK activity. What might be the mechanism responsible for the dissimilar activities of FAK at different subcellular domains? Earlier work demonstrated that integrin mobilized to lipid rafts upon activation [22]. Our results showed that the activity of integrin has been found as required for Src and FAK activities in lipid rafts in response to loading, and the activities of FAK in lipid rafts are highly colocalized with integrin activities. We further observed that FAK is required for Src activities in the lipid rafts as well as in the non-lipid rafts in response to loading, while Src inhibitor did not alter FAK activities under loading. It appears that FAK in lipid rafts that closely interacts with integrin, not that in non-lipid rafts, is essential in loading-induced Src/FAK signaling(Figure 3.8A). This proposed mechanism is further confirmed by pretreating cells with MβCD to disrupt lipid rafts, which consequently blocked KRas-Src activity under 5 and 20 μl/min fluid flow. To further validate Src in non-rafts, not that in lipid rafts, is crucial in inflammatory signaling, specifically blocking Src in lipid rafts and monitoring Src/FAK signaling under cytokines are preferred. However, at the present time, there are no techniques or drugs available that have the capability to inhibit Src at designated subcellular locations. In the future, drugs with higher specificity will contribute to the study of subcellular signaling activities, and more importantly, can target molecules responsible for diseases with fewer side effects.

TNFα and IL1β are known to activate proinflammatory signaling cascades and promote OA progress [37]. Our result is the first time to show that FAK and Src activities in different domains of plasma membrane have different activation patterns under TNFα and IL1β. We further demonstrated that upon the stimulation of cytokines, phosphorylated Pyk2 creats a binding site for SH2 domain of Src, resulting in Src activation in non-lipid rafts, which consequently activates FAK activities (Figure 3.8B). To the best of our knowledge, the schematic in Figure 3.8 have illustrated the first time the fundamentally new mechanisms that regulating Src and FAK activities at different microdomains in responds to different stimulus.

The 3D gel-cells system used in present study mimics physiological microenvironment experienced by cell *in vivo*, while the cell-ECM interaction, matrix stiffness and cell-cell interaction are still very different from those *in vivo*. Because imaging subcellular signaling activities *in vivo* is very challenging, to narrow the gap between 3D *in vitro* and *in vivo*, the chondrocytes in mouse cartilage explants embedded in agarose gel were transfected Src or FAK biosensor to test the effect of moderate loading on cytokine-induced Src/FAK activation. As to collagen in cartilage is a strong fluorophore, cartilage were cut to very thin slices to reduce strong autofluorescence and background noise [343,344,350]. Before mixed with gels, cartilage slices were further minced to small pieces to minimize its effect on flow conditions in gels. During imaging, only cells residing at the surface of the explant will be imaged. Interestingly, moderate loading (5 μl/min) reversed cytokine-induced Lyn-Src, KRas-Src and Lyn-FAK activation. These results suggest that moderate mechanical stimuli may be considered as a potential therapeutic strategy for prevention of OA progression due to excessive cytokine expression. We observed a discrepancy between 3D *in vitro* and *ex vivo* data of Lyn-Src activtiy by cytokine application: the Lyn-Src activity is not highly responsive to cytokine *in vitro*, while it get activated rapidly and strongly in the *ex vivo* model. Two possible factors might contribute this discrepancy. C28I2 is a human chondrocytic cell line, but the explants employed in this study were harvested from mouse. The variances between species might results in these different responses to cytokines. Second factor might be the different microenvironment that experienced by chondrocytes. The cell-ECM interaction, matrix stiffness, cell-cell interaction, and the mechanical loading applied on chondrocytes can leads to different activation pattern of Lyn-Src. Besides Lyn-Src, other Src/FAK activities obtained using the *ex vivo* model are highly similar to those from the 3D *in vivo* model, suggesting the collagen-coupled agarose gel system provides reliable data with much simpler experimental setup.

In summary, our findings of the distinct activation patterns of FAK and Src at different microdomains of plasma membrane first time suggested the different mech-

anisms of mechanical loading- and cytokine-induced signaling activities (Figure 3.8). By down-regulating cytokine-initiated Src and FAK activation, moderate fluid flow and Pyk2 depletion appear to promote cartilage health. Further study on the connection between Src/FAK signaling and ECM reorganization by chondrocytes under cytokine or loading stimulation may benefit in developing a therapeutic strategy for OA.

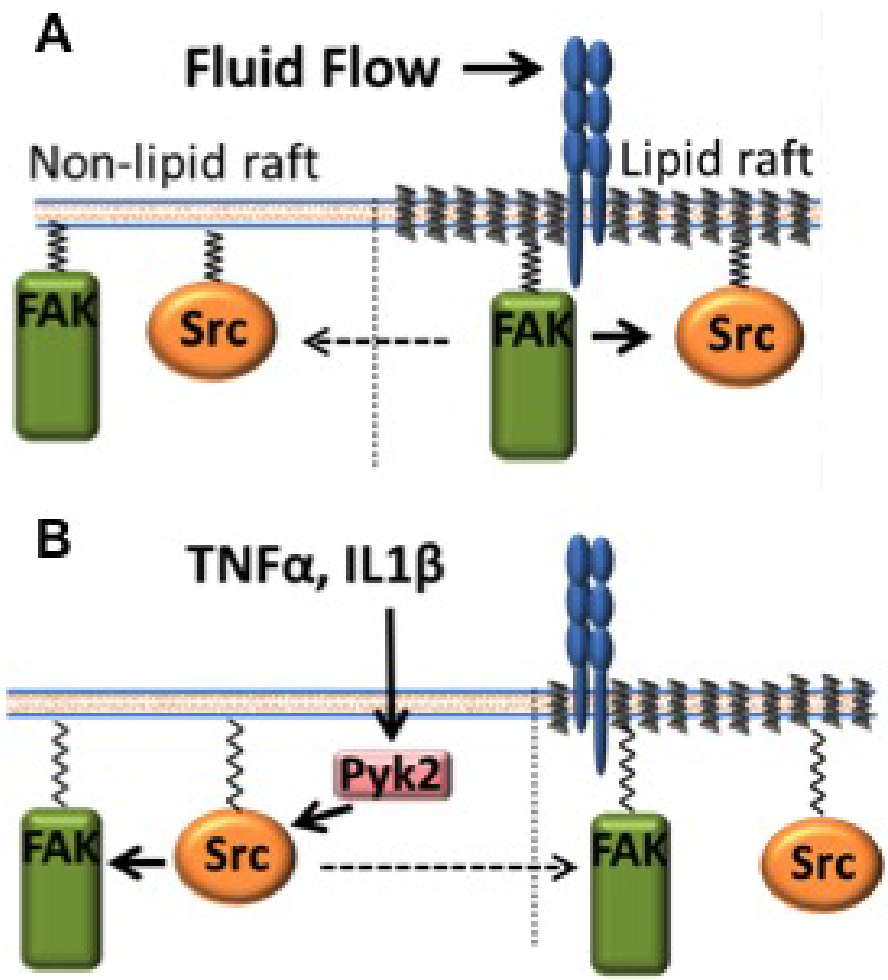

Fig. 3.8.: A proposed model of Src and FAK regulation under fluid flow and cytokines at different subcellular locations. (A) Fluid flow activates FAK in lipid rafts that closely linked with integrin, which subsequently activates Src in lipid rafts and Src in its adjacent non-lipid rafts. (B) TNFα and IL1β activate KRas-Src with the assistance of Pyk2, and eventually activate FAK activities.

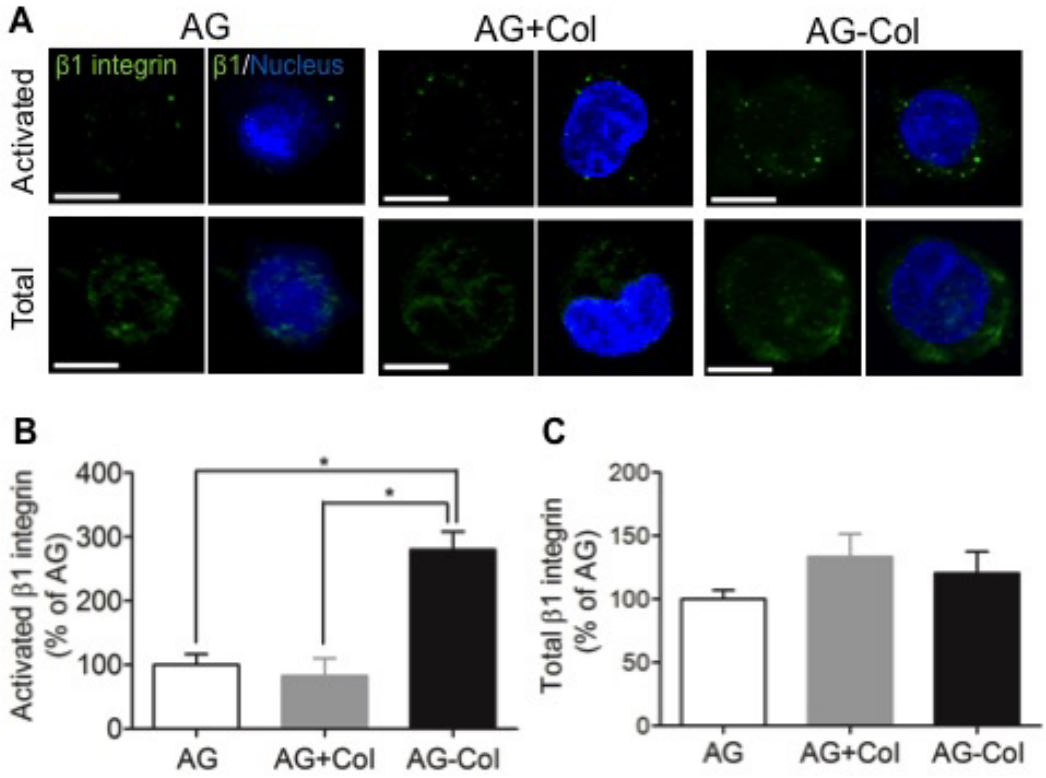

Fig. S 3.1.: Collagen-conjugated agarose gels enable fluid flow-induced Lyn-Src and Lyn-FAK activities via activated integrin. (A) Immunostaining images show that the level of activated and total integrin in collagen-conjugated agarose (AG-Col) gels, collagen-added agarose (AG+Col) gels and agarose (AG) gels. Scale bar, 10 μm. (B,C) The mean GFP values of activated β1 integrin (B) and total β1 integrin (C) in various types of agarose gels were obtained by measuring GFP intensity averaged over the whole cell, and mean values of each type of gels were normalized to the mean values of AG gels. n>6 cells. * p<0.05.

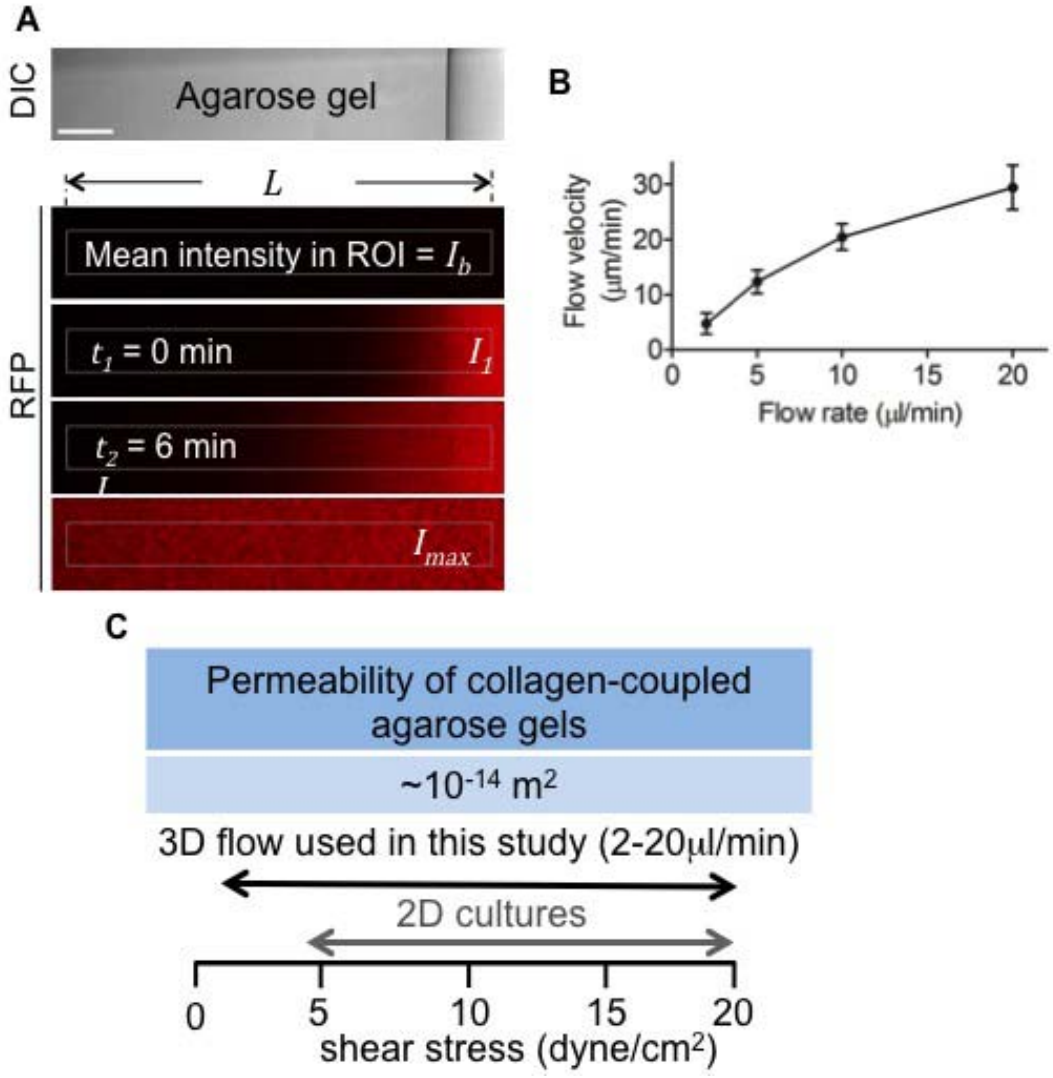

Fig. S 3.2.: Characterization of collagen-conjugated agarose gels. (A) Images illustrate the measurement of flow velocity (μm/min) through agarose gels under specific flow rate (μl/min). (B) The flow velocity through agarose gels corresponds to flow rate that applied. (C) The permeability of collagen-coupled agarose gels, and the shear stress experienced by C28/I2 cells in gels. Corresponding to 2-20 μl/min fluid flow that applied on gels, the shear stress generated is ranged from 2-20 dyne/cm^2. Sample number>7. Scale bar, 100 μm.

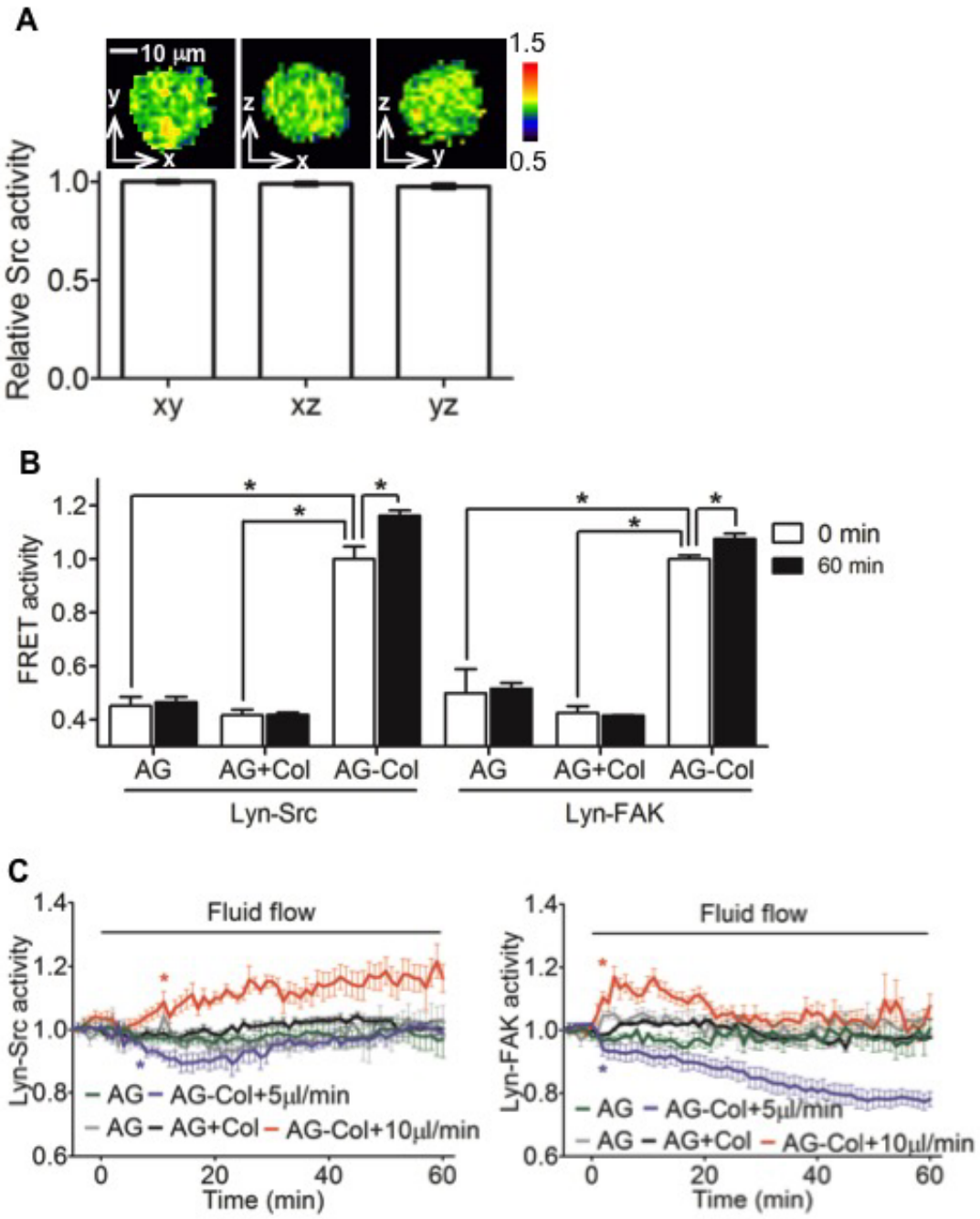

Fig. S 3.3.: Src activities from different orthogonal views have similar activation levels and patterns. (A) C28/I2 cells were transfected with the Lyn-Src biosensor. z-stack images were obtained to generate 3D cell constructs. The activities of Src from each orthogonal view were normalized to that from xy plane. (B) Src and FAK activities in response to 10 μl/min fluid flow in different types of gels. Activities were normalized to those at 0 min in AG-Col gels. (C) Src and FAK activities in response to 5 or 10 μl/min fluid flow in different types of gels. n>7 cells. Scale bar, 10 μm. * p<0.05.

4. THE DIFFERENTIAL ACTIVITIES OF AMPK IN VARIOUS CELLULAR ORGANELLES IN RESPONSE TO MECHANICAL LOADING

4.1 Introduction

It is increasingly recognized that cells growing on 2D flat and rigid substrate sometimes exhibit abnormal cellular functions, whereas 3D culture provides a more physiologically relevant microenvironment for cells. It has been found that the cell culture dimensionality is a crucial fate determinant that influences signaling activities, gene expression and functions of living cells [295]. Evidences have demonstrated that cells in 3D cultures function more similar to cells *in vivo*, as compared to 2D cultured cells [351]. Nevertheless, the mechanisms underlying how culture dimensionality alters cellular behavior is not well understood. One prevailing factor is changes in the cell-matrix interaction, leading to altered cell morphology, cell polarity [352], effective surface-to-volume ratio [289], and integrin-mediated adhesions [353] in 2D culture. The other factor is the mechanical microenvironment experienced by cells and the way of signaling transduction from the outside to the inside of cells are very different in 2D versus 3D culture [354, 355]. Cytoskeletal filaments are key mediators in transmission of mechanical signals and their networks are distinct in 2D versus 3D environment [293]. But so far, experimental evidence showing how culture dimensionality influences subcellular signaling activities in response to loading is lacking. We hypothesized that the culture dimensionality affect cellular signaling by changing the cytoskeletal structure.

AMP-activated protein kinase (AMPK) is a sensor and regulator of ATP levels that maintains the energy homeostasis [193]. Upon activation, AMPK phosphorylates multiple downstream signaling pathways to generate ATP whilst inhibiting

ATP-consuming cellular activities [356]. AMPK has been shown to play crucial roles in inhibiting tumor development [212,213,357], cardiovascular diseases [200,358,359], Type II diabetes [206, 360, 361], inflammatory disorders [219–221], neurodegenerative disorders [226, 227, 229] and most recently, OA [231, 233, 362], a progressive joint disease that is initiated by overuse of joint and progresses with inflammatory responses. It has been discovered that the highly elevated AMPK activity in healthy chondrocytes is suppressed with the progression of OA, and the activation of AMPK substantially downregulates the IL-1 and TNF-induced inflammatory signaling in chondrocytes by inhibiting NFκB signaling [235,362,363]. The inhibition of NFκB is known to preserve the cartilage matrix integrity [231].

AMPK performs various cellular functions and compartmentalization of AMPK is required for execution of multi-task within various cellular locations [273,316,364,365]. Recently, FRET-based AMPK biosensors targeting different subcellular compartments were developed to investigate the dynamics of AMPK at varying subcellular spaces of living cells, including endoplasmic reticulum (ER), mitochondria, nuclear, cytosol, plasma membrane and Golgi apparatus [278]. Although mechanical loading has been found to play pivot roles in OA development [366], the effect of mechanical forces on AMPK signlaing has been studied best in the context of skeletal muscle physiology, while how forces regulate compartmentalized AMPK activities in chondrocytes is unknown. We hypothesized that mechanical loading upregulates AMPK activities in chondrocytes.

In the current study, we employed six fluorescence resonance energy transfer (FRET)-based biosensors that selectively target different subcellular locations to visualize compartmentalized AMPK signaling of cells in a 2D culture or a 3D agarose gel-based model in response to physical stimulation. The cytoskeleton inhibitors, a integrin blocking antibody and a plasma membrane inhibitor were used to study how the signal transduction pathways in the 2D culture different from that in the 3D culture. Four types of siRNA were co-transfected with a AMPK biosensor to abolish

the linker of nucleoskeleton and cytoskeleton (LINC) complex, and the connection between cytoskeleton filaments and nucleus was examined.

4.2 Materials and Methods

4.2.1 AMPK biosensors

FRET-based biosensors were used for monitoring AMPK activities. The cytosolic AMPK (Cyto-AMPK) biosensor consists of the ECFP, an FHA1 domain, an AMPK substrate motif, and Venus cpV E172. Different sequences are fused to Cyto-AMPK to produce biosensors targeting various organelles: plasma membrane (PM-AMPK), Golgi apparatus (Golgi-AMPK), endoplasmic reticulum (ER-AMPK), nucleus (Nuc-AMPK) and mitochondria (Mito-AMPK). The phosphorylation of the AMPK substrate leads to the binding of FHA1 substrate to the binding domain, resulting in the fluorescence resonance transfer from the donor (ECFP) to the acceptor (YFP variant Venus). Hence, AMPK activities can be visualized as changes of the emission ratio of the YFP/CFP. The specificity of the biosensors has been characterized previously [278, 316].

4.2.2 Cell culture and transfection

The human chondrocyte cell line C28/I2 was used. Cells were cultured in Dulbecco's modified Eagle's medium (DMEM; Lonza) containing 10 % FBS (Hyclone) and 1 % penicillin/streptomycin (Lonza), and maintained at 37 °C, 5 % CO_2 in a humidified incubator. Neon transfection system (Invitrogen) was used to transfect AMPK biosensors and siRNA into the cells. After transfection, cells were cultured in serum-free and antibiotic-free DMEM for 24 hours before imaging.

4.2.3 Chemical reagents, antibodies and siRNAs

Sulfo-SANPAH (Sigma) was employed to crosslink agarose gel (Sigma) with Type II collagen (Sigma). Agarose (low melting temperature agarose; Lonza) was used to prepare 3D agarose gels. integrin $\beta 1$ antibody (Santa Cruz Biotechnology; A-4, 10 g/ml) was used to block integrin activities. Methyl-beta-cyclodextrin (MβCD; Sigma; 10 mM) was used to extract cholesterol from the lipid rafts of the plasma membrane. Cytochalasin D (Enzo life sciences; 1 μg/ml) was used to disrupt actin filaments. Blebbistatin (Toronto research chemicals; 50 μM) was used to inhibit myosin II. ML-7 (Biomol; 25 μM) was used to inhibit myosin light chain kinase. Nocodazole (Sigma; 1 μM) was used to inhibit microtubule. α-Tubulin-Alexa Fluor 488 was used to label microtubule and DyLight 554 Phalloidin was used to label actin filaments (Cell Signaling Technology). Plectin siRNA, Lamin A/C siRNA, SUN1 siRNA, and SUN2 siRNA (Santa Cruze Biotechnology) were used to selectively silence their activities.

4.2.4 Shear stress application in 2D

Fluid flow-induced shear stress regulates chondrocyte signaling and metabolism [367]. Because the shear stress of 2-20 dyne/cm^2 has been found to influence chondrocyte activities either positively or negatively [368–370], in this study, we used 5 and 20 dyne/cm^2 shear stress to stimulate chondrocytes growing on 2D culture. During imaging, an oscillatory flow at 2 Hz was applied to cells growing in the μ-slide cell culture chamber (Ibidi) [371]. The chamber was perfused with HEPES-buffered (20 mM), phenol red-free DMEM without serum. The fluid flow-induced shear stress was controlled by a peristaltic pump (Cole-Parmer) and two pulse dampeners (Cole-Parmer) were used to minimize pulsation of the flow.

4.2.5 3D agarose-chondrocytes constructs

The collagen-coupled agarose gels (AG-Col) were prepared as detailed described in Chapter 3. Briefly, the collagen solution was reacted with the sulfo-SANPAH to produce 1.2 mg/ml Type II collagen-sulfo-SANPAH solution. The 4 % (wt/vol) agarose solution was prepared, autoclaved, and cooled to 40 °C. Three parts of 4 % agarose were combined with one part of collagen-sulfo-SANPAH solution. The mixture was exposed under UV light for 20 min to conjugate the collagen to the agarose. After conjugation, the agarose mixture was washed with PBS thoroughly. Before transfection, 3 % modified agarose gels were melted down at 45 °C and cooled to 37 °C. Two parts of 3 % agarose gel were mixed with one part of 3 × DMEM containing transfected cells to produce the mixture of 2 % agarose and 1 × DMEM with cells. The mixture was injected into an flow chamber and cooled at room temperature for 30 min. The gel was supplemented with fresh 1 × phenol red-free serum-free DMEM and transferred to incubator for 24 hours before imaging.

4.2.6 Fluid flow application in 3D

Fluid flow-induced shear stress has been shown to play crucial roles in the development and progression of OA [372]. During imaging, the agarose gel construct in a flow chamber was perfused with HEPES buffered, phenol red-free and serum-free DMEM. During imaging, a syringe pump (Harvard Apparatus) was employed to apply pulsatile flow (0.2Hz) at 5, 10, and 20 μl/min for 1 hour, which will produce 5 to 20 dyne/cm^2 shear stress experienced by cells as characterized in Chapter 3.

4.2.7 FRET microscopy and image analysis

During imaging, cells were maintained at 37 °C and 5 % CO_2 using the gas incubation and heating system (Ibidi). Images were obtained using a Nikon Ti-E inverted microscope equipped with an electron-multiplying charge-coupled device (EMCCD)

camera (Evolve 512; Photometrics), a filter wheel controller (Sutter Instruments), and a Perfect Focus System (Nikon) that maintains the focus during time-lapse imaging. The following filter sets (Semrock) were used: CFP excitation: 438/24 (center wavelength/bandwidth in nm); CFP emission (483/32); YFP (FRET) emission: 542/27. To minimize photobleaching, cells were illuminated with a 100 W Hg lamp through an ND64 (∼1.5 % transmittance) neutral density filter. Images were acquired with a 40 × (0.75 numerical aperture) objective. FRET images for AMPK activities were generated with NIS-Elements software (Nikon) by computing an emission ratio of YFP/CFP for individual cells over time. For 3D images, the representative FRET ratio images were produced using ImageJ (NIH). All FRET images were scaled according to the color bar.

4.2.8 Immunostaining and confocal microscopy

C28/I2 cells cultured in collagen-conjugated agarose gels or on collagen-coated glass bottom dishes were incubated for 24 h before staining. For the 3D culture, gels were washed with PBS three time to remove medium. The cells were fixed with 4 % paraformldehyde for 45 min. After rinsing, the gels were permeabilized with 0.5 % Triton X-100 (Sigma) in PBS for 45 min at room temperature, and then incubated with blocking buffer (5 % BSA, serum, 20 % Polyvinylpyrrolidone (Amresco) in PBS combined into 1:1:1 ratio) for 2 hours at RT. For the 2D culture, cells were fixed following protocol from Cell Signaling Technology. Briefly, cells in the 2D culture were fixed with 4 % paraformldehyde for 15 min. After rinsing, cells were treated with blocking solution for 60 min. After fixation, samples were incubated with primary antibodies-conjugated with fluorescent dyes overnight at 4 °C. Before imaging, cell nuclei were labeled by DAPI (Sigma). An Olympus Fluoview FV1000 confocal microscope was used to visualize actin and microtubule structure. Images were acquired using a 60 × objective lens (1.2 numerical aperture; Olympus).

4.2.9 Statistical analysis

Statistical data is presented as the mean ± standard error of the mean (SEM). One-way ANOVA followed by Dunnett's post hoc test was used to determine the statistical differences. Student's t-test was used to compare two groups. Statistical analyses were conducted using Prism 5 software (GraphPad Software). $p<0.05$ was considered statistically significant. In the time course data, * indicates AMPK activity is significantly different from that before stimulation.

4.3 Results

4.3.1 AMPK activities at different subcellular organelles are substantially activated by shear stress in 2D culture

We first tested whether AMPK at various subcellular compartments of living chondrocytes respond to different magnitudes of shear stress in 2D environment. We transfected chondrocytes with one of the six FRET-based AMPK biosensors: Cyto-AMPK targeting cytosol, PM-AMPK targeting plasma membrane, Nuc-AMPK targeting nucleus, ER-AMPK targeting ER, Mito-AMPK targeting mitochondria, and Golgi-AMPK targeting Golgi apparatus. The AMPK activities were assessed by monitoring changes of the emission ratios of YFP/CFP of the biosensors in response to stimulus in the same cell. The AMPK activities were quantified over the whole cell and normalized to the ratio value at 0 min. In C28/I2 human chondrocytes growing on a 2D flow chamber, Cyto-AMPK activities were increased by the application of 5 and 20 dyne/cm^2 shear stress and reached its maximal at 18min by 5 dyne/cm^2 (7.5 % increase) and at 60 min by 20 dyne/cm^2 (12.8 % increase) (Figure 4.1A). The PM-, Nuc-, ER-, Mito- and Golgi-AMPK activities were also upregulated by shear stress application and reached a maximal by 5 dyne/cm^2 (PM: 14.5 % increase at 60 min; Nuc: 11.7 % increase at 12 min; ER: 17.0 % increase at 58 min; Mito: 4.1 % increase at 6 min; and Golgi: 8.8 % increase at 14 min), and by 20 dyne/cm^2 (PM: 8.3 % increase

at 38 min;Nuc: 11.0 % increase at 58 min; ER: 12.5 % increase at 20 min; Mito: 7.8 % increase at 20 min; and Golgi: 9.8 % increase at 26 min), correspondingly (Figure 4.1B-F). However, the activities of Mito-AMPK failed to maintain the activation and were returned to basal levels at latter timepoints. Statistical results showed that, except Mito-AMPK, 60 min after 5 dyne/cm^2 and 20 dyne/cm^2 shear stress stimulation, the activities of AMPK were significantly different from those at time 0 min ($p<0.05$).

4.3.2 AMPK activities in plasma membrane and nucleus are substantially activated by fluid flow-induced shear stress in 3D

We further investigated AMPK activities of C28/I2 cells embedded in 3D type II collagen-conjugated agarose gel scaffolds. The detailed characterization of the 3D agarose gel-based loading system was described in Chapter 3. The transfected cells were mixed with agarose gel, and the mixture was injected into a flow chamber. During imaging, we applied 5, 10 and 20 μl/min fluid flow through the chamber, which generate 5, 10 and 20 dyne/cm^2 shear stress experienced by chondrocytes, respectively. Results showed that only Nuc- and PM-AMPK activities were upregulated by loading, and reached maximum activities (Nuc + 5 μl/min: 9.9 % increase at 54 min; Nuc + 10 μl/min: 9.8 % increase at 26 min; Nuc + 20 μl/min: 11.0 % increase at 58 min; PM + 5 μl/min:16.0 % increase at 58 min; Nuc + 10 μl/min: 15.3 % increase at 36 min; and Nuc + 20 μl/min: 15.2 % increase at 56 min) (Figure 4.2B, C). However, the activities of Cyto-, ER-, Golgi and Mito-AMPK were not significantly altered by loading (Figure 4.2A, D-F). To characterized the temporal profiles of Nuc- and PM-AMPK in 2D versus in 3D, we determined $t_{\frac{1}{2}}$, which measured the time required for Nuc- and PM-AMPK to reach their half-maximal activity levels (Figure 4.2G, H). The results showed that the mean and standard deviation of $t_{\frac{1}{2}}$ of Nuc-AMPK in 2D (5 dyne/cm^2: 4.89 $\pm$ 0.56; and 20 dyne/cm^2: 4.15 $\pm$ 0.66) were not significantly different from those in 3D (5 μl/min: 4.22 $\pm$ 0.62; and 20 μl/min: 5.75 $\pm$ 0.75). The

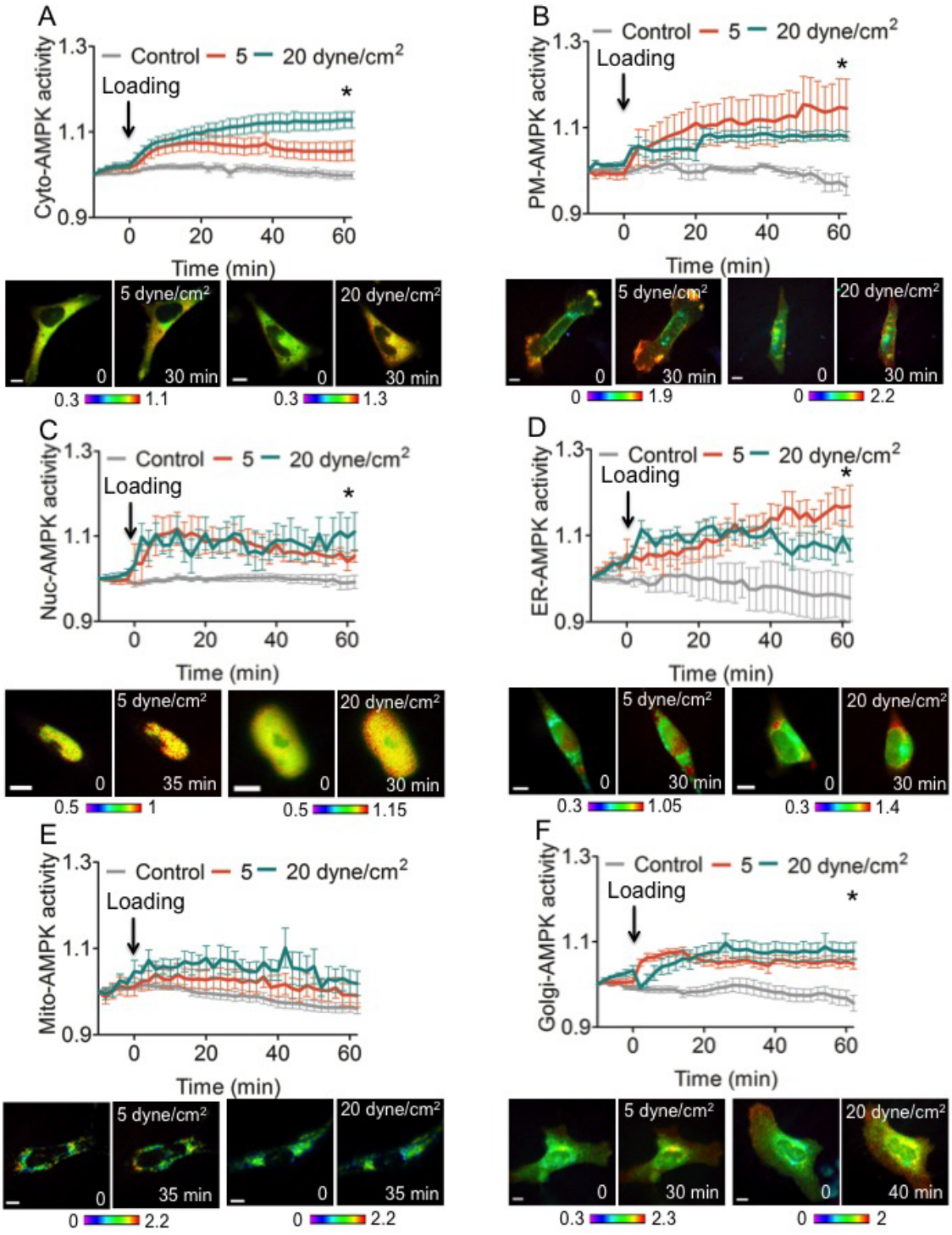

Fig. 4.1.: AMPK activities at differential subcellular organelles are upregulated by the application of shear stress in 2D culture. The YFP/CFP ratio images were scaled according to the corresponding color bar. (A-F) Cyto-AMPK, PM-AMPK, Nuc-AMPK, ER-AMPK, Mito-AMPK and Golgi-AMPK activities under shear stress in 2D. n>7 cells. Scale bar, 10 μm. * p<0.05.

mean and standard deviation of $t_{\frac{1}{2}}$ of PM-AMPK in 2D (5 dyne/cm^2: 21.33 $\pm$ 2.23; and 20 dyne/cm^2: 18.50 $\pm$ 2.19) were also not significantly different from those in 3D (5 μl/min: 20.25 $\pm$ 1.90; and 20 μl/min: 18.67 $\pm$ 1.95).

4.3.3 Cytoskeletal structure and integrin activity play roles in the regulation of AMPK activities by loading in 2D culture

Since the activation patterns of AMPK activities in 2D were different from those in 3D culture, we hypothesized cytoskeletal structure may be responsible for these altered signaling responses to loading in different culture dimensions. Immunostaining images showed actin and microtubule structure in C28/I2 human chondrocytes growing on a 2D plate (Figure 4.3A) or embedded in the 3D agarose gel (Figure 4.3B). In 2D, the chondrocyte generates strong actin fibrils through the whole cell, and has microtubules protruding away. However in 3D environment, microtubule tightly encapsulates the cell neuclei, and actin mostly concentrates near plasma membrane and only sparsely distributed as bright dots in cytosol. We hypothesized that the strengthened cytoskeletal networks on 2D substrates enhance the sensitivity of cells to mechanical loading.

To investigate factors contributing to the discrepancies of cellular signaling between cells in 2D and 3D model, cells transfected with one of AMPK biosensors were seeded on 2D flow chambers. Before imaging, cells were pretreated with one of reagents for 1 hour (integrin blocking antibody to silence integrin activity, MβCD to disrupt the lipid rafts of plasma membrane, CytoD to disrupt actin cytoskeleton, Bleb to inhibit myosin II, ML7 to inhibit myosin light chain kinase, and Nocodazole to disrupt microtubule). During imaging, cells were exposed to 10 dyne/cm^2 shear stress for 1 hour, and the AMPK activities before and after loading application were recorded. The AMPK activities at 60 min were normalized to the activity value at 0 min and $*$ denotes AMPK activities at 60 min are significantly different from their activities at 0 min (Figure 4.3C-H). The disruption of lipid rafts of plasma membrane

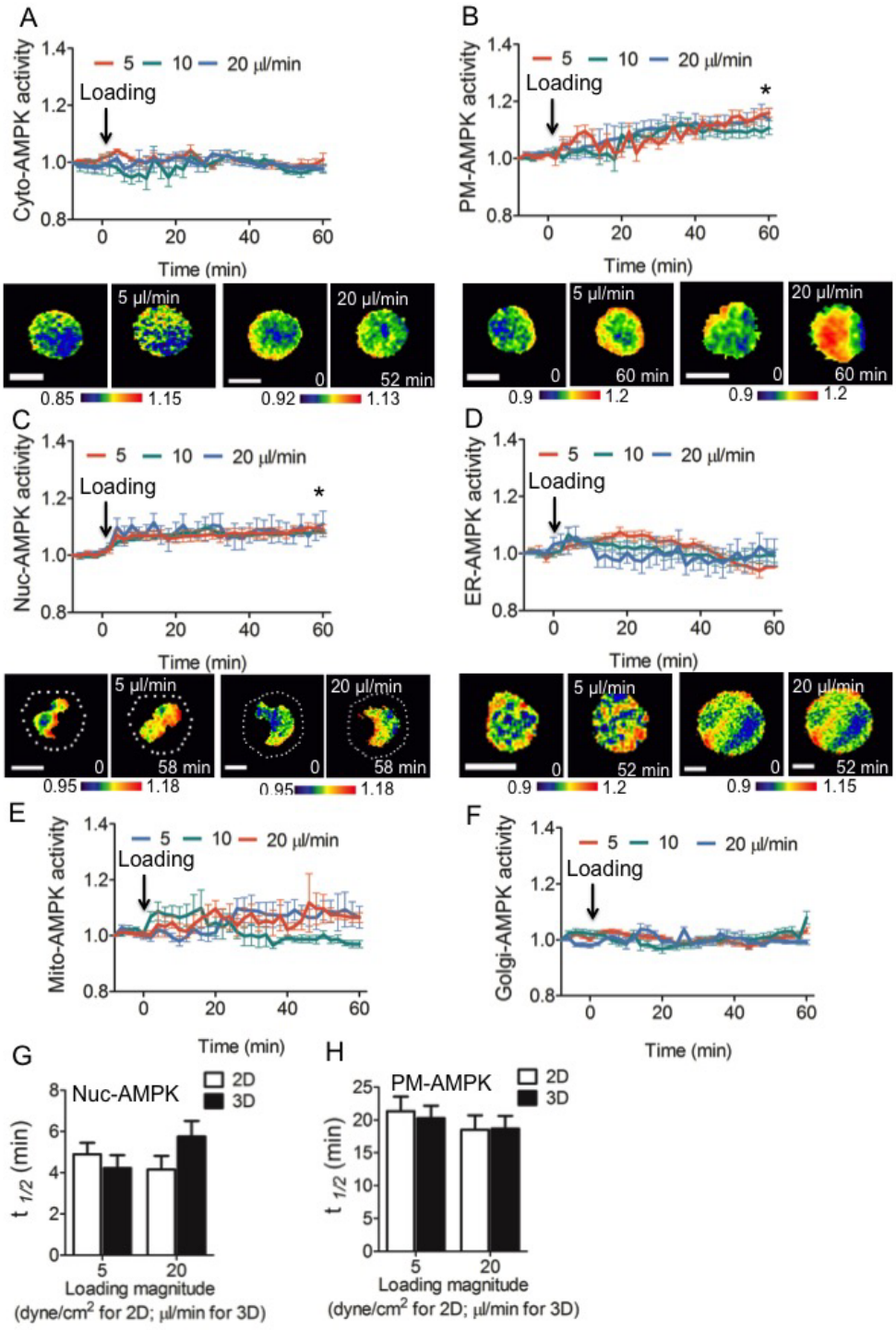

Fig. 4.2.: AMPK activities at plasma membrane and nucleus are upregulated by the application of shear stress in 3D culture. (A) Cyto-AMPK activities under shear stress in 3D. (B) PM-AMPK activities under shear stress in 3D. (C) Nuc-AMPK activities under shear stress in 3D. (D) ER-AMPK activities under shear stress in 3D. (E) Mito-AMPK activities under shear stress in 3D. (F) Golgi-AMPK activities under shear stress in 3D. n>7 cells. Scale bar, 10 μm. * p<0.05.

and actin cytoskeleton prevented Cyto-AMPK activation by shear stress (Control: 5.7 % increase; Anti-integrin: 6.5 % increase; MβCD: 0.2 % decrease; CytoD: 0.1 % increase; Bleb: 6.5 % increase; ML7: 5.1 % increase; and Nocodazole: 4.2 % increase); the silence of integrin activity and the disruption of plasma membrane abolished PM-AMPK activation by shear stress (Control: 8.2 % increase; Anti-integrin: 1.4 % decrease; MβCD: 0.1 % decrease; CytoD: 10.4 % increase; Bleb: 7.4 % increase; ML7: 8.0 % increase; and Nocodazole: 6.7 % increase); the integrin activation, the existence of lipid rafts as well as the integrity of cytoskeletal structure are required for the activation of Nuc-AMPK by shear (Control: 8.4 % increase; Anti-integrin: 1.1 % increase; MβCD: 0.1 % decrease; CytoD: 0.1 % increase; Bleb: 0.1 % decrease; ML7: 2.7 % increase; and Nocodazole: 0.7 % increase); the disruption of microtubule and plasma membrane prevented ER-AMPK activation by shear stress (Control: 10.3 % increase; Anti-integrin: 7.7 % increase; MβCD: 0.2 % decrease; CytoD: 6.1 % increase; Bleb: 7.4 % increase; ML7: 6.8 % increase; and Nocodazole: 0.5 % increase); the activities of Mito-AMPK are still not highly responsive to loading W/O treatments (Control: 3.1 % increase; Anti-integrin: 0.3 % increase; MβCD: 0.3 % decrease; CytoD: 1.2 % increase; Bleb: 0.4 % increase; ML7: 0.1 % decrease; and Nocodazole: 2.4 % increase); and microtubule is not required for Golgi-AMPK regulation by shear stress (Control: 8.3 % increase; Anti-integrin: 0.1 % increase; MβCD: 0.1 % decrease; CytoD: 0.3 % increase; Bleb: 2.5 % increase; ML7: 0.8 % increase; and Nocodazole: 7.5 % increase).

4.3.4 The integrin, cytoskeleton structure and LINC complex play roles in the regulation of Nuc-AMPK signaling by loading in 3D

While the integrin activity level and cytoskeletal structure in 3D are lower and weaker than those in 2D cultures, their potential roles in mechanotransduction have been studied [373]. To examine the importance of cytoskeleton and integrin activity in AMPK activation by mechanical loading in 3D cultures, chondrocytes transfected

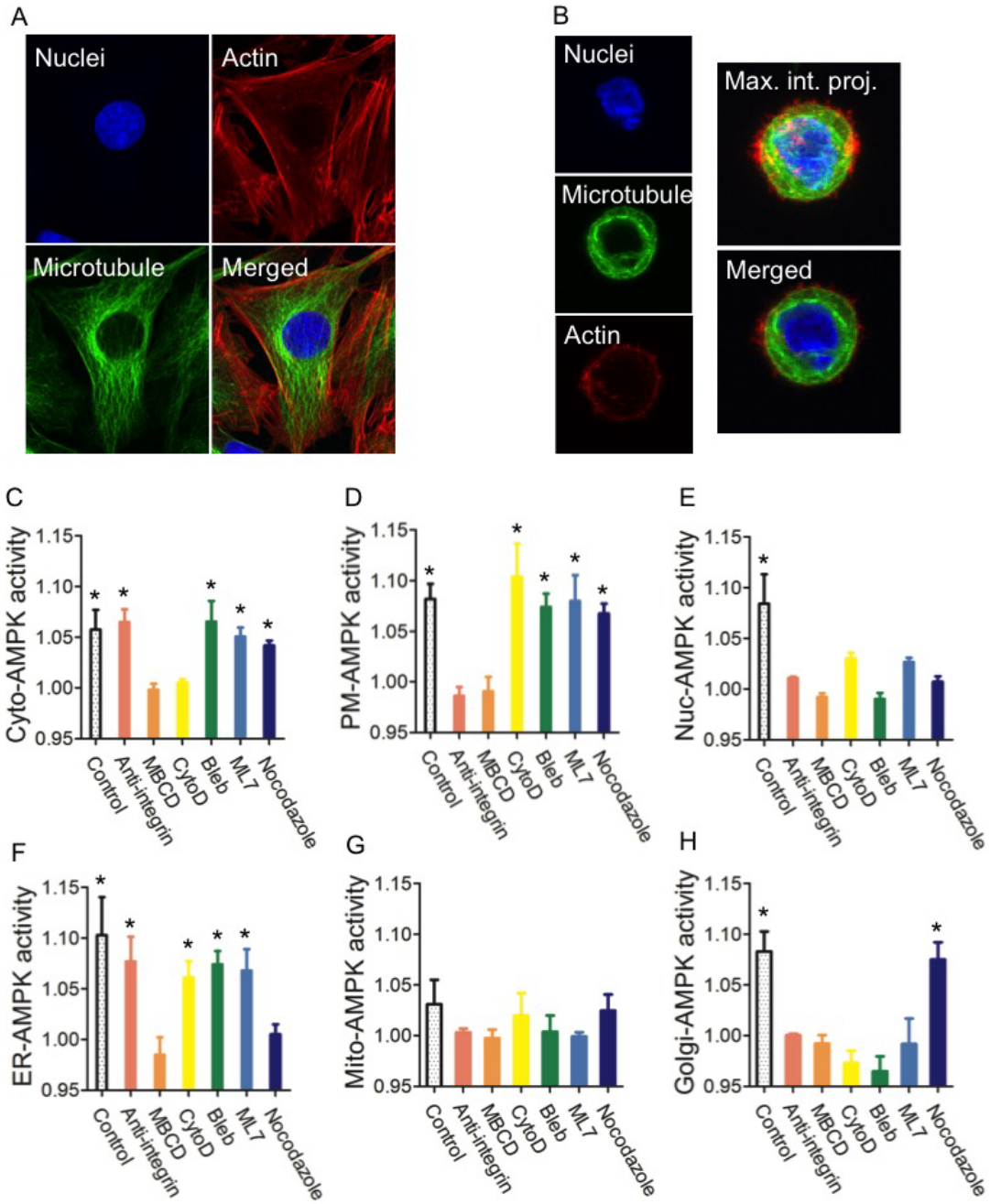

Fig. 4.3.: The roles of integrin and cytoskeleton in the regulation of AMPK by shear stress in 2D culture. (A) Immunostaining images showing the structure of actin and microtubule in the 2D culture. (B) Immunostaining images showing the structure of actin and microtubule in the 3D culture. The Max. int. proj. image generated from z-stack images showing the highest intensity of each XY coordinate along the Z-axis in a 2D image. (C-H) C28/I2 chondrocytes transfected with one of AMPK biosensors were pretreated with one of reagents for 1 hour before subjected to 10 dyne/cm^2 shear stress. n>7 cells. * p<0.05.

with one of AMPK biosensors were mixed with agarose gel to produce 3D cell-gel constructs in 3D flow chamber. Before imaging, cells were incubated with one of reagents for 1 hour. During imaging, cells were subjected to 10 μl/min fluid flow for 1 hour, and the AMPK activities at distinct subcellular locations at 0 and 60 min were recorded. The AMPK activities at 60 min were normalized to those at 0 min and $*$ denotes AMPK activities at 60 min are significantly different from their activities at 0 min. The PM-AMPK activation by fluid flow was abolished by the silence of integrin and the disruption of plasma membrane (Figure 4.4B) (Control: 10.8 % increase; Anti-integrin: 1.4 % decrease; MβCD: 0.1 % increase; CytoD: 11.8 % increase; Bleb: 8.2 % increase; ML7: 10.1 % increase; and Nocodazole: 13.9 % increase); the Nuc-AMPK activation by flow requires integrin activation, the integrity of lipid rafts as well as complete cytoskeletal structure (Figure 4.4C) (Control: 8.3 % increase; Anti-integrin: 1.1 % increase; MβCD: 1.6 % increase; CytoD: 1.8 % increase; Bleb: 2.5 % increase; ML7: 1.4 % increase; and Nocodazole: 2.6 % decrease); and Cyto-, Mito-, Golgi-, ER-AMPK activities were still not substantially altered by flow (Figure 4.4A, D-F).

LINC complex physically associates cytoskeletal filaments with the nuclear envelope [374]. To evaluate roles of LINC complex in Nuc-AMPK regulation by loading in 3D, chondrocytes co-transfected with one of siRNAs and one of AMPK biosensors were embedded in agarose gels. During imaging, cells were exposed to 10 μl/min fluid flow for 1 hour. The AMPK activities at 60 min were normalized to those at 0 min and $*$ denotes AMPK activities at 60 min are significantly different from their activities at 0 min. The silence of Lamin A/C, Plectin, SUN1 and SUN2 totally abolished Nuc-AMPK activation by fluid flow (Control: 8.3 % increase; Plectin siRNA: 0.1 % increase; SUN1 siRNA: 0.6 % increase; SUN2 siRNA: 0.1 % decrease; and Lamin A/C siRNA: 0.3 % decrease), while the activation of PM-AMPK by fluid flow was not significantly altered by the treatment of siRNAs (Control: 10.8 % increase; Plectin siRNA: 9.2 % increase; SUN1 siRNA: 8.9 % increase; SUN2 siRNA: 9.8 % increase; and Lamin A/C siRNA: 10.0 % increase). The Cyto-AMPK activities were

still not highly responsive to loading (Control: 1.5 % increase; Plectin siRNA: 0.1 % increase; SUN1 siRNA: 1.5 % increase; SUN2 siRNA: 1.4 % increase; and Lamin A/C siRNA: 1.6 % increase) (Figure 4.4G). The silence of LINC components didn't affect PM-AMPK activation by loading, and Cyto-AMPK activities were still not highly responsive to fluid flow.

4.4 Discussion

In this study, we used FRET-based AMPK biosensors targeting distinct subcellular compartments in conjunction with live cell imaging to investigate the spatiotemporal activities of AMPK at different subcellular locations in C28/I2 human chondrocytes cultured in a 2D or a 3D culture system. We employed six types of AMPK biosensors that specifically label AMPK activities in the cytosol, plasma membrane, nuclei, ER, mitochondria, and Golgi apparatus. Although the diverse-functions of AMPK at various cellular organelles have been documented [375–377], its responses to physiological stimuli at different compartments is poorly understood. Cells growing on 2D culture were exposed to 5 and 20 dyne/cm^2 shear stress for 1 hour. We found that AMPK at all five locations is upregulated by shear stress, but Mito-AMPK is not highly responsive to loading. AMPK has been found as a major regulator of mitochondrial biogenesis in response to AMPK signaling [378, 379], and the exact mechanism underlying why Mito-AMPK activity is not substantially activated by forces is not clear. Since in skeletal muscle cells, the physiological stimuli has been found to regulate AMPK signaling in a different way than nutrients [380], we hypothesized that mechanical loading and nutrients regulate AMPK activities via different mechanisms in chondrocytes. In this study, we mainly focused on the comparison between the 2D culture and the 3D culture. Future investigation of AMPK responses to different types of stimuli is an important subject and requires further consideration.

Using the 3D agarose-chondrocytes constructs described in the Chapter 3, we investigated compartmentalized AMPK activities under fluid flow-induced shear stress.

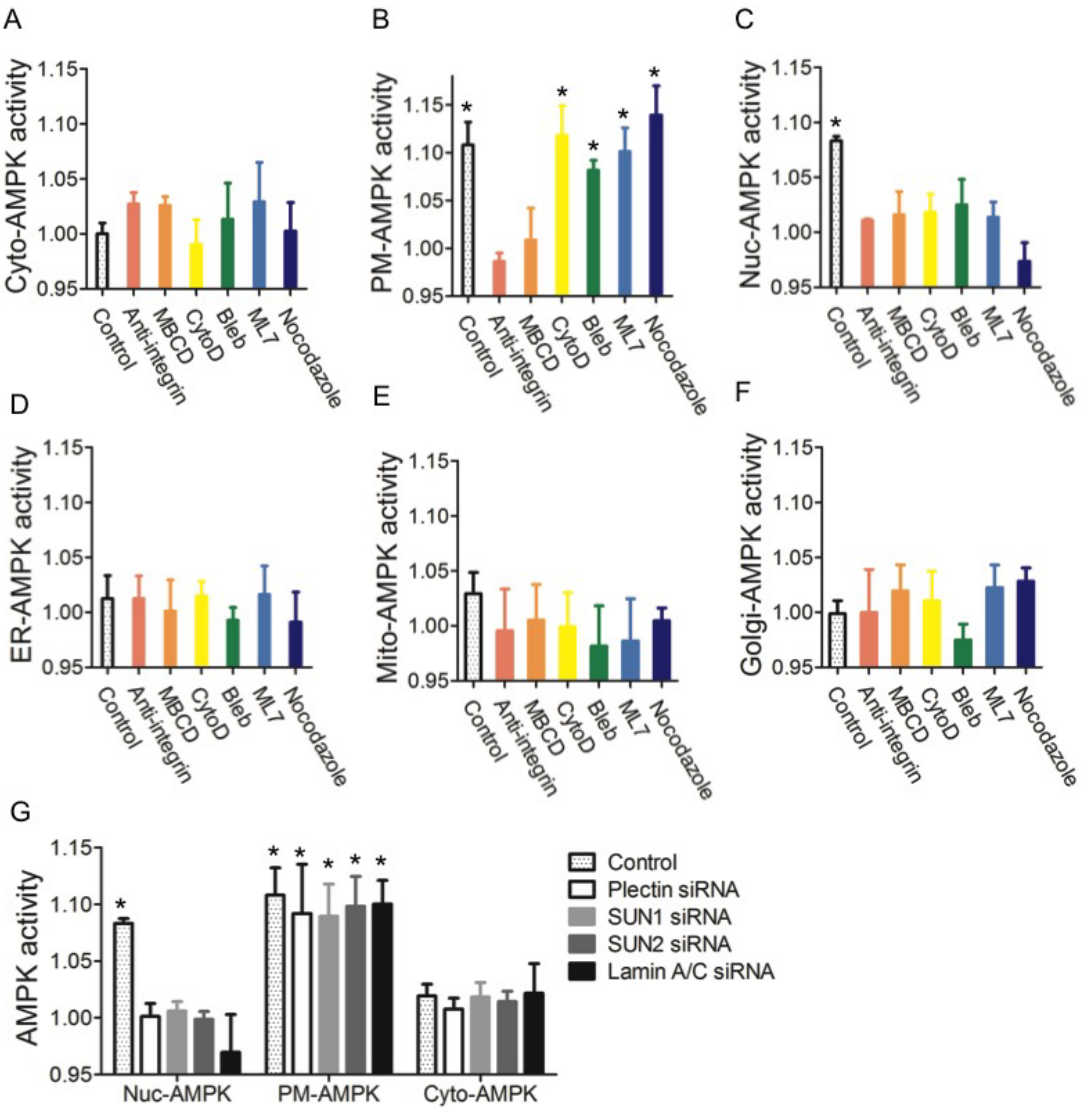

Fig. 4.4.: The roles of integrin, cytoskeleton structure and LINC complex in the regulation of Nuc- and PM-AMPK by fluid flow in 3D culture. (A-F) C28/I2 chondrocytes transfected with one of AMPK biosensors were pretreated with one of reagents for 1 hour before subjected to 10 μl/min fluid flow for another 1 hour. n>7 cells. * p<0.05. (G) C28/I2 cells co-transfected with one of AMPK biosensors and one of siRNAs were subjected to 10 μl/min fluid flow for 1 hour.

The forces experienced by cells in 3D culture are characterized in the Chapter 3: 5-20 μl/min fluid flow in 3D generates 5-20 dyne/cm^2 shear stress on 2D and the cell deformation is negligible (Figure S3.2). Thus, the results obtained from 3D loading model are comparable with those obtained from the 2D model. We observed that only PM- and Nuc-AMPK were significantly activated by fluid flow, while AMPK at other locations were not altered by loading. Since it has been found that AMPK translocates from cytoplasm to nucleus upon the application of stress, such as heat shock and oxidant exposure [381], it is possible that upon the application of forces, AMPK moves to nucleus via cytoskeleton and is activated. Another possibility is that mechanical signals transmit from plasma membrane to nucleus via the cytoskeleton and LINC complex, and activate the AMPK in nucleus [382]. AMPK has been shown to closely interact with integrin activity [383–385]. Our finding that the inhibition of integrins prevent PM-AMPK activation by loading in 3D suggests that integrins regulate the activation of AMPK near plasma membrane by forces and this activation is independent of the cytoskeleton. The activation pattern and level of Nuc- and PM-AMPK in 3D culture are highly similar to those in 2D culture, suggesting the factors (e.g. integrins and cytoskeleton) that control the AMPK activation in plasma membrane and nucleus might maintained their functionality in different culture dimensions. It is also possible that there are compensatory mechanisms involved, which requires further studies.

There are several reports suggesting that culture dimensions regulate cellular functions [386, 387] and cytoskeletal structures [388]. We imaged actin and microtubule structure of chondrocytes in 2D and 3D environment. Immunostaining images showed distinct cytoskeleton patterns in different dimensional cultures: in the 3D, microtubules wrap cell nucleus, and actin is mostly concentrated in the plasma membrane and sparsely distributed near the nucleus; while in 2D, both actin and microtubules are well developed and extend across the cytoplasm.

We further specifically disrupted cytoskeletal components or plasma membrane using drugs and monitored the loading-induced compartmentalized AMPK activities

of chondrocytes in 2D culture. The disruption of plasma membrane and actin cytoskeleton prevented the activation of AMPK in cytosol, suggesting the integrity of plasma membrane and actin fibrils are required for the mechanical signal transduction through cytosol. Our observation is consistent with the previous findings that mechanical forces distort membrane cortex and transmit physical signals to the cytosol [389] via actin cytoskeleton [390](Figure 4.5A). The silence of integrin and the disruption of plasma membrane prevented the activation of AMPK in plasma membrane. Integrin is reponsible for mechanochemical conversion near the plasma membrane. The integrin in plasma membrane is the key receptor of mechanical signals, and is capable of transmiting mechanical signals to regulate signaling molecules near cell surface without the assistance of cytoskeleton (Figure 4.5A). Both intact plasma membrane and cytoskeletal support are required for the regulation of AMPK activity in nucleus by loading (Figure 4.5A), which supports the earlier finding that integrins are physically connected to nuclear scaffolds via cytoskeletal networks [373,391]. The regulation of ER-AMPK activities by loading in the 2D culture requires intact plasma membrane and microtubule (Figure 4.5A). Since ER is highly correlated with microtubule [392], it either slides along or attaches to microtubules [393], we proposed the model that the distortion of plasma membrane transmit signals to ER through microtubule (Figure 4.5A). We did noticed that the inhibition of actin filaments, myosin kinase and myosin light chain II slightly reduced activation levels of ER-AMPK as compared to the control group, while they are not significantly different. The Mito-AMPK is not highly responsive to shear stress, suggesting that its regulation may be preferentially influenced by nutrients, not mechanical loading. The activation of Golgi-AMPK requires integrin, plasma membrane, actin filaments, myosin kinase and myosin light chain II, while microtubules are not involved (Figure 4.5A). We also observed that except Nuc- and PM-AMPK, the activation of Cyto-, ER- and Golgi-AMPK is independent of integrin activity. Although there are many differences between 2D and 3D conditions, our results suggest that the altered cytoskeletal

networks is a critical factor that contributes to the differential cellular signaling in the 2D versus the 3D culture.

While the cytoskeltal structure in 3D is dissimilar to that in 2D culture, it plays crucial roles in mechanotransduction of chondrocytes in 3D culture. The AMPK activation near plasma membrane requires integrins and intact plasma membrane; and the AMPK activation in nucleus requires integrins, plasma membrane as well as the cytoskeleton (Figure 4.5B). These results are consistent with those found in the 2D culture, suggesting that cells in the 2D model share similarities with cells in 3D environment. It has been known that SUN family members are inner nuclear membrane proteins that transmit signals to Lamins [394], and Lamins are an extended part of the LINC complex that transmit forces across the nuclear envelope to regulate signaling cascades and gene transcription [395]. However, most studies have been performed using the 2D model, and to our knowledge, this is the first study on the physical connection between cytoskeleton filaments and nucleus in 3D.

In summary, our findings of the distinct compartmentalized AMPK activation patterns in 2D and 3D cultures suggest the importance of culture dimensions on cellular signaling activities. By selectively inhibiting integrins, plasma membrane and cytoskeletal networks, we observed that the altered cytoskeletal structures influence the differential cellular activity of chondrocytes in 2D versus 3D culture. The LINC complex physically links the cytoskeleton and nucleus, and transmit mechanical signals to the nucleus. The work herein suggests that the different culture dimensions may influence cellular functions, which is, at least partially, due to the altered cytoskeletal structures.

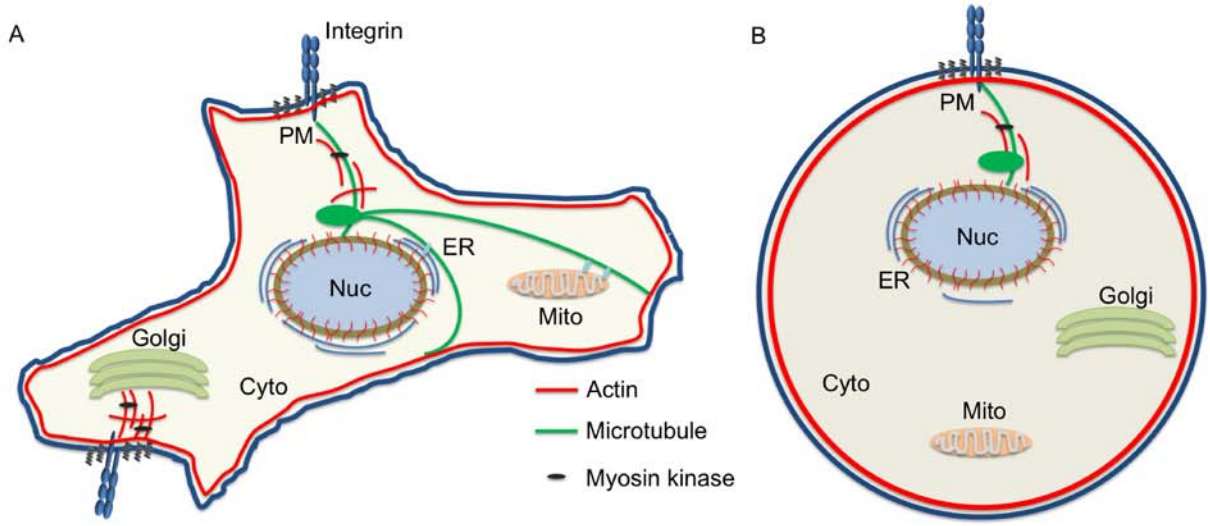

Fig. 4.5.: A proposed model of cytoskeleton connection with subcellular organelles in the 2D or 3D culture. (A) Strong microtubule and actin filaments are developed in cells in 2D culture, and responsible for AMPK activation by shear stress at different organelles. In cytosol, actin filaments transmit membrane distortion and regulate the AMPK activity in the cytosol; near plasma membrane, integrin on cell surface senses mechanical signals and activate AMPK activity; to activate AMPK in nucleus, integrin senses mechanical signals and transmit signals through cytoskeleton networks to nuclear envelops; near the ER, the distortion of plasma membrane regulates AMPK activity near the ER through microtubule; and to activate AMPK near Golgi, the integrin receives mechanical signals and regulate AMPK activity near Golgi via actin filaments. (B) The cytoskeletal structure of cells in 3D is distinct from that in 2D culture. The AMPK activity near plasma membrane gets activated with the assistance of integrin, and the signal transduction to nucleus requires integrin and cytoskeleton networks.

5. CONCLUSIONS AND FUTURE DIRECTIONS

Osteoarthritis aggressively affects millions of people worldwide. Conservative treatments include physical therapy and occupational therapy. In physical therapy, patients learn how to stretch stiff joints without damage them further; and in occupational therapy, patients learn how to change their living environment to reduce unnecessary motions that may further irritate joints. When conservative therapies no longer help, patients will be recommended to have joint replacement, in which the damaged joint will be replaced with plastic or metal materials. However, the surgical risks carried with this procedure, like infections, blood clots, and unsatisfied joint performance, as well as months pain, limited mobility, and vigorous rehabilitation, make it as a option only for severe symptomatic OA patients [396]. Although OA is common with aging and is a irreversible process, it is not inevitable. Doctors recommend individuals to maintain healthy weight, control blood sugar, take 30 minutes exercise five times a week and have healthy lifestyle. The importance of exercise and healthy weight is recognized in OA prevention [81], while the mechanism underlying how mechanical forces alters cartilage metabolism is not clearly understood.

Cartilage consists of ECM, chondrocytes and tissue fluid. Two most important ECM components in cartilage are proteoglycans and type II collagen, which generate ECM network responsible for retaining tissue fluid within cartilage and maintain the mechanical property of cartilage. Chondrocyte is the only cell type in healthy cartilage and is capable to maintain the balance of ECM synthesis and degradation. In the healthy cartilage, the degr adative and raparative activities are strictly controlled by chondrocytes, while due to aging, overweight or injuries-induced inflammation, this delicate balance will be broken and the cartilage degeneration happens [397]. In early studies, forms of arthritis are classified into rheumatoid arthritis (RA) and OA based on the existence of significant inflammatory cells. However, this definition has been

regarded as misnomers with the advancing understanding of the basic mechanisms behind arthritis. Recently, aberrant mechanical forces-induced cartilage inflammation at the molecular level is accepted as a major factor contributing to OA progression [398].

The abnormal mechanical loading experienced by chondrocytes in cartilage matrix, due to obesity, excessive exercise or injuries, has been identified to alter the biosynthetic activity of chondrocytes. In the first stage, chondrocytes upregulate MMPs/ADAMT expression to cleave collagen/aggrecans and downregulate matrix synthesis [399]. The breakdown of ECM network leads to swelling and soft cartilage tissue that is more sensitive and less resistant to mechanical loading. The second stage involves the increased expression of cytokines and chemokines as well as reactive oxygen species. Those molecules further elevate the gene expression of MMPs. The third stage involves chondrocyte death by necrosis or apoptosis. It has been discovered that the number of apoptotic cell death is positively correlated with OA grades, and it may responsible for irreversible progression of OA [400]. Interestingly, contrast to overloading, moderate loading has been identified as effective prevention therapy of OA [101]. However, the mechanisms underlying how chondrocytes sense different magnitudes of forces and determine their fates are not well understood.

Numerous efforts have been made to elucidate how mechanical loading and cytokines regulate OA at cellular levels. NF-κB is one main downstream signaling pathway that excessively activated by mechanical stress and inflammatory mediators in OA chondrocytes. The high activation of NF-κB is required for the excessive expression of MMPs, NOS2, COX2, and IL-1.The cleaved and released ECM molecules will further activate NF-κB signaling cascade. This positive feedback loop promotes the development of OA [401]. ERK/JNK/p38 kinase cascades is another important pathway in response to injurious loading and inflammatory stimuli in OA. The activation of this pathway upregulates catabolic activity and initiates inflammatory events by induction of trascription factors, like AP-1, ETS, and C/EBP [402]. Integrin-mediated signaling has been found as a key upstream mediator of ERK/JNK/p38

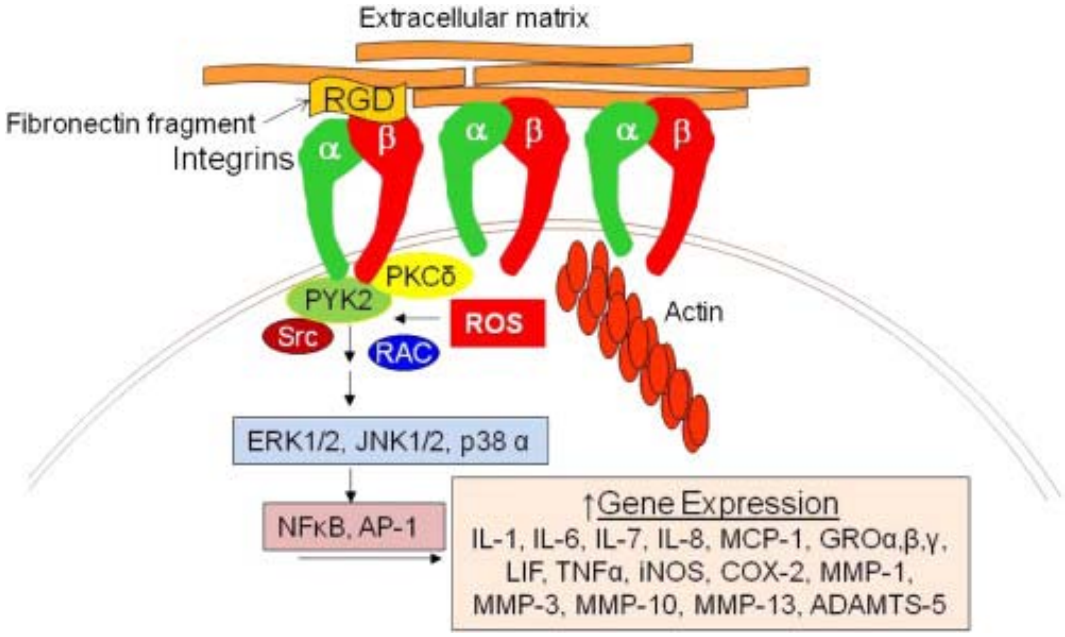

Fig. 5.1.: Integrin-mediated signaling pathways in chondrocytes. The integrin interacts with ECM and transduce mechanical signals to intercellular molecules to initiate downstream signaling pathways, including ERK/JNK/p38 AND NFκB. These activated pathways stimulate chondrocytes to produce pro-inflammatory cytokines and mediatros. [13]

as well as NFκB signaling pathways via FAK/Src [403] (Figure 5.1). While the importance of integrin-mediate signaling in OA, how integrin/FAK/Src signaling in response to different magnitudes of loading and inflammatory cytokines at subcellular level is unknown.

In the chapter 2, we evaluated how loading, cytokines and ER stress inhibition regulate integrin-mediated Src activity in cytosol or in lipid-rafts of plasma membrane. We firstly found the activities of Src at different subcellular locations exhibit differential activation temporal profiles under cytokine treatment. Upon the stimulation of cytokines, Src in cytosol reaches non-lipid rafts of plasma membrane faster than lipid-rafts. We hypothesized that the activation of Src at the lipid rafts requires its translocation from cytosol to lipid rafts through the actin cytoskeleton, while some

population of Src arriving at non-lipid rafts via diffusion and get activated quicker upon cytokine treatment. The ER inhibitor only downregulated Src in cytosol and failed to alter Src activity in lipid-rafts, indicating only cytosolic Src but not Src in the lipid rafts is a critical signaling node within an ER stress signaling pathway. ER stress inhibitors were capable to reverse cytokine-activated Src activity in cytosol, which provides a potential therapy target for OA prevention and treatment. The roles of shear stress on Src activities were investigated. Only the activity of Src in lipid rafts was regulated by loading in a magnitude-dependent manner, while Src in cytosol was not highly responsive to loading. The moderate loading substantially downregulated cytokine-stimulated Src activities in lipid rafts. These results provide evidences that moderate loading and ER inhibitors contribute to inflammation of OA, and Src at distinct subcellular compartments execute different cellular functions via different mechanisms. A combination of mechanical stimuli and subcellular location-targeting chemicals may present a potential therapeutic strategy for prevention of cartilage loss in OA.

The 2D monolayer culture on flat and rigid surfaces is popular in cell-based assays, while its limitations, including lack of ECM, abnormal cell morphology and unnatural polarity, have been increasingly recognized. As compared to 2D culture models, 3D culture systems mimic the microenvironment that cells experienced in tissues, and cells in the 3D culture are more morphologically and physiologically relevant to cells *in vivo* [295]. To obtain more predictive data for future *in vivo* tests, we developed a chondrocytes-agarose gel construct in the Chapter 3 and evaluated how mechanical loading and cytokines regulate FAK and Src activities at distinct subcellular locations.

Agarose gel is a type of hydrogel having porous structure and is widely used in chondrocyte studies [99]. We conjugated type II collagen with agarose gel to enhance the adhesion and activation of integrins on chondrocytes. Results shown that the conjugation of type II collagen with agarose is required for the regulation of Src and FAK activity by mechanical loading. We found that only Src and FAK in lipid rafts are responsive to loading. Since integrins concentrate to lipid rafts upon activation, we

hypothesized that the activation of Src and FAK in lipid rafts requires integrins. The treatment of integrin blocking antibody prevented Lyn-Src and FAK activation by flow, and the integrins were colocalized with FAK in lipid rafts, providing evidences that integrins in lipid rafts are required for FAK/Src signaling. The moderate loading reduced Src and FAK activities, which is consistent with the results in Chapter 2 that Src in lipid rafts can be inhibited with moderate loading in 2D model. Cytokines activate Src and FAK, except Src in lipid rafts. This finding, again, suggests differential signaling mechanism of Src and FAK at various locations. While the interaction between Src and FAK is increasingly recognized, most studies are performed at a cellular level, whether Src and FAK at different subcellular compartments interact via distinct mechanisms is unclear. We found that under mechanical stimulation, FAK in the lipid rafts is the key upstream mediator of Src; while under cytokine treatment, the Src is required for the FAK activation. Although the 3D agarose gel-based scaffold in this study provided a physiologically relevant microenvironment for chondrocytes, while the artificial ECM structure is still different from what cells experienced *in vivo*. We employed *ex vivo* cartilage explant to further test the effect of cytokines and mechanical loading on Src/FAK signaling at different compartments of plasma membrane, and found that moderate loading reversed cytokine-induced Src/FAK activation.

The current studies found that in 2D culture, Src activities were up- or down-regulated by physical forces depending on loading magnitudes, and moderate loading reversed cytokine-activated signaling activities. In the 3D culture, similarly, the activities of Src and FAK are regulated in a magnitude-dependent manner. One model for the role of membrane receptors (e.g. integrins) in mechanotransduction is that forces is transmitted through the receptors to regulate cellular signaling pathways and genetic programs [404], which is consistent with our results showing colocalization of integrins and FAK activities under loading. However, how integrins sense different loads and selectively activate or inhibit Src/FAK activities will need further studies.

We did observed discrepancies between data obtained from the 3D gel model and the *ex vivo* explant. The Src in lipid rafts in the 3D gel model was not significantly activated by cytokines, while it was upregulated by cytokine treatment in cartilage explant. Additionally, different from the 2D loading data in Chapter 2, in which the Src activity in lipid rafts was substantially reduced by loading, in 3D gel model, the Src in lipid rafts was slightly downregulated at earlier timepoints, but its activity returned back to basal level later. To further investigate the effect of dimensionality on cellular signaling, we compared signaling in chondrocytes in 2D versus 3D model in the Chapter 5.

AMPK is another upstream key mediator of NFκB and p38 [259, 405, 406]. It is closely linked with integrin/FAK/Src signaling [258]. It regulates cellular energy balance, and the malfunction of AMPK contributes to diabetes, atherosclerosis, cardiovascular diseases, cancers and OA. AMPK activity is decreased in OA chondrocytes, which promotes the catabolic activities in response to cytokines or injuries. To perform multiple tasks at different subcellular locations, AMPK has been shown to accumulate within specific compartments, like mitochondria, cytosol, nucleus, and plasma membrane [278]. However, the AMPK activities at various subcellular compartments in response to mechanical forces are not well understood. In Chapter 5, we employed six FRET-based AMPK biosensors targeting ER, mitochondria, Golgi apparatus, plasma membrane, nucleus and cytosol, to investigate potential factors contributing to differential cellular signaling in the 2D versus 3D culture.

In 2D culture, AMPK activities at different compartments were activated by mechanical loading, while in the 3D culture, only activities of AMPK in nucleus and near plasma membrane could be upregulated by loading. The flat and rigid substrates of 2D cultured changed cell morphology and cytoskeleton networks [295], while how these changes influence cell function is still under investigation. We found in 2D environment, different organelles required varying cytoskeletal filament to respond to physical stimulation. We further demonstrated that the altered cytoskeletal structure in the 2D model was a factor that enhances sensitivity of cells to loading in 2D

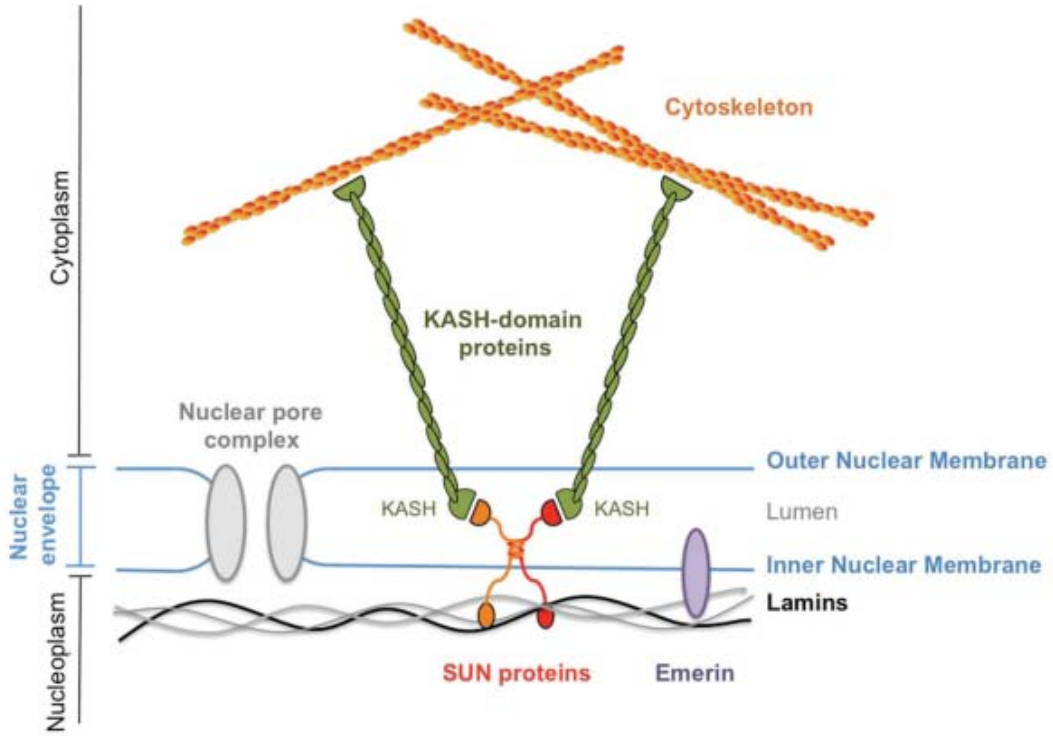

Fig. 5.2.: A model illustrating the LINC complex and its extended molecules. Plectins connect cytoskeletal filaments to LINC complex. The KASH domains are associated with the outer membrane of the nucleus and the SUN domains are located at the inner membrane of the nucleus, which interact with Lamin A/C [408]

culture. In addition to cell membrane receptors and cytoskeleton, the LINC complex and Lamin A/C are key mediators of mechanotransduction to nucleus. The LINC complex consists of KASH domain proteins in the outer nuclear membrane and SUN proteins in the inner nuclear membrane. The interaction of KASH and SUN domains transmit mechanical signals to Lamins [407]. The linkage between plasma membrane and nucleus is maintained similarly in cells in different culture dimensions.

Although there are several evident lines showing the interaction between AMPK and integrin/Src/FAK signaling: activation of AMPK reduced the abundance of β1-integrin on the cell surface [409, 410]; Src mediates the activation of AMPK in endothelial cells [411]. However, there is a study demonstrated the modulation of FAK

or Src failed to change AMPK sigaling correspondingly in cancer cells [412]. These results are obtained using different cell types and donor species, which might contribute to the discrepancy, while the relation between AMPK and integrin/Src/FAK signaling remains unclear. In our study, we found that different from Src and FAK activities by loading in Chapter 3 and 4, AMPK activities didn't show magnitude-dependent activation patterns, suggesting distinct regulation mechanisms of AMPK and Src/FAK. In addition to membrane surface receptors, ion channels can sense the membrane distortion produced by forces and alter the opening and closing rates, which consequently changes downstream signaling cascades [413]. It is possible that the ion channels and integrins synergistically regualte AMPK activities.

There are two types of 3D culture methods: cell aggregates that do not adhere to any culture substrates, and cell culture scaffolds that embed cells in gels. Although 3D biodegradable culture scaffolds (e.g. agarose gel) mimic *in vivo* microenvironment experienced by cells, those materials are prone to cause immune reactions and future infections *in vivo*. Various attempts have been made to develop scaffold-free engineered tissue [414]. During the incubation, chondrocytes have been found can produce collagens and proteoglycans *in vitro*, and this ECM production is accelerated under 3D culture environment [415, 416]. In the future study, chondrocytes spheroids can be placed in a specific culture mold, and incubate to allow the formation of ECM. Earlier study using spheroids produced cartilage tissue that has similar properties to native cartilage [417, 418]. Imaging techniques in conjunction with the cartilage-like construct that produced using cell spheroids will provide a novel model to study the signaling pathways *in vitro*.

Studies about the effects of moderate loading on the organization of ECM will provide direct evidence supporting moderate exercise as potential therapy of OA. Since the excessive degradation of ECM is the first sign of OA development and the type II collagen is the most abundant component of ECM, which is highly dynamic and under constant remodeling by chondrocytes [46, 47]. In the future studies, we can correlate the assembly of type II collagen in cartilage with signaling activities

to determine the physiological or pathological results by cytokines or loading. As we found in the current study, cellular signaling in a 2D model is different from that in a 3D model, this collagen and signaling study should be performed in the 3D environment. To monitor the type II collagen reorganization by chondrocytes, the fluorescent protein-coupled collagen (Figure 5.3) can be mixed with chondrocytes transfected with a biosensor. Collagen fibrils and sub-cellular signaling activities in the same live chondrocyte can be imaged simultaneously (Figure 5.4). Next, we can monitor site-specific signaling activities in chondrocytes under fluid flow in the presence or the absence of cytokines. The collagen fibril dynamics and cellular signaling will be further quantified using computational image analysis.

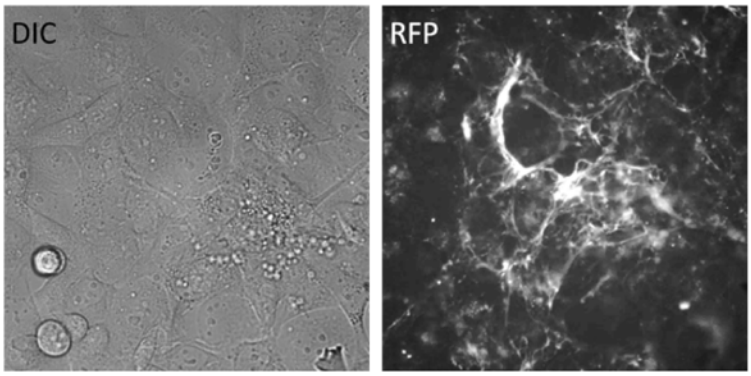

Fig. 5.3.: Collagen fibrils after 48 hour incubation. The type II collagen were labeled using an Alexa Fluor 568 (red fluorescent) protein labeling kit following the manufacturers instructions (Molecular Probes, Eugene, OR).

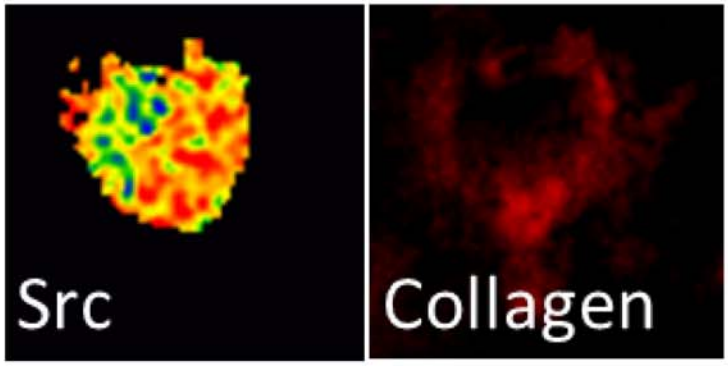

Fig. 5.4.: Collagen fibrils and Src activity after 48 hour incubation. Collagen fibrils and Src activity in the same live chondrocyte embedded in 3D agarose gel were imaged.

LIST OF REFERENCES

LIST OF REFERENCES

[1] S. Sutton, A. Clutterbuck, P. Harris, T. Gent, S. Freeman, N. Foster, R. Barrett-Jolley, and A. Mobasheri, "The contribution of the synovium, synovial derived inflammatory cytokines and neuropeptides to the pathogenesis of osteoarthritis," Vet J, vol. 179, no. 1, pp. 10–24, 2009.

[2] L. Ding, E. Heying, N. Nicholson, N. J. Stroud, G. A. Homandberg, J. A. Buckwalter, D. Guo, and J. A. Martin, "Mechanical impact induces cartilage degradation via mitogen activated protein kinases," Osteoarthritis Cartilage, vol. 18, no. 11, pp. 1509–17, 2010.

[3] C. Herberhold, S. Faber, T. Stammberger, M. Steinlechner, R. Putz, K. H. Englmeier, M. Reiser, and F. Eckstein, "In situ measurement of articular cartilage deformation in intact femoropatellar joints under static loading," J Biomech, vol. 32, no. 12, pp. 1287–95, 1999.

[4] C. Chen, D. T. Tambe, L. Deng, and L. Yang, "Biomechanical properties and mechanobiology of the articular chondrocyte," Am J Physiol Cell Physiol, vol. 305, no. 12, pp. C1202–8, 2013.

[5] B. D. Elder and K. A. Athanasiou, "Hydrostatic pressure in articular cartilage tissue engineering: from chondrocytes to tissue regeneration," Tissue Eng Part B Rev, vol. 15, no. 1, pp. 43–53, 2009.

[6] H. Yokota, M. B. Goldring, and H. B. Sun, "Cited2-mediated regulation of mmp-1 and mmp-13 in human chondrocytes under flow shear," J Biol Chem, vol. 278, no. 47, pp. 47275–80, 2003.

[7] K. Hamamura, P. Zhang, L. Zhao, J. W. Shim, A. Chen, T. R. Dodge, Q. Wan, H. Shih, S. Na, C. C. Lin, H. B. Sun, and H. Yokota, "Knee loading reduces mmp13 activity in the mouse cartilage," BMC Musculoskelet Disord, vol. 14, p. 312, 2013.

[8] F. Zhu, P. Wang, N. H. Lee, M. B. Goldring, and K. Konstantopoulos, "Prolonged application of high fluid shear to chondrocytes recapitulates gene expression profiles associated with osteoarthritis," PLoS One, vol. 5, no. 12, p. e15174, 2010.

[9] J. Fitzgerald, M. Jin, D. Dean, D. Wood, M. Zheng, and A. Grodzinsky, "Mechanical compression of cartilage explants induces multiple time-dependent gene expression patterns and involves intracellular calcium and cyclic amp," J Biol Chem, vol. 279, no. 19, pp. 19502 – 19511, 2004.

[10] K. W. Jang, J. A. Buckwalter, and J. A. Martin, "Inhibition of cell-matrix adhesions prevents cartilage chondrocyte death following impact injury," J Orthop Res, vol. 32, no. 3, pp. 448–54, 2014.

[11] Y. H. Kim and J. W. Lee, "Targeting of focal adhesion kinase by small interfering rnas reduces chondrocyte redifferentiation capacity in alginate beads culture with type ii collagen," J Cell Physiol, vol. 218, no. 3, pp. 623–30, 2009.

[12] P. Libby, P. M. Ridker, and A. Maseri, "Inflammation and atherosclerosis," Circulation, vol. 105, no. 9, pp. 1135–43, 2002.

[13] R. F. Loeser, "Integrins and cell signaling in chondrocytes," Biorheology, vol. 39, no. 1-2, pp. 119–24, 2002.

[14] K. Cheng, P. Xia, Q. Lin, S. Shen, M. Gao, S. Ren, and X. Li, "Effects of low-intensity pulsed ultrasound on integrin-fak-pi3k/akt mechanochemical transduction in rabbit osteoarthritis chondrocytes," Ultrasound Med Biol, vol. 40, no. 7, pp. 1609–18, 2014.

[15] W. Liang, K. Ren, F. Liu, W. Cui, Q. Wang, Z. Chen, and W. Fan, "Periodic mechanical stress stimulates the fak mitogenic signal in rat chondrocytes through erk1/2 activity," Cell Physiol Biochem, vol. 32, no. 4, pp. 915–30, 2013.

[16] I. Raizman, J. N. De Croos, R. Pilliar, and R. A. Kandel, "Calcium regulates cyclic compression-induced early changes in chondrocytes during in vitro cartilage tissue formation," Cell Calcium, vol. 48, no. 4, pp. 232–42, 2010.

[17] J. Seong, S. Lu, M. Ouyang, H. Huang, J. Zhang, M. C. Frame, and Y. Wang, "Visualization of src activity at different compartments of the plasma membrane by fret imaging," Chemistry and biology, vol. 16, no. 1, pp. 48–57, 2009.

[18] D. K. Kim, E. B. Cho, M. J. Moon, S. Park, J. I. Hwang, O. Kah, S. A. Sower, H. Vaudry, and J. Y. Seong, "Revisiting the evolution of gonadotropin-releasing hormones and their receptors in vertebrates: secrets hidden in genomes," Gen Comp Endocrinol, vol. 170, no. 1, pp. 68–78, 2011.

[19] Q. Wan, W. Xu, J. L. Yan, H. Yokota, and S. Na, "Distinctive subcellular inhibition of cytokine-induced src by salubrinal and fluid flow," PLoS One, vol. 9, no. 8, p. e105699, 2014.

[20] M. F. McCarty, "Ampk activation–protean potential for boosting healthspan," Age (Dordr), vol. 36, no. 2, pp. 641–63, 2014.

[21] R. Terkeltaub, B. Yang, M. Lotz, and R. Liu-Bryan, "Chondrocyte amp-activated protein kinase activity suppresses matrix degradation responses to proinflammatory cytokines interleukin-1beta and tumor necrosis factor alpha," Arthritis Rheum, vol. 63, no. 7, pp. 1928–37, 2011.

[22] A. D. Pearle, R. F. Warren, and S. A. Rodeo, "Basic science of articular cartilage and osteoarthritis," Clin Sports Med, vol. 24, no. 1, pp. 1–12, 2005.

[23] A. J. Sophia Fox, A. Bedi, and S. A. Rodeo, "The basic science of articular cartilage: structure, composition, and function," Sports Health, vol. 1, no. 6, pp. 461–8, 2009.

[24] S. L.-Y. Woo and J. A. Buckwalter, "Injury and repair of the musculoskeletal soft tissues. savannah, georgia, june 1820, 1987," Journal of Orthopaedic Research, vol. 6, no. 6, pp. 907–931, 1988.

[25] J. A. Buckwalter, H. J. Mankin, and A. J. Grodzinsky, "Articular cartilage and osteoarthritis," Instr Course Lect, vol. 54, pp. 465–80, 2005.

[26] V. C. Mow, M. H. Holmes, and W. M. Lai, "Fluid transport and mechanical properties of articular cartilage: a review," J Biomech, vol. 17, no. 5, pp. 377–94, 1984.

[27] D. J. Responte, R. M. Natoli, and K. A. Athanasiou, "Collagens of articular cartilage: structure, function, and importance in tissue engineering," Crit Rev Biomed Eng, vol. 35, no. 5, pp. 363–411, 2007.

[28] Y. Gao, S. Liu, J. Huang, W. Guo, J. Chen, L. Zhang, B. Zhao, J. Peng, A. Wang, Y. Wang, W. Xu, S. Lu, M. Yuan, and Q. Guo, "The ecm-cell interaction of cartilage extracellular matrix on chondrocytes," Biomed Res Int, vol. 2014, p. 648459, 2014.

[29] J. A. Buckwalter and L. C. Rosenberg, "Electron microscopic studies of cartilage proteoglycans," Electron Microsc Rev, vol. 1, no. 1, pp. 87–112, 1988.

[30] M. Pfaffle, M. Borchert, R. Deutzmann, K. von der Mark, M. P. Fernandez, O. Selmin, Y. Yamada, G. Martin, F. Ruggiero, and R. Garrone, "Anchorin cii, a collagen-binding chondrocyte surface protein of the calpactin family," Prog Clin Biol Res, vol. 349, pp. 147–57, 1990.

[31] J. A. Martin and J. A. Buckwalter, "Effects of fibronectin on articular cartilage chondrocyte proteoglycan synthesis and response to insulin-like growth factor-i," J Orthop Res, vol. 16, no. 6, pp. 752–7, 1998.

[32] J. M. Mansour, "Biomechanics of cartilage," Kinesiology: the mechanics and pathomechanics of human movement, pp. 66–79, 2003.

[33] A. Maroudas and P. Bullough, "Permeability of articular cartilage," Nature, vol. 219, no. 5160, pp. 1260–1261, 1968.

[34] Z. Y. García-Carvajal, D. Garciadiego-Cázares, C. Parra-Cid, R. Aguilar-Gaytán, C. Velasquillo, C. Ibarra, and J. S. C. Carmona, "Cartilage tissue engineering: the role of extracellular matrix (ecm) and novel strategies," Regenerative medicine and tissue engineering. Croatia: InTech, pp. 365–397, 2013.

[35] M. Demoor, D. Ollitrault, T. Gomez-Leduc, M. Bouyoucef, M. Hervieu, H. Fabre, J. Lafont, J.-M. Denoix, F. Audigi, F. Mallein-Gerin, F. Legendre, and P. Galera, "Cartilage tissue engineering: Molecular control of chondrocyte differentiation for proper cartilage matrix reconstruction," Biochimica et Biophysica Acta (BBA) - General Subjects, vol. 1840, no. 8, pp. 2414–2440, 2014.

[36] A. S. Lee, M. B. Ellman, D. Yan, J. S. Kroin, B. J. Cole, A. J. van Wijnen, and H. J. Im, "A current review of molecular mechanisms regarding osteoarthritis and pain," Gene, vol. 527, no. 2, pp. 440–7, 2013.

[37] M. B. Goldring and M. Otero, "Inflammation in osteoarthritis," Curr Opin Rheumatol, vol. 23, no. 5, pp. 471–8, 2011.

[38] J. Lutzner, P. Kasten, K.-P. Gunther, and S. Kirschner, "Surgical options for patients with osteoarthritis of the knee," Nat Rev Rheumatol, vol. 5, no. 6, pp. 309–316, 2009.

[39] F. H. Silver, G. Bradica, and A. Tria, "Elastic energy storage in human articular cartilage: estimation of the elastic modulus for type ii collagen and changes associated with osteoarthritis," Matrix Biol, vol. 21, no. 2, pp. 129–37, 2002.

[40] K. Gelse, E. Pschl, and T. Aigner, "Collagensstructure, function, and biosynthesis," Adv Drug Deliv Rev, vol. 55, no. 12, pp. 1531–1546, 2003.

[41] M. B. Goldring and S. R. Goldring, "Articular cartilage and subchondral bone in the pathogenesis of osteoarthritis," Ann N Y Acad Sci, vol. 1192, no. 1, pp. 230–237, 2010.

[42] N. Ishiguro, T. Kojima, and A. R. Poole, "Mechanism of cartilage destruction in osteoarthritis," Nagoya J Med Sci, vol. 65, no. 3-4, pp. 73–84, 2002.

[43] A. R. Poole, "An introduction to the pathophysiology of osteoarthritis," Front Biosci, vol. 4, pp. D662–70, 1999.

[44] J. P. Pelletier, F. Mineau, M. P. Faure, and J. Martel-Pelletier, "Imbalance between the mechanisms of activation and inhibition of metalloproteases in the early lesions of experimental osteoarthritis," Arthritis Rheum, vol. 33, no. 10, pp. 1466–76, 1990.

[45] L. C. Tetlow, D. J. Adlam, and D. E. Woolley, "Matrix metalloproteinase and proinflammatory cytokine production by chondrocytes of human osteoarthritic cartilage: associations with degenerative changes," Arthritis Rheum, vol. 44, no. 3, pp. 585–94, 2001.

[46] B. Bau, P. M. Gebhard, J. Haag, T. Knorr, E. Bartnik, and T. Aigner, "Relative messenger rna expression profiling of collagenases and aggrecanases in human articular chondrocytes in vivo and in vitro," Arthritis Rheum, vol. 46, no. 10, pp. 2648–57, 2002.

[47] D. W. Richardson and G. R. Dodge, "Effects of interleukin-1beta and tumor necrosis factor-alpha on expression of matrix-related genes by cultured equine articular chondrocytes," Am J Vet Res, vol. 61, no. 6, pp. 624–30, 2000.

[48] A. Liacini, J. Sylvester, W. Q. Li, W. Huang, F. Dehnade, M. Ahmad, and M. Zafarullah, "Induction of matrix metalloproteinase-13 gene expression by tnf- is mediated by map kinases, ap-1, and nf-b transcription factors in articular chondrocytes," Exp Cell Res, vol. 288, no. 1, pp. 208–217, 2003.

[49] L. Troeberg and H. Nagase, "Proteases involved in cartilage matrix degradation in osteoarthritis," Biochimica et Biophysica Acta (BBA)-Proteins and Proteomics, vol. 1824, no. 1, pp. 133–145, 2012.

[50] T. T. Chowdhury, D. M. Salter, D. L. Bader, and D. A. Lee, "Signal transduction pathways involving p38 mapk, jnk, nfkappab and ap-1 influences the response of chondrocytes cultured in agarose constructs to il-1beta and dynamic compression," Inflamm Res, vol. 57, no. 7, pp. 306–13, 2008.

[51] M. B. Goldring, J. Birkhead, L. J. Sandell, T. Kimura, and S. M. Krane, "Interleukin 1 suppresses expression of cartilage-specific types ii and ix collagens and increases types i and iii collagens in human chondrocytes," J Clin Invest, vol. 82, no. 6, pp. 2026–37, 1988.

[52] V. Lefebvre, C. Peeters-Joris, and G. Vaes, "Modulation by interleukin 1 and tumor necrosis factor alpha of production of collagenase, tissue inhibitor of metalloproteinases and collagen types in differentiated and dedifferentiated articular chondrocytes," Biochim Biophys Acta, vol. 1052, no. 3, pp. 366–78, 1990.

[53] Z. Fan, B. Bau, H. Yang, and T. Aigner, "Il-1beta induction of il-6 and lif in normal articular human chondrocytes involves the erk, p38 and nfkappab signaling pathways," Cytokine, vol. 28, no. 1, pp. 17–24, 2004.

[54] S. Bender, H. D. Haubeck, E. Van de Leur, G. Dufhues, X. Schiel, J. Lauwerijns, H. Greiling, and P. C. Heinrich, "Interleukin-1 beta induces synthesis and secretion of interleukin-6 in human chondrocytes," FEBS Lett, vol. 263, no. 2, pp. 321–4, 1990.

[55] C. Sommer and M. Kress, "Recent findings on how proinflammatory cytokines cause pain: peripheral mechanisms in inflammatory and neuropathic hyperalgesia," Neurosci Lett, vol. 361, no. 1-3, pp. 184–7, 2004.

[56] C. H. Evans, E. Gouze, J. N. Gouze, P. D. Robbins, and S. C. Ghivizzani, "Gene therapeutic approaches-transfer in vivo," Adv Drug Deliv Rev, vol. 58, no. 2, pp. 243–58, 2006.

[57] J. S. Smolen and G. Steiner, "Therapeutic strategies for rheumatoid arthritis," Nature Reviews Drug Discovery, vol. 2, no. 6, pp. 473–488, 2003.

[58] P. E. Auron, A. C. Webb, L. J. Rosenwasser, S. F. Mucci, A. Rich, S. M. Wolff, and C. A. Dinarello, "Nucleotide sequence of human monocyte interleukin 1 precursor cdna," Proc Natl Acad Sci U S A, vol. 81, no. 24, pp. 7907–11, 1984.

[59] B. J. de Lange-Brokaar, A. Ioan-Facsinay, G. J. van Osch, A. M. Zuurmond, J. Schoones, R. E. Toes, T. W. Huizinga, and M. Kloppenburg, "Synovial inflammation, immune cells and their cytokines in osteoarthritis: a review," Osteoarthritis Cartilage, vol. 20, no. 12, pp. 1484–99, 2012.

[60] M. U. Martin and H. Wesche, "Summary and comparison of the signaling mechanisms of the toll/interleukin-1 receptor family," Biochim Biophys Acta, vol. 1592, no. 3, pp. 265–80, 2002.

[61] J. M. Kyriakis and J. Avruch, "Mammalian mitogen-activated protein kinase signal transduction pathways activated by stress and inflammation," Physiol Rev, vol. 81, no. 2, pp. 807–69, 2001.

[62] S. Ghosh and M. Karin, "Missing pieces in the nf-kappab puzzle," Cell, vol. 109 Suppl, pp. S81–96, 2002.

[63] S. Agarwal, J. Deschner, P. Long, A. Verma, C. Hofman, C. H. Evans, and N. Piesco, "Role of nf-kappab transcription factors in antiinflammatory and proinflammatory actions of mechanical signals," Arthritis Rheum, vol. 50, no. 11, pp. 3541–8, 2004.

[64] M. S. Hayden and S. Ghosh, "Signaling to nf-kappab," Genes Dev, vol. 18, no. 18, pp. 2195–224, 2004.

[65] C. Melchiorri, R. Meliconi, L. Frizziero, T. Silvestri, L. Pulsatelli, I. Mazzetti, R. M. Borzi, M. Uguccioni, and A. Facchini, "Enhanced and coordinated in vivo expression of inflammatory cytokines and nitric oxide synthase by chondrocytes from patients with osteoarthritis," Arthritis Rheum, vol. 41, no. 12, pp. 2165–74, 1998.

[66] M. Grell, E. Douni, H. Wajant, M. Lohden, M. Clauss, B. Maxeiner, S. Georgopoulos, W. Lesslauer, G. Kollias, K. Pfizenmaier, and P. Scheurich, "The transmembrane form of tumor necrosis factor is the prime activating ligand of the 80 kda tumor necrosis factor receptor," Cell, vol. 83, no. 5, pp. 793–802, 1995.

[67] A. Matsuzawa, P. H. Tseng, S. Vallabhapurapu, J. L. Luo, W. Zhang, H. Wang, D. A. Vignali, E. Gallagher, and M. Karin, "Essential cytoplasmic translocation of a cytokine receptor-assembled signaling complex," Science, vol. 321, no. 5889, pp. 663–8, 2008.

[68] O. Micheau and J. Tschopp, "Induction of tnf receptor i-mediated apoptosis via two sequential signaling complexes," Cell, vol. 114, no. 2, pp. 181–90, 2003.

[69] J. Konopka, B. Richbourgh, and C. Liu, "The role of pgrn in musculoskeletal development and disease," Front Biosci (Landmark Ed), vol. 19, pp. 662–71, 2014.

[70] S. Das, J. Cho, I. Lambertz, M. A. Kelliher, A. G. Eliopoulos, K. Du, and P. N. Tsichlis, "Tpl2/cot signals activate erk, jnk, and nf-kappab in a cell-type and stimulus-specific manner," J Biol Chem, vol. 280, no. 25, pp. 23748–57, 2005.

[71] T. Ishitani, G. Takaesu, J. Ninomiya-Tsuji, H. Shibuya, R. B. Gaynor, and K. Matsumoto, "Role of the tab2-related protein tab3 in il-1 and tnf signaling," EMBO J, vol. 22, no. 23, pp. 6277–88, 2003.

[72] T. Silvestri, L. Pulsatelli, P. Dolzani, A. Facchini, and R. Meliconi, "Elevated serum levels of soluble interleukin-4 receptor in osteoarthritis," Osteoarthritis Cartilage, vol. 14, no. 7, pp. 717–9, 2006.

[73] M. Yorimitsu, K. Nishida, A. Shimizu, H. Doi, S. Miyazawa, T. Komiyama, Y. Nasu, A. Yoshida, S. Watanabe, and T. Ozaki, "Intra-articular injection of interleukin-4 decreases nitric oxide production by chondrocytes and ameliorates subsequent destruction of cartilage in instability-induced osteoarthritis in rat knee joints," Osteoarthritis Cartilage, vol. 16, no. 7, pp. 764–71, 2008.

[74] S. J. Millward-Sadler, M. O. Wright, L. W. Davies, G. Nuki, and D. M. Salter, "Mechanotransduction via integrins and interleukin-4 results in altered aggrecan and matrix metalloproteinase 3 gene expression in normal, but not osteoarthritic, human articular chondrocytes," Arthritis Rheum, vol. 43, no. 9, pp. 2091–9, 2000.

[75] T. D. Mueller, J. L. Zhang, W. Sebald, and A. Duschl, "Structure, binding, and antagonists in the il-4/il-13 receptor system," Biochim Biophys Acta, vol. 1592, no. 3, pp. 237–50, 2002.

[76] Y. Wang and S. Lou, "Direct protective effect of interleukin-10 on articular chondrocytes in vitro," Chin Med J (Engl), vol. 114, no. 7, pp. 723–5, 2001.

[77] S. V. Kotenko, C. D. Krause, L. S. Izotova, B. P. Pollack, W. Wu, and S. Pestka, "Identification and functional characterization of a second chain of the interleukin-10 receptor complex," The EMBO Journal, vol. 16, no. 19, pp. 5894–5903, 1997.

[78] D. Umulis, M. B. O'Connor, and S. S. Blair, "The extracellular regulation of bone morphogenetic protein signaling," Development, vol. 136, no. 22, pp. 3715–28, 2009.

[79] D. Jovanovic, J. P. Pelletier, N. Alaaeddine, F. Mineau, C. Geng, P. Ranger, and J. Martel-Pelletier, "Effect of il-13 on cytokines, cytokine receptors and inhibitors on human osteoarthritis synovium and synovial fibroblasts," Osteoarthritis Cartilage, vol. 6, no. 1, pp. 40–9, 1998.

[80] A. Bhattacharjee, M. Shukla, V. P. Yakubenko, A. Mulya, S. Kundu, and M. K. Cathcart, "Il-4 and il-13 employ discrete signaling pathways for target gene expression in alternatively activated monocytes/macrophages," Free Radic Biol Med, vol. 54, pp. 1–16, 2013.

[81] A. J. Grodzinsky, M. E. Levenston, M. Jin, and E. H. Frank, "Cartilage tissue remodeling in response to mechanical forces," Annu Rev Biomed Eng, vol. 2, pp. 691–713, 2000.

[82] F. Guilak, G. R. Erickson, and H. P. Ting-Beall, "The effects of osmotic stress on the viscoelastic and physical properties of articular chondrocytes," Biophysical Journal, vol. 82, no. 2, pp. 720–727, 2002.

[83] P. Manninen, H. Riihimki, M. Helivaara, and O. Suomalainen, "Physical exercise and risk of severe knee osteoarthritis requiring arthroplasty," Rheumatology, vol. 40, no. 4, pp. 432–437, 2001.

[84] E. M. Roos and L. Dahlberg, "Positive effects of moderate exercise on glycosaminoglycan content in knee cartilage: a four-month, randomized, controlled trial in patients at risk of osteoarthritis," Arthritis Rheum, vol. 52, no. 11, pp. 3507–14, 2005.

[85] K. L. Bennell, F. Dobson, and R. S. Hinman, "Exercise in osteoarthritis: moving from prescription to adherence," Best Pract Res Clin Rheumatol, vol. 28, no. 1, pp. 93–117, 2014.

[86] A. R. Poole, M. Kobayashi, T. Yasuda, S. Laverty, F. Mwale, T. Kojima, T. Sakai, C. Wahl, S. El-Maadawy, G. Webb, E. Tchetina, and W. Wu, "Type ii collagen degradation and its regulation in articular cartilage in osteoarthritis," Ann Rheum Dis, vol. 61 Suppl 2, pp. ii78–81, 2002.

[87] I. Kiviranta, M. Tammi, J. Jurvelin, A. M. Saamanen, and H. J. Helminen, "Moderate running exercise augments glycosaminoglycans and thickness of articular cartilage in the knee joint of young beagle dogs," J Orthop Res, vol. 6, no. 2, pp. 188–95, 1988.

[88] R. J. Todhunter, R. R. Minor, J. A. Wootton, L. Krook, N. Burton-Wurster, and G. Lust, "Effects of exercise and polysulfated glycosaminoglycan on repair of articular cartilage defects in the equine carpus," J Orthop Res, vol. 11, no. 6, pp. 782–95, 1993.

[89] D. J. Leong, X. I. Gu, Y. Li, J. Y. Lee, D. M. Laudier, R. J. Majeska, M. B. Schaffler, L. Cardoso, and H. B. Sun, "Matrix metalloproteinase-3 in articular cartilage is upregulated by joint immobilization and suppressed by passive joint motion," Matrix Biol, vol. 29, no. 5, pp. 420–6, 2010.

[90] T. T. Chowdhury, D. L. Bader, and D. A. Lee, "Anti-inflammatory effects of il-4 and dynamic compression in il-1beta stimulated chondrocytes," Biochem Biophys Res Commun, vol. 339, no. 1, pp. 241–7, 2006.

[91] T. T. Chowdhury, D. L. Bader, and D. A. Lee, "Dynamic compression counteracts il-1 beta-induced release of nitric oxide and pge2 by superficial zone chondrocytes cultured in agarose constructs," Osteoarthritis Cartilage, vol. 11, no. 9, pp. 688–96, 2003.

[92] J. Deschner, B. Rath-Deschner, and S. Agarwal, "Regulation of matrix metalloproteinase expression by dynamic tensile strain in rat fibrochondrocytes," Osteoarthritis Cartilage, vol. 14, no. 3, pp. 264–72, 2006.

[93] A. C. Shieh and K. A. Athanasiou, "Dynamic compression of single cells," Osteoarthritis Cartilage, vol. 15, no. 3, pp. 328–34, 2007.

[94] S. D. Waldman, C. G. Spiteri, M. D. Grynpas, R. M. Pilliar, J. Hong, and R. A. Kandel, "Effect of biomechanical conditioning on cartilaginous tissue formation in vitro," J Bone Joint Surg Am, vol. 85-A Suppl 2, pp. 101–5, 2003.

[95] T. Toyoda, B. B. Seedhom, J. Kirkham, and W. A. Bonass, "Upregulation of aggrecan and type ii collagen mrna expression in bovine chondrocytes by the application of hydrostatic pressure," Biorheology, vol. 40, no. 1-3, pp. 79–85, 2003.

[96] M. Ferretti, A. Srinivasan, J. Deschner, R. Gassner, F. Baliko, N. Piesco, R. Salter, and S. Agarwal, "Anti-inflammatory effects of continuous passive motion on meniscal fibrocartilage," J Orthop Res, vol. 23, no. 5, pp. 1165–71, 2005.

[97] M. Ferretti, R. Gassner, Z. Wang, P. Perera, J. Deschner, G. Sowa, R. B. Salter, and S. Agarwal, "Biomechanical signals suppress proinflammatory responses in cartilage: early events in experimental antigen-induced arthritis," J Immunol, vol. 177, no. 12, pp. 8757–66, 2006.

[98] T. Ikenoue, M. C. Trindade, M. S. Lee, E. Y. Lin, D. J. Schurman, S. B. Goodman, and R. L. Smith, "Mechanoregulation of human articular chondrocyte aggrecan and type ii collagen expression by intermittent hydrostatic pressure in vitro," J Orthop Res, vol. 21, no. 1, pp. 110–6, 2003.

[99] D. A. Lee and D. L. Bader, "Compressive strains at physiological frequencies influence the metabolism of chondrocytes seeded in agarose," J Orthop Res, vol. 15, no. 2, pp. 181–8, 1997.

[100] J. C. Shelton, D. L. Bader, and D. A. Lee, "Mechanical conditioning influences the metabolic response of cell-seeded constructs," Cells Tissues Organs, vol. 175, no. 3, pp. 140–50, 2003.

[101] H. B. Sun, "Mechanical loading, cartilage degradation, and arthritis," Ann N Y Acad Sci, vol. 1211, pp. 37–50, 2010.

[102] S. Mizuno and R. Ogawa, "Using changes in hydrostatic and osmotic pressure to manipulate metabolic function in chondrocytes," Am J Physiol Cell Physiol, vol. 300, no. 6, pp. C1234–45, 2011.

[103] B. Kurz, M. Jin, P. Patwari, D. M. Cheng, M. W. Lark, and A. J. Grodzinsky, "Biosynthetic response and mechanical properties of articular cartilage after injurious compression," J Orthop Res, vol. 19, no. 6, pp. 1140–6, 2001.

[104] C. T. Chen, N. Burton-Wurster, G. Lust, R. A. Bank, and J. M. Tekoppele, "Compositional and metabolic changes in damaged cartilage are peak-stress, stress-rate, and loading-duration dependent," J Orthop Res, vol. 17, no. 6, pp. 870–9, 1999.

[105] C. T. Chen, N. Burton-Wurster, C. Borden, K. Hueffer, S. E. Bloom, and G. Lust, "Chondrocyte necrosis and apoptosis in impact damaged articular cartilage," J Orthop Res, vol. 19, no. 4, pp. 703–11, 2001.

[106] P. A. Torzilli, R. Grigiene, J. Borrelli, J., and D. L. Helfet, "Effect of impact load on articular cartilage: cell metabolism and viability, and matrix water content," J Biomech Eng, vol. 121, no. 5, pp. 433–41, 1999.

[107] A. M. Loening, I. E. James, M. E. Levenston, A. M. Badger, E. H. Frank, B. Kurz, M. E. Nuttall, H. H. Hung, S. M. Blake, A. J. Grodzinsky, and M. W. Lark, "Injurious mechanical compression of bovine articular cartilage induces chondrocyte apoptosis," Arch Biochem Biophys, vol. 381, no. 2, pp. 205–12, 2000.

[108] J. B. Fitzgerald, M. Jin, D. H. Chai, P. Siparsky, P. Fanning, and A. J. Grodzinsky, "Shear- and compression-induced chondrocyte transcription requires mapk activation in cartilage explants," J Biol Chem, vol. 283, no. 11, pp. 6735–43, 2008.

[109] T. Pufe, A. Lemke, B. Kurz, W. Petersen, B. Tillmann, A. J. Grodzinsky, and R. Mentlein, "Mechanical overload induces vegf in cartilage discs via hypoxia-inducible factor," Am J Pathol, vol. 164, no. 1, pp. 185–92, 2004.

[110] B. Kurz, A. K. Lemke, J. Fay, T. Pufe, A. J. Grodzinsky, and M. Schunke, "Pathomechanisms of cartilage destruction by mechanical injury," Ann Anat, vol. 187, no. 5-6, pp. 473–85, 2005.

[111] Z. R. Healy, F. Zhu, J. D. Stull, and K. Konstantopoulos, "Elucidation of the signaling network of cox-2 induction in sheared chondrocytes: Cox-2 is induced via a rac/mekk1/mkk7/jnk2/c-jun-c/ebpβ-dependent pathway," American Journal of Physiology-Cell Physiology, vol. 294, no. 5, pp. C1146–C1157, 2008.

[112] A. Chakrabarti, A. W. Chen, and J. D. Varner, "A review of the mammalian unfolded protein response," Biotechnol Bioeng, vol. 108, no. 12, pp. 2777–93, 2011.

[113] N. Donnelly, A. M. Gorman, S. Gupta, and A. Samali, "The eif2alpha kinases: their structures and functions," Cell Mol Life Sci, vol. 70, no. 19, pp. 3493–511, 2013.

[114] M. Boyce, K. F. Bryant, C. Jousse, K. Long, H. P. Harding, D. Scheuner, R. J. Kaufman, D. Ma, D. M. Coen, D. Ron, and J. Yuan, "A selective inhibitor of eif2alpha dephosphorylation protects cells from er stress," Science, vol. 307, no. 5711, pp. 935–9, 2005.

[115] K. Hamamura, M. B. Goldring, and H. Yokota, "Involvement of p38 mapk in regulation of mmp13 mrna in chondrocytes in response to surviving stress to endoplasmic reticulum," Arch Oral Biol, vol. 54, no. 3, pp. 279–86, 2009.

[116] J. B. Fitzgerald, Chondrocyte gene expression and intracellular signaling pathways in cartilage mechanotransduction. PhD thesis, Massachusetts Institute of Technology, 2005.

[117] M. Zhang, M. Wang, and J. Wang, "[the role of the mapk pathway in mandibular condylar chondrocytes mechanotransduction].," Shanghai kou qiang yi xue= Shanghai journal of stomatology, vol. 13, no. 6, pp. 510–514, 2004.

[118] C. T. Hung, D. R. Henshaw, C. C. Wang, R. L. Mauck, F. Raia, G. Palmer, P. H. Chao, V. C. Mow, A. Ratcliffe, and W. B. Valhmu, "Mitogen-activated protein kinase signaling in bovine articular chondrocytes in response to fluid flow does not require calcium mobilization," J Biomech, vol. 33, no. 1, pp. 73–80, 2000.

[119] S. R. Tew, O. Vasieva, M. J. Peffers, and P. D. Clegg, "Post-transcriptional gene regulation following exposure of osteoarthritic human articular chondrocytes to hyperosmotic conditions," Osteoarthritis Cartilage, vol. 19, no. 8, pp. 1036–46, 2011.

[120] F. Guilak, R. A. Zell, G. R. Erickson, D. A. Grande, C. T. Rubin, K. J. McLeod, and H. J. Donahue, "Mechanically induced calcium waves in articular chondrocytes are inhibited by gadolinium and amiloride," Journal of orthopaedic research, vol. 17, no. 3, pp. 421–429, 1999.

[121] S. R. Roberts, M. M. Knight, D. A. Lee, and D. L. Bader, "Mechanical compression influences intracellular ca2+ signaling in chondrocytes seeded in agarose constructs," Journal of Applied Physiology, vol. 90, no. 4, pp. 1385–1391, 2001.

[122] C. E. Yellowley, C. R. Jacobs, and H. J. Donahue, "Mechanisms contributing to fluid-flow-induced ca2+ mobilization in articular chondrocytes," Journal of cellular physiology, vol. 180, no. 3, pp. 402–408, 1999.

[123] J. Browning, K. Saunders, J. Urban, and R. Wilkins, "The influence and interactions of hydrostatic and osmotic pressures on the intracellular milieu of chondrocytes," Biorheology, vol. 41, no. 3-4, pp. 299–308, 2004.

[124] G. R. Erickson, L. G. Alexopoulos, and F. Guilak, "Hyper-osmotic stress induces volume change and calcium transients in chondrocytes by transmembrane, phospholipid, and g-protein pathways," Journal of biomechanics, vol. 34, no. 12, pp. 1527–1535, 2001.

[125] M. N. Phan, H. A. Leddy, B. J. Votta, S. Kumar, D. S. Levy, D. B. Lipshutz, S. H. Lee, W. Liedtke, and F. Guilak, "Functional characterization of trpv4 as an osmotically sensitive ion channel in porcine articular chondrocytes," Arthritis Rheum, vol. 60, no. 10, pp. 3028–37, 2009.

[126] R. F. Loeser, "Chondrocyte integrin expression and function," Biorheology, vol. 37, no. 1-2, pp. 109–16, 2000.

[127] S. Jalali, M. A. del Pozo, K. Chen, H. Miao, Y. Li, M. A. Schwartz, J. Y. Shyy, and S. Chien, "Integrin-mediated mechanotransduction requires its dynamic interaction with specific extracellular matrix (ecm) ligands," Proc Natl Acad Sci U S A, vol. 98, no. 3, pp. 1042–6, 2001.

[128] M. O. Wright, K. Nishida, C. Bavington, J. L. Godolphin, E. Dunne, S. Walmsley, P. Jobanputra, G. Nuki, and D. M. Salter, "Hyperpolarisation of cultured human chondrocytes following cyclical pressure-induced strain: evidence of a role for alpha 5 beta 1 integrin as a chondrocyte mechanoreceptor," J Orthop Res, vol. 15, no. 5, pp. 742–7, 1997.

[129] M. A. Wozniak, R. Desai, P. A. Solski, C. J. Der, and P. J. Keely, "Rock-generated contractility regulates breast epithelial cell differentiation in response to the physical properties of a three-dimensional collagen matrix," J Cell Biol, vol. 163, no. 3, pp. 583–95, 2003.

[130] S. K. Mitra, D. A. Hanson, and D. D. Schlaepfer, "Focal adhesion kinase: in command and control of cell motility," Nat Rev Mol Cell Biol, vol. 6, no. 1, pp. 56–68, 2005.

[131] M. O. Wright, K. Nishida, C. Bavington, J. L. Godolphin, E. Dunne, S. Walmsley, P. Jobanputra, G. Nuki, and D. M. Salter, "Hyperpolarisation of cultured human chondrocytes following cyclical pressure-induced strain: Evidence of a role for 51 integrin as a chondrocyte mechanoreceptor," Journal of Orthopaedic Research, vol. 15, no. 5, pp. 742–747, 1997.

[132] M. M. Knight, T. Toyoda, D. A. Lee, and D. L. Bader, "Mechanical compression and hydrostatic pressure induce reversible changes in actin cytoskeletal organisation in chondrocytes in agarose," J Biomech, vol. 39, no. 8, pp. 1547–51, 2006.

[133] J. J. Parkkinen, M. J. Lammi, R. Inkinen, M. Jortikka, M. Tammi, I. Virtanen, and H. J. Helminen, "Influence of short-term hydrostatic pressure on organization of stress fibers in cultured chondrocytes," J Orthop Res, vol. 13, no. 4, pp. 495–502, 1995.

[134] M. M. Knight, B. D. Idowu, D. A. Lee, and D. L. Bader, "Temporal changes in cytoskeletal organisation within isolated chondrocytes quantified using a novel image analysis technique," Med Biol Eng Comput, vol. 39, no. 3, pp. 397–404, 2001.

[135] D. R. Haudenschild, B. Nguyen, J. Chen, D. D. D'Lima, and M. K. Lotz, "Rho kinase-dependent ccl20 induced by dynamic compression of human chondrocytes," Arthritis Rheum, vol. 58, no. 9, pp. 2735–42, 2008.

[136] B. A. Kerr, T. Otani, E. Koyama, T. A. Freeman, and M. Enomoto-Iwamoto, "Small gtpase protein rac-1 is activated with maturation and regulates cell morphology and function in chondrocytes," Exp Cell Res, vol. 314, no. 6, pp. 1301–12, 2008.

[137] D. L. Long, J. S. Willey, and R. F. Loeser, "Rac1 is required for matrix metalloproteinase 13 production by chondrocytes in response to fibronectin fragments," Arthritis Rheum, vol. 65, no. 6, pp. 1561–8, 2013.

[138] K. Ren, F. Liu, Y. Huang, W. Liang, W. Cui, Q. Wang, and W. Fan, "Periodic mechanical stress activates integrinbeta1-dependent src-dependent plcgamma1-independent rac1 mitogenic signal in rat chondrocytes through erk1/2," Cell Physiol Biochem, vol. 30, no. 4, pp. 827–42, 2012.

[139] N. Takeshita, E. Yoshimi, C. Hatori, F. Kumakura, N. Seki, and Y. Shimizu, "Alleviating effects of as1892802, a rho kinase inhibitor, on osteoarthritic disorders in rodents," J Pharmacol Sci, vol. 115, no. 4, pp. 481–9, 2011.

[140] A. Méjat, "Linc complexes in health and disease," Nucleus, vol. 1, no. 1, pp. 40–52, 2010.

[141] W. Chang, H. J. Worman, and G. G. Gundersen, "Accessorizing and anchoring the linc complex for multifunctionality," The Journal of cell biology, vol. 208, no. 1, pp. 11–22, 2015.

[142] M. D. Schaller, J. D. Hildebrand, J. D. Shannon, J. W. Fox, R. R. Vines, and J. T. Parsons, "Autophosphorylation of the focal adhesion kinase, pp125fak, directs sh2-dependent binding of pp60src," Mol Cell Biol, vol. 14, no. 3, pp. 1680–8, 1994.

[143] J. Ivaska, L. Bosca, and P. J. Parker, "Pkc[epsi] is a permissive link in integrin-dependent ifn-[gamma] signalling that facilitates jak phosphorylation of stat1," Nat Cell Biol, vol. 5, no. 4, pp. 363–369, 2003.

[144] T. Gemba, J. Valbracht, S. Alsalameh, and M. Lotz, "Focal adhesion kinase and mitogen-activated protein kinases are involved in chondrocyte activation by the 29-kda amino-terminal fibronectin fragment," J Biol Chem, vol. 277, no. 2, pp. 907–11, 2002.

[145] Y. Zhang, A. A. Thant, Y. Hiraiwa, Y. Naito, T. T. Sein, Y. Sohara, S. Matsuda, and M. Hamaguchi, "A role for focal adhesion kinase in hyluronan-dependent mmp-2 secretion in a human small-cell lung carcinoma cell line, qg90," Biochem Biophys Res Commun, vol. 290, no. 3, pp. 1123–7, 2002.

[146] K. Shibata, F. Kikkawa, A. Nawa, A. A. Thant, K. Naruse, S. Mizutani, and M. Hamaguchi, "Both focal adhesion kinase and c-ras are required for the enhanced matrix metalloproteinase 9 secretion by fibronectin in ovarian cancer cells," Cancer Res, vol. 58, no. 5, pp. 900–3, 1998.

[147] K. S. Gill, F. Beier, and H. A. Goldberg, "Rho-rock signaling differentially regulates chondrocyte spreading on fibronectin and bone sialoprotein," Am J Physiol Cell Physiol, vol. 295, no. 1, pp. C38–49, 2008.

[148] N. P. Whitney, A. C. Lamb, T. M. Louw, and A. Subramanian, "Integrin-mediated mechanotransduction pathway of low-intensity continuous ultrasound in human chondrocytes," Ultrasound Med Biol, vol. 38, no. 10, pp. 1734–43, 2012.

[149] Z. F. Lu, B. Zandieh Doulabi, C. L. Huang, R. A. Bank, and M. N. Helder, "Beta1 integrins regulate chondrogenesis and rock signaling in adipose stem cells," Biochem Biophys Res Commun, vol. 372, no. 4, pp. 547–52, 2008.

[150] X. D. Ren, W. B. Kiosses, D. J. Sieg, C. A. Otey, D. D. Schlaepfer, and M. A. Schwartz, "Focal adhesion kinase suppresses rho activity to promote focal adhesion turnover," J Cell Sci, vol. 113 (Pt 20), pp. 3673–8, 2000.

[151] S. J. Parsons and J. T. Parsons, "Src family kinases, key regulators of signal transduction," Oncogene, vol. 23, no. 48, pp. 7906–9, 2004.

[152] J. L. Guan, J. E. Trevithick, and R. O. Hynes, "Fibronectin/integrin interaction induces tyrosine phosphorylation of a 120-kda protein," Cell Regulation, vol. 2, no. 11, pp. 951–964, 1991.

[153] S. K. Akiyama, S. S. Yamada, K. M. Yamada, and S. E. LaFlamme, "Transmembrane signal transduction by integrin cytoplasmic domains expressed in single-subunit chimeras," J Biol Chem, vol. 269, no. 23, pp. 15961–4, 1994.

[154] J. Sinnett-Smith, I. Zachary, A. M. Valverde, and E. Rozengurt, "Bombesin stimulation of p125 focal adhesion kinase tyrosine phosphorylation. role of protein kinase c, ca2+ mobilization, and the actin cytoskeleton," J Biol Chem, vol. 268, no. 19, pp. 14261–8, 1993.

[155] Z. Xing, H. C. Chen, J. K. Nowlen, S. J. Taylor, D. Shalloway, and J. L. Guan, "Direct interaction of v-src with the focal adhesion kinase mediated by the src sh2 domain," Mol Biol Cell, vol. 5, no. 4, pp. 413–21, 1994.

[156] J. A. Cooper and B. Howell, "The when and how of src regulation," Cell, vol. 73, no. 6, pp. 1051–4, 1993.

[157] B. S. Cobb, M. D. Schaller, T. H. Leu, and J. T. Parsons, "Stable association of pp60src and pp59fyn with the focal adhesion-associated protein tyrosine kinase, pp125fak," Mol Cell Biol, vol. 14, no. 1, pp. 147–55, 1994.

[158] D. D. Schlaepfer, S. K. Hanks, T. Hunter, and P. v. d. Geer, "Integrin-mediated signal transduction linked to ras pathway by grb2 binding to focal adhesion kinase," Nature, vol. 372, no. 6508, pp. 786–791, 1994.

[159] H. Sabe, A. Hata, M. Okada, H. Nakagawa, and H. Hanafusa, "Analysis of the binding of the src homology 2 domain of csk to tyrosine-phosphorylated proteins in the suppression and mitotic activation of c-src," Proc Natl Acad Sci U S A, vol. 91, no. 9, pp. 3984–8, 1994.

[160] S. T. Lim, "Nuclear fak: a new mode of gene regulation from cellular adhesions," Mol Cells, vol. 36, no. 1, pp. 1–6, 2013.

[161] D. A. Hsia, S. K. Mitra, C. R. Hauck, D. N. Streblow, J. A. Nelson, D. Ilic, S. Huang, E. Li, G. R. Nemerow, J. Leng, K. S. Spencer, D. A. Cheresh, and D. D. Schlaepfer, "Differential regulation of cell motility and invasion by fak," J Cell Biol, vol. 160, no. 5, pp. 753–67, 2003.

[162] Y. N. Yang, F. Wang, W. Zhou, Z. Q. Wu, and Y. Q. Xing, "Tnf-alpha stimulates mmp-2 and mmp-9 activities in human corneal epithelial cells via the activation of fak/erk signaling," Ophthalmic Res, vol. 48, no. 4, pp. 165–70, 2012.

[163] N. N. Mon, H. Hasegawa, A. A. Thant, P. Huang, Y. Tanimura, T. Senga, and M. Hamaguchi, "A role for focal adhesion kinase signaling in tumor necrosis factor-alpha-dependent matrix metalloproteinase-9 production in a cholangiocarcinoma cell line, ccks1," Cancer Res, vol. 66, no. 13, pp. 6778–84, 2006.

[164] C. S. Lee, I. H. Bae, J. Han, G. Y. Choi, K. H. Hwang, D. H. Kim, M. H. Yeom, Y. H. Park, and M. Park, "Compound k inhibits mmp-1 expression through suppression of c-src-dependent erk activation in tnf-alpha-stimulated dermal fibroblast," Exp Dermatol, vol. 23, no. 11, pp. 819–24, 2014.

[165] S. T. Lim, N. L. Miller, X. L. Chen, I. Tancioni, C. T. Walsh, C. Lawson, S. Uryu, S. M. Weis, D. A. Cheresh, and D. D. Schlaepfer, "Nuclear-localized focal adhesion kinase regulates inflammatory vcam-1 expression," J Cell Biol, vol. 197, no. 7, pp. 907–19, 2012.

[166] D. D. Schlaepfer, S. Hou, S. T. Lim, A. Tomar, H. Yu, Y. Lim, D. A. Hanson, S. A. Uryu, J. Molina, and S. K. Mitra, "Tumor necrosis factor-alpha stimulates focal adhesion kinase activity required for mitogen-activated kinase-associated interleukin 6 expression," J Biol Chem, vol. 282, no. 24, pp. 17450–9, 2007.

[167] M. Funakoshi-Tago, Y. Sonoda, S. Tanaka, K. Hashimoto, K. Tago, S. Tominaga, and T. Kasahara, "Tumor necrosis factor-induced nuclear factor kappab activation is impaired in focal adhesion kinase-deficient fibroblasts," J Biol Chem, vol. 278, no. 31, pp. 29359–65, 2003.

[168] W.-C. Huang, J.-J. Chen, and C.-C. Chen, "c-src-dependent tyrosine phosphorylation of ikk is involved in tumor necrosis factor--induced intercellular adhesion molecule-1 expression," Journal of Biological Chemistry, vol. 278, no. 11, pp. 9944–9952, 2003.

[169] C. L. Tsai, W. C. Chen, H. L. Hsieh, P. L. Chi, L. D. Hsiao, and C. M. Yang, "Tnf-alpha induces matrix metalloproteinase-9-dependent soluble intercellular adhesion molecule-1 release via traf2-mediated mapks and nf-kappab activation in osteoblast-like mc3t3-e1 cells," J Biomed Sci, vol. 21, p. 12, 2014.

[170] K. Ren, Y. Ma, Y. Huang, W. Liang, F. Liu, Q. Wang, W. Cui, Z. Liu, G. Yin, and W. Fan, "Periodic mechanical stress activates mek1/2-erk1/2 mitogenic signals in rat chondrocytes through src and plcgamma1," Braz J Med Biol Res, vol. 44, no. 12, pp. 1231–42, 2011.

[171] H. S. Lee, S. J. Millward-Sadler, M. O. Wright, G. Nuki, and D. M. Salter, "Integrin and mechanosensitive ion channel-dependent tyrosine phosphorylation of focal adhesion proteins and beta-catenin in human articular chondrocytes after mechanical stimulation," J Bone Miner Res, vol. 15, no. 8, pp. 1501–9, 2000.

[172] R. F. Loeser, C. S. Carlson, and M. P. McGee, "Expression of beta 1 integrins by cultured articular chondrocytes and in osteoarthritic cartilage," Exp Cell Res, vol. 217, no. 2, pp. 248–57, 1995.

[173] H. Yu, X. Li, G. S. Marchetto, R. Dy, D. Hunter, B. Calvo, T. L. Dawson, M. Wilm, R. J. Anderegg, L. M. Graves, and H. S. Earp, "Activation of a novel calcium-dependent protein-tyrosine kinase. correlation with c-jun n-terminal kinase but not mitogen-activated protein kinase activation," J Biol Chem, vol. 271, no. 47, pp. 29993–8, 1996.

[174] D. D. Schlaepfer, S. K. Mitra, and D. Ilic, "Control of motile and invasive cell phenotypes by focal adhesion kinase," Biochim Biophys Acta, vol. 1692, no. 2-3, pp. 77–102, 2004.

[175] S. K. Hanks, L. Ryzhova, N. Y. Shin, and J. Brabek, "Focal adhesion kinase signaling activities and their implications in the control of cell survival and motility," Front Biosci, vol. 8, pp. d982–96, 2003.

[176] E. Kiyokawa, Y. Hashimoto, T. Kurata, H. Sugimura, and M. Matsuda, "Evidence that dock180 up-regulates signals from the crkii-p130(cas) complex," J Biol Chem, vol. 273, no. 38, pp. 24479–84, 1998.

[177] G. Baillat, C. Siret, E. Delamarre, and J. Luis, "Early adhesion induces interaction of fak and fyn in lipid domains and activates raft-dependent akt signaling in sw480 colon cancer cells," Biochim Biophys Acta, vol. 1783, no. 12, pp. 2323–31, 2008.

[178] Y. Wei, X. Yang, Q. Liu, J. A. Wilkins, and H. A. Chapman, "A role for caveolin and the urokinase receptor in integrin-mediated adhesion and signaling," J Cell Biol, vol. 144, no. 6, pp. 1285–94, 1999.

[179] E. K. Park, M. J. Park, S. H. Lee, Y. C. Li, J. Kim, J. S. Lee, J. W. Lee, S. K. Ye, J. W. Park, C. W. Kim, B. K. Park, and Y. N. Kim, "Cholesterol depletion induces anoikis-like apoptosis via fak down-regulation and caveolae internalization," J Pathol, vol. 218, no. 3, pp. 337–49, 2009.

[180] T. Hitosugi, M. Sato, K. Sasaki, and Y. Umezawa, "Lipid raft specific knockdown of src family kinase activity inhibits cell adhesion and cell cycle progression of breast cancer cells," Cancer Res, vol. 67, no. 17, pp. 8139–48, 2007.

[181] A. Kasai, T. Shima, and M. Okada, "Role of src family tyrosine kinases in the down-regulation of epidermal growth factor signaling in pc12 cells," Genes Cells, vol. 10, no. 12, pp. 1175–87, 2005.

[182] B. Guo, R. M. Kato, M. Garcia-Lloret, M. I. Wahl, and D. J. Rawlings, "Engagement of the human pre-b cell receptor generates a lipid raft-dependent calcium signaling complex," Immunity, vol. 13, no. 2, pp. 243–53, 2000.

[183] X. Gao and J. Zhang, "Spatiotemporal analysis of differential akt regulation in plasma membrane microdomains," Mol Biol Cell, vol. 19, no. 10, pp. 4366–73, 2008.

[184] Y. Wang, E. L. Botvinick, Y. Zhao, M. W. Berns, S. Usami, R. Y. Tsien, and S. Chien, "Visualizing the mechanical activation of src," Nature, vol. 434, no. 7036, pp. 1040–5, 2005.

[185] J. Seong, M. Ouyang, T. Kim, J. Sun, P. C. Wen, S. Lu, Y. Zhuo, N. M. Llewellyn, D. D. Schlaepfer, J. L. Guan, S. Chien, and Y. Wang, "Detection of focal adhesion kinase activation at membrane microdomains by fluorescence resonance energy transfer," Nat Commun, vol. 2, p. 406, 2011.

[186] P. de Diesbach, T. Medts, S. Carpentier, L. D'Auria, P. Van Der Smissen, A. Platek, M. Mettlen, A. Caplanusi, M. F. van den Hove, D. Tyteca, and P. J. Courtoy, "Differential subcellular membrane recruitment of src may specify its downstream signalling," Exp Cell Res, vol. 314, no. 7, pp. 1465–79, 2008.

[187] S. Lev, H. Moreno, R. Martinez, P. Canoll, E. Peles, J. M. Musacchio, G. D. Plowman, B. Rudy, and J. Schlessinger, "Protein tyrosine kinase pyk2 involved in ca(2+)-induced regulation of ion channel and map kinase functions," Nature, vol. 376, no. 6543, pp. 737–45, 1995.

[188] A. E. Brinson, T. Harding, P. A. Diliberto, Y. He, X. Li, D. Hunter, B. Herman, H. S. Earp, and L. M. Graves, "Regulation of a calcium-dependent tyrosine kinase in vascular smooth muscle cells by angiotensin ii and platelet-derived growth factor. dependence on calcium and the actin cytoskeleton," J Biol Chem, vol. 273, no. 3, pp. 1711–8, 1998.

[189] M. Okigaki, C. Davis, M. Falasca, S. Harroch, D. P. Felsenfeld, M. P. Sheetz, and J. Schlessinger, "Pyk2 regulates multiple signaling events crucial for macrophage morphology and migration," Proc Natl Acad Sci U S A, vol. 100, no. 19, pp. 10740–10745, 2003.

[190] M. D. Schaller, "Cellular functions of fak kinases: insight into molecular mechanisms and novel functions," J Cell Sci, vol. 123, no. Pt 7, pp. 1007–13, 2010.

[191] Y. Lim, S. T. Lim, A. Tomar, M. Gardel, J. A. Bernard-Trifilo, X. L. Chen, S. A. Uryu, R. Canete-Soler, J. Zhai, H. Lin, W. W. Schlaepfer, P. Nalbant, G. Bokoch, D. Ilic, C. Waterman-Storer, and D. D. Schlaepfer, "Pyk2 and fak connections to p190rho guanine nucleotide exchange factor regulate rhoa activity, focal adhesion formation, and cell motility," J Cell Biol, vol. 180, no. 1, pp. 187–203, 2008.

[192] X. R. Ren, Q. S. Du, Y. Z. Huang, S. Z. Ao, L. Mei, and W. C. Xiong, "Regulation of cdc42 gtpase by proline-rich tyrosine kinase 2 interacting with psgap, a novel pleckstrin homology and src homology 3 domain containing rhogap protein," J Cell Biol, vol. 152, no. 5, pp. 971–84, 2001.

[193] D. Carling, V. A. Zammit, and D. G. Hardie, "A common bicyclic protein kinase cascade inactivates the regulatory enzymes of fatty acid and cholesterol biosynthesis," FEBS Lett, vol. 223, no. 2, pp. 217–22, 1987.

[194] S. A. Hawley, M. Davison, A. Woods, S. P. Davies, R. K. Beri, D. Carling, and D. G. Hardie, "Characterization of the amp-activated protein kinase kinase from rat liver and identification of threonine 172 as the major site at which it phosphorylates amp-activated protein kinase," J Biol Chem, vol. 271, no. 44, pp. 27879–87, 1996.

[195] J. W. Scott, D. G. Norman, S. A. Hawley, L. Kontogiannis, and D. G. Hardie, "Protein kinase substrate recognition studied using the recombinant catalytic domain of amp-activated protein kinase and a model substrate," J Mol Biol, vol. 317, no. 2, pp. 309–23, 2002.

[196] B. Xiao, M. J. Sanders, D. Carmena, N. J. Bright, L. F. Haire, E. Underwood, B. R. Patel, R. B. Heath, P. A. Walker, S. Hallen, F. Giordanetto, S. R. Martin, D. Carling, and S. J. Gamblin, "Structural basis of ampk regulation by small molecule activators," Nat Commun, vol. 4, 2013.

[197] B. Xiao, M. J. Sanders, E. Underwood, R. Heath, F. V. Mayer, D. Carmena, C. Jing, P. A. Walker, J. F. Eccleston, L. F. Haire, P. Saiu, S. A. Howell, R. Aasland, S. R. Martin, D. Carling, and S. J. Gamblin, "Structure of mammalian ampk and its regulation by adp," Nature, vol. 472, no. 7342, pp. 230–3, 2011.

[198] D. G. Hardie, F. A. Ross, and S. A. Hawley, "Ampk: a nutrient and energy sensor that maintains energy homeostasis," Nature reviews Molecular cell biology, vol. 13, no. 4, pp. 251–262, 2012.

[199] X. H. Zeng, X. J. Zeng, and Y. Y. Li, "Efficacy and safety of berberine for congestive heart failure secondary to ischemic or idiopathic dilated cardiomyopathy," Am J Cardiol, vol. 92, no. 2, pp. 173–6, 2003.

[200] F. A. Masoudi, S. E. Inzucchi, Y. Wang, E. P. Havranek, J. M. Foody, and H. M. Krumholz, "Thiazolidinediones, metformin, and outcomes in older patients with diabetes and heart failure: an observational study," Circulation, vol. 111, no. 5, pp. 583–90, 2005.

[201] J. P. Cooke, "The pivotal role of nitric oxide for vascular health," Can J Cardiol, vol. 20 Suppl B, pp. 7b–15b, 2004.

[202] A. Salminen, J. M. Hyttinen, and K. Kaarniranta, "Amp-activated protein kinase inhibits nf-kappab signaling and inflammation: impact on healthspan and lifespan," J Mol Med (Berl), vol. 89, no. 7, pp. 667–76, 2011.

[203] M. H. Gollob, M. S. Green, A. S. Tang, T. Gollob, A. Karibe, A. S. Ali Hassan, F. Ahmad, R. Lozado, G. Shah, L. Fananapazir, L. L. Bachinski, and R. Roberts, "Identification of a gene responsible for familial wolff-parkinson-white syndrome," N Engl J Med, vol. 344, no. 24, pp. 1823–31, 2001.

[204] Y. Zhang, T. S. Lee, E. M. Kolb, K. Sun, X. Lu, F. M. Sladek, G. S. Kassab, J. Garland, T., and J. Y. Shyy, "Amp-activated protein kinase is involved in endothelial no synthase activation in response to shear stress," Arterioscler Thromb Vasc Biol, vol. 26, no. 6, pp. 1281–7, 2006.

[205] V. T. Samuel, K. F. Petersen, and G. I. Shulman, "Lipid-induced insulin resistance: unravelling the mechanism," Lancet, vol. 375, no. 9733, pp. 2267–77, 2010.

[206] H. M. O'Neill, S. J. Maarbjerg, J. D. Crane, J. Jeppesen, S. B. Jorgensen, J. D. Schertzer, O. Shyroka, B. Kiens, B. J. van Denderen, M. A. Tarnopolsky, B. E. Kemp, E. A. Richter, and G. R. Steinberg, "Amp-activated protein kinase (ampk) beta1beta2 muscle null mice reveal an essential role for ampk in maintaining mitochondrial content and glucose uptake during exercise," Proc Natl Acad Sci U S A, vol. 108, no. 38, pp. 16092–7, 2011.

[207] S. A. Hawley, F. A. Ross, C. Chevtzoff, K. A. Green, A. Evans, S. Fogarty, M. C. Towler, L. J. Brown, O. A. Ogunbayo, A. M. Evans, and D. G. Hardie, "Use of cells expressing gamma subunit variants to identify diverse mechanisms of ampk activation," Cell Metab, vol. 11, no. 6, pp. 554–65, 2010.

[208] M. A. Iglesias, J. M. Ye, G. Frangioudakis, A. K. Saha, E. Tomas, N. B. Ruderman, G. J. Cooney, and E. W. Kraegen, "Aicar administration causes an apparent enhancement of muscle and liver insulin action in insulin-resistant high-fat-fed rats," Diabetes, vol. 51, no. 10, pp. 2886–94, 2002.

[209] B. Cool, B. Zinker, W. Chiou, L. Kifle, N. Cao, M. Perham, R. Dickinson, A. Adler, G. Gagne, R. Iyengar, G. Zhao, K. Marsh, P. Kym, P. Jung, H. S. Camp, and E. Frevert, "Identification and characterization of a small molecule ampk activator that treats key components of type 2 diabetes and the metabolic syndrome," Cell Metab, vol. 3, no. 6, pp. 403–16, 2006.

[210] G. Zhou, R. Myers, Y. Li, Y. Chen, X. Shen, J. Fenyk-Melody, M. Wu, J. Ventre, T. Doebber, N. Fujii, N. Musi, M. F. Hirshman, L. J. Goodyear, and D. E. Moller, "Role of amp-activated protein kinase in mechanism of metformin action," J Clin Invest, vol. 108, no. 8, pp. 1167–74, 2001.

[211] M. D. Fullerton, S. Galic, K. Marcinko, S. Sikkema, T. Pulinilkunnil, Z.-P. Chen, H. M. O'Neill, R. J. Ford, R. Palanivel, M. O'Brien, D. G. Hardie, S. L. Macaulay, J. D. Schertzer, J. R. B. Dyck, B. J. van Denderen, B. E. Kemp, and G. R. Steinberg, "Single phosphorylation sites in acc1 and acc2 regulate lipid homeostasis and the insulin-sensitizing effects of metformin," Nat Med, vol. 19, no. 12, pp. 1649–1654, 2013.

[212] J. M. Evans, L. A. Donnelly, A. M. Emslie-Smith, D. R. Alessi, and A. D. Morris, "Metformin and reduced risk of cancer in diabetic patients," Bmj, vol. 330, no. 7503, pp. 1304–5, 2005.

[213] C. W. Lee, L. L. Wong, E. Y. Tse, H. F. Liu, V. Y. Leong, J. M. Lee, D. G. Hardie, I. O. Ng, and Y. P. Ching, "Ampk promotes p53 acetylation via phosphorylation and inactivation of sirt1 in liver cancer cells," Cancer Res, vol. 72, no. 17, pp. 4394–404, 2012.

[214] M. Nakau, H. Miyoshi, M. F. Seldin, M. Imamura, M. Oshima, and M. M. Taketo, "Hepatocellular carcinoma caused by loss of heterozygosity in lkb1 gene knockout mice," Cancer Res, vol. 62, no. 16, pp. 4549–53, 2002.

[215] D. Grahame Hardie, "Amp-activated protein kinase: a key regulator of energy balance with many roles in human disease," J Intern Med, vol. 276, no. 6, pp. 543–59, 2014.

[216] M. F. McCarty, "mtorc1 activity as a determinant of cancer risk–rationalizing the cancer-preventive effects of adiponectin, metformin, rapamycin, and low-protein vegan diets," Med Hypotheses, vol. 77, no. 4, pp. 642–8, 2011.

[217] X. Huang, S. Wullschleger, N. Shpiro, V. A. McGuire, K. Sakamoto, Y. L. Woods, W. McBurnie, S. Fleming, and D. R. Alessi, "Important role of the lkb1-ampk pathway in suppressing tumorigenesis in pten-deficient mice," Biochem J, vol. 412, no. 2, pp. 211–21, 2008.

[218] H. Noto, A. Goto, T. Tsujimoto, and M. Noda, "Cancer risk in diabetic patients treated with metformin: a systematic review and meta-analysis," PLoS One, vol. 7, no. 3, p. e33411, 2012.

[219] D. Sag, D. Carling, R. D. Stout, and J. Suttles, "Adenosine 5'-monophosphate-activated protein kinase promotes macrophage polarization to an anti-inflammatory functional phenotype," J Immunol, vol. 181, no. 12, pp. 8633–41, 2008.

[220] C. M. Krawczyk, T. Holowka, J. Sun, J. Blagih, E. Amiel, R. J. DeBerardinis, J. R. Cross, E. Jung, C. B. Thompson, R. G. Jones, and E. J. Pearce, "Toll-like receptor-induced changes in glycolytic metabolism regulate dendritic cell activation," Blood, vol. 115, no. 23, pp. 4742–9, 2010.

[221] S. Galic, M. D. Fullerton, J. D. Schertzer, S. Sikkema, K. Marcinko, C. R. Walkley, D. Izon, J. Honeyman, Z. P. Chen, B. J. van Denderen, B. E. Kemp, and G. R. Steinberg, "Hematopoietic ampk beta1 reduces mouse adipose tissue macrophage inflammation and insulin resistance in obesity," J Clin Invest, vol. 121, no. 12, pp. 4903–15, 2011.

[222] N. Nath, M. Khan, M. K. Paintlia, I. Singh, M. N. Hoda, and S. Giri, "Metformin attenuated the autoimmune disease of the central nervous system in animal models of multiple sclerosis," J Immunol, vol. 182, no. 12, pp. 8005–14, 2009.

[223] X. Ma, Y. Jiang, A. Wu, X. Chen, R. Pi, M. Liu, and Y. Liu, "Berberine attenuates experimental autoimmune encephalomyelitis in c57 bl/6 mice," PLoS One, vol. 5, no. 10, p. e13489, 2010.

[224] N. Nath, S. Giri, R. Prasad, M. L. Salem, A. K. Singh, and I. Singh, "5-aminoimidazole-4-carboxamide ribonucleoside: a novel immunomodulator with therapeutic efficacy in experimental autoimmune encephalomyelitis," J Immunol, vol. 175, no. 1, pp. 566–74, 2005.

[225] S. A. Hawley, M. D. Fullerton, F. A. Ross, J. D. Schertzer, C. Chevtzoff, K. J. Walker, M. W. Peggie, D. Zibrova, K. A. Green, K. J. Mustard, B. E. Kemp, K. Sakamoto, G. R. Steinberg, and D. G. Hardie, "The ancient drug salicylate directly activates amp-activated protein kinase," Science, vol. 336, no. 6083, pp. 918–22, 2012.

[226] J. Puyal, V. Ginet, Y. Grishchuk, A. C. Truttmann, and P. G. Clarke, "Neuronal autophagy as a mediator of life and death: contrasting roles in chronic neurodegenerative and acute neural disorders," Neuroscientist, vol. 18, no. 3, pp. 224–36, 2012.

[227] D. Y. Lu, C. H. Tang, Y. H. Chen, and I. H. Wei, "Berberine suppresses neuroinflammatory responses through amp-activated protein kinase activation in bv-2 microglia," J Cell Biochem, vol. 110, no. 3, pp. 697–705, 2010.

[228] V. Vingtdeux, P. Chandakkar, H. Zhao, C. d'Abramo, P. Davies, and P. Marambaud, "Novel synthetic small-molecule activators of ampk as enhancers of autophagy and amyloid-beta peptide degradation," Faseb j, vol. 25, no. 1, pp. 219–31, 2011.

[229] C. C. Hsu, M. L. Wahlqvist, M. S. Lee, and H. N. Tsai, "Incidence of dementia is increased in type 2 diabetes and reduced by the use of sulfonylureas and metformin," J Alzheimers Dis, vol. 24, no. 3, pp. 485–93, 2011.

[230] A. Salminen and K. Kaarniranta, "Amp-activated protein kinase (ampk) controls the aging process via an integrated signaling network," Ageing Res Rev, vol. 11, no. 2, pp. 230–41, 2012.

[231] F. Petursson, M. Husa, R. June, M. Lotz, R. Terkeltaub, and R. Liu-Bryan, "Linked decreases in liver kinase b1 and amp-activated protein kinase activity modulate matrix catabolic responses to biomechanical injury in chondrocytes," Arthritis Res Ther, vol. 15, no. 4, p. R77, 2013.

[232] K. Takayama, K. Ishida, T. Matsushita, N. Fujita, S. Hayashi, K. Sasaki, K. Tei, S. Kubo, T. Matsumoto, H. Fujioka, M. Kurosaka, and R. Kuroda, "Sirt1 regulation of apoptosis of human chondrocytes," Arthritis Rheum, vol. 60, no. 9, pp. 2731–40, 2009.

[233] T. Matsushita, H. Sasaki, K. Takayama, K. Ishida, T. Matsumoto, S. Kubo, T. Matsuzaki, K. Nishida, M. Kurosaka, and R. Kuroda, "The overexpression of sirt1 inhibited osteoarthritic gene expression changes induced by interleukin-1beta in human chondrocytes," J Orthop Res, vol. 31, no. 4, pp. 531–7, 2013.

[234] O. Gabay, C. Sanchez, M. Dvir-Ginzberg, V. Gagarina, K. J. Zaal, Y. Song, X. H. He, and M. W. McBurney, "Sirtuin 1 enzymatic activity is required for cartilage homeostasis in vivo in a mouse model," Arthritis Rheum, vol. 65, no. 1, pp. 159–66, 2013.

[235] P. F. Hu, W. P. Chen, J. L. Tang, J. P. Bao, and L. D. Wu, "Protective effects of berberine in an experimental rat osteoarthritis model," Phytother Res, vol. 25, no. 6, pp. 878–85, 2011.

[236] A. Woods, S. R. Johnstone, K. Dickerson, F. C. Leiper, L. G. Fryer, D. Neumann, U. Schlattner, T. Wallimann, M. Carlson, and D. Carling, "Lkb1 is the upstream kinase in the amp-activated protein kinase cascade," Curr Biol, vol. 13, no. 22, pp. 2004–8, 2003.

[237] G. J. Gowans, S. A. Hawley, F. A. Ross, and D. G. Hardie, "Amp is a true physiological regulator of amp-activated protein kinase by both allosteric activation and enhancing net phosphorylation," Cell Metab, vol. 18, no. 4, pp. 556–66, 2013.

[238] G. Herrero-Martin, M. Hoyer-Hansen, C. Garcia-Garcia, C. Fumarola, T. Farkas, A. Lopez-Rivas, and M. Jaattela, "Tak1 activates ampk-dependent cytoprotective autophagy in trail-treated epithelial cells," Embo j, vol. 28, no. 6, pp. 677–85, 2009.

[239] R. A. Screaton, M. D. Conkright, Y. Katoh, J. L. Best, G. Canettieri, S. Jeffries, E. Guzman, S. Niessen, r. Yates, J. R., H. Takemori, M. Okamoto, and M. Montminy, "The creb coactivator torc2 functions as a calcium- and camp-sensitive coincidence detector," Cell, vol. 119, no. 1, pp. 61–74, 2004.

[240] Y. Nakahata, S. Sahar, G. Astarita, M. Kaluzova, and P. Sassone-Corsi, "Circadian control of the nad+ salvage pathway by clock-sirt1," Science, vol. 324, no. 5927, pp. 654–7, 2009.

[241] F. Lan, J. M. Cacicedo, N. Ruderman, and Y. Ido, "Sirt1 modulation of the acetylation status, cytosolic localization, and activity of lkb1. possible role in amp-activated protein kinase activation," J Biol Chem, vol. 283, no. 41, pp. 27628–35, 2008.

[242] E. L. Greer, D. Dowlatshahi, M. R. Banko, J. Villen, K. Hoang, D. Blanchard, S. P. Gygi, and A. Brunet, "An ampk-foxo pathway mediates longevity induced by a novel method of dietary restriction in c. elegans," Curr Biol, vol. 17, no. 19, pp. 1646–56, 2007.

[243] M. C. Hu, D. F. Lee, W. Xia, L. S. Golfman, F. Ou-Yang, J. Y. Yang, Y. Zou, S. Bao, N. Hanada, H. Saso, R. Kobayashi, and M. C. Hung, "Ikappab kinase promotes tumorigenesis through inhibition of forkhead foxo3a," Cell, vol. 117, no. 2, pp. 225–37, 2004.

[244] Y. Hattori, K. Suzuki, S. Hattori, and K. Kasai, "Metformin inhibits cytokine-induced nuclear factor kappab activation via amp-activated protein kinase activation in vascular endothelial cells," Hypertension, vol. 47, no. 6, pp. 1183–8, 2006.

[245] J. W. Lee, S. Park, Y. Takahashi, and H.-G. Wang, "The association of ampk with ulk1 regulates autophagy," PLoS ONE, vol. 5, no. 11, p. e15394, 2010. PONE-D-10-00025[PII] 21072212[pmid] PLoS One.

[246] H. Hatakeyama and M. Kanzaki, "Regulatory mode shift of tbc1d1 is required for acquisition of insulin-responsive glut4-trafficking activity," Mol Biol Cell, vol. 24, no. 6, pp. 809–17, 2013.

[247] N. B. Ruderman, J. M. Cacicedo, S. Itani, N. Yagihashi, A. K. Saha, J. M. Ye, K. Chen, M. Zou, D. Carling, G. Boden, R. A. Cohen, J. Keaney, E. W. Kraegen, and Y. Ido, "Malonyl-coa and amp-activated protein kinase (ampk): possible links between insulin resistance in muscle and early endothelial cell damage in diabetes," Biochem Soc Trans, vol. 31, no. Pt 1, pp. 202–6, 2003.

[248] H. U. Park, S. Suy, M. Danner, V. Dailey, Y. Zhang, H. Li, D. R. Hyduke, B. T. Collins, G. Gagnon, B. Kallakury, D. Kumar, M. L. Brown, A. Fornace, A. Dritschilo, and S. P. Collins, "Amp-activated protein kinase promotes human prostate cancer cell growth and survival," Mol Cancer Ther, vol. 8, no. 4, pp. 733–41, 2009.

[249] K. Kato, T. Ogura, A. Kishimoto, Y. Minegishi, N. Nakajima, M. Miyazaki, and H. Esumi, "Critical roles of amp-activated protein kinase in constitutive tolerance of cancer cells to nutrient deprivation and tumor formation," Oncogene, vol. 21, no. 39, pp. 6082–90, 2002.

[250] E. E. Mendoza, M. G. Pocceschi, X. Kong, D. B. Leeper, J. Caro, K. H. Limesand, and R. Burd, "Control of glycolytic flux by amp-activated protein kinase in tumor cells adapted to low ph," Transl Oncol, vol. 5, no. 3, pp. 208–16, 2012.

[251] M. Buzzai, D. E. Bauer, R. G. Jones, R. J. Deberardinis, G. Hatzivassiliou, R. L. Elstrom, and C. B. Thompson, "The glucose dependence of akt-transformed cells can be reversed by pharmacologic activation of fatty acid beta-oxidation," Oncogene, vol. 24, no. 26, pp. 4165–73, 2005.

[252] C. E. Massie, A. Lynch, A. Ramos-Montoya, J. Boren, R. Stark, L. Fazli, A. Warren, H. Scott, B. Madhu, N. Sharma, H. Bon, V. Zecchini, D. M. Smith, G. M. Denicola, N. Mathews, M. Osborne, J. Hadfield, S. Macarthur, B. Adryan, S. K. Lyons, K. M. Brindle, J. Griffiths, M. E. Gleave, P. S. Rennie, D. E. Neal, and I. G. Mills, "The androgen receptor fuels prostate cancer by regulating central metabolism and biosynthesis," Embo j, vol. 30, no. 13, pp. 2719–33, 2011.

[253] H. Yun, M. Lee, S. S. Kim, and J. Ha, "Glucose deprivation increases mrna stability of vascular endothelial growth factor through activation of amp-activated protein kinase in du145 prostate carcinoma," J Biol Chem, vol. 280, no. 11, pp. 9963–72, 2005.

[254] B. G. Ha, J. E. Park, H. J. Cho, Y. B. Lim, and Y. H. Shon, "Inhibitory effects of proton beam irradiation on integrin expression and signaling pathway in human colon carcinoma ht29 cells," Int J Oncol, vol. 46, no. 6, pp. 2621–8, 2015.

[255] W. C. Chen, Y. S. Chang, H. P. Hsu, M. C. Yen, H. L. Huang, C. Y. Cho, C. Y. Wang, T. Y. Weng, P. T. Lai, C. S. Chen, Y. J. Lin, and M. D. Lai, "Therapeutics targeting cd90-integrin-ampk-cd133 signal axis in liver cancer," Oncotarget, vol. 6, no. 40, pp. 42923–37, 2015.

[256] Y. S. Park, S. Hwang, Y. M. Jin, Y. Yu, S. A. Jung, S. C. Jung, K. H. Ryu, H. S. Kim, and I. Jo, "Ccn1 secreted by tonsil-derived mesenchymal stem cells promotes endothelial cell angiogenesis via integrin alphav beta3 and ampk," J Cell Physiol, vol. 230, no. 1, pp. 140–9, 2015.

[257] J. J. Park, S. M. Seo, E. J. Kim, Y. J. Lee, Y. G. Ko, J. Ha, and M. Lee, "Berberine inhibits human colon cancer cell migration via amp-activated protein kinase-mediated downregulation of integrin beta1 signaling," Biochem Biophys Res Commun, vol. 426, no. 4, pp. 461–7, 2012.

[258] E. Ross, R. Ata, T. Thavarajah, S. Medvedev, P. Bowden, J. G. Marshall, and C. N. Antonescu, "Amp-activated protein kinase regulates the cell surface proteome and integrin membrane traffic," PLoS One, vol. 10, no. 5, p. e0128013, 2015.

[259] C. H. Tang and M. E. Lu, "Adiponectin increases motility of human prostate cancer cells via adipor, p38, ampk, and nf-kappab pathways," Prostate, vol. 69, no. 16, pp. 1781–9, 2009.

[260] V. Randriamboavonjy, J. Isaak, T. Fromel, B. Viollet, B. Fisslthaler, K. T. Preissner, and I. Fleming, "Ampk alpha2 subunit is involved in platelet signaling, clot retraction, and thrombus stability," Blood, vol. 116, no. 12, pp. 2134–40, 2010.

[261] Q. Tang, S. Zhao, J. Wu, F. Zheng, L. Yang, J. Hu, and S. S. Hann, "Inhibition of integrin-linked kinase expression by emodin through crosstalk of ampkalpha and erk1/2 signaling and reciprocal interplay of sp1 and c-jun," Cell Signal, vol. 27, no. 7, pp. 1469–77, 2015.

[262] S. Mizrachy-Schwartz, N. Kravchenko-Balasha, H. Ben-Bassat, S. Klein, and A. Levitzki, "Optimization of energy-consuming pathways towards rapid growth in hpv-transformed cells," PLoS One, vol. 2, no. 7, p. e628, 2007.

[263] S. Mizrachy-Schwartz, N. Cohen, S. Klein, N. Kravchenko-Balasha, and A. Levitzki, "Up-regulation of ampk in cancer cell lines is mediated through c-src activation," Journal of Biological Chemistry, 2011.

[264] P. Fan, O. L. Griffith, F. A. Agboke, P. Anur, X. Zou, R. E. McDaniel, K. Creswell, S. H. Kim, J. A. Katzenellenbogen, J. W. Gray, and V. C. Jordan, "c-src modulates estrogen-induced stress and apoptosis in estrogen-deprived breast cancer cells," Cancer Res, vol. 73, no. 14, pp. 4510–20, 2013.

[265] E. Yamada and C. C. Bastie, "Disruption of fyn sh3 domain interaction with a proline-rich motif in liver kinase b1 results in activation of amp-activated protein kinase," PLoS One, vol. 9, no. 2, p. e89604, 2014.

[266] M. H. Zou, X. Y. Hou, C. M. Shi, S. Kirkpatick, F. Liu, M. H. Goldman, and R. A. Cohen, "Activation of 5'-amp-activated kinase is mediated through c-src and phosphoinositide 3-kinase activity during hypoxia-reoxygenation of bovine aortic endothelial cells. role of peroxynitrite," J Biol Chem, vol. 278, no. 36, pp. 34003–10, 2003.

[267] E. K. Lee, J. U. Jeong, J. W. Chang, W. S. Yang, S. B. Kim, S. K. Park, J. S. Park, and S. K. Lee, "Activation of amp-activated protein kinase inhibits albumin-induced endoplasmic reticulum stress and apoptosis through inhibition of reactive oxygen species," Nephron Exp Nephrol, vol. 121, no. 1-2, pp. e38–48, 2012.

[268] J. O. Lee, S. K. Lee, J. H. Kim, N. Kim, G. Y. You, J. W. Moon, S. J. Kim, S. H. Park, and H. S. Kim, "Metformin regulates glucose transporter 4 (glut4) translocation through amp-activated protein kinase (ampk)-mediated cbl/cap signaling in 3t3-l1 preadipocyte cells," J Biol Chem, vol. 287, no. 53, pp. 44121–9, 2012.

[269] L. Vucicevic, M. Misirkic, K. Janjetovic, U. Vilimanovich, E. Sudar, E. Isenovic, M. Prica, L. Harhaji-Trajkovic, T. Kravic-Stevovic, V. Bumbasirevic, and V. Trajkovic, "Compound c induces protective autophagy in cancer cells through ampk inhibition-independent blockade of akt/mtor pathway," Autophagy, vol. 7, no. 1, pp. 40–50, 2011.

[270] K. C. Chan, M. C. Lin, C. N. Huang, W. C. Chang, and C. J. Wang, "Mulberry 1-deoxynojirimycin pleiotropically inhibits glucose-stimulated vascular smooth muscle cell migration by activation of ampk/rhob and down-regulation of fak," J Agric Food Chem, vol. 61, no. 41, pp. 9867–75, 2013.

[271] M. Kodiha, J. G. Rassi, C. M. Brown, and U. Stochaj, "Localization of amp kinase is regulated by stress, cell density, and signaling through the mek–¿erk1/2 pathway," Am J Physiol Cell Physiol, vol. 293, no. 5, pp. C1427–36, 2007.

[272] A. Suzuki, S. Okamoto, S. Lee, K. Saito, T. Shiuchi, and Y. Minokoshi, "Leptin stimulates fatty acid oxidation and peroxisome proliferator-activated receptor alpha gene expression in mouse c2c12 myoblasts by changing the subcellular localization of the alpha2 form of amp-activated protein kinase," Mol Cell Biol, vol. 27, no. 12, pp. 4317–27, 2007.

[273] K. I. Mitchelhill, B. J. Michell, C. M. House, D. Stapleton, J. Dyck, J. Gamble, C. Ullrich, L. A. Witters, and B. E. Kemp, "Posttranslational modifications of the 5'-amp-activated protein kinase beta1 subunit," J Biol Chem, vol. 272, no. 39, pp. 24475–9, 1997.

[274] J. S. Oakhill, Z. P. Chen, J. W. Scott, R. Steel, L. A. Castelli, N. Ling, S. L. Macaulay, and B. E. Kemp, "beta-subunit myristoylation is the gatekeeper for initiating metabolic stress sensing by amp-activated protein kinase (ampk)," Proc Natl Acad Sci U S A, vol. 107, no. 45, pp. 19237–41, 2010.

[275] A. Vazquez-Martin, C. Oliveras-Ferraros, and J. A. Menendez, "The active form of the metabolic sensor: Amp-activated protein kinase (ampk) directly binds the mitotic apparatus and travels from centrosomes to the spindle midzone during mitosis and cytokinesis," Cell Cycle, vol. 8, no. 15, pp. 2385–98, 2009.

[276] C. Boehlke, F. Kotsis, V. Patel, S. Braeg, H. Voelker, S. Bredt, T. Beyer, H. Janusch, C. Hamann, M. Godel, K. Muller, M. Herbst, M. Hornung, M. Doerken, M. Kottgen, R. Nitschke, P. Igarashi, G. Walz, and E. W. Kuehn, "Primary cilia regulate mtorc1 activity and cell size through lkb1," Nat Cell Biol, vol. 12, no. 11, pp. 1115–22, 2010.

[277] P. Tsou, B. Zheng, C. H. Hsu, A. T. Sasaki, and L. C. Cantley, "A fluorescent reporter of ampk activity and cellular energy stress," Cell Metab, vol. 13, no. 4, pp. 476–86, 2011.

[278] T. Miyamoto, E. Rho, V. Sample, H. Akano, M. Magari, T. Ueno, K. Gorshkov, M. Chen, H. Tokumitsu, J. Zhang, and T. Inoue, "Compartmentalized ampk signaling illuminated by genetically encoded molecular sensors and actuators," Cell Reports, vol. 11, no. 4, pp. 657–670.

[279] L. Bian, E. G. Lima, S. L. Angione, K. W. Ng, D. Y. Williams, D. Xu, A. M. Stoker, J. L. Cook, G. A. Ateshian, and C. T. Hung, "Mechanical and biochemical characterization of cartilage explants in serum-free culture," Journal of Biomechanics, vol. 41, no. 6, pp. 1153–1159, 2008.

[280] M. B. Goldring and S. R. Goldring, "Osteoarthritis," J Cell Physiol, vol. 213, no. 3, pp. 626–634, 2007.

[281] K. Von Der Mark, V. Gauss, H. Von Der Mark, and P. Muller, "Relationship between cell shape and type of collagen synthesised as chondrocytes lose their cartilage phenotype in culture," Nature, vol. 267, no. 5611, pp. 531–532, 1977.

[282] O. W. Petersen, L. Rnnov-Jessen, A. R. Howlett, and M. J. Bissell, "Interaction with basement membrane serves to rapidly distinguish growth and differentiation pattern of normal and malignant human breast epithelial cells," Proceedings of the National Academy of Sciences of the United States of America, vol. 89, no. 19, pp. 9064–9068, 1992.

[283] M. Banerjee and R. R. Bhonde, "Application of hanging drop technique for stem cell differentiation and cytotoxicity studies," Cytotechnology, vol. 51, no. 1, pp. 1–5, 2006.

[284] P. Benya and J. Shaffer, "Dedifferentiated chondrocytes reexpress the differentiated collagen phenotype when cultured in agarose gels," Cell, vol. 30, no. 1, pp. 215 – 224, 1982.

[285] J. T. Emerman and D. R. Pitelka, "Maintenance and induction of morphological differentiation in dissociated mammary epithelium on floating collagen membranes," In Vitro, vol. 13, no. 5, pp. 316–28, 1977.

[286] J. A. Hickman, R. Graeser, R. de Hoogt, S. Vidic, C. Brito, M. Gutekunst, H. van der Kuip, et al., "Three-dimensional models of cancer for pharmacology and cancer cell biology: Capturing tumor complexity in vitro/ex vivo," Biotechnology journal, vol. 9, no. 9, pp. 1115–1128, 2014.

[287] L. M. McCaffrey and I. G. Macara, "Epithelial organization, cell polarity and tumorigenesis," Trends in Cell Biology, vol. 21, no. 12, pp. 727–735.

[288] V. M. Weaver, S. Lelivre, J. N. Lakins, M. A. Chrenek, J. C. R. Jones, F. Giancotti, Z. Werb, and M. J. Bissell, "4 integrin-dependent formation of polarized three-dimensional architecture confers resistance to apoptosis in normal and malignant mammary epithelium," Cancer cell, vol. 2, no. 3, pp. 205–216, 2002.

[289] J. Meyers, J. Craig, and D. J. Odde, "Potential for control of signaling pathways via cell size and shape," Curr Biol, vol. 16, no. 17, pp. 1685–93, 2006.

[290] J. B. Kim, "Three-dimensional tissue culture models in cancer biology," Semin Cancer Biol, vol. 15, no. 5, pp. 365–77, 2005.

[291] M. A. Wozniak, K. Modzelewska, L. Kwong, and P. J. Keely, "Focal adhesion regulation of cell behavior," Biochimica et Biophysica Acta (BBA) - Molecular Cell Research, vol. 1692, no. 23, pp. 103–119, 2004.

[292] B. M. Baker and C. S. Chen, "Deconstructing the third dimension–how 3d culture microenvironments alter cellular cues," J Cell Sci, vol. 125, no. 13, pp. 3015–3024, 2012.

[293] C. P. Soares, V. Midlej, M. E. W. de Oliveira, M. Benchimol, M. L. Costa, and C. Mermelstein, "2d and 3d-organized cardiac cells shows differences in cellular morphology, adhesion junctions, presence of myofibrils and protein expression," PloS one, vol. 7, no. 5, p. e38147, 2012.

[294] S. Breslin and L. ODriscoll, "Three-dimensional cell culture: the missing link in drug discovery," Drug Discovery Today, vol. 18, no. 56, pp. 240–249, 2013.

[295] R. Edmondson, J. J. Broglie, A. F. Adcock, and L. Yang, "Three-dimensional cell culture systems and their applications in drug discovery and cell-based biosensors," Assay and Drug Development Technologies, vol. 12, no. 4, pp. 207–218.

[296] W. E. Hennink and C. F. van Nostrum, "Novel crosslinking methods to design hydrogels," Adv Drug Deliv Rev, vol. 54, no. 1, pp. 13–36, 2002.

[297] R. A. Marklein and J. A. Burdick, "Controlling stem cell fate with material design," Adv Mater, vol. 22, no. 2, pp. 175–89, 2010.

[298] E. Knight and S. Przyborski, "Advances in 3d cell culture technologies enabling tissue-like structures to be created in vitro," J Anat, vol. 227, no. 6, pp. 746–56, 2015.

[299] H. Muir, P. Bullough, and A. Maroudas, "The distribution of collagen in human articular cartilage with some of its physiological implications," J Bone Joint Surg Br, vol. 52, no. 3, pp. 554–63, 1970.

[300] M.-T. Sheu, J.-C. Huang, G.-C. Yeh, and H.-O. Ho, "Characterization of collagen gel solutions and collagen matrices for cell culture," Biomaterials, vol. 22, no. 13, pp. 1713–1719, 2001.

[301] T. Koide and M. Daito, "Effects of various collagen crosslinking techniques on mechanical properties of collagen film," Dent Mater J, vol. 16, no. 1, pp. 1–9, 1997.

[302] B. Chevallay and D. Herbage, "Collagen-based biomaterials as 3d scaffold for cell cultures: applications for tissue engineering and gene therapy," Med Biol Eng Comput, vol. 38, no. 2, pp. 211–8, 2000.

[303] T. Andersen, P. Auk-Emblem, and M. Dornish, "3d cell culture in alginate hydrogels," Microarrays, vol. 4, no. 2, p. 133, 2015.

[304] V. M. Rodriquez, B. B. Vega, Z. R. Romao, K. D. Saldana, and O. L. Quinones, "Chitosan and its potential use as a scaffold for tissue engineering in regenerative medicine," BioMed Research International, vol. 2015, p. 15, 2015.

[305] E. Santos, R. M. Hernandez, J. L. Pedraz, and G. Orive, "Novel advances in the design of three-dimensional bio-scaffolds to control cell fate: translation from 2d to 3d," Trends Biotechnol, vol. 30, no. 6, pp. 331–41, 2012.

[306] P. D. Benya and S. R. Padilla, "Dihydrocytochalasin b enhances transforming growth factor-beta-induced reexpression of the differentiated chondrocyte phenotype without stimulation of collagen synthesis," Exp Cell Res, vol. 204, no. 2, pp. 268–77, 1993.

[307] M. Buschmann, Y. Gluzband, A. Grodzinsky, and E. Hunziker, "Mechanical compression modulates matrix biosynthesis in chondrocyte/agarose culture," J Cell Sci, vol. 108, no. Pt 4, pp. 1497 – 1508, 1995.

[308] M. D. Buschmann, Y. A. Gluzband, A. J. Grodzinsky, J. H. Kimura, and E. B. Hunziker, "Chondrocytes in agarose culture synthesize a mechanically functional extracellular matrix," J Orthop Res, vol. 10, no. 6, pp. 745–58, 1992.

[309] D. A. Lee and D. L. Bader, "The development and characterization of an in vitro system to study strain-induced cell deformation in isolated chondrocytes," In Vitro Cell Dev Biol Anim, vol. 31, no. 11, pp. 828–35, 1995.

[310] R. L. Sah, J. Y. Doong, A. J. Grodzinsky, A. H. Plaas, and J. D. Sandy, "Effects of compression on the loss of newly synthesized proteoglycans and proteins from cartilage explants," Arch Biochem Biophys, vol. 286, no. 1, pp. 20–9, 1991.

[311] J. Smetana, K., "Cell biology of hydrogels," Biomaterials, vol. 14, no. 14, pp. 1046–50, 1993.

[312] C. N. Soparkar, J. F. Wong, J. R. Patrinely, and D. Appling, "Growth factors embedded in an agarose matrix enhance the rate of porous polyethylene implant biointegration," Ophthal Plast Reconstr Surg, vol. 16, no. 5, pp. 341–6, 2000.

[313] C. N. Soparkar, J. F. Wong, J. R. Patrinely, J. K. Davidson, and D. Appling, "Porous polyethylene implant fibrovascularization rate is affected by tissue wrapping, agarose coating, and insertion site," Ophthal Plast Reconstr Surg, vol. 16, no. 5, pp. 330–6, 2000.

[314] Y. Wang and N. Wang, "Fret and mechanobiology," Integrative Biology, vol. 1, no. 10, pp. 565–573, 2009.

[315] A. Y. Ting, K. H. Kain, R. L. Klemke, and R. Y. Tsien, "Genetically encoded fluorescent reporters of protein tyrosine kinase activities in living cells," Proceedings of the National Academy of Sciences, vol. 98, no. 26, pp. 15003–15008, 2001.

[316] P. Tsou, B. Zheng, C. H. Hsu, A. T. Sasaki, and L. C. Cantley, "A fluorescent reporter of ampk activity and cellular energy stress," Cell Metab, vol. 13, no. 4, pp. 476–86, 2011.

[317] H. Yoshizaki, Y. Ohba, K. Kurokawa, R. E. Itoh, T. Nakamura, N. Mochizuki, K. Nagashima, and M. Matsuda, "Activity of rho-family gtpases during cell division as visualized with fret-based probes," J Cell Biol, vol. 162, no. 2, pp. 223–232, 2003.

[318] N. Mochizuki, S. Yamashita, K. Kurokawa, Y. Ohba, T. Nagai, A. Miyawaki, and M. Matsuda, "Spatio-temporal images of growth-factor-induced activation of ras and rap1," Nature, vol. 411, no. 6841, pp. 1065–8, 2001.

[319] R. E. Itoh, K. Kurokawa, Y. Ohba, H. Yoshizaki, N. Mochizuki, and M. Matsuda, "Activation of rac and cdc42 video imaged by fluorescent resonance energy transfer-based single-molecule probes in the membrane of living cells," Mol Cell Biol, vol. 22, no. 18, pp. 6582–91, 2002.

[320] A. Miyawaki, J. Llopis, R. Heim, J. M. McCaffery, J. A. Adams, M. Ikura, and R. Y. Tsien, "Fluorescent indicators for ca2+ based on green fluorescent proteins and calmodulin," Nature, vol. 388, no. 6645, pp. 882–7, 1997.

[321] R. D. Mitra, C. M. Silva, and D. C. Youvan, "Fluorescence resonance energy transfer between blue-emitting and red-shifted excitation derivatives of the green fluorescent protein," Gene, vol. 173, no. 1 Spec No, pp. 13–7, 1996.

[322] L. M. DiPilato, X. Cheng, and J. Zhang, "Fluorescent indicators of camp and epac activation reveal differential dynamics of camp signaling within discrete subcellular compartments," Proc Natl Acad Sci U S A, vol. 101, no. 47, pp. 16513–16518, 2004.

[323] B. Ananthanarayanan, Q. Ni, and J. Zhang, "Signal propagation from membrane messengers to nuclear effectors revealed by reporters of phosphoinositide dynamics and akt activity," Proc Natl Acad Sci U S A, vol. 102, no. 42, pp. 15081–15086, 2005.

[324] M. Kim, C. V. Carman, and T. A. Springer, "Bidirectional transmembrane signaling by cytoplasmic domain separation in integrins," Science, vol. 301, no. 5640, pp. 1720–1725, 2003.

[325] M. C. Dodla and R. V. Bellamkonda, "Anisotropic scaffolds facilitate enhanced neurite extension in vitro," J Biomed Mater Res A, vol. 78, no. 2, pp. 213–21, 2006.

[326] S. Na, O. Collin, F. Chowdhury, B. Tay, M. Ouyang, Y. Wang, and N. Wang, "Rapid signal transduction in living cells is a unique feature of mechanotransduction," Proceedings of the National Academy of Sciences, vol. 105, no. 18, pp. 6626–6631, 2008.

[327] V. J. Fincham, M. Unlu, V. G. Brunton, J. D. Pitts, J. A. Wyke, and M. C. Frame, "Translocation of src kinase to the cell periphery is mediated by the actin cytoskeleton under the control of the rho family of small g proteins," J Cell Biol, vol. 135, no. 6 Pt 1, pp. 1551–64, 1996.

[328] P. Tsaytler, H. P. Harding, D. Ron, and A. Bertolotti, "Selective inhibition of a regulatory subunit of protein phosphatase 1 restores proteostasis," Science, vol. 332, no. 6025, pp. 91–4, 2011.

[329] M. T. Brown and J. A. Cooper, "Regulation, substrates and functions of src," Biochimica et Biophysica Acta (BBA)-Reviews on Cancer, vol. 1287, no. 2, pp. 121–149, 1996.

[330] V. G. Brunton and M. C. Frame, "Src and focal adhesion kinase as therapeutic targets in cancer," Current opinion in pharmacology, vol. 8, no. 4, pp. 427–432, 2008.

[331] S. M. Thomas and J. S. Brugge, "Cellular functions regulated by src family kinases," Annual review of cell and developmental biology, vol. 13, no. 1, pp. 513–609, 1997.

[332] S. K. Mitra and D. D. Schlaepfer, "Integrin-regulated fak-src signaling in normal and cancer cells," Curr Opin Cell Biol, vol. 18, no. 5, pp. 516–23, 2006.

[333] S. Li, M. Kim, Y.-L. Hu, S. Jalali, D. D. Schlaepfer, T. Hunter, S. Chien, and J. Y. Shyy, "Fluid shear stress activation of focal adhesion kinase linking to mitogen-activated protein kinases," Journal of Biological Chemistry, vol. 272, no. 48, pp. 30455–30462, 1997.

[334] J. Seong, A. Tajik, J. Sun, J.-L. Guan, M. J. Humphries, S. E. Craig, A. Shekaran, A. J. García, S. Lu, M. Z. Lin, et al., "Distinct biophysical mechanisms of focal adhesion kinase mechanoactivation by different extracellular matrix proteins," Proceedings of the National Academy of Sciences, vol. 110, no. 48, pp. 19372–19377, 2013.

[335] S. Shahrara, H. P. Castro-Rueda, G. K. Haines, and A. E. Koch, "Differential expression of the fak family kinases in rheumatoid arthritis and osteoarthritis synovial tissues," Arthritis research & therapy, vol. 9, no. 5, p. 1, 2007.

[336] L. Bursell, A. Woods, C. G. James, D. Pala, A. Leask, and F. Beier, "Src kinase inhibition promotes the chondrocyte phenotype," Arthritis research & therapy, vol. 9, no. 5, p. 1, 2007.

[337] E. Cukierman, R. Pankov, D. R. Stevens, and K. M. Yamada, "Taking cell-matrix adhesions to the third dimension," Science, vol. 294, no. 5547, pp. 1708–1712, 2001.

[338] B. M. Baker and C. S. Chen, "Deconstructing the third dimension–how 3d culture microenvironments alter cellular cues," J Cell Sci, vol. 125, no. 13, pp. 3015–3024, 2012.

[339] S. I. Fraley, Y. Feng, R. Krishnamurthy, D.-H. Kim, A. Celedon, G. D. Longmore, and D. Wirtz, "A distinctive role for focal adhesion proteins in three-dimensional cell motility," Nature cell biology, vol. 12, no. 6, pp. 598–604, 2010.

[340] H. C. Brinkman, "A calculation of the viscous force exerted by a flowing fluid on a dense swarm of particles," Applied Scientific Research, vol. 1, no. 1, pp. 27–34, 1949.

[341] D. K. Cullen, M. C. Lessing, and M. C. LaPlaca, "Collagen-dependent neurite outgrowth and response to dynamic deformation in three-dimensional neuronal cultures," Ann Biomed Eng, vol. 35, no. 5, pp. 835–46, 2007.

[342] S. Sakai, I. Hashimoto, and K. Kawakami, "Synthesis of an agarose-gelatin conjugate for use as a tissue engineering scaffold," J Biosci Bioeng, vol. 103, no. 1, pp. 22–6, 2007.

[343] H. B. Manning, M. B. Nickdel, K. Yamamoto, J. L. Lagarto, D. J. Kelly, C. B. Talbot, G. Kennedy, J. Dudhia, J. Lever, C. Dunsby, P. French, and Y. Itoh, "Detection of cartilage matrix degradation by autofluorescence lifetime," Matrix Biol, vol. 32, no. 1, pp. 32–8, 2013.

[344] J. M. Menter, "Temperature dependence of collagen fluorescence," Photochem Photobiol Sci, vol. 5, no. 4, pp. 403–10, 2006.

[345] K. M. Skubitz, K. D. Campbell, and A. P. Skubitz, "Cd63 associates with cd11/cd18 in large detergent-resistant complexes after translocation to the cell surface in human neutrophils," FEBS Lett, vol. 469, no. 1, pp. 52–6, 2000.

[346] W. J. Polacheck, R. Li, S. G. Uzel, and R. D. Kamm, "Microfluidic platforms for mechanobiology," Lab Chip, vol. 13, no. 12, pp. 2252–67, 2013.

[347] Q. Wan, S. J. Kim, H. Yokota, and S. Na, "Differential activation and inhibition of rhoa by fluid flow induced shear stress in chondrocytes," Cell Biol Int, 2013.

[348] E. A. Jares-Erijman and T. M. Jovin, "Fret imaging," Nat Biotechnol, vol. 21, no. 11, pp. 1387–95, 2003.

[349] A. D. Hoppe, S. L. Shorte, J. A. Swanson, and R. Heintzmann, "Three-dimensional fret reconstruction microscopy for analysis of dynamic molecular interactions in live cells," Biophys J, vol. 95, no. 1, pp. 400–18, 2008.

[350] I. Georgakoudi, B. C. Jacobson, M. G. Muller, E. E. Sheets, K. Badizadegan, D. L. Carr-Locke, C. P. Crum, C. W. Boone, R. R. Dasari, J. Van Dam, and M. S. Feld, "Nad(p)h and collagen as in vivo quantitative fluorescent biomarkers of epithelial precancerous changes," Cancer Res, vol. 62, no. 3, pp. 682–7, 2002.

[351] K. Shield, M. L. Ackland, N. Ahmed, and G. E. Rice, "Multicellular spheroids in ovarian cancer metastases: Biology and pathology," Gynecologic oncology, vol. 113, no. 1, pp. 143–148, 2009.

[352] V. M. Weaver, S. Lelivre, J. N. Lakins, M. A. Chrenek, J. C. R. Jones, F. Giancotti, Z. Werb, and M. J. Bissell, "4 integrin-dependent formation of polarized three-dimensional architecture confers resistance to apoptosis in normal and malignant mammary epithelium," Cancer cell, vol. 2, no. 3, pp. 205–216, 2002.

[353] E. Cukierman, R. Pankov, D. R. Stevens, and K. M. Yamada, "Taking cell-matrix adhesions to the third dimension," Science, vol. 294, no. 5547, pp. 1708–1712, 2001.

[354] J. Eyckmans, T. Boudou, X. Yu, and C. S. Chen, "A hitchhiker's guide to mechanobiology," Developmental Cell, vol. 21, no. 1, pp. 35–47, 2011.

[355] B. D. Hoffman, C. Grashoff, and M. A. Schwartz, "Dynamic molecular processes mediate cellular mechanotransduction," Nature, vol. 475, no. 7356, pp. 316–323, 2011. 10.1038/nature10316.

[356] D. G. Hardie, "Amp-activated/snf1 protein kinases: conserved guardians of cellular energy," Nat Rev Mol Cell Biol, vol. 8, no. 10, pp. 774–85, 2007.

[357] J. R. Fay, V. Steele, and J. A. Crowell, "Energy homeostasis and cancer prevention: the amp-activated protein kinase," Cancer Prev Res (Phila), vol. 2, no. 4, pp. 301–9, 2009.

[358] N. A. Shirwany and M. H. Zou, "Ampk in cardiovascular health and disease," Acta Pharmacol Sin, vol. 31, no. 9, pp. 1075–84, 2010.

[359] X. H. Zeng, X. J. Zeng, and Y. Y. Li, "Efficacy and safety of berberine for congestive heart failure secondary to ischemic or idiopathic dilated cardiomyopathy," Am J Cardiol, vol. 92, no. 2, pp. 173–6, 2003.

[360] K. A. Coughlan, R. J. Valentine, N. B. Ruderman, and A. K. Saha, "Ampk activation: a therapeutic target for type 2 diabetes?," Diabetes, Metabolic Syndrome and Obesity: Targets and Therapy, vol. 7, pp. 241–253, 2014.

[361] V. T. Samuel, K. F. Petersen, and G. I. Shulman, "Lipid-induced insulin resistance: unravelling the mechanism," Lancet, vol. 375, no. 9733, pp. 2267–77, 2010.

[362] R. Terkeltaub, B. Yang, M. Lotz, and R. Liu-Bryan, "Chondrocyte amp-activated protein kinase activity suppresses matrix degradation responses to proinflammatory cytokines interleukin-1beta and tumor necrosis factor alpha," Arthritis Rheum, vol. 63, no. 7, pp. 1928–37, 2011.

[363] A. Salminen, J. M. Hyttinen, and K. Kaarniranta, "Amp-activated protein kinase inhibits nf-κb signaling and inflammation: impact on healthspan and lifespan," Journal of molecular medicine, vol. 89, no. 7, pp. 667–676, 2011.

[364] S. M. Warden, C. Richardson, J. O'Donnell, J., D. Stapleton, B. E. Kemp, and L. A. Witters, "Post-translational modifications of the beta-1 subunit of amp-activated protein kinase affect enzyme activity and cellular localization," Biochem J, vol. 354, no. Pt 2, pp. 275–83, 2001.

[365] A. Vazquez-Martin, C. Oliveras-Ferraros, and J. A. Menendez, "The active form of the metabolic sensor: Amp-activated protein kinase (ampk) directly binds the mitotic apparatus and travels from centrosomes to the spindle midzone during mitosis and cytokinesis," Cell Cycle, vol. 8, no. 15, pp. 2385–98, 2009.

[366] K. Hamamura, P. Zhang, L. Zhao, J. W. Shim, A. Chen, T. R. Dodge, Q. Wan, H. Shih, S. Na, C. C. Lin, H. B. Sun, and H. Yokota, "Knee loading reduces mmp13 activity in the mouse cartilage," BMC Musculoskelet Disord, vol. 14, p. 312, 2013.

[367] R. Lane Smith, M. C. Trindade, T. Ikenoue, M. Mohtai, P. Das, D. R. Carter, S. B. Goodman, and D. J. Schurman, "Effects of shear stress on articular chondrocyte metabolism," Biorheology, vol. 37, no. 1-2, pp. 95–107, 2000.

[368] Q. Wan, S. J. Kim, H. Yokota, and S. Na, "Differential activation and inhibition of rhoa by fluid flow induced shear stress in chondrocytes," Cell Biol Int, vol. 37, no. 6, pp. 568–76, 2013.

[369] R. L. Smith, B. S. Donlon, M. K. Gupta, M. Mohtai, P. Das, D. R. Carter, J. Cooke, G. Gibbons, N. Hutchinson, and D. J. Schurman, "Effects of fluid-induced shear on articular chondrocyte morphology and metabolism in vitro," J Orthop Res, vol. 13, no. 6, pp. 824–31, 1995.

[370] R. L. Smith, D. R. Carter, and D. J. Schurman, "Pressure and shear differentially alter human articular chondrocyte metabolism: a review," Clin Orthop Relat Res, no. 427 Suppl, pp. S89–95.

[371] Q. Wan, E. Cho, H. Yokota, and S. Na, "Rac1 and cdc42 gtpases regulate shear stress-driven beta-catenin signaling in osteoblasts," Biochem Biophys Res Commun, vol. 433, no. 4, pp. 502–7, 2013.

[372] F. Zhu, P. Wang, N. H. Lee, M. B. Goldring, and K. Konstantopoulos, "Prolonged application of high fluid shear to chondrocytes recapitulates gene expression profiles associated with osteoarthritis," PLoS One, vol. 5, no. 12, p. e15174, 2010.

[373] A. J. Maniotis, C. S. Chen, and D. E. Ingber, "Demonstration of mechanical connections between integrins, cytoskeletal filaments, and nucleoplasm that stabilize nuclear structure," Proceedings of the National Academy of Sciences, vol. 94, no. 3, pp. 849–854, 1997.

[374] C. M. Hale, A. L. Shrestha, S. B. Khatau, P. J. Stewart-Hutchinson, L. Hernandez, C. L. Stewart, D. Hodzic, and D. Wirtz, "Dysfunctional connections between the nucleus and the actin and microtubule networks in laminopathic models," Biophys J, vol. 95, no. 11, pp. 5462–75, 2008.

[375] K. I. Mitchelhill, B. J. Michell, C. M. House, D. Stapleton, J. Dyck, J. Gamble, C. Ullrich, L. A. Witters, and B. E. Kemp, "Posttranslational modifications of the 5-amp-activated protein kinase β1 subunit," Journal of Biological Chemistry, vol. 272, no. 39, pp. 24475–24479, 1997.

[376] A. Vazquez-Martin, C. Oliveras-Ferraros, and J. A. Menendez, "The active form of the metabolic sensor amp-activated protein kinase α (ampkα) directly binds the mitotic apparatus and travels from centrosomes to the spindle midzone during mitosis and cytokinesis," Cell Cycle, vol. 8, no. 15, pp. 2385–2398, 2009.

[377] P. Tsou, B. Zheng, C.-H. Hsu, A. T. Sasaki, and L. C. Cantley, "A fluorescent reporter of ampk activity and cellular energy stress," Cell metabolism, vol. 13, no. 4, pp. 476–486, 2011.

[378] Y. Wang, X. Zhao, M. Lotz, R. Terkeltaub, and R. Liu-Bryan, "Mitochondrial biogenesis is impaired in osteoarthritis chondrocytes but reversible via peroxisome proliferator–activated receptor γ coactivator 1α," Arthritis & Rheumatology, vol. 67, no. 8, pp. 2141–2153, 2015.

[379] D. G. Hardie, "Amp-activated/snf1 protein kinases: conserved guardians of cellular energy," Nature reviews Molecular cell biology, vol. 8, no. 10, pp. 774–785, 2007.

[380] N. Nakai, F. Kawano, and K. Nakata, "Mechanical stretch activates mammalian target of rapamycin and amp-activated protein kinase pathways in skeletal muscle cells," Molecular and cellular biochemistry, vol. 406, no. 1-2, pp. 285–292, 2015.

[381] T.-C. Ju, H.-M. Chen, J.-T. Lin, C.-P. Chang, W.-C. Chang, J.-J. Kang, C.-P. Sun, M.-H. Tao, P.-H. Tu, C. Chang, et al., "Nuclear translocation of ampk-α1 potentiates striatal neurodegeneration in huntingtons disease," The Journal of cell biology, vol. 194, no. 2, pp. 209–227, 2011.

[382] N. Wang, J. D. Tytell, and D. E. Ingber, "Mechanotransduction at a distance: mechanically coupling the extracellular matrix with the nucleus," Nature reviews Molecular cell biology, vol. 10, no. 1, pp. 75–82, 2009.

[383] V. Randriamboavonjy, J. Isaak, T. Frömel, B. Viollet, B. Fisslthaler, K. T. Preissner, and I. Fleming, "Ampk α2 subunit is involved in platelet signaling, clot retraction, and thrombus stability," Blood, vol. 116, no. 12, pp. 2134–2140, 2010.

[384] R. Kaiser, D. Friedrich, E. Chavakis, M. Böhm, and E. B. Friedrich, "Effect of hypoxia on integrin-mediated adhesion of endothelial progenitor cells," Journal of cellular and molecular medicine, vol. 16, no. 10, pp. 2387–2393, 2012.

[385] W. Chen, Y. Chang, H. Hsu, M. Yen, H. Huang, C. Cho, C. Wang, T. Weng, P. Lai, C. Chen, et al., "Therapeutics targeting cd90-integrin-ampk-cd133 signal axis in liver cancer.," Oncotarget, vol. 6, no. 40, pp. 42923–42937, 2015.

[386] C. P. Soares, V. Midlej, M. E. W. de Oliveira, M. Benchimol, M. L. Costa, and C. Mermelstein, "2d and 3d-organized cardiac cells shows differences in cellular morphology, adhesion junctions, presence of myofibrils and protein expression," PloS one, vol. 7, no. 5, p. e38147, 2012.

[387] C. M. Kraning-Rush, S. P. Carey, J. P. Califano, B. N. Smith, and C. A. Reinhart-King, "The role of the cytoskeleton in cellular force generation in 2d and 3d environments," Physical biology, vol. 8, no. 1, p. 015009, 2011.

[388] Y. Matsuda, T. Ishiwata, Y. Kawamoto, K. Kawahara, W.-X. Peng, T. Yamamoto, and Z. Naito, "Morphological and cytoskeletal changes of pancreatic cancer cells in three-dimensional spheroidal culture," Medical molecular morphology, vol. 43, no. 4, pp. 211–217, 2010.

[389] V. Vogel and M. Sheetz, "Local force and geometry sensing regulate cell functions," Nature reviews molecular cell biology, vol. 7, no. 4, pp. 265–275, 2006.

[390] A. S. Sechi and J. Wehland, "The actin cytoskeleton and plasma membrane connection: Ptdins (4, 5) p (2) influences cytoskeletal protein activity at the plasma membrane," Journal of cell science, vol. 113, no. 21, pp. 3685–3695, 2000.

[391] E. G. Fey, K. M. Wan, and S. Penman, "Epithelial cytoskeletal framework and nuclear matrix-intermediate filament scaffold: three-dimensional organization and protein composition.," The Journal of Cell Biology, vol. 98, no. 6, pp. 1973–1984, 1984.

[392] M. Terasaki, L. B. Chen, and K. Fujiwara, "Microtubules and the endoplasmic reticulum are highly interdependent structures.," The Journal of Cell Biology, vol. 103, no. 4, pp. 1557–1568, 1986.

[393] C. M. Waterman-Storer and E. Salmon, "Endoplasmic reticulum membrane tubules are distributed by microtubules in living cells using three distinct mechanisms," Current Biology, vol. 8, no. 14, pp. 798–807, 1998.

[394] C. Guilluy and K. Burridge, "Nuclear mechanotransduction: Forcing the nucleus to respond," Nucleus, vol. 6, no. 1, pp. 19–22, 2015.

[395] P. Isermann and J. Lammerding, "Nuclear mechanics and mechanotransduction in health and disease," Current Biology, vol. 23, no. 24, pp. R1113–R1121, 2013.

[396] S. M. Seed, K. C. Dunican, and A. M. Lynch, "Osteoarthritis: a review of treatment options," Formulary, vol. 44, no. 5, pp. 143–152, 2009.

[397] H. Muir, "The chondrocyte, architect of cartilage. biomechanics, structure, function and molecular biology of cartilage matrix macromolecules," Bioessays, vol. 17, no. 12, pp. 1039–1048, 1995.

[398] R. F. Loeser, "Molecular mechanisms of cartilage destruction: mechanics, inflammatory mediators, and aging collide," Arthritis & Rheumatism, vol. 54, no. 5, pp. 1357–1360, 2006.

[399] J. H. Lee, J. B. Fitzgerald, M. A. DiMicco, and A. J. Grodzinsky, "Mechanical injury of cartilage explants causes specific time-dependent changes in chondrocyte gene expression," Arthritis & Rheumatism, vol. 52, no. 8, pp. 2386–2395, 2005.

[400] S. Hashimoto, R. L. Ochs, F. Rosen, J. Quach, G. McCabe, J. Solan, J. E. Seegmiller, R. Terkeltaub, and M. Lotz, "Chondrocyte-derived apoptotic bodies and calcification of articular cartilage," Proceedings of the National Academy of Sciences, vol. 95, no. 6, pp. 3094–3099, 1998.

[401] K. B. Marcu, M. Otero, E. Olivotto, R. M. Borzí, and M. B. Goldring, "Nf-κb signaling: multiple angles to target oa," Current drug targets, vol. 11, no. 5, p. 599, 2010.

[402] K. Nishitani, H. Ito, T. Hiramitsu, R. Tsutsumi, S. Tanida, T. Kitaori, H. Yoshitomi, M. Kobayashi, and T. Nakamura, "Pge2 inhibits mmp expression by suppressing mkk4–jnk map kinase–c-jun pathway via ep4 in human articular chondrocytes," Journal of cellular biochemistry, vol. 109, no. 2, pp. 425–433, 2010.

[403] K. R. Legate, S. A. Wickström, and R. Fässler, "Genetic and cell biological analysis of integrin outside-in signaling," Genes & development, vol. 23, no. 4, pp. 397–418, 2009.

[404] M. A. Schwartz, "Integrins and extracellular matrix in mechanotransduction," Cold Spring Harbor perspectives in biology, vol. 2, no. 12, p. a005066, 2010.

[405] S.-Y. Chien, C.-Y. Huang, C.-H. Tsai, S.-W. Wang, Y.-M. Lin, and C.-H. Tang, "Interleukin-1β induces fibroblast growth factor 2 expression and subsequently promotes endothelial progenitor cell angiogenesis in chondrocytes," Clinical Science, vol. 130, no. 9, pp. 667–681, 2016.

[406] E. Kang, Y. Lee, T. Kim, C. Chang, J.-H. Chung, K. Shin, E. Lee, E. Lee, and Y. Song, "Adiponectin is a potential catabolic mediator in osteoarthritis cartilage," Arthritis Research and Therapy, vol. 12, no. 6, p. R231, 2010.

[407] D. I. Kim, B. KC, and K. J. Roux, "Making the linc: Sun and kash protein interactions," Biological chemistry, vol. 396, no. 4, pp. 295–310, 2015.

[408] A. Méjat, "Linc complexes in health and disease," Nucleus, vol. 1, no. 1, pp. 40–52, 2010.

[409] E. Ross, R. Ata, T. Thavarajah, S. Medvedev, P. Bowden, J. G. Marshall, and C. N. Antonescu, "Amp-activated protein kinase regulates the cell surface proteome and integrin membrane traffic," PloS one, vol. 10, no. 5, p. e0128013, 2015.

[410] R. Kaiser, D. Friedrich, E. Chavakis, M. Böhm, and E. B. Friedrich, "Effect of hypoxia on integrin-mediated adhesion of endothelial progenitor cells," Journal of cellular and molecular medicine, vol. 16, no. 10, pp. 2387–2393, 2012.

[411] M.-H. Zou, X.-Y. Hou, C.-M. Shi, S. Kirkpatick, F. Liu, M. H. Goldman, and R. A. Cohen, "Activation of 5-amp-activated kinase is mediated through c-src and phosphoinositide 3-kinase activity during hypoxia-reoxygenation of bovine aortic endothelial cells role of peroxynitrite," Journal of Biological Chemistry, vol. 278, no. 36, pp. 34003–34010, 2003.

[412] A. Sundararaman, U. Amirtham, and A. Rangarajan, "Calcium-oxidant signaling network regulates ampk activation upon matrix-deprivation," Journal of Biological Chemistry, pp. jbc–M116, 2016.

[413] D. E. Ingber, "Cellular mechanotransduction: putting all the pieces together again," The FASEB journal, vol. 20, no. 7, pp. 811–827, 2006.

[414] V. Mironov, R. P. Visconti, V. Kasyanov, G. Forgacs, C. J. Drake, and R. R. Markwald, "Organ printing: tissue spheroids as building blocks," Biomaterials, vol. 30, no. 12, pp. 2164–2174, 2009.

[415] S. Grogan, F. Rieser, V. Winkelmann, S. Berardi, and P. Mainil-Varlet, "A static, closed and scaffold-free bioreactor system that permits chondrogenesis in vitro," Osteoarthritis and cartilage, vol. 11, no. 6, pp. 403–411, 2003.

[416] W. Ando, K. Tateishi, D. A. Hart, D. Katakai, Y. Tanaka, K. Nakata, J. Hashimoto, H. Fujie, K. Shino, H. Yoshikawa, et al., "Cartilage repair using an in vitro generated scaffold-free tissue-engineered construct derived from porcine synovial mesenchymal stem cells," Biomaterials, vol. 28, no. 36, pp. 5462–5470, 2007.

[417] W. Ando, K. Tateishi, D. A. Hart, D. Katakai, Y. Tanaka, K. Nakata, J. Hashimoto, H. Fujie, K. Shino, H. Yoshikawa, et al., "Cartilage repair using an in vitro generated scaffold-free tissue-engineered construct derived from porcine synovial mesenchymal stem cells," Biomaterials, vol. 28, no. 36, pp. 5462–5470, 2007.

[418] T. Nagai, K. S. Furukawa, M. Sato, T. Ushida, and J. Mochida, "Characteristics of a scaffold-free articular chondrocyte plate grown in rotational culture," Tissue Engineering Part A, vol. 14, no. 7, pp. 1183–1193, 2008.

VITA

VITA

Qiaoqiao Wan was born on May 16, 1989 to Xianchun Wan and Runfeng Ni. Upon graduation form high school in 2006, she attended East China University of Science and Technology where she graduated with a Bachelor of Bioengineering degree in 2010. In 2009, she joined the laboratory of Dr. Jingxiu Bi in Adelaide University, Australia to work as research assistant on optimization of transfection using PEG. In 2010, Qiaoqiao joined the master program of Biomedical Engineering at Indiana University-Purdue University Indianapolis. At IUPUI, Qiaoqiao joined the laboratory of Dr. Na where she studied the mechanotransduction in cartilage and bone cells. After two years mater study with Dr. Na, Qiaoqiao decided to apply form Ph.D. program of Biomedical Engineering at Purdue University to continue her study. During her Ph.D. study, she focused on signaling in chondrocytes in response to mechanical loading as well as cytokines.